UNIVERSITY OF MODENA AND REGGIO EMILIA

Doctorate School in
INDUSTRIAL INNOVATION ENGINEERING

XXXV cycle

Methodological developments in the LCA analysis about chemicals dispersion model on local scale and effects evaluation model on the environment and human health

Candidate: Grazia Maria Cappucci

Tutor: Prof. Anna Maria Ferrari

School Director/Coordinator: Prof. Franco Zambonelli

Index

Abstract

Nowadays, the environmental problem most feared by our society and, in particular, by the new generations, is climate change. Its devastating effects can be felt by every person almost daily, with winters that are increasingly mild and not very rainy, summers characterized by violent and short thunderstorms alternating with dry and torrid periods. The effects of climate change are visible on a global scale, and it is precisely the vast territorial impact that unites activists around the world. If attention is shifted to local-scale effects, it is the pollution of the ecosystem that is of greatest concern to people along with climate change. The widespread diffusion of the phenomenon within all environmental compartments casts suspicion on the air that is breathed, the food that is eaten and the water that is drunk. In addition, people are wary of chemicals or fuels used by companies because of the ever growing potential effects on human health, once these substances have reached the final "target". Several physical and mathematical models have been developed in order to provide an answer to the dispersion problem, trying to increase knowledge about the pathways of substances into ecosystem once they have been emitted into environment. These models, according to their accuracy and completeness, can take into account substance-specific characteristics, although there are inevitably assumptions and simplifications, due to the complexity of the phenomenon of dispersion in the whole ecosystem. The Life Cycle Assessment (LCA) methodology provides a quantification of the damage caused by these emissions, through the implementation of models that assess toxicological and carcinogenic effects on human health and on the ecosystem in general based on the dose-response correlation. These models, which, first of all, estimate the migration of pollutants, in addition to the effect assessment, represent a first attempt to represent the reality, as the local dimension of the effects is not yet fully considered or it is limited to certain environmental compartments. The current study addresses the above issues, aiming at enhancing the modelling of the dispersion of pollutants at local level and their effects on human health and the ecosystem, from a toxicological point of view. In particular, the core activity is represented by the evaluation of the dispersion of a pollutant in air, water, soil, up to fauna and vegetation and human beings, once it is emitted from a local source. The reference is the box model described in Multimedia Environmental Models by Donald Mackay (2001), integrated, in a second step of the work, with a current calculation method for LCA, USEtox 2.0 (Fantke et al. 2017). The results of the methodological research are put at the service of the LCA methodology, in order to obtain a damage result based on models that take into account the complexity of the substance-specific dispersion process, starting from the input data related to an emission in an environmental compartment. The research activity, applying the LCA to a complex system as the one mentioned above, has the goal to analyse, with case studies and, if possible, in an experimental way, some methodological aspects that have not yet been thoroughly investigated to date. The project is a big challenge to be faced with a Life Cycle Thinking approach, but it is also a great opportunity to study the weak aspects of the current LCA-based environmental assessment models.

Summary

The aim of this study was to develop an assessment model applicable to Life Cycle Assessment (LCA) for damage on human and ecosystem health near emitting point caused by local emissions in air, water and soil. The definition of local characterization factors (CFs), the result of the toxicity pathway modelling of chemicals and that allow to convert inventoried emissions amounts into the corresponding toxicological impact and damage on human health and ecosystem, was found to be missing in literature and in current calculation methods (chapter 1) and constituted the main target of the present work.

The in-depth study of the current toxicity pathway approach in LCA (chapter 2) allowed to define a specific framework for the calculation of local CFs, at the end-point level expressed for human toxicity in disability adjusted life years (DALYs) per kg of chemical emitted and for ecotoxicity in potentially disappeared fraction of species (PDFs) multiplied with volume compartment per daily unit emission. They were achieved by building two models according to the stationary well-mixed box model (i.e. III level) described in Multimedia Environmental Models by Donald Mackay (2001) with the fugacity approach for a reference chemical (chapter 3), i.e. benzene, accounting, respectively, for the local scale alone, called “local model” (chapter 3.2) and the locale scale nested in a continental scale, called “local-continental model” (chapter 3.3), under the constraint of the local compartments as unique emitting ones.

The first model took into account 7 compartments, including aquatic and terrestrial biota, and 3 possible emitting scenarios, in air, water and soil compartments. All environmental intermedia partitioning within each compartment and inter-compartments transfer processes reported by Mackay were included and described in fluxes balance equations for each compartment. The second one considered a simplified system made of 3 compartments for each scale, scales that are linked with advective processes. A system of 6 fluxes balance equations was defined accordingly.

The models were built as Excel spreadsheets (Local model.xlsx and Local-continental model.xlsx, described in chapters 3.2.2 and 3.3.1, respectively), organized in sheets, and providing CFs calculation for each emitting compartment adopting the resolution matrix approach of the system of equations for the calculation of fugacities and concentrations in the receiving compartments.

The toxicity pathway for the calculation of CFs for both models follow USEtox 2.12 framework (Fantke et al. 2017), the UNEP/SETAC scientific consensus model for characterizing human and ecotoxicological impacts of chemical emissions in life cycle impact assessment, thanks to the definition of fate factors (FFs), that recall the concentration results of the resolution matrix, exposure factors (XFs), taking into account for human toxicity the exposure routes of the local population, and the effect factors (EFs). EFs of benzene for human toxicity were based on USEtox database, while eco-toxicity assessment was expanded compared to the current toxicity framework in LCA, adding terrestrial and air toxicities through the definition of specific EFs (chapter 3.2.6). A preliminary framework for the evaluation of a comprehensive ecotoxicity of benzene was built following the structure of freshwater ecotoxicity of USEtox 2.12 model and additional data collection about toxicological effects of benzene on terrestrial and air species were retrieved from literature and government reports/databases. The gap in the conversion procedure from a generic toxicity level into concentrations affecting 50% of species (EC_{50}) for terrestrial and air species was filled with the adoption of freshwater extrapolation factors, used as proxy.

In the second part of the study, the relevance of the locale scale was tested introducing it into a current model for LCA, in particular, USEtox 2.12 was taken as reference (chapter 5). This was achieved thanks to the collaboration with Prof. Peter Fantke of Quantitative Sustainability Assessment Division, Department of Management Engineering, Technical University of Denmark (DTU), USEtox director, first of all by translating the fugacity-based rate constants, previously developed for the models described above, into mass-based rates (chapter 5.1 and Appendix – A.4. The calculation is performed in the Excel spreadsheet Mass-based local-continental model.xlsx, in particular in the sheets "Conversion Local" and "Conversion Continental"). Then, an expansion of the current excel matrices of USEtox for the introduction of a 4 compartments local scale with local rate constants (chapter 5.1) was performed and an Excel spreadsheet (USEtox2.12-local.xlsm) was built.

An analysis and interpretation of the results of USEtox model modified with the local scale was performed for a unit emission of benzene first (chapters from 5.3.1 to 5.3.3) and extended at a later stage to 10 chemicals, whose amounts emitted were also defined in a sensitivity analysis according to real European emitting scenarios (chapter 5.2.2), and the results were compared with those of the original model (chapters 5.3.4 and 5.3.5).

The analysis of the local model results (chapter 3.2.3) allowed to identify the relevant processes for each compartment, advective for air and water and diffusive for soil, and the trend in mass distribution for each emitting scenario.

The fate results of the local model were tested (chapter 4) with a similar model made by Trent University (CA), that considered the III level of Mackay models as well, adapting the original Excel spreadsheet with landscape parameters used in the local model, providing similar results in almost all emitting scenarios, while reasons of differences were identified and discussed. Moreover, a comparison of the well-mixed box model with a Gaussian distribution of concentration, i.e. the Plume model, a semi-empirical stationary model frequently used in the air fate modelling in small scales, was performed to check whether, under appropriate conditions, there can be a similarity in the concentration results.

Summarising the findings about the local-continental model (chapter 3.3.2), the damage on human health on the local scale appears relevant, since it is comparable (i.e. same order of magnitude) to the continental one. Water emitting scenario shows the higher damage, because of the low degradation rate in water of benzene and the direct exposure route of the local population. Ecotoxicity results show the relevance of the compartments volume on the final score, attributing the greatest damage to the continental scale (up to + 3 orders of magnitude compared to the local scale). The damage expressed by PDFs alone is based on the assumption that the number of species present in each compartment is proportional to the volume of the compartment. Therefore, a high concentration in the local scale will produce a number of affected species in the same scale that is lower than in the continental scale, however, in proportion to the volume of the compartment, the fraction of affected species is higher in the local scale due to the higher concentration. This result is not visible because the unit of measure of ecotoxicity also considers compartment volume, balancing the results obtained for PDFs alone. Soil emitting scenario generates the highest damage score, mainly because of the absence of advective process.

The relevance of the local scale in LCA was proved also comparing the local impacts to larger emitting scales impacts provided by the current model modified with the local dimension, considering a unit emission for 10 chemicals (chapter

5.3.4). Local scale results to be relevant in terms of damage (i.e. CFs) to human health (DALYs), up to + 3 orders of magnitude compared to the emission in the continental freshwater compartment (Naphthalene), mainly due to the high concentration to which the local population is exposed to. Physico-chemical properties that lead to more or less significant presence (i.e. concentration) of chemicals at the local scale were identified and discussed.

Unlike human health, ecotoxicity CF is marginally affected by the presence of the local scale, as reported for the local-continental model.

Secondly, in the comparison of the impact scores generated by the model with the local dimension and by a current model without the local dimension, the consideration of average real amounts emitted in Europe shows that the neglecting local emissions leads to underestimating the damage especially for water and soil emissions (chapter 5.3.5).

As illustrated in chapter 6, a final test was performed, in particular, a comparison of the fate results of the local-continental model with the modified USEtox 2.12 model with the local scale. For this purpose some landscape parameters of the local-continental model were equated with those in use in the modified USEtox 2.12 model with the local scale. All emitting scenarios show a good correspondence in the concentration results between the two models, since differences concern only three cases, i.e. concentrations in local soil and continental water compartments, with opposite trends compared to the modified USEtox model. An analysis of the reasons to explain these differences, even if partially, was hypothesised to be related to the lack of some removal processes, that are not considered in the local-continental model.

Because of the relevance of the local damage, assessed with the building of a new model, the local-continental model, and by adapting a current LCA model (i.e. USEtox 2.12), local CFs are highly recommended for LCA.

The proposed model could be adapted to represent specific environments and local population exposure conditions, shifting from the generic standard environment to site-specific environment, in relation to the ultimate purpose of the proposed model, i.e. reflecting the potential hazard that an emission could generate on the surrounding community and ecosystem first, expression of the high level of damage achieved by individuals exposed to high concentrations.

Further methodological developments are needed, both on the fate and effect modelling side, in the first case considering mathematical representations of the environmental processes more suitable for local conditions, i.e. overcoming the well-mixed box assumption and adopting spatialized approach, and further implementing the robustness of the EFs calculated for air and soil, with specific extrapolation factors and broader and more reliable toxicological data.

1 Introduction

The role of Life Cycle Thinking (LCT) has become central in the last decade as support to public decision making. The increasing number of policies that, from the early 90's, recalled LCT principles demonstrates the legislator's high regard and trust in it (Sala et al. 2021), culminating with the European Green Deal (European Commission 2019), where LCT was designated as a fundamental approach to guide the European Union towards an ecological transition.

The commitment of the European Commission's Joint Research Center (JRC) from early 2004 in promoting the permeation of LCT-related practices into the decision-making processes of policy makers and companies led to a great number of initiatives and projects, such as the European Platform on LCA (EP-LCA), the contribution to product and organization environmental footprint (PEF/POEF) and definitions of methods to include LCT in waste management, resource use for energy production and building future scenarios (Sonnemann et al. 2017). Among the deliverables of EP-LCA it is worth mentioning the International Reference Life Cycle Data System (ILCD) Handbook (2010), representing the key guidelines for practical inclusion of LCT both in market and public services.

The perfect synthesis of the perception of the role the LCT can play was reported in the preface of the EU communication "EU Life Cycle Policy and Support" (Pennington et al. 2007): "Life cycle thinking is now maturing, moving from its academic origins and limited uses primarily in house in large companies to more powerful approaches that can efficiently support the provision of more sustainable goods and services through efficient use in product development, external communications, in support of customer choice, and in public debates."

Among the life cycle-based methodologies, the Life Cycle Assessment (LCA) (UNI EN ISO 2021a, 2021b) provides a quantification framework to assess the damage related to a complete life cycle of a product or a service, accounting, with a systemic approach, for all impacts related to inputs and outputs of the studied system. Damage is attributed to resources depletion and chemical emissions on ecosystems, through characterizing their multimedia fate, human and ecological exposure and toxicological effects.

While global attention is focused on the devastating effects of climate change, there is a firm and vigilant resistance from local communities to the installation of manufacturing and waste treatment plants, often addressed as the NIMBY (not-in-my-backyard) syndrome (Buffoli et al. 2016), concerned about the environmental repercussions of any toxic emissions. Particularly, a wide variety of installations are involved, such as landfills, livestock farms and waste processing plants, contributing also to the reduction of land availability.

The experience that posed the need for further methodological developments in LCA, deepen in this work, is placed in the context of support from the scientific community to local authorities and to citizens, when italian city council of Coriano (RN) in the Emilia-Romagna region, pressed by citizens' committees, in 2015 asked to the LCA practitioners of the LCA Working Group of University of Modena and Reggio Emilia to investigate the potential harmful effect caused by the local incinerator of municipal waste. The people living near the treatment plant were concerned not only about direct exposure, but also about indirect routes, such as ingestion of food grown near the incinerator.

At the same time, the city council of Coriano, observed that the Emilia-Romagna Regional Waste Management Plan addressed the plant choice on the basis of the results of just three LCA impact categories, i.e. Global warming potential,

Acidification and Resource consumption (Municipality of Coriano and Riccione (RN) 2018), thus neglecting other fundamental categories like Human toxicity and Eco-toxicity.

The mentioned local authority correctly interpreted the mission of LCA in policy making, that aims at avoiding the shift of burdens between environmental impact categories, in space, i.e. between world regions, and in time (Sala et al. 2016; Sanyé-Mengual and Sala 2022).

The request highlighted a gap currently present in the LCA, i.e. the local scale is scarcely considered in the chemical multimedia fate and exposure of calculation models for LCA, or limited to certain environmental compartments, i.e. air compartment in the urban scale. The main reason behind this choice is that usually in LCA of products the point of emission usually is not known through the value chain (Fantke et al. 2017) and, therefore, damage is sought at continental or global level. This criticality results in the absence of characterisation factors (CFs), the main output of calculation methods, for emissions in the environmental compartments at the local scale.

Other authors (Loiseau et al. 2018) have considered the role of LCA methodology applied to the territory, in particular the so-called territorial LCA has been analyzed by considering a precise activity in a defined local context and considering a local context as a whole, including all the anthropogenic activities present. In both cases, it turns out to be adapted to the local context the goal and scope and inventory phases of the studies only, while it has been admitted that the application of site-specific LCIA methods could be useful.

CFs aim at translating inventory data of LCA, such as chemical emissions in the environmental compartments, to the corresponding damage on human health and ecosystem quality. The CFs are defined for each emitting compartment and they quantify the whole damage per kg of emitted substance that occurs on each receiving compartment.

CFs vary among scales because concentrations and the number of people exposed are different from one scale to another. While continental CFs are commonly calculated by current LCA models, smaller emitting scales are not included.

1.1 Literature analysis

CFs link inventory data to the corresponding impact, encompassing the quantification of the environmental concentration thanks to *fate models*, that take into account all transport and removal processes according to chemical's properties, the quantification of the *intake mass* by targets – e.g. taking into account the exposure route, the number of people exposed - through exposure to the concentration, the calculation of *adverse effect* based on toxicological tests results (Figure 1).

Usually damage in LCA is expressed in Disability Adjusted Life Years (DALYs) for human health, i.e. the number of years lost due to premature death or morbidity, and in Potentially Disappeared Fraction of species integrated over space and time (PDF m^3 d).

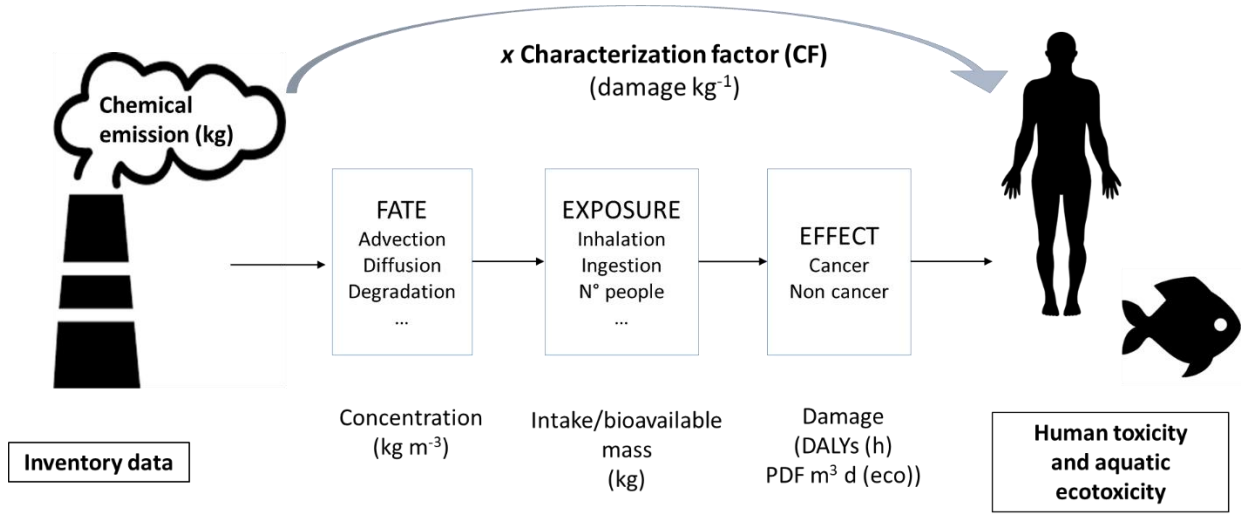

Figure 1 General impact pathway in LCA

These steps are not made explicit to a practitioner during an LCA, who might use the calculation method as a black box, ignoring the complexity and the meaning behind the definition of each CF.

An analysis of calculation methods is reported below, focusing on the presence of the local scale first, and, secondly, on the current approach adopted to evaluate ecotoxicity.

Currently, to the best of the author knowledge, calculation methods available in calculation software for LCA, like SimaPro 9.3 (PRé Consultants 2021) that take into account potential effects on high population urban scale due to air emissions, with CF for air compartment and high population, are listed hereafter:

- USEtox 2.12 (Fantke et al. 2017), the UNEP/SETAC scientific consensus model for characterizing human and ecotoxicological impacts of chemical emissions in life cycle impact assessment;
- methods whose toxicity impacts are based on USEtox, such as LC-IMPACT (Verones et al. 2020), the regionalized method that provides damage assessment to related to three areas of protection (human health, ecosystem quality, natural resources), TRACI 2.1 (Bare 2011), the calculation method originated from the broader impact assessment tool developed by U.S. specifically for the U.S. locations, and EF 3.0 Method (Fazio et al. 2018), the impact assessment method adopted in Environmental footprint transition phase of the European Commission;
- EN 15804 + A2 method (JRC 2019) intended for application to construction products in Environmental Product Declaration (EPD) certification programmes and based on EF 3.0 framework;
- IMPACT World+ (Bulle et al. 2019), the globally regionalized method based on USEtox population density archetypes for urban and rural emissions for specific pollutants.

It is also worth mentioning the preliminary method by Ferrari et al. (2019), that aims to implement indoor and local human effects within IMPACT 2002+ (Jolliet et al. 2003) method, considering only air compartment. It has been built following Eco-indicator 99 (Goedkoop and Spriemsma 2000) framework and the Gaussian Plume Modeling (Zannetti 1990), a stationary model used to simulate the air pollutants dispersion into air emitted from a chimney.

About ecotoxicity, nowadays, the most studied compartment is freshwater, so much so that it was included in the USEtox v. 2.1 evaluation framework (and, consequently, in the methods based on it listed above), thanks to the great amount of test data and databases collecting toxicity evidences on various taxonomic groups and species at different effect levels.

Toxicity study related to other compartments is currently under development, since for some of them it is considered essential by the scientific community in order to fully assess ecosystem toxicity. In particular, the most wanted compartments are sediments, about to be included in the framework of USEtox thanks to the improved data availability, and soil, whose toxicity analysis was probably postponed because of the possibility of deriving it for porewater phase from water toxicity (Fantke et al. 2018), as in the case of IMPACT2002+ method (Jolliet et al. 2003).

Soil toxicity was addressed until now as porewater phase toxicity by several methods, like Eco-indicator 99 (Goedkoop and Spriemsma 2000), in which the effects on micro-organisms, plants, worms were obtained from no observed effect level concentrations (NOECs) values of test data, according to the National Institute for Public Health and the Environment (RIVM) method for the Dutch Environmental Outlook (Klepper and van de Meent 1997). The toxicity level represented by NOECs is nowadays considered suitable for risk assessment for conservative purpose rather than Life Cycle Impact Assessment (LCIA), where more robust, average indicator like EC_{50} is recommended (Peter Fantke, Aurisano, et al. 2018; Jolliet et al. 2006; Larsen and Hauschild 2006a), as better discussed in chapter 2.3. Among the most recent calculation methods, LC-IMPACT (Verones et al. 2020) considers vascular plants as proxy for terrestrial species to evaluate toxicity due to exposure medium porewater phase.

Air toxicity is not directly addressed by any calculation method, but some species are currently of great concern for the scientific community, such as pollinators (Crenna et al. 2017) and predatory birds (Golsteijn et al. 2012).

Beyond the LCA methodology, several researchers have analyzed the local dimensions of chemicals fate and transport, more rarely the effects on human or ecosystem health, focusing on specific emission compartments. The analyzed literature reports two main models: nested box models, where every scale is assimilated to a well-mixed, homogeneous standard environment of the “Mackay type” (Mackay 2001), communicating only with the bigger box that contains it, and spatialized environments, divided in cells of a defined or varying resolution, where each cell communicates with more adjacent cells. While the latter is more complex due to the large number of mass balance equations to be solved, it allows the variation in landscape and demographic parameters to be represented more accurately. Both of them could be run under steady-state or dynamic conditions.

Hollander et al. (2007) have performed a simulation of PCB-153 emissions in Europe from 1981 to 2000 and have compared the concentration results in air and soil provided by LOTUS-EUROS (Schaap et al. 2008), a dynamic spatially resolved model with 14000 cells of 25 x 25 km^2, with those resulting from SimpleBox 3.0 (Den Hollander et al. 2004), the nested multi-media fate model, made of forty well-mixed, homogeneous compartments distributed on a local, regional, continental and global scale. The type IV (dynamic, non-steadystate) of SimpleBox 3.0 has been taken into account in the study, with a local environment sizing the same grid cell resolution. SimpleBox 3.0 returns higher average concentrations across scales in both air and soil compartments, namely twice and 1.5-3 times, in particular the lower range of concentrations (occurring on the regional-continental scale) is overestimated, due to the averaging of regional

and continental emissions, whereas the peaks on the local scale are comparable and confirmed by measured values. Generally, local air concentrations have resulted to be 2 orders of magnitude higher than continental concentrations.

In a later version, in SimpleBox 4.0 (Hollander et al. 2016) the local scale has been removed in order to improve the simplicity of the model.

Brandt et al. (2001) and Giannouli et al. (2011) have combined the gaussian plume modeling with the box model to evaluate the concentration at street level of pollutant emitted with exhaust gases in air. In particular, the latter compared the so defined small scale concentrations of PM_{10} and NO_2 with the urban scale, sizing 5 x 5 km^2, in 20 European cities, according to three emitting scenarios. In particular, NO_2 concentrations have shown a significant additional street increment to the urban background concentrations for almost all European cities considered, up to about twice or 3 times the urban one.

Among highly spatialized models that have investigated local-regional conditions, with quite large grid resolution, from 12 to over 100 km (Breivik et al. 2021; Cooter et al. 2012; Dennis et al. 2010; Derognat et al. 2003; Humbert et al. 2009; Seigneur et al. 2004; Van Zelm et al. 2007), Wannaz et al. (2018) have applied the Pangea modeling framework, the multimedia box model consisting of a set of compartments combined with multiscale varying grids, to finer resolution of 7 x 7 km^2 around the point of emission, for the evaluation of local up to global concentrations in the region of north-east of France in steady-state conditions for three chemicals (2,3,7,8-tetrachlorodibenzo-p-dioxin (TCDD), benzene and benzo[a]pyrene (B[a]P)). Air, water and agricultural soil concentrations, due to emissions from 126 solid waste treatment plants, and consequent population intake fractions at local and global scale, have been estimated and compared, showing an extended area invested by high concentration of benzene in air (up to 9 orders of magnitude higher than global concentration), while freshwater and agricultural soil are afflicted extensively by 2,3,7,8-tetrachlorodibenzo-p-dioxin (TCDD). The major intake occurs via inhalation of benzene, with local peaks of intake up to 6 times higher than the continental one.

In less recent years, the use of EUSES tool (Lijzen & Rikken 2004) can be highlighted. It is a decision-support system for the evaluation of the risks of substances to human health and the environment commissioned by European Commission, that models the concentration in three main nested spatial scales (local, regional and continental) with a hybrid mode. In particular, in local air the Gaussian plume is applied to an emitting point of 10 m and the resulting concentration is calculated at 100 m from the source point, while in local freshwater complete mixing and dilution are considered. For both local compartments, degradation and other removal processes are not taken into account, since considered negligible. Regional and continental scale are adapted to SimpleBox 3.0 (Hollander et al. 2004).

EUSES has been applied by several authors (Jaworskal et al. 1999; Kawamoto et al. 2012; Van De Meent et al. 2010) to evaluate local concentrations in different emitting scenarios. Van De Meent et al. (2010) have performed the most complete analysis by evaluating concentrations of petroleum hydrocarbons for every compartment (air, freshwater, natural and agricultural soils), assuming a daily steady-state emission ratios of 1:10:100 in air, respectively for local, regional and continental scales, reporting that the first ones are higher than those found at regional and continental scales, ranging, in terms of orders of magnitude, from + 5 to + 6 for air, from + 4 to + 6 for freshwater and from +1 to + 3 for soils.

1.2 Scope of the present work

Compared to the mentioned studies, the scope of the present study is assessing the magnitude of concentration and the consequent damage on human and environmental health caused by local emissions, i.e. emissions that occur in a small scale. Damage is assessed for a unit emission of a reference substance, i.e. benzene, with the final purpose of calculating local CFs for LCA analyses and to provide an answer to the "local issue". This issue is recognized to be addressed by the Health Risk Assessment (HRA) procedure, primarily to assess risk at the local site-specific level, however, it is believed that this task can also be accomplished in a LCT prospective by the LCA methodology, combining different levels of site-specificity depending on the focus of the study.

The calculation model of local CFs is proposed in two versions, the local scale alone (made of 7 compartments) with a surface area of 1 x 1 km^2 and the local scale connected with the continental scale (with 3 compartments for each scale), under the assumption of the stationary well-mixed boxes.

In both cases the proposed approach concern:

- the evaluation of damage that occurs near the point of emission, located in air, water and soil, on human health and ecosystem health due to the exposure to local concentrations;
- the evaluation of toxicity for air and soil compartments in terms of loss of biodiversity, in order to provide eco-toxicity results comprehensive of all environmental compartments.

In the proposed models the emitting point is always considered occurring in the local scale by default. According to the point of view of the author and of the LCA WG research group (Unimore), continental points of emission do not exist in reality, since every emitting point has effects in the surrounding area first and, then, the chemical is transported on larger scales.

The present work does not aim in providing a robust framework in evaluating ecotoxicity for every receiving compartment. Considerable amount of test data as well as adequate protocols in data selection and modelling are to be found from the scientific community.

A preliminary assessment for ecotoxicity was performed within this work just for one chemical in order to provide a complete assessment of damage in the whole system considered.

Moreover, the relevance of the local issue was deepened also in the context of a current model for LCA, i.e. USEtox v. 2.12. The presence of USEtox chemicals database gave the opportunity to study the behaviour of the local scale on a wider range of chemicals, in order to provide indications on the recommended use of the local scale according to the physico-chemical properties of chemicals.

2 Life Cycle Toxicity Assessment

LCA methodology is part of the *comparative assessment*, in which environmental impacts are referred to a functional unit, such as a product, that fulfils a certain function. The attempts to mitigate impacts along the life cycle are addressed to the preservation of the function, through comparative analyses of different products or production systems (Fantke et al. 2017; Olsen et al. 2001). In contrast to environmental *risk assessment*, which, being focused on harmful effect to the final receptor, uses a precautionary approach in order to indicate which scenario is safe for humans and the ecosystem, the life cycle impact assessment (LCIA) step is based on robust statistical quantities in order to provide an optimal estimate of the effect (Fantke et al. 2018; Frischknecht and Jolliet 2016), useful for the comparative purposes mentioned above.

The global consensus framework of the scientific community regarding Life Cycle Toxicity Assessment was defined in 2003 as part of the Life Cycle Initiative, a public-private, multi-stakeholder partnership enabling the global use of credible life cycle knowledge by private and public decision makers and hosted by UN Environment, with the contribution of a panel of experts in the fields of pollutant dispersion, human and ecosystem exposure and toxicology. These specific skills, combined with each other, form the basis of the CFs used by the calculation methods in LCA studies to convert the masses of toxic emissions resulting from life cycle inventory processing into the corresponding damage to human and ecosystem health, in terms of loss of life years and loss of biodiversity, respectively.

The years of life lost by humans due to a given cause are expressed by a statistical quantity defined by the World Health Organisation as Disability Adjusted Life Years (DALYs), equal to “the sum of the years of life lost due to premature mortality and the years of healthy life lost due to disability for people living in states of less than good health”. For this type of indicator, quantification with integers is carried out since the interest is on individuals, where “a DALY represents the loss of the equivalent of one year of full health” (Wold Health Organization (WHO) 2020).

Biodiversity has been defined by the United Nations as follows (United Nations (UN) 1992):

“Biological diversity" means the variability among living organisms from all sources including, inter alia, terrestrial, marine and other aquatic ecosystems and the ecological complexes of which they are part: this includes diversity within species, between species and of ecosystems.”

The quality of the ecosystem and the protection of biodiversity in the LCA analysis is placed at the species level, rather than the individual level (Jolliet et al. 2003), which is difficult to quantify due to the great variety of species on different levels of the food chain that populate a compartment, a variety that crosses not only the different compartments that make up the ecosystem (mainly air, water and soil), but also the different scales considered. The quantification of the damage occurs, therefore, in terms of Potentially Disappeared Fraction of species (PDF), integrated in the area or volume of the compartment under analysis and over time. An analysis of this unit of measurement is proposed in chapter 2.4.1.

The assessment framework generally consists of three main steps:

- modelling and quantification of pollutant dispersion following emission in a compartment, called *fate* analysis;

- modelling and quantification of human population/species exposure to a concentration in a compartment, called *exposure* analysis;
- modelling and quantification of human and ecosystem health effects as a result of exposure, called *effect* analysis.

From each of these analyses, a factor is defined and their product returns the characterisation factor for each substance emitted in a given compartment according to the generic formula (Eq. 1) (Jolliet et al. 2006; Rosenbaum et al. 2008):

$$CF = FF \times XF \times EF \quad \text{(Eq. 1)}$$

where CF is the characterization factor, FF is the fate factor, XF is the exposure factor and EF is the effect factor. The first and last factors are specific to the pollutant, the characteristics of the environmental system considered and the final receptor, the second depends solely on the environmental system considered and the final receptor.

The task of the CF is to take the LCA analysis from the phase of quantifying the masses emitted (kg) in the inventory of an LCA to the quantification of the corresponding damage on human and ecosystem health. Therefore, the unit of measurement of CF is the damage (DALYs or PDF area/volume time) for a unit emission in an environmental compartment.

The matrix resolution approach proposed by Rosenbaum et al. (2007) is integrated within USEtox 2.12 (Fantke et al. 2017), the United Nations Environment Programme (UNEP) / Society of Environmental Toxicology and Chemistry (SETAC) scientific consensus model for characterising human and ecotoxicological impacts of chemical emissions in life cycle assessment. The model provides CFs for assessing the ecotoxicity of organic and inorganic chemicals on human health and freshwater.

USEtox 2.12 is taken as a reference in the present study to explore, in a second step of this work, the characteristics of the local scale within a current calculation method, as described in chapter 5.

A synthetic discussion of the matrices and the physical significance they represent is given below.

2.1 Fate factor

The modelling of pollutant dispersion in USEtox 2.12 is based on SimpleBox 2.0 (Brandes et al. 1996), a nested multimedia fate model for evaluating the environmental fate of chemicals, in which the environmental compartments are represented as well-mixed boxes, in which environmental transport and degradation processes occur according to first-order kinetics and under steady-state conditions. The scales present are indoor (air), urban (air), continental (air, fresh water, seawater, continental soil, agricultural soil) and global (same compartments as continental scale). Each scale is nested into the larger one. In USEtox, all compartments are considered to be emitters and receivers at the same time and the mass increase following a daily emission is evaluated for each of them with a mass balance equation, based on the generic formula (Eq. 2), which takes into account all processes occurring in a given compartment i:

$$\frac{dm_i(t)}{dt} = EMIS_i + IMT_{j \to i} \times m_j - IMT_{i \to j} \times m_i - DEG_i \times m_i - OUT_i \times m_i \quad \text{(Eq. 2)}$$

Where:

- m_i (kg) is the mass of the chemical in box i;
- t (d) is the time;
- $EMIS_i$ $(kg\ d^{-1})$ is the emission rate of the chemical into box i;
- $IMT_{j\to i}(d^{-1})$ is the intermedia transfer rate of the chemical from box j into box i;
- $IMT_{i\to j}(d^{-1})$ is the intermedia transfer rate of the chemical from box i into box j;
- DEG_i (d^{-1}) is the degradation rate of the chemical from box i;
- OUT_i (d^{-1}) is the transfer rate of the chemical from box i to outside the system.

The unknowns of the equations are the masses that, under steady-state conditions, stabilise within the compartments, which are directly or indirectly connected to the emitting compartment.

The system of n equations in n unknowns is solved with a matrix $\bar{k}$ $(\mathrm{n}\times\mathrm{m})$, populated by the known terms of the equations, i.e. the rates of the different environmental processes, and where the columns represent the emitting compartments and the rows the receiving compartments. Each receiving compartment can in turn be an emitter, thus obtaining a square matrix of the type shown below:

$$\begin{array}{c} \\ i \\ j \end{array}\begin{array}{c} \begin{array}{ccc} i & & j \end{array} \\ \begin{bmatrix} k_{i,tot} & \cdots & k_j \\ \vdots & \ddots & \vdots \\ k_i & \cdots & k_{j,tot} \end{bmatrix} \end{array}$$

The matrix $\bar{k}$ presents on the diagonal elements the sums of the removal processes from the corresponding compartment in the column. By dividing the off-diagonal element by the diagonal element of the respective column, the fraction of removal to each receiving compartment (removed fraction) can be measured.

Equation 2 can then be rewritten in the synthetic form (Eq. 3):

$$\frac{dM\,(t)}{dt} = \vec{M}\times\bar{k}+\vec{S} \qquad \text{(Eq. 3)}$$

where $\vec{M}$ (kg) represents the vector of unknown pollutant masses for the compartments under analysis, $\bar{k}$ (d^{-1}) is the matrix of constant rates affecting all environmental processes, $\vec{S}$ $(kg\ d^{-1})$ is the vector of emissions in the compartments.

In steady-state conditions $\frac{dM\,(t)}{dt}=0$ and the Eq. 3 could be rewritten (Eq. 4 and Eq. 5) to provide the unknown $\vec{M}$:

$$\vec{M}\times\bar{k}+\vec{S}=0 \qquad \text{(Eq. 4)}$$

$$\vec{M}=-\bar{k}^{-1}\times\vec{S} \qquad \text{(Eq. 5)}$$

The system is then solved by inverting the matrix $\bar{k}$ and changing the sign. The resulting matrix $-\bar{k}^{-1}$ correspond to the matrix $\overline{FF}$ (d), fate factor matrix, made as follows:

$$\begin{matrix} & i & & j \\ i & \begin{bmatrix} FF_i & \cdots & FF_{j,i} \\ \vdots & \ddots & \vdots \\ FF_{i,j} & \cdots & FF_j \end{bmatrix} \\ j & \end{matrix}$$

Each FF has time as its unit of measurement, but its physical meaning can be traced back to mass; in fact, it represents the mass of a unit emission in the receiving compartment for a unit emission in the compartment corresponding to the column.

Since S unit of measure is $kg\ d^{-1}$, FF could be expressed as $\frac{kg}{kg\ d^{-1}}$.

This meaning can be explained by imagining multiplying the matrix $\overline{FF}$ with an identity emission matrix $\bar{S}$, i.e. a matrix with 1 on the diagonal, indicating an emission in each emitting compartment.

The resulting matrix $\bar{M}$ (kg) of unknown masses will show the same values of the matrix $\overline{FF}$:

$$\begin{bmatrix} a & b \\ c & d \end{bmatrix} (d) \times \begin{bmatrix} 1 & 0 \\ 0 & 1 \end{bmatrix} (kg\ d^{-1}) = \begin{bmatrix} a & b \\ c & d \end{bmatrix} (kg)$$

The resulting matrix $\bar{M}$ will therefore have as many columns as the emitting compartments and as many rows as the receiving compartments. Each element represents the mass present in the receiving compartment for an emission in the compartment corresponding to the column.

The sum of the elements of a column returns the total mass present in the system for an emission in the compartment corresponding to the column.

The diagonal elements of matrix $\overline{FF}$ also represent the residence times in the compartment corresponding to the column, since, for a daily unit emission, these also represent the mass present in the compartment.

It may be useful to define a further quantity, the transfer fraction $f_{i\to j}$, the mass fraction that moves from compartment i to j compared to the emitted mass in i-th compartment (Eq. 6):

$$f_{i\to j} = \frac{FF_{j,i}}{FF_i} \qquad \text{(Eq. 6)}$$

A demonstration of this equation is given below on a simplified two-compartment air-water system, in which diffusion (volatilisation and adsorption), degradation and advection processes occur for each compartment.

The matrix $\bar{k}\ (2 \times 2)$ could be written as follows:

$$\begin{matrix} & \text{A} & \text{W} \\ \text{A} & \begin{bmatrix} k_{a,tot} & k_{volat,w,a} \\ k_{abs,a,w} & k_{w,tot} \end{bmatrix} \\ \text{W} & \end{matrix}$$

From which the inversion the matrix $\overline{FF}$ is made:

$$\begin{array}{cc} & \begin{array}{cc} A & W \end{array} \\ \begin{array}{c} A \\ W \end{array} & \begin{bmatrix} \frac{k_{w,tot}}{det} & \frac{-k_{volat,w,a}}{det} \\ \frac{-k_{abs,a,w}}{det} & \frac{k_{a,tot}}{det} \end{bmatrix} \end{array}$$

where:

- $k_{a,tot} = -k_{abs,a,w} - k_{deg,a} - k_{adv,a}$ (Eq. 7)
- $k_{w,tot} = -k_{volat,w,a} - k_{deg,w} - k_{adv,w}$ (Eq. 8)
- $\det = (k_{a,tot} \times k_{w,tot}) - (k_{volat,w,a} \times k_{abs,a,w})$ (Eq. 9)

$FF_{a,w}$ could be obtained as follows (Eq. 10) on the basis of (Eq. 9):

$$FF_{a,w} = \frac{-k_{volat,w,a}}{det} \quad \text{(Eq. 10)}$$

$$= \frac{-k_{volat,w,a}}{(k_{a,tot} \times k_{w,tot}) - (k_{volat,w,a} \times k_{abs,a,w})}$$

$$= \frac{-k_{volat,w,a}}{((k_{abs,a,w} + k_{deg,a} + k_{adv,a}) \times (k_{volat,w,a} + k_{deg,w} + k_{adv,w})) - (k_{volat,w,a} \times k_{abs,a,w})}$$

$$= \frac{-k_{volat,w,a}}{\left(k_{volat,w,a} + k_{deg,w} + k_{adv,w}\right) \times \left[(k_{abs,a,w} + k_{deg,a} + k_{adv,a}) - \frac{(k_{volat,w,a} \times k_{abs,a,w})}{\left(k_{volat,w,a} + k_{deg,w} + k_{adv,w}\right)}\right]}$$

$$= \frac{-k_{volat,w,a}}{\left(k_{volat,w,a} + k_{deg,w} + k_{adv,w}\right)} \times \frac{1}{\left[(k_{abs,a,w} + k_{deg,a} + k_{adv,a}) - \frac{(k_{volat,w,a} \times k_{abs,a,w})}{\left(k_{volat,w,a} + k_{deg,w} + k_{adv,w}\right)}\right]}$$

$$= \frac{-k_{volat,w,a}}{\left(k_{volat,w,a} + k_{deg,w} + k_{adv,w}\right)} \times FF_a$$

It can be shown that FF_a corresponds to the second ratio of the latest development of Eq. 10 by developing the following steps (Eq. 11):

$$FF_a = \frac{1}{\left[(k_{abs,a,w}+k_{deg,a}+k_{adv,a}) - \frac{(k_{volat,w,a} \times k_{abs,a,w})}{\left(k_{volat,w,a}+k_{deg,w}+k_{adv,w}\right)}\right]} \quad \text{(Eq. 11)}$$

$$= \frac{1}{\left\{\frac{\left[(k_{abs,a,w} + k_{deg,a} + k_{adv,a}) \times \left(k_{volat,w,a} + k_{deg,w} + k_{adv,w}\right)\right] - (k_{volat,w,a} \times k_{abs,a,w})}{\left(k_{volat,w,a} + k_{deg,w} + k_{adv,w}\right)}\right\}}$$

$$= \frac{\left(k_{volat,w,a} + k_{deg,w} + k_{adv,w}\right)}{\left[(k_{abs,a,w} + k_{deg,a} + k_{adv,a}) \times \left(k_{volat,w,a} + k_{deg,w} + k_{adv,w}\right)\right] - (k_{volat,w,a} \times k_{abs,a,w})}$$

$$= \frac{k_{w,tot}}{\left(k_{a,tot} \times k_{w,tot}\right) - (k_{volat,w,a} \times k_{abs,a,w})}$$

$$= \frac{k_{w,tot}}{det}$$

as obtained with inversion of matrix $\bar{k}$.

The first fraction of the latest development of Eq. 10, on the other hand, represents the fraction evaporating $-k_{volat,w,a}$, i.e. moving from water to air, compared to the total moving out of water $k_{w,tot}$ (Eq. 12):

$$f_{w\to a} = \frac{-k_{volat,w,a}}{k_{w,tot}} \qquad \text{(Eq. 12)}$$

The ratio between the two FFs, therefore, returns the transfer fraction $f_{i\to j}$, as reported below (Eq. 13):

$$\frac{FF_{a,w}}{FF_a} = \frac{f_{w\to a}\times FF_a}{FF_a} = f_{w\to a} \qquad \text{(Eq. 13)}$$

In this simplified two-compartment case, the transfer fraction corresponds to the removed fraction, since there are no third-party compartments through which dispersion into the receiving compartment occurs. In more complex cases, where the compartments are not all directly connected, the transfer fraction also takes into account all possible pathways through third medium.

The compartments are represented as homogeneous boxes, i.e. within them the concentration of the chemical is uniformly distributed and shared between the different phases that compose them according to coefficients, which are discussed in more detail in chapter 3.1, expressing the constant ratios between the concentrations in the different phases at chemical equilibrium.

When defining the rates of the different processes, reference is made to the phases of the compartments responsible for these processes, which will, then, be accompanied by the mass fraction of chemical residing in the phase.

Eq. 177 to Eq. 182 in Appendix - A.1 show the procedure for deriving these mass fractions on the basis of the partition processes, depending on the different compartments.

2.2 Exposure factor

The purpose of the exposure factor is to quantify the intake by living beings exposed to a certain concentration.
As with the FF, the modelling of exposure is based on the matrix approach.
The calculation for the exposure factor XF is differentiated between human health and ecosystem health, because the subsequent steps of the analysis take the human dose and the bioavailable environmental concentration for the ecosystem as the starting point for determining the effect, respectively. The quantification of exposure for human health, therefore, is made on the basis of the intake mass, for the ecosystem on the basis of the bioavailable concentration, as explained in more detail in chapter 2.3 below.
Two distinct matrices are created, $\overline{XF_{hum}}$ for human intake, where the columns represent the receiving compartments and the rows the possible routes of exposure, and $\overline{XF_{eco}}$ for ecosystem exposure, where the columns represent the compartments and the rows the mass fractions of bioavailable chemicals in each compartment corresponding to the column. Therefore, the latter matrix is only populated in the diagonal elements.

In the matrix $\overline{XF_{hum}}$ it is possible to distinguish direct exposure routes, i.e. inhalation of air and ingestion of water, from indirect exposure routes, represented by intake through ingestion of food, such as meat, dairy produce, vegetables, and fish. The latter do not represent compartments in the USEtox model, so the corresponding concentration is calculated using a bioaccumulation factor (BAF) model. BAF represents the biotransfer from an environmental medium into a substrate and subsequent bioaccumulation within the substrate, represented, in general, by the ratio of the concentration present in the food to the concentration present in the medium to which it is exposed. For a complete discussion of BAF, please refer to the USEtox documentation.

Elements of matrix $\overline{XF_{hum}}$ have the following formula, differentiating between direct exposure (Eq. 14 and Eq. 15) and indirect exposure (Eq. 16):

$$XF_{inh,S}^{direct} = \frac{IR_{inh} \times Pop_S}{V_{a,S}} \quad \text{(Eq. 14)}$$

where $XF_{inh,S}^{direct}(d^{-1})$ is the XF for inhalation on the considered scale, $IR_{inh}(m^3 d^{-1})$ is the individual human inhalation rate, Pop_S is the population declined in the different scales, and $V_{a,S}$ (m^3) is the volume of the global, continental, and urban air compartment, respectively.

$$XF_{ing,w,S}^{direct} = \frac{IR_{ing,w} \times Pop_S}{V_{w,S} \times 1000} \quad \text{(Eq. 15)}$$

where $XF_{inh,S}^{direct}(d^{-1})$ is the XF for water ingestion on the considered scale, $IR_{ing,w}(L\ d^{-1})$ is the individual human water ingestion rate, Pop_S is the population declined in the different scales, and $V_{w,S}$ (m^3) is the volume of the global and continental water compartment, respectively, $1000\ L\ m^{-3}$ is the unit conversion factor or water density.

$$XF_{ing,xp,i,S}^{indirect} = \frac{BAF_{xp,i} \times IR_{ing,xp} \times Pop_S}{V_{i,S} \times \rho_i} \quad \text{(Eq. 16)}$$

Where $XF_{ing,xpi,S}^{indirect}$ (d^{-1}) is the XF for ingestion through route xp, i on the considered scale, $BAF_{xp,i} = \frac{C_{xp,i}}{C_i}$ $(kg_{xp,i}\ kg_i^{-1})$ is the bioaccumulation factor, $IR_{ing,xp}(kg\ d^{-1})$ is the individual human ingestion rate through route xp, i, Pop_S is the population declined in the different scales, $V_{i,S}$ (m^3) is the volume of the medium connected to route xp, i on the considered scale, ρ_i $(kg\ m^{-3})$ is the medium density.

About the ecosystem, since toxicity is only assessed in the freshwater compartment, the formula for calculating XF (Eq. 17) makes explicit the fraction of chemical present in the dissolved water phase, i.e. that which is bioavailable for the different aquatic species:

$$XF_{eco,x,w,S} = \frac{1}{1 + K_{susp,x} \times \frac{C_{susp,fw}}{1000} + K_{doc,x} \times \frac{C_{doc,fw}}{1000} + BAF_{fish,fw,x} \times \frac{C_{biota,fw}}{1000}} \quad \text{(Eq. 17)}$$

where $K_{susp,x}$ $(L\ kg^{-1})$ is suspended solids/water partitioning coefficient of chemical x, $C_{susp,fw}$ $(kg\ m^{-3})$ is the concentration suspended matter in freshwater, $K_{doc,x}$ $(L\ kg^{-1})$ is the dissolved (colloidal) organic carbon/water partition coefficient of chemical x, $C_{doc,fw}$ $(kg\ m^{-3})$ is the concentration of dissolved (colloidal) organic carbon in freshwater, $BAF_{fish,fw,x}$ $(L\ kg^{-1})$ is the bioaccumulation factor for freshwater fish of chemical x, $C_{biota,fw}$ $(kg\ m^{-3})$ is the concentration of biota in freshwater.

The above equation is obtained from a ratio of the mass in the dissolved water phase to the mass in the total water compartment, taking into account all phases present, similar to Eq. 179.

2.3 Effect factor

The calculation of the effect factor, both for human health and ecosystem quality, is based on toxicological evidence.

A definition of toxicology is "the study of the adverse effects of chemical, physical, or biological agents on living organisms and the ecosystem". The effects may be targeted on certain organs or affect the entire body of the living being.

The degree of toxicity of a chemical substance is assessed by direct studies on animals or, less frequently, by measurements on humans or by epidemiological studies on humans.

The studies that can be carried out experimentally on living beings differ in the way they are performed, particularly in relation to the duration of the test (acute/chronic toxicity) and the quantity (dose) of substance administered, providing different information on the effects generated. The main concepts involved in the definition of toxicological tests are outlined below:

- Dose, is the amount of substance administered at one time. It is related to the body weight of the living being to which it is administered and the time of administration (e.g. mg kg_{bw}^{-1} d^{-1}), especially for repeated administrations over time. It is also differentiated by the type of effect generated, whether lethal (Lethal Dose, LD) or a different generic effect analysed (Effect Dose, ED), and by the number of subjects statistically affected by the adverse effect. In relation to the latter concept, the definition of the dose-response curve is essential for relating a dose to the subjects affected, as shown below;
- Acute toxicity, experienced after the administration of a single dose or a series of doses received within a 24-hour period, to such an extent as to cause very serious effects, up to and including death;
- Sub-chronic toxicity, by which the effects induced after repeated and prolonged doses for more than 10% of the life of the treated living being are identified or in any case from a few weeks to a few months. Their study makes possible to determine how the effects evolve.
- Chronic toxicity, by which the effects induced after repeated and prolonged administration for more than 50% of the life of the living being treated are identified. Their study make possible to determine latency periods, bioaccumulation phenomena and the reversibility of the effects (Musmeci 2007).
- Routes of exposure, define the mode of administration of the toxic substance, through inhalation, ingestion of water or food, dermal and ocular exposure.

In order to be able to define the dose-response curve, some references to statistical quantities are given below.

Generally speaking, the frequency (absolute or relative) of adverse effects in a number of subjects in a population (y-axis) exposed to a certain increasing dose (x-axis) presents a trend that can be approximated by a 'bell-shaped', or Gaussian, curve, where the greatest number of subjects present an adverse response to an average dose (Figure 2).

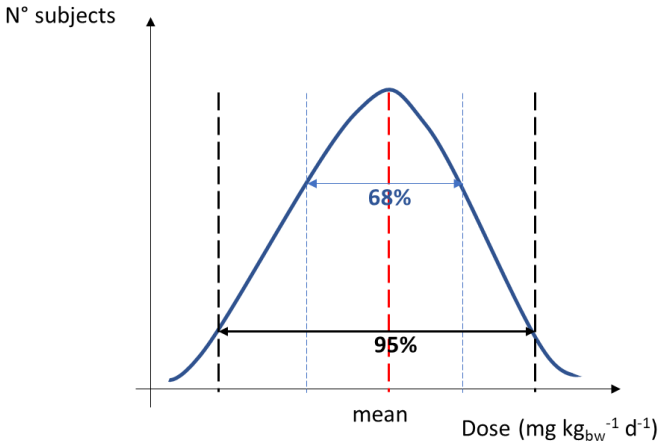

Figure 2 Gaussian distribution of adverse effects on a population

The standard deviation σ, i.e. the dispersion of the results around the mean value, is used to accompany a dose response value under analysis and it was noted that, statistically, 68% of the subjects is within the range of -1 σ and +1 σ, while 95% of the subjects is within the range -2 σ and +2 σ.

More precisely, referring to the concentration of a pollutant, this is a continuous variable, i.e. it is not a quantity that can be counted or measured, since all instruments have finite precision and can take on all real values in a limited range. In this case, it would not be possible to calculate the probability of a given adverse effect that corresponds to a given concentration value, as it can only be made in the presence of a discrete value of x. In this case, the probability density is used.

The probability density function $f(x)$, also expressed with the acronym PDF, of harmful effects for a given concentration value (continuous variable x) is generally described for this type of event by the Gaussian, or normal, distribution according to the following equation (Eq. 18):

$$f(x) = \frac{1}{\sqrt{2\pi\sigma^2}} e^{-\frac{(x-\mu)^2}{2\sigma^2}} \qquad \text{(Eq. 18)}$$

where x represents the concentration value under analysis, μ is the mean value and σ is the standard deviation.

The distribution function $F(x_0)$ (Eq. 19) associates to a given value of x_0 the probability that the continuous variable takes on a value no greater than x_0 itself.

$$F(x_0) = \int_{-\infty}^{x_0} f(x)dx \qquad \text{(Eq. 19)}$$

This probability is represented by the area to the left of a certain value x_0 subtended by the Gaussian curve with respect to the total area (Figure 3).

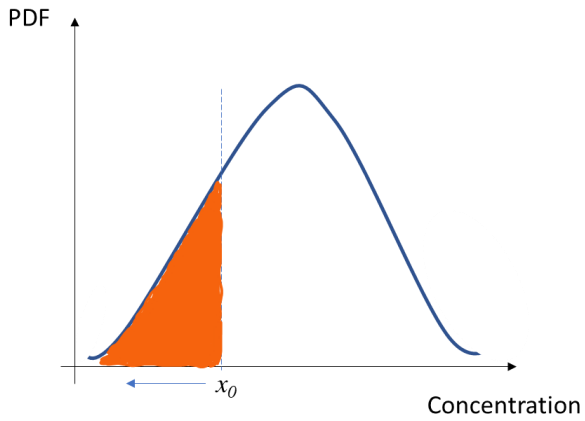

Figure 3 Probability density function of effects in an ecosystem

From the concentration, the corresponding dose can be calculated, as shown in sub-chapter 2.4. Through the cumulative integral of the Gaussian curve, it is possible to obtain the dose-response curve, usually an S-shaped or sigmoidal curve, in which the x-axis shows the dose taken over a lifetime, usually on a 10-based logarithmic scale to allow results corresponding to doses of very different orders of magnitude to be easily visualised on a single graph, and the y-axis shows the probability for an individual to manifest an adverse response (case). From the curve (Figure 4) it is possible to identify some known values, for example (only some of those mentioned are shown on the graph so as not to compromise readability):

- No observed adverse effect level (NOAEL), i.e. the highest dose that showed no effect on subjects in a population;
- Lowest observed adverse effect level (LOAEL), i.e. the lowest dose that showed effects on subjects in a population;
- Effect dose 10% (ED_{10}), the dose that showed effects on 10%of the subjects in a population;
- Effect dose 20% (ED_{20}), the dose that showed effects on 20%of the subjects in a population;
- Effect dose 50% (ED_{50}), the dose that showed effects on 50% of the subjects in a population;
- Effect dose 100% (ED_{100}), the dose that showed effects on 100% of the subjects in a population.

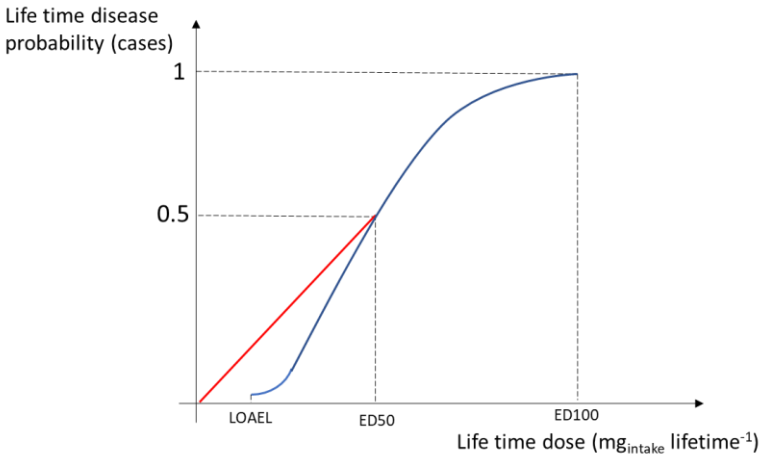

Figure 4 Dose-response curve for human toxicity

With regard specifically to the definition of the EF for human health, guidelines have been provided by the United Nations Environment Program (UNEP)/SETAC Life Cycle Initiative (McKone et al. 2006) in which ED_{50} values are recommended for the determination of effects to be included in the impact pathway of the LCA, rather than NOAEL or LOAEL values, which present problems related to the structure of the laboratory test, i.e. the concentrations tested. Indeed, it has been noted that the NOAEL, being determined as the highest measured value, is not statistically lower than the lowest dose at which the chronic effect actually occurs for the tested organism (LOAEL).

Values resulting from chronic tests are preferable to acute ones (Jolliet et al. 2006), since LCA studies typically deal with case studies involving continuous and constant emissions over time, due, for example, to steady-state production systems, which are more similar to chronic test conditions. For this reason, the S-curve depicted shows the probability results over an individual's lifetime.

Depending on the effect of the substance, whether carcinogenic or non-carcinogenic, a different data selection protocol is adopted by USEtox for deriving the ED_{50} for human health. Particular reference is made to the carcinogenic effect of the *low-dose slope factor* q_1^*, defined as the ratio of the unit of risk (U.R.), i.e. the increased probability for an individual to develop cancer if exposed to a concentration of 1 μg m^{-3} for his life (conventionally assumed to be 70 years), and the corresponding daily dose (μg kg_{bw}^{-1} d^{-1}).

This factor, if directly available for humans, is reported from the IRIS US EPA database (US EPA 2022), otherwise tumour dose 50% (TD_{50}) values from the CPDB (Gold et al. 1991) or low-dose slope factor for animals from the IRIS US EPA database can be used.

About the non-carcinogenic effects, there are generally insufficient data available to calculate the ED_{50} value with dose-response models. Therefore, NOAEL or LOAEL values are used, thus obtaining ED_{50} values with appropriate extrapolation factors (Huijbregts et al. 2005).

Formulas for calculating ED_{50}s are given below (Fantke et al. 2017). Eq. 20 represents the general formula for calculating the ED_{50} on a human being from an ED_{50} of a test animal for both a carcinogenic and a non-carcinogenic effect, while the calculation of the ED_{50} for a test animal for a carcinogenic effect uses q_1^* (Eq. 21) and the NOAEL/LOAEL for a non-carcinogenic effect (Eq. 22 and Eq. 23):

$$ED_{50,j,h} = \frac{ED_{50,a,t,j} \times BW \times LT \times N}{AF_a \times AF_t \times 10^6} \quad \text{(Eq. 20)}$$

Where $ED_{50,j,h}$ is the lifetime dose for a human through exposure route j (inhalation or oral), $ED_{50,a,t,j}$ is the daily dose for animal a and time duration t per kg body weight that causes a disease probability of 50% for the same exposure route j (mg kg_{bw}^{-1} d^{-1}), AF_a is the extrapolation factor for interspecies differences, $AF_t = 2$ (from subchronic to chronic) and $= 5$ (from subacute to chronic) is the extrapolation factor for differences in time of exposure, $BW = 70\ kg$ is the average body weight of humans, $LT = 70\ yr$ is the average lifetime of humans, $N = 365\ d\ yr^{-1}$.

$$ED_{50,canc,a,t,j} = \frac{1}{q^*_{1,a,t,j}} \times AF_q \quad \text{(Eq. 21)}$$

where $q^*_{1,a,t,j}$ is the carcinogenic, low-dose, slope factor for animal a and time duration t for exposure route j (kg_{bw} d mg^{-1}), and $AF_q = 0.8$ is the extrapolation factor to ED_{50};

$$ED_{50,noncanc,a,t,j} = NOAEL_{a,t,j} \times AF_N \quad \text{(Eq. 22)}$$

where $NOAEL_{a,t,j}$ is highest the daily dose per kg body weight or concentration for animal a and time duration t that causes no observed adverse effects for exposure route j (mg kg_{bw}^{-1} d^{-1}), and $AF_N = 9$ is the extrapolation factor to ED_{50}.

If not available directly, the NOAEL can be derived from LOAEL values according to the following formula (Eq. 23):

$$NOAEL_{a,t,j} = \frac{LOAEL_{a,t,j}}{AF_L} \quad \text{(Eq. 23)}$$

where $LOAEL_{a,t,j}$ is the lowest daily dose per kg body weight or concentration for animal a and time duration t that causes observed adverse effects for exposure route j (mg kg_{bw}^{-1} d^{-1}), and $AF_L = 4$ is the extrapolation factor to NOAEL.

The EF_{HH} definition is based on a linearity assumption for all dose-response models, where ED_{50} constitutes the working point, i.e. the point at which the slope of the line approximating the sigmoidal curve (red line in Figure 5b) is to be assessed, according to the general formula below (Eq. 24):

$$EF_{HH,canc/noncanc,j} = \frac{0.5}{ED_{50,canc/noncanc,j,h}} \quad \text{(Eq. 24)}$$

where 0.5 is the probability to develop the cancer or non cancer effect (cases) corresponding to the $ED_{50,canc/noncanc,j,h}$ (mg $person^{-1}$ $lifetime^{-1}$) through exposure route j.

About ecosystem, toxicity is measured in terms of biodiversity loss, so the toxicological test data used in the calculation referred to the bioavailable environmental concentration of a certain substance in a certain compartment to which the animal and plant species inhabiting that compartment are exposed to, and not to the intake dose. In fact, it is not possible to determine a single exposure mode for the living species occupying a certain compartment, due to the great variety of taxonomic groups, therefore the damage is related to the bioavailable concentration in the compartment, which can be calculated with dispersion models.

In particular, the concentration recommended within the UNEP/SETAC Life Cycle Initiative (Jolliet et al. 2006) is the hazardous concentration 50% (HC_{50}), i.e. the concentration of the compartment corresponding to 50% of the species exposed above their EC_{50} value and is equal to the geometric mean of the EC_{50} concentrations that caused 50% of the effects on the individual species in the compartment (Eq. 25) (Fantke et al. 2017).

$$HC_{50} = 10^{\frac{1}{n}\sum_{i=1}^{n}\frac{1}{m}\sum_{j=1}^{m} log_{10}(EC_{50,i,j})} \quad \text{(Eq. 25)}$$

where $EC_{50,i,j}$ are the individual j chronic EC50 values $j \in \{1,\ldots,m\}$ for i-th species $i \in \{1,\ldots,n\}$.
The geometric mean is used as it has been noted to provide a more robust result than other averages (Larsen and Hauschild 2006b), however it requires the data distribution to be lognormal (Eq. 26).

$$f(x) = \frac{1}{x\sqrt{2\pi\sigma^2}}\, e^{-\frac{(\log x-\mu)^2}{2\sigma^2}} \qquad \text{(Eq. 26)}$$

Where x is the continous variable, μ is the average value and σ is the standard deviation.

Therefore, assuming a log-normal distribution of the probability density data that a species is for 50% affected when subjected to a given concentration (Figure 5a, image adapted from Larsen and Hauschild 2006a), the derivation of the HC_{50} is made from the species sensitivity distribution (SSD), or PAF curve, potentially affected fraction of species, obtained, similarly to the dose-response curve, by the cumulative integral of the probability density curve, as shown in Figure 5b (image adapted from Larsen and Hauschild 2006a).

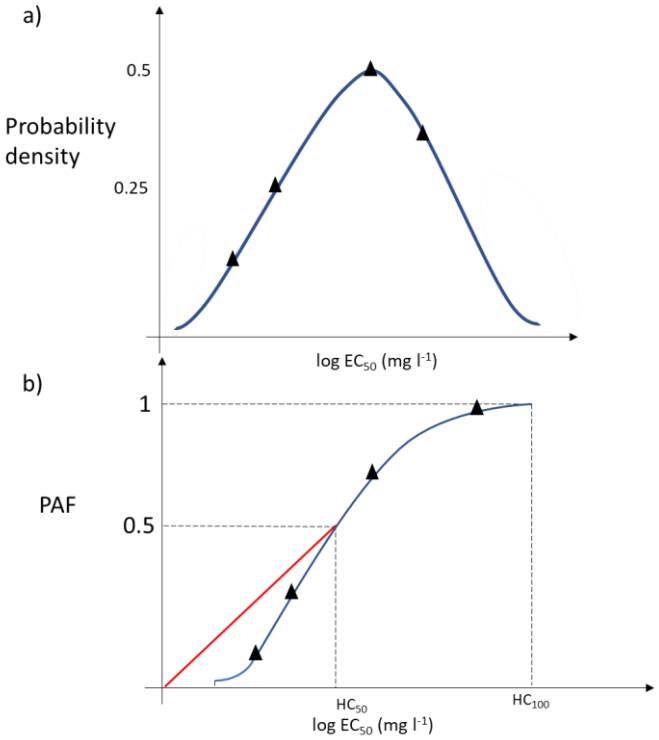

Figure 5 a) Probability density function in an ecosystem. b) PAF curve. Image adapted from (Larsen and Hauschild 2006a)

The area under the curve to the left of a given EC_{50} value represents the relative probability, compared to the total area under the curve, of selecting a species with a lower EC_{50} value (Figure 5a).

The trend of the PAF curve for a log-normal distribution is described by the cumulative distribution function, CDF, equation (Eq. 27):

$$PAF = \frac{1}{2} + \frac{1}{2}\,\mathrm{erf}\left(\frac{\log C-\mu}{\sqrt{2\sigma^2}}\right) \qquad \text{(Eq. 27)}$$

The curve in Figure 5b is substance-specific and the effects are given by the sum of the effects on the individual species. Similar to ED_{50}, it is recommended to consider HC_{50} rather than other levels expressing lower or non-existent effects as these are statistically more robust magnitudes.

The definition of EF_{ECO} is, therefore, based on an assumption of linearity for all PAF curve models, whereby HC_{50} constitutes the working point, i.e. the point at which the slope of the line approximating the sigmoidal curve (red line in Figure 5b) is to be assessed, according to the general formula below (Eq. 28):

$$EF_{ECO,i} = \frac{0.5}{HC_{50,i}} \quad \text{(Eq. 28)}$$

where i represents the receiving compartment whose toxicity is to be assessed.

Within the USEtox v. 2.12 calculation method, ecotoxicity is only assessed for the freshwater compartment. Recommended aquatic ecotoxicological effect factors must be based on test data of at least three different species for at least three different species group, representing three different trophic level in the food web chain (typically algae, crustaceans and fish), in order to obtain a sufficiently robust calculation of the fraction of species potentially affected (Fantke et al. 2017).

2.4 Characterization factor

The multiplication between FF and XF yields a different magnitude between human health and ecosystem quality.

In the former case, an intake factor is obtained, i.e. the mass of chemical taken up by humans through the different exposure routes (Eq. 29):

$$iF = FF \times XF \quad \text{(Eq. 29)}$$
$$= \frac{kg_{comp}}{kg_{em}d^{-1}} \times \frac{m^3_{inh}}{d\ pers} \times \frac{Pop}{V_{comp}}$$
$$= \frac{1}{kg_{em}d^{-1}} \times \frac{kg_{comp}}{V_{comp}} \times \frac{m^3_{inh}}{d\ pers} \times Pop$$
$$= \frac{1}{kg_{em}d^{-1}} \times C_{comp} \times \frac{m^3_{inh}}{d\ pers} \times Pop$$
$$= \frac{1}{kg_{em}} \times kg_{intake}$$

Note how time disappears from the equation, suggesting that only intake mass is decisive in calculating human toxicity.

In the second case, a bioavailable mass (Eq. 30) is obtained:

$$M_{bioav.} = FF \times XF \quad \text{(Eq. 30)}$$
$$= \frac{kg_{comp}}{kg_{em}d^{-1}} \times fract_{bioav.}$$
$$= \frac{kg_{bioav.}}{kg_{em}d^{-1}}$$

The calculation of CF starts from the result of this multiplication to express toxicity, in the first case using the correlation existing between the individual probability of suffering an effect in lifetime and the corresponding dose taken in lifetime (Eq. 31), in the second case the correlation existing between the fraction of species potentially affected and the corresponding environmental concentration (Eq. 32).

$$CF_{HH} = \frac{kg_{intake}}{kg_{em}} \times \frac{disease\ probability\ lifetime^{-1}}{kg_{intake} lifetime^{-1}} = \frac{n\ cases}{kg_{em}} \quad \text{(Eq. 31)}$$

$$CF_{ECO} = \frac{kg_{bioav.}}{kg_{em}\ d^{-1}} \times \frac{PAF}{kg_{comp}\ m^{-3}_{comp.}} = \frac{PAF\ m^{3}_{comp.}\ d}{kg_{em}} \quad \text{(Eq. 32)}$$

For both end receptors, the damage relative to 1 kg emitted is then expressed, for the purpose of applicability in the LCA.

2.4.1 Interpretation of USEtox CFs

From the calculation of human toxicity and eco-toxicity reported in the previous paragraph, interpretations are proposed and reported below about two aspects.

The first concerns the temporal discrepancy between the intake, which considers the mass taken in as a result of emission and the relative intake of a day, and the effect factor, which considers the individual's lifetime. The latter, however, could be assumed valid for any period, since, dimensionally, the life time is simplified into the fraction, relying on the total mass taken in to estimate the corresponding effect. As shown in Eq. 29, the same simplification can also be made on the intake mass.

Exploiting this relationship, therefore, the intake mass expressed by the iF is related to the damage it causes (Figure 6).

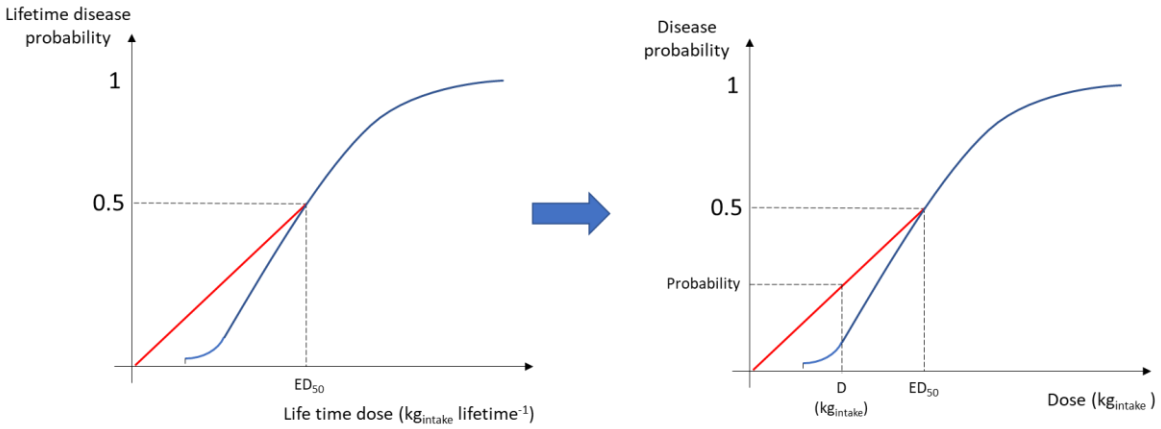

Figure 6 Interpretation of EF in USEtox for human toxicity

Mid-point toxicity to the aquatic ecosystem is measured as $\mathrm{PAF}\ m^3\ \mathrm{d}\ kg^{-1}$, i.e. the fraction of affected species integrated in the compartment volume and time for a unit emission of 1 kg, whereas the SSD curve, in general, has the PAF in the abscissa and the environmental concentration to which the species are exposed to in the ordinate. A change of variable is therefore made in the SSD curve, as shown in Figure 7.

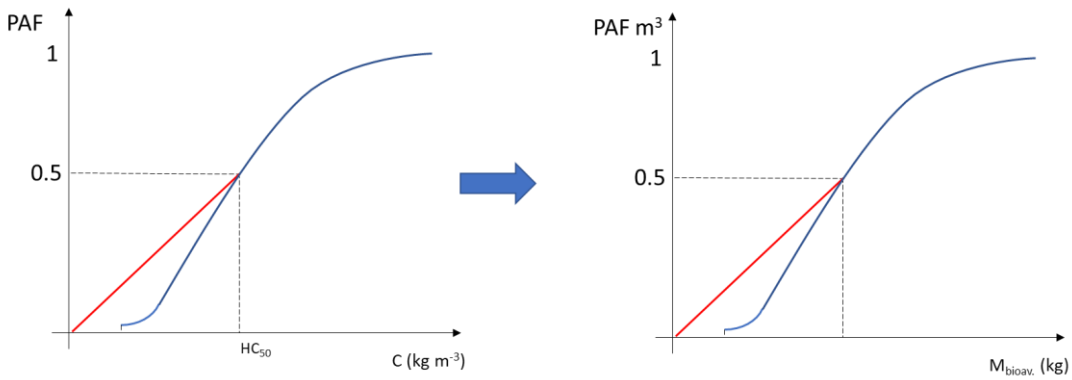

Figure 7 Interpretation of EF in USEtox for eco-toxicity. Hypothesis: V_{comp} = 1 m^3

The motivation behind this change could be driven by the following two necessities:

1. the multiplication between FF and XF for the ecosystem returns the bioavailable mass for a daily emission, i.e. the mass present in the phase taken up by the species, and not the concentration;

2. it is not possible to sum PAFs from different compartments and scales, since, in reality, they relate to a different number of species, depending on the extent of the compartment. Integrating PAFs into the compartment volume would allow this diversity to be taken into account.

Unlike the calculation of human toxicity, where the number of people present is taken into account, in the calculation of eco-toxicity the impact is calculated for a fraction of affected species, without assessing the total number of species involved. This approximation is necessary because, in general, it is very difficult to know the number of species present in an ecosystem.

However, if it is possible and of interest to the analyst, it is possible to estimate the number of species affected on a local scale by extrapolating the value of PAFs from the unit of measurement considered in the CF and multiplying it by the number of species present, if known.

Alternatively, the calculated PAF value alone can be used to express the magnitude of the impact generated on the total number of species present in each compartment.

The calculation of PAFs alone can be performed using the SSD curve approximated by the straight line with EF as its angular coefficient (Eq. 33):

$$PAF_i = C_i \times EF_i \qquad \text{(Eq. 33)}$$

where PAF_i is the fraction of affected species in the i-th receiving compartment, C_i $(kg\ m^{-3})$ is the concentration in the i-th receiving compartment, EF_i $(PAF\ m^3\ kg^{-1})$ is the effect factor calculated for the i-th receiving compartment, representing the ratio of the effect on 50% of the species exposed to the HC_{50} concentration to the HC_{50} concentration.

The value of PAF can, alternatively, also be derived by dividing the value of $PAF\ m^3 d\ kg^{-1}$ for the volume of the compartment where eco-toxicity is assessed, the emission time being 1 day.

2.4.2 Latest developments on the calculation of EFs for human health

Within the framework of the Life Cycle Initiative, workshops were held from 2014 to 2017 with the aim of overcoming criticisms shared by the scientific community on the current approach to toxicity assessment in LCIA (Fantke et al. 2021; Fantke et al. 2018). Linearity in the dose-response correlation correctly describes carcinogenic effects, whereas recent studies have shown it to be inadequate for different effects at the population level. This was demonstrated in the study on fine particulate matter (Frischknecht and Jolliet 2016) and endocrine disruptors (Fagin 2012).

Extrapolation of the dose-response correlation from zero to the point where the probability is 50% overestimates the harmful effect that would occur for realistically assumed doses, since, with all good evidence, such levels of harm are not reached.

The global scientific consensus model USEtox has been designated as the bearer of such advances in the LCIA, in particular with regard to the definition of new effect factors for non-carcinogenic effects on human health (Fantke et al. 2021), which considers two substantial novelties: the replacement of the zero slope with a marginal slope at a given working point, representing an existing population exposure condition (background exposure level), and a procedure for identifying a suitable point of departure (POD) for the subsequent steps of extrapolating toxicological effects on humans.

With regard to the first point, ED_{10} is identified as the working point for a direct extrapolation to zero, since the resulting slope approximates the marginal slope for a working point of 1% (ED_{01}), considered to be a realistic exposure level for the population (Fantke et al. 2019) (Figure 8).

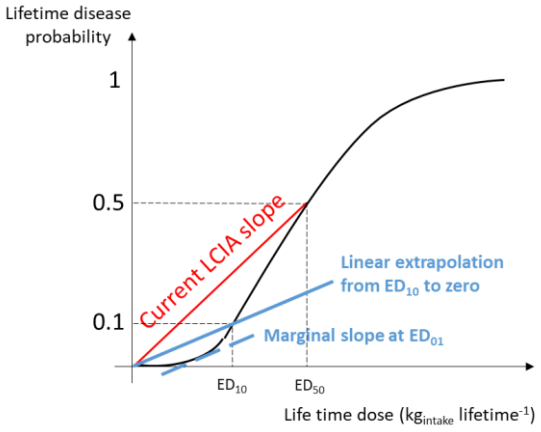

Figure 8 New EF for human toxicity. Image adapted from Fantke et al. (2018) *and* Fantke et al. (2021)

3 Experimental part: the proposed models for damage assessment on a local scale

The model built for the assessment of local damage due to emissions in the three main environmental compartments was based on Donald Mackay's description of the world unit in *Multimedia Environmental Models* (Mackay 2001), in which the author uses an assessment environment to describe the environmental processes between the compartments.

Specifically, in the present study, the same chemical-physical quantities used by Mackay to represent environmental processes and the same environmental compartments were used within an Excel spreadsheet-based calculation tool to simulate the dispersion of pollutants on a local scale. Within the same tool, the calculation of human and ecosystem exposure to environmental concentrations and the toxic effect that can be generated on these were included. This second part of the tool was created on the basis of the USEtox v.2.12 framework, with the aim of obtaining characterisation factors that can be used in Life Cycle Assessments (LCA).

Two versions of this tool were produced:

- a model with a local scale composed of 7 compartments, henceforth called “local model”;
- a model with a local scale of 3 compartments grafted onto a continental scale of 3 compartments, henceforth referred to as the "local - continental model".

The local scale is delimited in this study as the volume of small world units located near the emission point, in order to assess the dispersion of pollutants in all compartments and the effect on human health and the ecosystem.

The characteristics of the local scale are:

- small world unit (A_{max} = 1 km^2);
- high population density, similar to the urban scale;
- emission source within the world unit.

For the second model, fluxes entering the world unit by advection with air and water from larger, communicating scales, such as regional/continental, are also allowed.

The differences of the local scale with respect to the urban scale concern precisely the proximity to the emissive source, as the urban scale can also be distant from the emissive point (e.g. in USEtox air urban is a receiving compartment with emissions also occurring on a continental/global scale) and population density, as an urban scale certainly has a high population density, while a local scale can also consider a peripheral area with lower population density.

Therefore, when the “local effect” is mentioned, the author is implicitly referring to an assessment of pollutant effects close to the emissive source, which is the first step of pollutant dispersion, before moving on to a continental and global scale.

The local scale could be seen as a magnifying glass on the emissive point, which centralises the unit of the world under consideration. In this way, it would be possible to connect the local scale with larger communicating scales, such as the continental, which would then be a receiving scale.

The final characterisation factors would be calculated with respect to the emitting compartment, but the dispersion, and hence the effects, would overwhelm all receiving compartments, on all scales involved.

Therefore, a local emission would have a characterisation factor expressing the damage at the local and continental scales. The main differences between continental and local scales would, therefore, be related to size, meteorological parameters, and population density for human health, while for ecosystem quality, a generic ecosystem is assumed as an example, as further explained below.

3.1 Fugacity model by D. Mackay

D. Mackay's fugacity model aims to give a representation of the distribution of a chemical substance following its release into the environment. The physical quantity underlying this modelling is fugacity, introduced in 1901 by the chemist-physicist Gilbert Lewis.

Fugacity, or chemical potential, is denoted by the letter ***f*** and measured in Pascal and can be defined as the tendency of a substance, introduced into a phase, to move out of it under isothermal conditions and redistribute itself in its surroundings to reach equilibrium. The concept of equilibrium is defined by the zero law of thermodynamics which states that when two bodies are in thermal equilibrium, i.e. there is no net flow of heat in any direction, their temperatures are equal.

In the case where movement is attributable to a diffusive process, a parallelism between temperature and fugacity can therefore be identified: the former concept is the criterion for thermal equilibrium, i.e. of heat flows, the latter for the equilibrium of mass flows. Following an emission, the emitted substance will tend to move until the compartments involved have the same fugacity. What, therefore, will determine the mass movement of a substance is the difference in fugacity Δf, which will direct the *mass flow* $\boldsymbol{F}$ (mol h^{-1}) from the compartment with the higher fugacity to the compartment with the lower fugacity, acting as a driving force, analogous to the temperature T in the case of heat conduction, as illustrated in Eq. 34 for a diffusive process:

$$F = \Delta \mathrm{f} \times \mathrm{D} \qquad \text{(Eq. 34)}$$

where $\mathrm{D}\ (\mathrm{mol}\ h^{-1}\ Pa^{-1})$ is a coefficient specific to each process, as explained in detail in sub–chapters 3.1.2. At equilibrium, therefore, it will be $\Delta \mathrm{f}\ (\mathrm{Pa}) = 0$.

A different approach to describe the partitioning of chemicals from that of fugacity, as also emphasised by Mackay, is that of the $\boldsymbol{K_{XY}}$ *partition coefficients*, which express in what ratio the concentrations of the same substance are in communicating phases x and y (Eq. 35).

$$K_{XY} = \frac{C_X\ (mol\ m^{-3})}{C_Y\ (mol\ m^{-3})} \quad \text{(Eq. 35)}$$

In this case, the diffusive flux under steady-state conditions is generated by the concentration difference ΔC (Figure 9).

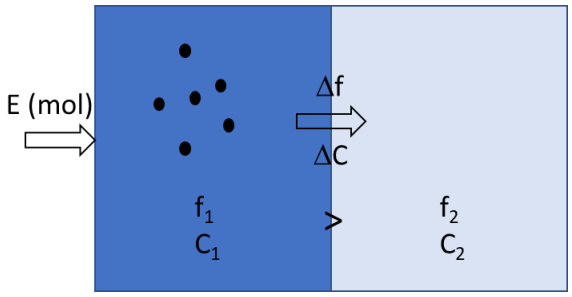

Figure 9 Diffusion process between two phases

Fugacity can be related to concentration, and thus to mass, by means of the *fugacity capacity*, denoted by the letter $\boldsymbol{Z}$, and having the unit mol m^{-3} Pa^{-1}. This quantity depends on both substance and compartment and expresses the tendency of the compartment to retain the substance, as indicated by the unit of measurement similar to a concentration per unit of fugacity. Fugacity capacity can be defined either by compartment or by any phase that makes up the compartment, as shown in detail in Eq. 72.

For this quantity, similarly to concentration, the constancy relationship expressed by the partition coefficient for two phases at equilibrium (Eq. 36) is applied:

$$K_{XY} = \frac{Z_X\ (mol\ m^{-3}Pa^{-1})}{Z_Y\ (mol\ m^{-3}Pa^{-1})} \quad \text{(Eq. 36)}$$

The relationship linking these two quantities is shown below (Eq. 37):

$$C\ (mol\ m^{-3}) = f\ (Pa) \times Z\ (mol\ m^{-3}Pa^{-1}) \quad \text{(Eq. 37)}$$

The balance between these two opposite quantities therefore determines the mass per unit volume that resides in a given compartment. The mass $\boldsymbol{M}$ (mol) can be obtained by multiplying the concentration by the compartment volume $\boldsymbol{V}$ (m^3).

For both approaches, the aim is to provide a measure of the concentration in a receiving compartment placed in contact with an emitting compartment long enough to reach equilibrium.

Under equilibrium conditions, the concentrations between two compartments are in constant ratio, so the partition coefficient is constant.

The following is an example of a description of the partitioning of a mass of a chemical in a system consisting of four generic compartments (Eq. 38), respecting the mass balance, when equilibrium has been reached, according to the two different modes, partition coefficient (Eq. 39) and fugacity (Eq. 40) respectively (Mackay 2001).

$$M = m_1 + m_2 + m_3 + m_4 \quad \text{(Eq. 38)}$$

$$= C_1V_1 + C_2V_2 + C_3V_3 + C_4V_4 \quad \text{(Eq. 39)}$$

$$= Z_1f\,V_1 + Z_2f\,V_2 + Z_3f\,V_3 + Z_4f\,V_4$$

$$= f\,(Z_1V_1 + Z_2V_2 + Z_3V_3 + Z_4V_4) \quad \text{(Eq. 40)}$$

where $M(mol)$ is the mass of chemical present in a system, $m_i(mol)$ is the mass present in the i-th compartment, $C_i(mol)$ is the concentration in the i-th compartment, $f(Pa)$ is the fugacity of the compartments, equal for all since at equilibrium, $Z_i(mol\ m^{-3}Pa^{-1})$ is the capacity fugacity of the i-th compartment and $V_i(m^3)$ is the volume of the i-th compartment. The advantage of using fugacity is that, at equilibrium for a system, fugacity is unique for all compartments and only one equation is needed to find the final unknowns, i.e. the masses in each compartment, since Z_i and V_i are known and constant.

3.1.1 Levels for box model pollutant dispersion

In order to describe partitioning, it is necessary to describe all the processes that lead to the redistribution of mass. The description of partitioning is presented on four levels, of increasing complexity with the degree of approximation of the described system to reality.

Naturally, the description of the processes also depends heavily on the partitions considered in the system, and a detailed description of these will be provided in the following sub-chapters.

The *first level* proposed considers a *closed system, at equilibrium and non-reacting*, i.e., there is a mass $\boldsymbol{M}$ of pollutant in the system, distributed among the different compartments that are at equilibrium with each other according to diffusive processes, i.e. of mutual mass exchange, where the chemical is conserved since there are no exits from the system and there is no degradation. This is the case described with Eq. 38.

The *second level* considers an *open system, at equilibrium and reacting*, where there is a continuous and constant input of substance into the system over time (steady-state conditions), distributed between the different compartments that are at equilibrium with each other, where there are outputs and there is degradation.

These processes are accompanied by a specific velocity of the compartment and substance, generally defined as *rate* $\boldsymbol{k}$ with first-order kinetics and having the inverse of time (e.g. h^{-1}) as unit. Under steady-state conditions, the principle of

equality between inputs and outputs from the system (input = output) and the general linear equation are applied to describe the mass balance of a generic system (Eq. 41):

$$E_{input} = \sum F_{degi} + \sum F_{outi} \quad \text{(Eq. 41)}$$

where E_{input} $(mol\ h^{-1})$ is the continuous and constant emission over time in the system, $\sum F_{degi}$ $(mol\ h^{-1})$ is the summation of mass flows by degradation in the i-th compartment and $\sum F_{outi}$ $(mol\ h^{-1})$ is the summation of mass flows that exit from the i-th compartment. The fluxes of the different processes can be expressed as a function of fugacity, as mentioned above, or with concentration.

Using the fugacity approach, the system being in equilibrium, it is, therefore, necessary to write a single equation for the mass balance, which describes the entire system, since the fugacity is the same.

In the *third level*, diffusive flow resistances are considered, due to the different physical and chemical nature of the compartments. The presence of such resistances located at the interface of the compartments result in unequal diffusive flows in the two directions, generating imbalances in the fugacities, and, thus, the loss of equilibrium. The concentrations between the compartments are therefore no longer in a constant ratio, and the partition coefficients can no longer be used alone to describe these exchanges.

To calculate the masses present in each compartment, it is therefore necessary to calculate the different fugacities, each representative of a compartment, the number of which will determine the number of equations to be written.

The general equation describing this type of model for an i-th compartment is (Eq. 42):

$$E_i + \sum F_{j-i} = \sum F_{i-j} - F_{outi} - F_{degi} \quad \text{(Eq. 42)}$$

where E_i $(mol\ h^{-1})$ is the continuous and constant emission over time in the i-th compartment, $\sum F_{j-i}$ $\left(mol\ h^{-1}\right)$ and $\sum F_{i-j}$ $\left(mol\ h^{-1}\right)$ are, respectively, the summations of flows from the j-th to i-th compartments and viceversa, $F_{degi}(mol\ h^{-1})$ is the mass flux that degradates in the i-th compartment and $F_{outi}(mol\ h^{-1})$ is the mass flux that exits from the i-th compartment. The fluxes of the different processes can be expressed as a function of fugacity, as mentioned above, or with concentration.

For all three levels mentioned above, an assumption is made of compartments as well-mixed boxes, or continous stirred tank reactors (CSTR), where the concentration achieved under stationary conditions becomes instantaneously homogeneous and equal at every point in the compartment.

In the *fourth level*, the assumption of stationarity is abandoned in order to achieve a more realistic representation of environmental dispersion: it is unlikely that an emission will always be equal and constant over time, even for production systems with continuous steady-state production, although it may be an acceptable approximation that does not entail too great an error.

Not only that, phenomena that are typically non-stationary, i.e. that vary over time, are those that precede the attainment of stationarity, such as the beginning of emission, or that describe the final behaviour of a pollutant, when emission ceases to exist. In this case, the equation to be written is differential with respect to time. The lack of stationarity implies that the balance between what goes in and what comes out is no longer respected, but rather a variation of the mass distributed in the compartment over time is determined.

In addition, non-stationary phenomena, in which there is a discontinuity of concentration in time, are also accompanied in reality by a variation of concentration in space: three variables are obtained, fugacity (and thus concentration), time and space.

The general equation describing this type of model for an i-th compartment is Eq. 43:

$$\frac{dM_i(t)}{dt} = E_i(t) + \sum F_{j-i}(t) - \sum F_{i-j}(t) - F_{outi}(t) - F_{degi}(t) \qquad \text{(Eq. 43)}$$

where $\frac{dM_i(t)}{dt}$ (mol) represents the mass variation in time in the i-th compartment, $E_i(t)\left(mol\ h^{-1}\right)$ is the emission changing with time in the i-th compartment, $\sum F_{j-i}(t)\left(mol\ h^{-1}\right)$ and $\sum F_{i-j}(t)\left(mol\ h^{-1}\right)$ are the sum of fluxes from j-th to i-th compartments and viceversa, $F_{degi}(t)\left(mol\ h^{-1}\right)$ is the mass flux that degradates in the i-th compartment and $F_{outi}(t)\left(mol\ h^{-1}\right)$ is the mass flux that exits in the i-th compartment. The fluxes of the different processes can be expressed as a function of fugacity, as mentioned above, or with concentration.

The *third level* is the one commonly used to represent the dynamics of pollutants in LCA calculation methods, as it allows the system of equations to be solved with reduced mathematical complexity, although it is not suitable for representing transient or extraordinary phenomena. The assumption of stationarity, i.e. of a continuous and constant emission over time, which is intended to represent the "steady state" conditions of a plant's operation, is consistent with the choice of adopting chronic toxicity data in the evaluation of effects.

For the above reasons, the third level, relating to an open, non-equilibrium, reacting and stationary system, is also adopted in the present work.

3.1.2 Environmental processes

There are three main categories of processes: advective, diffusive and degradative. Each process results in a mass flow $F\ (mol\ h^{-1})$, expressed with Eq. 44:

$$F = f \times D \qquad \text{(Eq. 44)}$$

As mentioned above, the coefficient $D\ (mol\ h^{-1}\ Pa^{-1})$ is specific to each process and expresses the speed at which a given process occurs, and $f\ (Pa)$ is the fugacity of the compartment.

This equation can also be used for the diffusive process, although it is different from Eq. 44 presented above.

As reported, diffusive flow occurs under a driving force, in this case the difference in fugacity between two communicating compartments. However, as reported in Whitman (1923), in which the author stipulated the *double-film theory* to demonstrate the existence of two resistances placed at the diffusive exchange interface between two compartments, and which will be discussed in more detail in sub-chapter 3.1.2, it is possible to approximate the diffusive flux as depending solely on the fugacity of the emitting compartment, since the fugacity of the receiving compartment is negligible by comparison.

If fugacities are the unknowns of the system following an emission, an analysis of D rates is reported below. Since the concept of fugacity is not commonly used, it is useful to derive D values from the concentration approach.

About the *advective processes*, these are mainly due to a moving medium in which the pollutant is dispersed. They are of a different nature and connect different compartments, the main ones are:

- Advection due to wind velocity in air or water current;
- Wet and dry deposition from air to water and soil, mainly;
- Runoff from the soil to the water;
- Irrigation from water to soil;
- Uptake by vegetation with roots from the soil.

For these, therefore, a flow rate of the medium can be defined as $G\ (m^3h^{-1})$ or, more generally, as the product of a velocity $v\ (m\ h^{-1})$ for the area transverse to the direction of motion $A\ (m^2)$ (Eq. 45):

$$G = v \times A \qquad \text{(Eq. 45)}$$

Every advective mass flux $F\ (mol\ h^{-1})$, expressed with concentration $C\ (mol\ m^{-3})$, is written as (Eq. 46):

$$F = C \times G \qquad \text{(Eq. 46)}$$

Based on the relationship expressed in Eq. 37, it is possible to rewrite the flux in terms of fugacity as follows (Eq. 47):

$$F\ (mol\ h^{-1}) = f\ (Pa) \times Z\ (mol\ m^{-3}Pa^{-1}) \times G\ (m^3h^{-1}) \qquad \text{(Eq. 47)}$$

The value of D for an advection process is, therefore, set equal to (Eq. 48):

$$D_{adv}\ (mol\ h^{-1}Pa^{-1}) = Z\ (mol\ m^{-3}Pa^{-1}) \times G\ (m^3h^{-1}) = Z\ (mol\ m^{-3}Pa^{-1}) \times v\ (m\ h^{-1}) \times A\ (m^2) \qquad \text{(Eq. 48)}$$

The advective D rates depend to a large extent on the medium, especially the contribution made by the flow rate, while the Z value depends on the compartment and the substance, as explained below in the sub-chapters on compartments.

Degradative processes that follow first-order kinetics are characterised by rates k (h^{-1}) specific of the substance in a given medium. The k -rates are obtained from an experimental datum, i.e. the half-life of the substance in a given medium, $\tau_{1/2}$ (h), i.e. the time it takes to achieve a halving of the concentration, according to Eq. 49 below:

$$k\ (h^{-1}) = \frac{0.693}{\tau_{1/2}\ (h)} \qquad \text{(Eq. 49)}$$

This equality is obtained from the equation describing the reduction in concentration over time (Eq. 50):

$$\frac{dC}{dt} = -C \times k \qquad \text{(Eq. 50)}$$

Solving for separation of variables gives (Eq. 51):

$$\frac{dC}{C} = -k\ dt \qquad \text{(Eq. 51)}$$

Solving by integral with the initial condition C_0 with t = 0 (Eq. 52):

$$\ln\left(\frac{C}{C_0}\right) = -k \times t \qquad \text{(Eq. 52)}$$

By definition, when $t = \tau_{1/2}$, $C = 0.5\ C_0$. Then (Eq. 53):

$$\ln(0.5) = -0.693 = -k \times \tau_{1/2} \qquad \text{(Eq. 53)}$$

The degradative flux is given by the equation expressed with the concentration (Eq. 54):

$$F\ (mol\ h^{-1}) = V\ (m^3) \times C\ (mol\ m^{-3}) \times k\ (h^{-1}) = V\ (m^3) \times f\ (Pa) \times Z\ (mol\ m^{-3} Pa^{-1}) \times k\ (h^{-1}) \qquad \text{(Eq. 54)}$$

The value of D for a degradation process is, therefore, set equal to (Eq. 55):

$$D_{deg}(mol\ h^{-1} Pa^{-1}) = V\ (m^3) \times Z\ (mol\ m^{-3} Pa^{-1}) \times k\ (h^{-1}) \qquad \text{(Eq. 55)}$$

Diffusive processes require more in-depth treatment, due to the more complex dynamics described in the double-film theory (Whitman 1923). As already mentioned, diffusive mass flow can be compared to the flow of heat between two rooms separated by a wall, where the flow must overcome three resistances placed in series: that of the air in the room with the higher temperature, that of the wall and that of the room with the lower temperature.

Similarly, in mass flow, e.g. in volatilisation from water to air where the driving force is the difference in concentration or fugacity, there are three resistances, relating to as many phases that are encountered in succession during motion: a first resistance on the water side, from the bulk of the water phase to a layer, called the *boundary layer*, of a thickness ***Y*** straddling the interface, usually few mm, which, in turn, opposes its own resistance and, finally, the resistance on the air side, from the boundary layer to the bulk of the phase.

In bulk phases, the concentration profiles are linear, due to the assumption of concentration homogeneity, there will therefore be a bulk C_A and a bulk C_W. In the boundary layer, the concentration decreases on the water side and increases on the air side with an exponential trend, although it never coincides at the interface. Therefore, two further concentrations are determined, C_{AI} and C_{WI}.

Regarding the type of motion, in the bulk phase the diffusive motion is turbulent, with more rapid and chaotic currents, while in the boundary layer the motion is slower and more linear. In the latter phase, the resistance is completely negligible compared to the other two, due to the easier conditions for motion. Therefore, *partial mass transfer coefficients* can be defined for the two bulk phases $\boldsymbol{k_a}$ and $\boldsymbol{k_w}$ with velocity unit of measure (m h^{-1}) that govern the motion, while within the boundary layer one can assume that there is equilibrium and the relationship between the concentrations C_{AI} and C_{WI} in the two main phases at the interface is described by the partition coefficient K_{AW} (Eq. 56).

$$K_{AW} = \frac{C_{AI}\,(mol\,m^{-3})}{C_{WI}\,(mol\,m^{-3})} \qquad \text{(Eq. 56)}$$

Under these conditions, the fugacity at the interface is the same for both phases, which greatly facilitates the writing of the diffusive motion equation.

In general, the partial mass transfer coefficient k_x of an x phase can be calculated from the between *diffusivity* $\boldsymbol{B_x}$ *(*m^2 h^{-1}*)*, or *diffusion coefficient*, chemical specific, and the thickness of the boundary layer *Y* (Eq. 57*):*

$$k_x = \frac{B_x}{Y} \qquad \text{(Eq. 57)}$$

Diffusivities $\boldsymbol{B_a}$ and $\boldsymbol{B_w}$, air and water respectively, can be derived from two semi-experimental USEtox equations (Fantke et al. 2017) that take into account the molecular weight of the substance and the two media (Eq. 58 and Eq. 59):

$$B_a = 0.000000002 \times \sqrt[2]{\frac{32}{MW}} \qquad \text{(Eq. 58)}$$

$$B_w = 0.0000257 \times \sqrt[2]{\frac{18}{MW}} \qquad \text{(Eq. 59)}$$

where 32 g mol^{-1} and 18 g mol^{-1} are, namely, air and water molecular weight, MW ($g\ mol^{-1}$) is the chemical molecular weight.

As an alternative to Eq. 57, there are two semi-experimental USEtox equations (Fantke et al. 2017) that allow the calculation of the partial mass transfer coefficient of air and water $\boldsymbol{k_a}$ and $\boldsymbol{k_w}$ (m h^{-1}) based on wind speed and phase molecular weights (Eq. 60 and Eq. 61):

$$k_a = 0.01 \times (0.0004 + 0.0004 \times 3^2) \times \left(\frac{0.032}{v_{air}}\right)^{0.5 \times 0.5} \times 3600 \quad \text{(Eq. 60)}$$

$$k_w = 0.01 \times (0.3 + 0.2 \times 3^2) \times \left(\frac{0.018}{v_{air}}\right)^{0.67 \times 0.5} \times 3600 \quad \text{(Eq. 61)}$$

Starting from the concentration approach, for ease of communication, the diffusive equation of motion is composed of two flows in series, according to the concentration gradient, the first relating to the crossing of the water bulk phase chemical to the interface, the second relating to the movement from the interface to the air bulk phase (Eq. 62):

$$F_{diffWA} = k_w A\,(C_W - C_{WI}) = k_a A\,(C_{AI} - C_A) \quad \text{(Eq. 62)}$$

where F_{diffWA} $(mol\ h^{-1})$ is the diffusive flux from water to air, k_w $(m\ h^{-1})$ is the mass transfer coefficient water side, A (m^2) is the contact surface between air and water, C_W $(mol\ m^{-3})$ is the bulk water concentration, C_{WI} $(mol\ m^{-3})$ is the interface concentration water side, k_a $(m\ h^{-1})$ is the mass transfer coefficient air side, C_{AI} $(mol\ m^{-3})$ is the interface concentration air side, C_A $(mol\ m^{-3})$ is the bulk air concentration.

The product of the mass transfer coefficient and the contact surface between air and water gives a flow rate ($m^3\ h^{-1}$).

Expressing the equation using the fugacity approach and exploiting the equilibrium at the interface, the two flows in series can be rewritten as (Eq. 63):

$$F_{diffWA} = k_w A\,Z_W(f_W - f_I) = k_a A\,Z_A(f_I - f_A) \quad \text{(Eq. 63)}$$

where F_{diffWA} $(mol\ h^{-1})$ is the diffusive flux from water to air, k_w $(m\ h^{-1})$ is the mass transfer coefficient water side, A (m^2) is the contact surface between air and water, Z_W $(mol\ m^{-3}\ Pa^{-1})$ is the water capacity fugacity, f_W (Pa) is the water fugacity, f_I (Pa) is the interface fugacity, k_a $(m\ h^{-1})$ is the mass transfer coefficient air side, f_A (Pa) is the air fugacity.

The factors can be combined within the partial diffusive exchange D rate, as follows (Eq. 64 and Eq. 65):

$$D_{diffW} = k_w A\,Z_W \quad \text{(Eq. 64)}$$

$$D_{diffA} = k_a A\,Z_A \quad \text{(Eq. 65)}$$

where D_{diffW} $(mol\ h^{-1}Pa^{-1})$ is the diffusive rate from water and D_{diffA} $(mol\ h^{-1}Pa^{-1})$ is the diffusive rate from air.

The flux is, then (Eq. 66):

$$F_{diffWA} = D_{diffW}(f_W - f_I) = D_{diffA}(f_I - f_A) \quad \text{(Eq. 66)}$$

Simplifying member by member f_I and combining the two partial rates D into a single rate D (Eq. 67):

$$F_{diffWA} = D_{diffAW}(f_W - f_A) \quad \text{(Eq. 67)}$$

where D_{diffAW} $(mol\ h^{-1}Pa^{-1})$ is the total diffusion air-water rate. In this case, the rate D can be compared to thermal conductivity and is therefore equal to the inverse of resistance. For resistors in series, additivity provides a single value of resistance to motion (Eq. 68 and Eq. 69):

$$R_{diffAW} = R_{diffW} + R_{diffA} \quad \text{(Eq. 68)}$$

$$\frac{1}{D_{diffAW}} = \frac{1}{D_{diffW}} + \frac{1}{D_{diffA}} \quad \text{(Eq. 69)}$$

As mentioned above, it is possible to approximate the diffusive flux as depending solely on the fugacity of the emitting compartment, since the fugacity of the receiving compartment is negligible by comparison (Whitman 1923). Therefore, the volatilisation diffusive flux from water to air can be written as (Eq. 70):

$$F_{diffWA} = D_{diffAW}\, f_W \quad \text{(Eq. 70)}$$

Similarly, the diffusive absorption flux from air to water will be (Eq. 71):

$$F_{diffAW} = D_{diffAW}\, f_A \quad \text{(Eq. 71)}$$

The coefficient D_{diffAW} is used for flows in both directions as it combines the sum of the two series resistances, which are equal for both processes.

3.2 The local model

The considered i_{th}-compartments in the world unit were 7, 3 of them are both emitting and receiving (E/R) and the others are receiving only (R):

- Air (A) (E/R);
- Water (W) (E/R);
- Soil (S) (E/R);
- Groundwater (GW) (R);
- Sediments (SED) (R);
- Fish (FISH) (R);
- Terrestrial vegetation (VEG) (R).

The layout of the local world unit, sizing 1000 m x 1000 m x 250 m, is represented below (Figure 10), where also dimensions and main landscape parameters are reported.

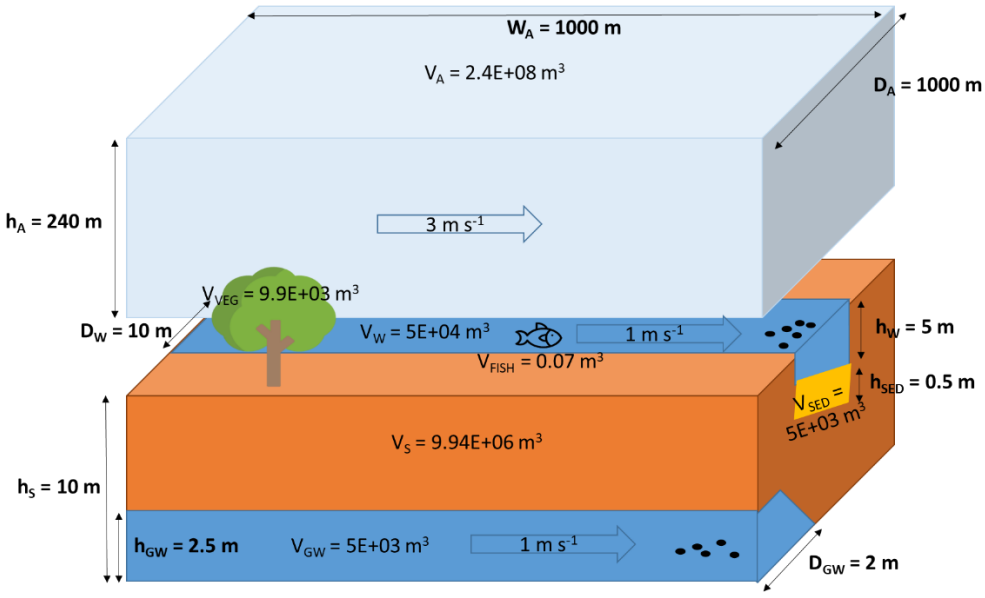

Figure 10 Local world unit

There are some landscape constraints to be respected:

- the area of air overlies all compartments, i.e. it is the compartment with the greatest extension;
- the area considered in the diffusive and advective exchanges of soil with air is equal to the area of air minus the area of surface water;
- the area taken into account in the diffusive and advective exchanges of surface water with air is equal to the area of surface water;
- the volume of the surface water is given by subtracting the size of the surface water from the volume occupied by the fish;
- the volume of fish was estimated by varying the figure suggested by Mackay (7 m^3 of fish per 10^6 m^3 of surface water) with the volume of surface water of the world unit considered;
- the volume of soil was given by subtracting the volume of the block below the air from the volume of groundwater, surface water and sediment;
- the volume of vegetation was estimated by varying the figure suggested by Mackay (2001) (3000 m^3 of terrestrial biota per 1000 m x 300 m of surface soil) with the soil surface area of the world unit considered;
- the particles present in surface and groundwater are a fraction of the respective compartments equal to 2.5E-05 (Mackay 2001).

The other data considered to sketch the world unit refer to the Po Valley (Emilia-Romagna region, Italy), in particular:

- a local wind speed of 3 m s^{-1} (Arpae Emilia-Romagna 2022). This parameter is used to calculate the advective flow rate;
- a surface water velocity of 1 m s^{-1} (Agenzia Interregionale per il fiume Po (AIPo) 2011). The same velocity was also assumed for groundwater, since site-specific data were not found. This parameter is used to calculate the advective flow rate.

In general, compartments can consist of one or more phases in equilibrium with each other, i.e. the fugacity is unique for each compartment. In fact, the compartments are considered to be well mixed internally and homogeneous (continuously stirred tank reactor - CSTR), therefore, the outlet concentration - by adduction, reaction, diffusion - will be the same as that present in the compartment.

For compartments characterised by the presence of more than one phase, it may be useful to define a bulk capacity value Z of bulk composed of other phases in equilibrium with each other, according to a weighted average with respect to the volume of each phase (Eq. 72):

$$Z_{ibulk} = v_{x,i}Z_x + v_{y,i}Z_y \quad \text{(Eq. 72)}$$

where Z_{ibulk} $(mol\ m^{-3}Pa^{-1})$ is the i-th compartment fugacity capacity, $v_{x,i}$ and $v_{y,i}$ are the volume fraction of phases x and y of the total volume of the i-th compartment, Z_x $(mol\ m^{-3}Pa^{-1})$ and Z_y $(mol\ m^{-3}Pa^{-1})$ are the fugacity capacity of phases x and y of the i-th compartment.

Multiplying the fugacity of the i-th compartment with Z_{ibulk} total compartment concentration will be obtained, while multiplying the fugacity with Z_x and Z_y single phase concentration will be obtained. However, these cannot be directly summed to obtain the bulk concentration. To do so, it is first necessary to refer them all to the same value represented by the total volume contained in the volume fractions v.

Since phase equilibrium exists, the partition of the chemical can be described by the partition coefficients K. These express the ratios between the concentrations of the phases in pairs, and in doing so, the entire compartment may be lost sight of when it consists of more than two phases.

Therefore, partition coefficients between an entire compartment and a specific reference phase are defined z, for example, in order to relate the concentration of a phase to that of the entire compartment. The latter is expressed as the sum of the products of the volume fraction of a phase and the partition coefficient between the phase x and the reference z (Eq. 73). Obviously, the volume fraction of the reference phase is multiplied by 1 ($K_{zz} = C_z/C_z = 1$).

$$K_{z,itot} = v_{x,i} \times K_{xz} + v_{z,i} + v_{y,i} \times K_{yz} \quad \text{(Eq. 73)}$$

Therefore, the calculation of the Z of the phases of a composite compartment could also be expressed using partition coefficients (Eq. 74):

$$Z_z = K_{iz} \times Z_{ibulk} \quad \text{(Eq. 74)}$$

This specification could be useful, as mentioned above, when calculating the phase concentration of a composite compartment.

For the complete description of all processes, attention must be paid to the role of organic matter, especially organic carbon. In a solid phase, the adsorption and accumulation of an organic chemical occurs by organic carbon and lipid content. In general, this capacity is described by a comparison with the adsorptive power of octanol, denoted by the letter $\boldsymbol{O}$, since it has a carbon-oxygen ratio similar to that of lipids.

The quantity most commonly used to describe the behaviour of a substance is the octanol-water partition coefficient $\boldsymbol{K_{OW}}$. Being equal to the ratio of the substance's concentrations in octanol and water, it expresses the substance's preference to partition into organic matter over water, thus giving information about its hydrophobicity.

From this property, all other phase-specific properties were derived, i.e. both partition coefficients between phases, adjusting them with factors that take into account the fraction of organic carbon y present in each phase, and fugacity capacities for each phase, according to Table 1. The genesis of the reported quantities is discussed in the following sections on the description of the compartments.

It is also preparatory to the definition of the fugacity capacity for the gas phase Z_A, which does not depend on the substance, but only on the system, according to Eq. 75. Starting with the Z_A it is possible to obtain Z_w (Eq. 76 Table 1), correlating it with a property commonly studied for organic substances, namely the air-water partition coefficient K_{AW}, according to Eq. 74 above.

Table 1 Main fugacity capacities Z and partition coefficients K used in the local model with fugacity approach

Name	Formula	Note	N° eq.
Fugacity capacity of gas phase	$Z_A\ (mol\ m^3 Pa^{-1}) = \frac{1}{R \times T}$	$R = 8.314\ Pa\ m^3 mol^{-1} K^{-1}$ perfect gases constant, T (K) temperature	Eq. 75
Fugacity capacity of water phase	$Z_w\ (mol\ m^3 Pa^{-1}) = Z_A \times K_{AW}$		Eq. 76
Octanol water partition coefficient	$K_{OA} = \frac{K_{OW}}{K_{AW}}$		Eq. 77
Aerosol air partition coefficient	$K_{QA} = y_{OM} \times K_{OA} \times \frac{\rho_Q}{1000}$	$y_{OM} = 3.6E-02$, mass fraction of organic matter in aerosols $\rho_Q = 1500\ kg\ m^{-3}$, aerosol density	Eq. 78
Organic carbon water partition coefficient	$K_{OC}\ (L\ kg^{-1}) = 0.41 \times K_{OW}$	0.41 L kg^{-1} experimental constant	Eq. 79
Soil organic carbon water partition coefficient	$K_{SW} = y_{OCsoil} \times K_{OC} \times \frac{\rho_{solid}}{1000}$	y_{OCsoil} = 0.02 mass fraction of organic carbon in soil $\rho_{solid} = 1500\ kg\ m^{-3}$, solid density of suspended solids and sediments	Eq. 80
Sediment/suspended solids organic carbon water partition coefficient	$K_{PW} = y_{OCsusp/sed} \times K_{OC} \times \frac{\rho_{solid}}{1000}$	$y_{OCsusp/sed}$ = 0.04 mass fraction of organic carbon in suspended solids and sediment $\rho_{solid} = 1500\ kg\ m^{-3}$, solid density of suspended solids and sediments	Eq. 81
Vegetation air partition coefficient	$K_{VEGA} = y_{OCVEG} \times K_{OA}$	$y_{OCVEG} = 0.01$ mass fraction of organic carbon in vegetation	Eq. 82
Fish water partition coefficient	$K_{FW} = 0.048 \times K_{OW}$	0.048 fish lipid content	Eq. 83
Fugacity capacity of aerosols	$Z_Q\ (mol\ m^3 Pa^{-1}) = Z_A \times K_{QA}$		Eq. 84
Fugacity capacity of soil solid (organic carbon)	$Z_S\ (mol\ m^3 Pa^{-1}) = Z_W \times K_{SW}$		Eq. 85
Fugacity capacity of water suspended solids	$Z_P\ (mol\ m^3 Pa^{-1}) = Z_W \times K_{PW}$		Eq. 86
Fugacity capacity of fish	$Z_F\ (mol\ m^3 Pa^{-1}) = Z_W \times K_{FW}$		Eq. 87
Fugacity capacity of vegetation	$Z_{VEG}\ (mol\ m^3 Pa^{-1}) = Z_A \times K_{VEGA}$		Eq. 88

Air

Air is the compartment that dominates the entire world unit in the modelling and is in contact with all compartments except fish, groundwater and sediment. Within it there is a gaseous phase, generically indicated in this work by the letter A, a dispersed solid phase consisting of aerosols, indicated by the letter Q according to a certain volume fraction, defined by Mackay ("World unit data" sheet of the Excel tool), and an aqueous phase, indicated by the letter W.

Aerosols, due to the presence of organic matter believed to be responsible for the adsorption of chemicals in solid phases, can transport chemical according to the phenomena that characterise them.

In general, degradation, diffusion and advection reactions can take place in air, which includes deposition.

The latter involves the processes of dry deposition of aerosol, wet deposition of chemical washed out of the gas phase by rain, and wet deposition of aerosol transported by rain. All processes will be characterised by a Z value that depends on the phase responsible for the process: Z_Q for wet and dry aerosol deposition and Z_W for wet deposition. Furthermore, these processes are defined by certain velocity values, defined by Mackay and listed in the summary table of model parameters ("World unit data" sheet of the Excel tool).

Dispersed solid phases that absorb the chemical, by virtue of their organic carbon content, are represented by partition coefficients expressing the ratio between the volume of the phase containing them (L), e.g. gas phase and dissolved water phase, and the mass of the absorbing solid phase (kg).

Therefore, as far as aerosol deposition phenomena are concerned, the volume fraction of aerosols in air $v_{q,A}$ must also be considered in the D-rate, because of the air-aerosol partition coefficient unit K_{QA} which, in a first version of the formula, is calculated from the K_P (L kg^{-1}), aerosols being a dispersed solid phase. This partition coefficient, in fact, needs to be multiplied by the concentration of the dispersed phase in the compartment X_Q (kg L^{-1}) (Eq. 89):

$$X_Q = \rho_Q \times v_{q,A} \qquad \text{(Eq. 89)}$$

where $X_Q\left(kg_Q\, L_A^{-1}\right)$ is the mass of aerosol per volume of air, $\rho_Q\left(kg_Q\, L_Q^{-1}\right)$ is the aerosol density, $v_{q,A}\left(L_Q\, L_A^{-1}\right)$ volume fraction of aerosols in air.

Density is included in the calculation of the $K_{QA,}$ while the volume fraction is expressed in the deposition rate D.

Mackay demonstrates the analogy with using K_{OA} instead of K_P and in subsequent formulae, the second version is always proposed, however, the use of the volume fraction remains.

The wet deposition of aerosols is also described with regard to the volume of air that is washed away by aerosols from the rain unit volume and represented by the dimensionless coefficient Q.
In addition, there is the exit advection from the air according to a flow rate determined by the wind ("World unit data" sheet of the Excel tool), which is referred to the volume fraction of the gas phase only $v_{g,A}$, which is included in the present work in view of the subsequent translation of D rates into rates k for the inclusion of the local scale in USEtox, as discussed in chapter 5.1 and Appendix - A.4.

About degradation, again as air is composed of several phases, the actual degradation value should take into account not only the degradation in the gas phase, but also aerosols. In the present study, only the degradation occurring in the gas phase is roughly taken into account, as it is the dominant phase in volume fraction. The volume fraction of the gas phase $v_{g,A}$ is, thus, included in the present work in view of the subsequent translation of D rates into rates k for the inclusion of the local scale in USEtox, as discussed in chapter 5.1 and Appendix - A.4.

Similarly, diffusion from the air to the other compartments is only supposed to occur from the gas phase.

Freshwater

Water is the compartment that in modelling is represented by a river flowing through the middle of the soil and is in contact with all compartments except vegetation and groundwater. Within it, there is a liquid dissolved phase, as the water dissolved phase and referred to by the letter W, and a dispersed phase consisting of the suspended solids according to a certain volume fraction, defined by Mackay ("World unit data" sheet of the Excel tool), and referred to as $SUSP$.

Suspended solids, due to the presence of organic matter containing organic carbon, can adsorb the chemical and transport it into their phenomena.

Dispersed solid phases that adsorb the chemical, by virtue of their organic carbon content, are represented through partition coefficients expressing the ratio between the volume of the phase containing them (L), e.g. gas phase and dissolved water phase, and the mass of the adsorbing solid phase (kg).

Therefore, with regard to the deposition phenomena of suspended solids on sediments, the volume fraction of these $v_{susp,W}$ in the water must also be considered in the D-rate, due to the unit of measurement of the water-suspended solids partition coefficient K_{PW} which is calculated from the K_P (L kg^{-1}) (Eq. 81 of Table 1), suspended solids being a dispersed solid phase. this partition coefficient, in fact, needs to be multiplied by the concentration of the dispersed phase in the compartment X_{SUSP} (kg L^{-1}) (Eq. 90):

$$X_{SUSP} = \rho_{SUSP} \times v_{susp,W} \qquad \text{(Eq. 90)}$$

where $X_{SUSP}(kg_{SUSP}\ L_W^{-1})$ is the mass of suspended solids per volume of water, $\rho_{SUSP}(kg_{SUSP}\ L_{SUSP}^{-1})$ is the density of suspended solids, $v_{susp,W}$ $(L_{SUSP}\ L_W^{-1})$ is the volume fraction of suspended solids on water.

Density is included in the calculation of the $K_{PW,}$ while the volume fraction is not made explicit in the deposition rate D, since it is already included in the deposition rate U_D, as shown by Mackay.

In general, degradation, diffusion and advection reactions can take place in water.

There is advection exiting water according to a flow rate ("World unit data" sheet of the Excel tool), which also carries suspended solids with it, each phase represented by its own Z value in relation to its flow rate.

About degradation, again as water consists of several phases, the actual degradation value should take into account not only the degradation in the dissolved phase, but also the suspended solids. In the present study, the degradation occurring only in the dissolved phase is roughly taken into account, as it represents the main phase. Similarly, diffusion (i.e. volatilisation) from water to air is assumed to occur only from the dissolved phase of water, so the Z_W is, thus, included in the present work in view of the subsequent translation of D rates into rates k for the inclusion of the local scale in USEtox, as discussed in chapter 5.1 and Appendix - A.4.

Soil

Soil is in contact with all compartments except fish and sediment. Within it there are 3 phases: air (20%), water (30%), solid phase (50%). The latter contains organic matter and, therefore, organic carbon, which is mainly responsible for the

adsorption of chemical, according to a certain volume fraction, defined by Mackay ("World unit data" sheet of the Excel tool).

In general, degradation, diffusion and advection reactions can take place in the soil.

Advection from the soil is represented by runoff due to rainfall, which also brings with it solid particles, each phase represented by its own Z value (respectively, Z_W and Z_P) in relation to its flow rate, where the speed of the process is defined by Mackay ("World unit data" sheet of the Excel tool), and leaching, always due to rain, to groundwater, therefore, the Z_W will be used to describe this process. Since the soil is a rather static compartment, other advective phenomena are not considered.

About degradation, again as soil is composed of several phases, the actual degradation value should take into account not only the degradation in the solid phase, but also water and air. In the present study, degradation occurring only in the solid phase is roughly taken into account, referring in particular to organic carbon, therefore, the Z_{OC} is, thus, included in the present work in view of the subsequent translation of D rates into rates k for the inclusion of the local scale in USEtox, as discussed in chapter 5.1 and Appendix - A.4.

The diffusion from the soil to the air deserves further investigation, as it occurs from all the phases in it, all being in direct contact with the air (Figure 11).

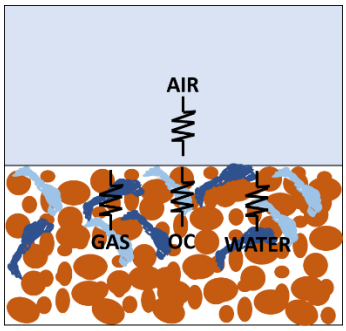

Figure 11 Diffusive resistances in air-soil diffusion

Therefore, the diffusion rate D air-soil and valid for both absorption and volatilisation will be given by the sum of the air-soil series resistances, in which there are three resistances in parallel (Eq. 91):

$$\frac{1}{D_{diffAS}} = \frac{1}{D_{diffE}} + \frac{1}{(D_{diffA} + D_{diffW} + D_{diffOC})} \qquad \text{(Eq. 91)}$$

where D_{diffAS} $(mol\ m^{-3}Pa^{-1})$ is the air-soil diffusion rate, D_{diffE} $(mol\ m^{-3}Pa^{-1})$ is the partial diffusion rate air side, D_{diffA} $(mol\ m^{-3}Pa^{-1})$ is the partial diffusion rate of air phase soil side, D_{diffW} $(mol\ m^{-3}Pa^{-1})$ is the partial diffusion rate of water phase soil side, D_{diffOC} $(mol\ m^{-3}Pa^{-1})$ is the partial diffusion rate of organic carbon phase soil side. It should be pointed out that the Mackay model does not envisage that diffusion can also occur by soil organic carbon, its introduction was made for the present study as it is assumed that the solid part of the soil, being generally porous, although of course porosity depends on the type of soil, could contribute to this phenomenon. This assumption is also confirmed in the model adopted by USEtox regarding air-soil diffusion.

The partial diffusion rates for soil are derived from the partial diffusivities, reduced according to the volume fractions occupied by each of the phases (Eq. 92, Eq. 93 and Eq. 94):

$$B_{AS} = \frac{B_A \times v_{g,S}^{\frac{10}{3}}}{\left(v_{g,S}+v_{w,S}+v_{oc,S}\right)^2} \quad \text{(Eq. 92)}$$

$$B_{WS} = \frac{B_W \times v_{w,W}^{\frac{10}{3}}}{\left(v_{g,S}+v_{w,S}+v_{oc,S}\right)^2} \quad \text{(Eq. 93)}$$

$$B_{OCS} = \frac{B_{OC} \times v_{oc,S}^{\frac{10}{3}}}{\left(v_{g,S}+v_{w,S}+v_{oc,S}\right)^2} \quad \text{(Eq. 94)}$$

where B_{AS} (m^2h^{-1}), B_{WS} (m^2h^{-1}), B_{OCS} (m^2h^{-1}) are, namely, the diffusivities of the air, water and soil organic carbon phases, B_A (m^2h^{-1}), B_W (m^2h^{-1}), B_{OC} (m^2h^{-1}) the diffusivities of the air, water and soil organic carbon, $v_{g,S}$, $v_{w,S}$, $v_{oc,S}$ are, namely, the volume fractions of the air, water and soil organic carbon phases of soil.

Each partial diffusion rate will be relative to the phase involved and the Z value will be determined accordingly, analogous to air-water diffusion.

Air also exerts wet and dry deposition processes on the soil in the same way as described above.

Sediments

Sediment is only in contact with surface water. Within it, there is a solid phase, which partly contains organic carbon, according to a certain volume fraction, defined by Mackay ("World unit data" sheet of the Excel tool).

In general, degradation, diffusion and advection reactions can take place in sediments.

Advection in sediments is represented by the resuspension of solids towards water and burial, i.e. the burial of solids towards the lower layers, processes accompanied by the Z_{SUSP} where the speed of the process is defined by Mackay ("World unit data" sheet of the Excel tool). As sediment is a rather static compartment, other advective phenomena are not considered.

The sediment is assumed within the present study not to be characterised by the presence of biota, which could be affected by toxic effects due to the concentration in it. However, this assumption is a strong approximation, which should be overcome in future developments.

Groundwater

The groundwater compartment is not mentioned by Mackay as one of the compartments that may represent the world unit. Within the present study, it was decided to include it in order to quantify the concentration that is established and that could be used in the further development of the present work for CF modelling.

Groundwater is schematised in the present study as a subterranean river flowing under part of the soil and only in contact with it. Within it a dissolved phase and a solid phase consisting of particles are considered, some of which contain organic carbon, according to a certain volume fraction, defined by Mackay, each phase represented by its own

Z-value in relation to its flow rate, where the process velocity is defined by Mackay ("World unit data" sheet of the Excel tool).

In general, degradation, diffusion and advection reactions can take place in groundwater.

The advection of groundwater is governed by its flow rate and the velocity of the flow, which also carries suspended particles with it.

The groundwater is assumed in this study not to be characterised by the presence of biota, which could be affected by toxic effects due to the concentration in it.

In reality, this is an approximation that should be overcome in a future development, as groundwater could be considered to be drunk by humans or terrestrial biota.

Fish

The fish compartment is of great interest mainly because of the phenomenon of bioaccumulation. This differs from bioconcentration, which occurs as a result of uptake through the gills by respiration from the water, as it also adds uptake through food. Biomagnification, on the other hand, represents the increase in concentration along the food chain, a phenomenon that occurs especially for chemicals that are difficult to metabolise, where the log K_{OW} > 5.

The fish communicates, of course, only with the water compartment and has two intake modes, by respiration of the dissolved water phase with a rate k_1 and with food with a rate k_A. The latter is approximated in the Mackay Model as the water phase, therefore, both processes will be characterised by values of Z_W, while the rates accompanying these processes are defined in "World unit data" sheet of the Excel tool. In particular, the first is given by Eq. 95:

$$k_1 = \frac{Q_{WUPTAKE}}{V_F} \quad \text{(Eq. 95)}$$

where k_1 (h^{-1}) represents the rate of uptake through the gills by respiration, $Q_{WUPTAKE}$ $(m^3\ h^{-1})$ is the breathing rate and V_F (m^3) is the volume of the fish. Fish exit processes take into account exit through respiration, degradation by metabolism, exit by egestion and concentration reduction as the fish grows.

The first exit process is characterised by a rate k_2 which can be related to k_1 through K_{FW}, which represents the bioconcentration factor.

It is defined from the equation (Eq. 96) showing the concentration trend in fish C_F immersed in water in which a certain concentration of pollutant is present C_W, in which uptake through respiration occurs according to a rate k_1 and the exit with k_2:

$$\frac{dC_F}{dt} = k_1 C_W - k_2 C_F \quad \text{(Eq. 96)}$$

Integrating by $t = 0$ when $C_{F0} = 0$ and C_W is constant, the equation can be written as (Eq. 97):

$$C_F = \frac{k_1}{k_2} C_W [1 - exp(-k_2 t)] \quad \text{(Eq. 97)}$$

After prolonged exposure, for high values of t (Eq. 98 and Eq. 99) :

$$C_F = \frac{k_1}{k_2}\, C_W \quad \text{(Eq. 98)}$$

$$\frac{C_F}{C_W} = \frac{k_1}{k_2} = K_{FW} \quad \text{(Eq. 99)}$$

The other fish output phenomena are, in turn, defined by rate values that can be added to Eq. 96 to obtain the complete balance for the fish (Eq. 100):

$$\frac{dC_F}{dt} = k_1 C_W + k_A C_A - C_F\,(k_2 + k_M + k_E + k_G) \quad \text{(Eq. 100)}$$

where k_M (h^{-1}) represents the degradation rate due to metabolism, k_E (h^{-1}) represents the degradation rate due to egestion and k_G (h^{-1}) represents the degradation rate due to growth, the fish volume increase.

In steady state conditions $\frac{dC_F}{dt} = 0$ and (Eq. 101):

$$C_F = \frac{k_1 C_W + k_A C_A}{k_2 + k_M + k_E + k_G} \quad \text{(Eq. 101)}$$

All of the above processes can be converted into fugacity terms on the basis of Eq. 37 and the relevant D-rates, shown in Table 3, can be derived. The bioconcentration factor K_{FW} becomes (Eq. 102):

$$K_{FW} = \frac{Z_F\ (mol\ m^{-3} Pa^{-1})}{Z_W\ (mol\ m^{-3} Pa^{-1})} \quad \text{(Eq. 102)}$$

Terrestrial vegetation

The vegetation compartment is mentioned by Mackay as one of the 7 compartments that can represent the world unit, although in the developed 4-compartment model, vegetation is neglected. In the present study, it was decided to include it in order to quantify the concentration that is established and used in the subsequent steps of CF modelling.

In the present study, the vegetation compartment has been assimilated with the maize plant, so all size parameters and the root uptake rate are related to this type of crop.

Vegetation is considered to be mainly composed of a water phase and an organic carbon phase and is in communication with the air and soil compartments. In particular, there are diffusive exchanges from the former and it receives wet and dry deposition in the same way as the water and soil compartments. The diffusive process was included as found in the literature (Smyrnova et al. 2012), similarly to the soil, a diffusion rate D air-vegetation and valid for both absorption and volatilisation, given by the sum of the air-vegetation series resistances, in which there are two resistances in parallel, one for each vegetation phase (Eq. 103):

$$\frac{1}{D_{diffAVEG}} = \frac{1}{D_{diffE}} + \frac{1}{(D_{diffW} + D_{diffOC})} \quad \text{(Eq. 103)}$$

where $D_{diffAVEG}$ $(mol\ m^{-3} Pa^{-1})$ is the air-vegetation diffusion rate, D_{diffE} $(mol\ m^{-3} Pa^{-1})$ is the partial diffusion rate air side, D_{diffW} $(mol\ m^{-3} Pa^{-1})$ is the partial diffusion rate of water phase vegetation side, D_{diffOC} $(mol\ m^{-3} Pa^{-1})$ is the partial diffusion rate of organic carbon phase vegetation side.

The partial diffusion rates for vegetation are derived from the partial diffusivities, reduced according to the volume fractions occupied by each of the phases (Eq. 104 and Eq. 105):

$$B_{WVEG} = \frac{B_W \times v_W^{\frac{10}{3}}}{\left(v_{w,VEG} + v_{oc,VEG}\right)^2} \quad \text{(Eq. 104)}$$

$$B_{OCVEG} = \frac{B_{OC} \times v_{oc,VEG}^{\frac{10}{3}}}{\left(v_{w,VEG} + v_{oc,VEG}\right)^2} \quad \text{(Eq. 105)}$$

where B_{WVEG} (m^2h^{-1}), B_{OCVEG} (m^2h^{-1}) are, namely, the diffusivity of the water and organic carbon phases of vegetation, B_W (m^2h^{-1}), B_{OC} (m^2h^{-1}) are, respectively, the diffusivities of the water and organic carbon phases, $v_{w,VEG}$ and $v_{oc,VEG}$ are the volume fractions of the water and organic carbon phases of vegetation, respectively. The volume fractions were defined on the basis of Mackay and the literature, the parameter values and sources are given in "World unit data" sheet of the Excel tool.

Air also exerts wet and dry deposition processes on the vegetation in the same manner as described above.

For modelling the surface area of the vegetation, which affects the processes from air by deposition and diffusive exchange, the leaf area was not taken into account, but this was calculated as the ratio of volume to height. The area thus obtained could be lower or higher than the actual area, depending on the vegetation considered. Furthermore, the value of partial mass transfer coefficient on the air side for diffusion was assumed to be equal to the value in diffusive exchange with the soil, as a proxy. These critical points could be overcome in a future development of this work.

The process connecting it with the soil is advective and concerns the uptake with the roots of the water phase, therefore, the process will be accompanied by a rate and the Z_W, since soil water is the carrier that transports the chemical into the vegetation.

The degradative process in vegetation is present and the D rate is characterised by the presence of the Z_{VEG}, according to Eq. 88 of Table 1.

3.2.1 Summary of the chemical used as test substance

In the present work, benzene was considered as the test substance, as it is one of the most extensively studied organic substances, both in terms of its physico-chemical properties and toxicity. The required physico-chemical properties and toxicological data were searched and entered into the calculation tool, as an integrated database with substances properties was not available. The required physico-chemical properties are shown in the table below (Table 2):

Table 2 Main physico-chemical properties of benzene

Type of data			Source
logK_{ow}	2.13		Mackay (2001)
Vapour pressure Ps (Pa)	12700		Mackay (2001)
Solubility Sw (kg m^{-3})	1.78E+00		Mackay (2001)
MW (kg mol^{-1})	7.81E-02		Mackay (2001)
Density in s.c. (kg m^{-3})	876.5		
Compartment	**Rate constant k (h^{-1})**	**Degradation Half-lives $\tau_{1/2}$ (h)**	
Air	4.08E-02	17	Mackay (2001)
Water	4.08E-03	170	Mackay (2001)
Soil	1.26E-03	550	Mackay (2001)
Sediments	4.08E-04	1700	Mackay (2001)
Groundwater	4.08E-03	170	Mackay (2001)
Fish metabolism	3.94E-01	-	Formula 17 from Radomyski et al. (2016) Chemical half-life in fish 1.2 days (28.8 h) Allometric constant: 0.25
Fish growth	2.96E-02	30720	Fish lifetime (1280 days from Radomyski et al. (2016))
Vegetation	2.15E-02	267.6	Degradation rate of hexacloro benzene (proxy) (Fantke et al. 2014)

Toxicity data are reported in the section dedicated to EF calculation (chapter 3.2.6).

The following table (Table 3) summarise all D-rates and the formulas used for their calculation, for each compartment and process.

Table 3 D rates calculation for each type of environmental process in the local model

Local	D diffusion (mol h^{-1} Pa^{-1})	Formula (k = mass transfer coeff., m h^{-1})
D_{VA}	8.99E-02	$k_A \times A_{AW} \times Z_A$
D_{VW}	3.56E+02	$k_W \times A_{AW} \times Z_W$
D_E	1.53E+03	$k_V \times A_{AS} \times Z_A$
D_T	8.97E-07	$k_T \times A_{WSED} \times Z_W$
D_{AS}	1.56E+02	$B_{AS}\ Y^{-1} \times A_{AS} \times Z_A$
D_{WS}	2.73E-01	$B_{WS}\ Y^{-1} \times A_{AS} \times Z_W$
D_{OCS}	1.39E-09	$B_{OCS}\ Y^{-1} \times A_{AS} \times Z_S$
D_{VAW}	8.98E-02	$(1/D_{VA} + 1/D_{VW})^{-1}$
D_{VAS}	1.41E+02	$(1/D_E + 1/(D_{AS} + D_{WS} + D_{OCS}))^{-1}$
D_{VAVEG}	2.58E-10	$(1/D_{EVEG} + 1/(D_{WVEG} + D_{OCVEG}))^{-1}$
D_{WVEG}	2.50E-10	$B_{VEGW}\ Y^{-1} \times A_{VEG} \times Z_W$
D_{OCVEG}	7.64E-12	$B_{VEGOC}\ Y^{-1} \times A_{VEG} \times Z_{VEG}$
D_{EVEG}	7.66E+00	$k_{VVEG} \times A_{VEG} \times Z_A$

Local	D degradation (mol h^{-1} Pa^{-1})	Formula (k = rate constant, h^{-1})
$D_{DEG,\ A}$	4.02E+03	$k_A \times V_A \times v_{g,A} \times Z_A$
$D_{DEG,\ W}$	3.66E-01	$k_W \times V_W \times v_{w,W} \times Z_W$
$D_{DEG,\ S}$	7.83E-01	$k_S \times V_S \times v_{oc,S} \times Zs$
$D_{DEG,\ SED}$	1.21E-02	$k_{SED} \times V_{SED} \times Z_{SED}$
$D_{DEG,\ GW}$	3.66E-02	$k_{GW} \times V_{GW} \times Z_{GW}$
$D_{DEG,\ VEG}$	5.14E-01	$k_{VEG} \times V_{VEG} \times Z_{VEG}$

Local	D advection (mol h^{-1} Pa^{-1})	Formula
$D_{ADV,\ A}$	1.06E+06	$G_A \times Z_A$
$D_{ADV,\ W}$	3.23E+02	$G_W \times Z_W + G_{PW} \times Z_P$
D_{QAW}	2.59E-08	$U_Q \times v_{q,A} \times A_{AW} \times Z_Q$
D_{MAW}	1.08E-03	$U_M \times A_{AW} \times Z_W$
D_{CAW}	3.11E-08	$U_M \times A_{AW} \times Q \times v_{q,A} \times Z_Q$
D_{QAS}	2.57E-06	$U_Q \times v_{q,A} \times A_{AS} \times Z_Q$
D_{MAS}	1.07E-01	$U_M \times A_{AS} \times Z_W$
D_{CAS}	3.08E-06	$U_M \times A_{AS} \times Q \times v_{q,A} \times Z_Q$
D_{QAVEG}	1.28E-08	$U_Q \times v_{q,A} \times A_{AVEG} \times Z_Q$
D_{MAVEG}	5.33E-04	$U_M \times A_{AVEG} \times Z_W$
D_{CAVEG}	1.54E-08	$U_M \times A_{AVEG} \times Q \times v_{q,A} \times Z_Q$
D_L	1.40E-04	$U_L \times A_{GW} \times Z_W$
D_{GW}	3.23E+01	$G_I \times Z_W$
$D_{RUNOFF,S}$	6.78E-05	$A_S \times U_{Solid} \times Z_S$
$D_{RUNOFF,W}$	6.93E-02	$A_S \times U_W \times Z_W$
D_D	2.74E-06	$U_D \times A_{SED} \times Z_P$
D_R	6.55E-07	$U_R \times A_{SED} \times Z_{SED}$
D_B	2.74E-06	$U_B \times A_{SED} \times Z_{SED}$
D_{IRRIG}	1.05E-03	$U_{IRRIG} \times A_S \times Z_W$
D_{VWF}	5.83E-03	$k_1 \times V_F \times Z_W$
D_{VFW}	5.83E-03	$k_2 \times V_F \times Z_F$
D_{AF}	5.24E-07	$G_{AF} \times Z_A$
D_{EF}	1.31E-07	$D_{AF}\ Q_F^{-1}$
D_{MF}	3.20E-04	$k_{MF} \times V_F \times Z_F$
D_{GF}	2.41E-05	$k_{GF} \times V_F \times Z_F$
D_{VEGS}	5.24E-08	$U_{UPTAKEROOTS} \times A_{STEMVEG} \times Z_W$

3.2.2 Excel calculation tool and resolution matrix

An Excel spreadsheet (Local model.xlsx) was created for collecting all required data and calculating fate dispersion. It contains all the required types of parameters, organized in sheets as follows:

- World unit data (highlighted in red in the Excel file): this sheet contains landscape parameters and compartments details, such as specific processes velocities and phases composition. These parameters are adaptable to specific situations to represent the local world unit under study. The emission vector $\vec{E}$ [E_A; E_W; E_S] is present in this sheet in cells B24-B27 (highlighted in red in the Excel file);
- Substance data: this sheet contains physico-chemical properties and toxicity data. These parameters are adaptable to the specific chemical under study;
- Partition coefficients $\boldsymbol{K}$ sheet: this sheet is automatically filled in on the basis of the information in Substance data sheet;
- Capacity of fugacities $\boldsymbol{Z}$: this sheet is automatically filled in on the basis of the information in Substance data sheet;
- Diffusivities $\boldsymbol{B}$ and mass transfer coefficients $\boldsymbol{k}$ sheet: this sheet presents fixed parameters and other parameters that are automatically filled in on the basis of the information in Substance data and World unit data sheets;
- D values sheet: this sheet is automatically filled in on the basis of the information in Substance data and World unit data sheets;
- Fugacities and concentrations: this sheet contains the equations, the matrix resolution, fugacities vector $\vec{f}$ (cells K50:K56), masses $\vec{M}$ (cells L50:L56) and concentrations $\boldsymbol{C}$, as well as a synthetic world unit mass balance (cells B79 and B81) and mass fluxes results (cells C86:C102). It is automatically filled in on the basis of the information in Substance data and World unit data sheets;
- Mass balance: this sheet contains a detailed mass balance, for each compartment. It is connected to the emission vector $\vec{E}$ in the World unit data sheet and it is automatically filled in on the basis of the information in Substance data and World unit data sheets;
- Fate factors $\boldsymbol{FF}$: this sheet is automatically filled on the basis of the information in Substance data and World unit data sheets;
- Exposure factors $\boldsymbol{XF}$: this sheet contains the population parameter (adaptable to specific conditions) and is automatically filled on the basis of the information in World unit data sheet;
- Effect factors $\boldsymbol{EF}$: this sheet and is automatically filled on the basis of the information in Substance data sheet;
- Mid-point characterization factors for local air emissions $\boldsymbol{CF_{LOC,A}}$: this sheet and is automatically filled for emission vector $\vec{E}$ = [1;0;0] in World unit data sheet;
- Mid-point characterization factors for local water emissions $\boldsymbol{CF_{LOC,W}}$: this sheet and is automatically filled for emission vector $\vec{E}$ = [0;1;0] in World unit data sheet;
- Mid-point characterization factors for local soil emissions $\boldsymbol{CF_{LOC,S}}$: this sheet and is automatically filled for emission vector $\vec{E}$ = [0;0;1] in World unit data sheet;

- End-point characterization factors for local air emissions $\boldsymbol{CF_{LOC,A}}$: this sheet is connected with the mid-point $\boldsymbol{CF_{LOC,A}}$;
- End-point characterization factors for local water emissions $\boldsymbol{CF_{LOC,W}}$: this sheet is connected with the mid-point $\boldsymbol{CF_{LOC,W}}$;
- End-point characterization factors for local soil emissions $\boldsymbol{CF_{LOC,S}}$: this sheet is connected with the mid-point $\boldsymbol{CF_{LOC,S}}$.

Similarly to the USEtox model, the matrix model is adopted to solve the system of 7 equations in 7 unknowns, one for each compartment, according to Eq. 2.

Similarly to Eq. 4 and Eq. 5, the same procedure will be performed for the calculation of fugacity under stationary conditions.

The system to be solved for Level III is of the type (Eq. 106 and Eq. 107):

$$\vec{E} + \vec{f} \times \overline{D} = 0 \qquad \text{(Eq. 106)}$$

$$\vec{f} = -\overline{D}^{-1} \times \vec{E} \qquad \text{(Eq. 107)}$$

where $\vec{f}\ (Pa)$ is the vector of unknowns, i.e. fugacities, $\overline{D}\ (mol\ h^{-1}Pa^{-1})$ is the rate matrix D, and $\vec{E}\ (mol\ h^{-1})$ is the vector of known terms, i.e. direct emissions.

The 7 equations, set up on the basis of the mass balance on the model of Eq. 2 for the third level and reported in Appendix - A.3, are given below (from Eq. 108 to Eq. 121). The equations were written in a first step by explicating all the flows present, then the D rates were aggregated into coefficients whose names are made up of two letters XY, X denotes the starting compartment, Y the arrival compartment.

The equations describe the stationary conditions of environmental processes, in which everything entering a compartment is equal to everything leaving it. Under these conditions, the accumulation of new chemicals in the compartments cannot occur, but only remain unchanged over time from a previous non-stationary condition that originated it. The mass calculation performed below, therefore, refers to the amount of chemical generated in a non-stationary phase prior to the current conditions, which preserve it, and which will accompany the rates of all environmental processes exiting each compartment.

<u>AIR</u>:

$$E_A + f_w \times D_{VAW} - f_A \times D_{VAW} - f_A \times D_{MAW} - f_A \times D_{QAW} - f_A \times D_{CAW} - f_A \times D_{MAS} - f_A \times D_{QAS} - f_A \times D_{CAS} - f_A \times D_{MAVEG} - f_A \times D_{QAVEG} - f_A \times D_{CAVEG} - f_A \times D_{DEGA} - f_A \times D_{ADV,A} + f_S \times D_{VAS} - f_A \times D_{VAS} + f_{VEG} \times D_{VAVEG} - f_A \times D_{VAVEG} = 0 \qquad \text{(Eq. 108)}$$

where:

- $E_A\ (mol\ h^{-1})$ is the emission vector relating only to continuous and constant air emission;
- $f_w \times D_{VAW}\ (mol\ h^{-1})$ is the flux entering the air by volatilisation from water;

- $-f_A \times D_{VAW}\ (mol\ h^{-1})$ is the outflow from the air by absorption to the water;
- $-f_A \times D_{MAW}\ (mol\ h^{-1})$ is the outflow from the air by wet deposition to the water;
- $-f_A \times D_{QAW}\ (mol\ h^{-1})$ is the outflow from the air by dry aerosol deposition to the water;
- $-f_A \times D_{CAW}\ (mol\ h^{-1})$ is the outflow from the air by wet deposition of aerosols to water;
- $-f_A \times D_{MAS}\ (mol\ h^{-1})$ is the outflow from the air by wet deposition towards the soil;
- $-f_A \times D_{QAS}\ (mol\ h^{-1})$ is the outflow from the air by dry aerosol deposition towards the soil;
- $-f_A \times D_{CAS}\ (mol\ h^{-1})$ is the outflow from the air by moist aerosol deposition towards the soil;
- $-f_A \times D_{MAVEG}\ (mol\ h^{-1})$ is the outflow from the air by wet deposition towards the vegetation;
- $-f_A \times D_{QAVEG}\ (mol\ h^{-1})$ is the outflow from the air by dry aerosol deposition towards vegetation;
- $-f_A \times D_{CAVEG}\ (mol\ h^{-1})$ is the outflow from the air by wet aerosol deposition towards vegetation;
- $-f_A \times D_{ADV,A}\ (mol\ h^{-1})$ is the outflow from the air by advection;
- $-f_A \times D_{DEG,A}\ (mol\ h^{-1})$ is the outflow from the air by degradation;
- $f_S \times D_{VAS}\ (mol\ h^{-1})$ is the flow entering the air by volatilisation from the soil;
- $-f_A \times D_{VAS}\ (mol\ h^{-1})$ is the flow out of the air by absorption towards the soil;
- $f_{VEG} \times D_{VAVEG}\ (mol\ h^{-1})$ is the flux entering the air by volatilisation from vegetation;
- $-f_A \times D_{VAVEG}\ (mol\ h^{-1})$ is the outflow from the air by absorption into the vegetation.

The equation is then rewritten as follows (Eq. 109), highlighting the unknowns in red and collecting the sum of the air outputs in the coefficient AA and the known term C_A the emission:

$$f_A \times AA - f_W \times D_{VAW} - f_S \times D_{VAS} - f_{VEG} \times D_{VAVEG} = C_A \qquad \text{(Eq. 109)}$$

where:

- $AA\ (mol\ h^{-1}Pa^{-1}) = D_{VAW} + D_{MAW} + D_{QAW} + D_{CAW} + D_{MAS} + D_{QAS} + D_{CAS} + D_{MAVEG} + D_{QAVEG} + D_{CAVEG} + D_{DEGA} + D_{ADV,A} + D_{VAS} + D_{VAVEG}$
- $C_A\ (mol\ h^{-1}) = E_A$

The known term C_A would also include airflow from outside the local system if it communicated with a larger scale or an adjacent box, an eventuality not foreseen in the present model, but introduced in the simplified model with the continental scale.

WATER:

$$E_W - f_w \times D_{VAW} + f_A \times D_{VAW} + f_A \times D_{MAW} + f_A \times D_{QAW} + f_A \times D_{CAW} - f_W \times D_{DEGW} - f_W \times D_{ADV,W} + f_{SED} \times D_T - f_W \times D_T + f_{SED} \times D_{RESUSP} - f_W \times D_D + f_S \times D_{RUNOFF} - f_W \times D_{IRRIG} - f_W \times D_{VWF} + f_F \times D_{VWF} - f_W \times D_{AF} = 0 \qquad \text{(Eq. 110)}$$

where:

- $E_W\ (mol\ h^{-1})$ is the emission vector relative to continuous and constant water emission only;
- $-f_w \times D_{VAW}\ (mol\ h^{-1})$ is the outflow by volatilisation from water to air;

- $f_A \times D_{VAW}\ (mol\ h^{-1})$ is the inflow from the air by absorption to the water;
- $f_A \times D_{MAW}\ (mol\ h^{-1})$ is the inflow from the air by wet deposition to the water;
- $f_A \times D_{QAW}\ (mol\ h^{-1})$ is the incoming flow from the air by dry aerosol deposition to the water;
- $f_A \times D_{CAW}\ (mol\ h^{-1})$ is the incoming flow from air by wet deposition of aerosols to water;
- $-f_W \times D_{ADV,W}\ (mol\ h^{-1})$ is the outflow from the water by advection;
- $-f_W \times D_{DEG,W}\ (mol\ h^{-1})$ is the outflow from the water by degradation;
- $-f_W \times D_{IRRIG}\ (mol\ h^{-1})$ is the outflow from irrigation water to the soil;
- $-f_W \times D_D\ (mol\ h^{-1})$ is the outflow from the water by deposition to the sediments;
- $f_{SED} \times D_T\ (mol\ h^{-1})$ is the flow entering the water by diffusion from the sediments;
- $-f_W \times D_T\ (mol\ h^{-1})$ is the outflow from the water by diffusion to the sediments;
- $f_{SED} \times D_{RESUSP}\ (mol\ h^{-1})$ is the flux entering the water by resuspension from the sediments;
- $-f_W \times D_{VWF}\ (mol\ h^{-1})$ is the outflow from the water for uptake by respiration to the fish;
- $f_F \times D_{VWF}\ (mol\ h^{-1})$ is the outflow from the fish by respiration into the water;
- $-f_W \times D_{AF}\ (mol\ h^{-1})$ is the outflow from the water by uptake through the food to the fish.

The equation is then rewritten as follows (Eq. 111), highlighting the unknowns in red and gathering in the coefficients WW the sum of the contributions from water, AW the sum of the contributions from air, SEDW the sum of the contributions from sediment and in the known term CW the emission:

$$-f_A \times AW + f_W \times WW - f_S \times D_{RUNOFF} - f_{SED} \times SEDW - f_F \times D_{VFW} = C_W \qquad \text{(Eq. 111)}$$

where:

- $WW\ (mol\ h^{-1}Pa^{-1}) = D_{VAW} + D_{DEGW} + D_{ADV,W} + D_T + D_D + D_{IRRIG} + D_{VWF} + D_{AF}$
- $AW\ (mol\ h^{-1}Pa^{-1}) = D_{VAW} + D_{MAW} + D_{QAW} + D_{CAW}$
- $SEDW\ (mol\ h^{-1}Pa^{-1}) = D_T + D_{RESUSP}$
- $C_W\ (mol\ h^{-1}) = E_W$

GROUNDWATER:

$$-f_{GW} \times D_{DEGW} - f_{GW} \times D_{ADV,GW} + f_S \times D_L = 0 \qquad \text{(Eq. 112)}$$

where:

- $-f_{GW} \times D_{DEGW}\ (mol\ h^{-1})$ is the outflow by degradation from groundwater;
- $-f_{GW} \times D_{ADVGW}\ (mol\ h^{-1})$ is the outflow by advection from the groundwater;
- $f_S \times D_L\ (mol\ h^{-1})$ is the incoming flow from the soil by leaching.

The equation is then rewritten as follows (Eq. 113), highlighting the unknowns in red and collecting the sum of the groundwater releases in the GWGW coefficient. There is no known term for this compartment as there can be no direct emission.

$$f_S \times D_L - f_{GW} \times GWGW = 0 \quad \text{(Eq. 113)}$$

where:

$$GWGW\ (mol\ h^{-1}Pa^{-1}) = D_{DEGW} + D_{ADV,GW}$$

SOIL:

$$E_S - f_S \times D_{VAS} + f_A \times D_{VAS} - f_S \times D_L + f_A \times D_{MAS} + f_A \times D_{QAS} + f_A \times D_{CAS} - f_S \times D_{DEGS} - f_S \times D_{RUNOFF} + f_W \times D_{IRRIG} - f_S \times D_{VEGS} = 0 \quad \text{(Eq. 114)}$$

Where:

- $E_S\ (mol\ h^{-1})$ is the emission vector relative to continuous and constant soil emission only;
- $f_A \times D_{MAS}\ (mol\ h^{-1})$ is the flow entering the soil by wet deposition from the air;
- $f_A \times D_{QAS}\ (mol\ h^{-1})$ is the flux entering the soil by dry aerosol deposition from the air;
- $f_A \times D_{CAS}\ (mol\ h^{-1})$ is the flow entering the soil by wet deposition of aerosols from the air;
- $-f_S \times D_{VAS}\ (mol\ h^{-1})$ is the outflow from the ground by volatilisation into the air;
- $f_A \times D_{VAS}\ (mol\ h^{-1})$ is the flux entering the soil by absorption from the air;
- $f_W \times D_{IRRIG}\ (mol\ h^{-1})$ is the flow entering the soil by irrigation from water;
- $-f_S \times D_{VEGS}\ (mol\ h^{-1})$ is the flow out of the soil by uptake with the roots towards the vegetation;
- $-f_S \times D_{DEG,S}\ (mol\ h^{-1})$ is the outflow from the soil by degradation;
- $-f_S \times D_{RUNOFF}\ (mol\ h^{-1})$ is the outflow from the soil for runoff to the water;
- $-f_S \times D_L\ (mol\ h^{-1})$ is the outflow from the soil by leaching to the groundwater.

The equation is then rewritten as follows (Eq. 115), highlighting the unknowns in red and gathering in the coefficients SS the sum of the contributions from the ground, AS the sum of the contributions from the air, and in the known term C_S the emission:

$$-f_A \times AS - f_W \times D_{IRRIG} + f_S \times SS = C_S \quad \text{(Eq. 115)}$$

where:

- $SS\ (mol\ h^{-1}Pa^{-1}) = D_{VAS} + D_L + D_{DEGS} + D_{RUNOFF} + D_{VEGS}$
- $AS\ (mol\ h^{-1}Pa^{-1}) = D_{VAS} + D_{MAS} + D_{QAS} + D_{CAS}$
- $C_S\ (mol\ h^{-1}) = E_S$

SEDIMENTS:

$$f_w \times D_T - f_{SED} \times D_T - f_{SED} \times D_{DEGSED} - f_{SED} \times D_B - f_{SED} \times D_{RESUSP} + f_W \times D_D = 0 \quad \text{(Eq. 116)}$$

Where:

- $-f_{SED} \times D_{DEG,SED}\ (mol\ h^{-1})$ is the outflow from the sediment by degradation;
- $f_W \times D_D\ (mol\ h^{-1})$ is the flux entering the sediment by deposition from the water;
- $-f_{SED} \times D_T\ (mol\ h^{-1})$ is the outflow from the sediment by diffusion to the water;
- $f_W \times D_T\ (mol\ h^{-1})$ is the flow entering the sediment by diffusion from the water;
- $-f_{SED} \times D_{RESUSP}\ (mol\ h^{-1})$ is the outflow from the sediment by resuspension to the water;
- $-f_{SED} \times D_B\ (mol\ h^{-1})$ is the outflow from the sediment for burial to the lower layers.

The equation is then rewritten as follows (Eq. 117), highlighting the unknowns in red and gathering in the SEDSED coefficient the sum of the releases from sediment and WSED the sum of the contributions from water. There is no known term for this compartment as there can be no direct emission.

$$-f_W \times WSED + f_{SED} \times SEDSED = 0 \qquad \text{(Eq. 117)}$$

where:

- $SEDSED\ (mol\ h^{-1}Pa^{-1}) = D_{DEG,SED} + D_T + D_{RESUSP} + D_B$
- $WSED\ (mol\ h^{-1}Pa^{-1}) = D_D + D_T$

FISH:

$$f_W \times D_{VWF} - f_F \times D_{VWF} - f_F \times D_G - f_F \times D_M - f_F \times D_E + f_W \times D_{AF} = 0 \qquad \text{(Eq. 118)}$$

Where:

- $f_W \times D_{VWF}\ (mol\ h^{-1})$ is the flux entering the fish by uptake by respiration from the water;
- $-f_F \times D_{VWF}\ (mol\ h^{-1})$ is the outflow from the fish by respiration into the water;
- $f_W \times D_{AF}\ (mol\ h^{-1})$ is the flow entering the fish by uptake through food from the water;
- $-f_F \times D_G\ (mol\ h^{-1})$ is the outflow from the fish for growth;
- $-f_F \times D_M\ (mol\ h^{-1})$ is the outflow from the fish for metabolism;
- $-f_F \times D_E\ (mol\ h^{-1})$ is the outflow from the fish for egestion.

The equation is then rewritten as follows (Eq. 119), highlighting the unknowns in red and gathering in the FF coefficient the sum of the outputs from the fish and WF the sum of the contributions from the water. There is no known term for this compartment as there can be no direct emission.

$$-f_W \times WF + f_F \times FF = 0 \qquad \text{(Eq. 119)}$$

where:

- $FF\ (mol\ h^{-1}Pa^{-1}) = D_{VWF} + D_G + D_M + D_E$
- $WF\ (mol\ h^{-1}Pa^{-1}) = D_{VWF} + D_{AF}$

VEGETATION:

$$f_A \times D_{MAVEG} + f_A \times D_{QAVEG} + f_A \times D_{CAVEG} - f_{VEG} \times D_{DEGVEG} - f_{VEG} \times D_{VAVEG} + f_A \times D_{VAVEG} + f_S \times D_{VEGS} = 0 \quad \text{(Eq. 120)}$$

where:

- $f_A \times D_{MAVEG}\ (mol\ h^{-1})$ is the flow entering the vegetation by wet deposition from the air;
- $f_A \times D_{QAVEG}\ (mol\ h^{-1})$ is the flux entering the vegetation by dry aerosol deposition from the air;
- $f_A \times D_{CAVEG}\ (mol\ h^{-1})$ is the flow entering the vegetation by wet deposition of aerosols from the air;
- $-f_{VEG} \times D_{DEG,VEG}\ (mol\ h^{-1})$ is the outflow from the vegetation by degradation;
- $-f_{VEG} \times D_{VAVEG}\ (mol\ h^{-1})$ is the outflow from the vegetation by volatilisation into the air;
- $f_A \times D_{VAVEG}\ (mol\ h^{-1})$ is the flux entering the vegetation by absorption from the air.

The equation is then rewritten as follows (Eq. 121), highlighting the unknowns in red and gathering in the coefficient VEGVEG the sum of the outputs from vegetation and AVEG the sum of the contributions from the air. The known term is not present for this compartment as there can be no direct emission.

$$f_{VEG} \times VEGVEG - f_A \times AVEG - f_S \times D_{VEGS} = 0 \quad \text{(Eq. 121)}$$

where:

- $VEGVEG\ (mol\ h^{-1}Pa^{-1}) = D_{VAVEG} + D_{DEGVEG}$
- $AVEG\ (mol\ h^{-1}Pa^{-1}) = D_{MAVEG} + D_{QAVEG} + D_{CAVEG} + D_{VAVEG}$

The determined coefficients are then introduced into a square matrix, called $-\overline{D}$, where the D coefficients have been changed by sign, shown below (Table 4), where the rows represent the individual compartments for which the balance equation is written, the columns represent the compartments that interact with the compartments under analysis. When there is no process connecting two compartments, a value of zero is entered. The diagonal cells represent the output from the compartment represented by the row, with a positive sign for all compartments as their sign has been changed to isolate the emission vector.

Table 4 Resolution matrix with equations coefficients of the local model

	Contributing compartment						
Analyzed compartment	**A**	**W**	**S**	**SED**	**GW**	**F**	**VEG**
A	AA	$-D_{VAW}$	$-D_{VAS}$	0	0	0	$-D_{VAVEG}$
W	-AW	WW	$-D_{RUNOFF}$	-SEDW	0	$-D_{VFW}$	0
S	-AS	$-D_{IRRIG}$	SS	0	0	0	0
SED	0	-WSED	0	SEDSED	0	0	0
GW	0	0	$-D_L$	0	GWGW	0	0
F	0	-WF	0	0	0	FF	0
VEG	-AVEG	0	$-D_{VEGS}$	0	0	0	VEGVEG

The result of the matrix construction is shown below $-\overline{D}$, constant for each emitting scenario (Table 5).

Table 5 Resolution matrix with equations coefficients for benzene emission in the local model

	Contributing compartment						
Analyzed compartment	**A**	**W**	**S**	**SED**	**GW**	**F**	**VEG**
A	1.07E+06	-8.98E-02	-1.41E+02	0	0	0	-2.58E-10
W	-9.09E-02	3.23E+02	-6.93E-02	-1.55E-06	0	-5.83E-03	0
S	-1.42E+02	-1.05E-03	1.42E+02	0	0	0	0
SED	0	-3.64E-06	0	1.21E-02	0	0	0
GW	0	0	-1.40E-04	0	3.23E+01	0	0
F	0	-5.83E-03	0	0	0	6.18E-03	0
VEG	-5.33E-04	0	-5.24E-08	0	0	0	5.14E-01

The matrix $-\overline{D}$ is then inverted, i.e. the $-\overline{D}^{-1}$ is calculated, in which the inverse terms have units Pa h mol^{-1}. The matrix inversion operation makes it possible to obtain the unknown, i.e. the fugacity, which can be traced back to the concentration and hence the mass, by multiplication with the vector of known terms $\vec{E}$, in which the elements have units mol h^{-1}.

A more in-depth analysis of the significance of the values resulting from the matrix inversion will be carried out in a future development of this paper.

The vector of known terms $\vec{E}$ is structured in such a way as to have as many rows as there are compartments in the system and a single column, in which the direct and continuous emission (Table 6):

Table 6 Vector of known terms C (emission vector $\vec{E}$)

Emitting compartment	
A	C_A
W	C_W
S	C_S
SED	0
GW	0
F	0
VEG	0

In order to obtain characterisation factors for each individual emitting compartment, the known terms must be equal to 1 mol h^{-1} only for the sub-fund for which the CF is to be calculated.

However, it is also possible to model the dispersion according to different emitting scenarios, in which case the purpose is to assess the damage due to emissions and not to calculate CFs for an LCA analysis.

The result of the multiplication returns the vector $\vec{f}$ of unknowns (Table 7):

Table 7 Vector of unknown terms (fugacity vector $\vec{f}$)

Compartment	
A	f_A
W	f_W
S	f_S
SED	f_{SED}
GW	f_{GW}
F	f_F
VEG	f_{VEG}

From this the different concentrations are derived C (mol m^{-3}), either by bulk, i.e. by compartments consisting of several phases, or by single phase, through the product of the Z_{ibulk} and of Z_x, namely (Eq. 122 and Eq. 123):

$$C_i = f_i \times Z_{ibulk} \quad \text{(Eq. 122)}$$

$$C_x = f_i \times Z_x \quad \text{(Eq. 123)}$$

Through multiplication with volume V (m^3) masses are obtained M (mol), converted with molecular weight in kg.

3.2.3 Fugacities and concentrations results

The fugacities and concentration results for benzene emissions in air in the local model are summarised in Table 8.

Table 8 Fugacities and concentration results for benzene emission in air in the local model

Compartments (emitting = E)	Fugacity (Pa)	C_{bulk} (mol m^{-3})	Phase	C_{phase} (mol m^{-3})	Phase	C_{phase} (mol m^{-3})	Phase	C_{phase} (mol m^{-3})
Air (E)	9.36E-07	3.84E-10	Agas	3.84E-10	Aaerosol	1.21E-08		
Water	4.63E-10	8.31E-13	Wdiss	8.30E-13	Wsusps	2.76E-12		
Soil	9.31E-07	6.36E-10	Ssolid	2.77E-09	Swater	1.67E-09	Sair	3.82E-10
Sediments	1.39E-13	-	SED	8.25E-16				
Ground water	4.03E-12	-	GW	7.23E-15				
Fish	4.37E-10	-	F	5.08E-12				
Vegetation	9.70E-10	-	VEG	2.35E-12				

Analysing the **air emission scenario** (1 mol h^{-1}) (Table 8) shows that:

- **fugacity** is highest for the air compartment, followed by soil, which has a slightly lower value. A high fugacity value for soil is determined by the magnitude of the input D values for soil, in particular through absorption (D_{VAS} = 1.41E+02 mol h^{-1} Pa^{-1}), not as effective for diffusive exchange with water, which is 4 orders of magnitude lower (D_{VAW} = 8.98E-02 mol h^{-1} Pa^{-1}). The higher diffusive velocity towards the ground is determined by the value of D at air-side diffusion (D_E = 1.53E+03 mol h^{-1} Pa^{-1}) and, in particular, by the high exchange surface area

between air and soil, which is about two orders of magnitude greater than the air-water exchange (A_{AW} = 1.00E+04 m^2; A_{AS} = 9.90E+05 m^2). The relevance of the contact surface is also valid for deposition phenomena from the air to the soil.

In addition, outflows from the air are larger than from the ground due to degradation, which is 4 orders of magnitude greater ($D_{DEG, A}$ = 4.02E+03 mol h^{-1} Pa^{-1}; $D_{DEG, S}$ = 7. 83E-01 mol h^{-1} Pa^{-1}), mainly due to the low half-life in air for benzene compared to soil ($\tau_{1/2, A}$ = 17 h; $\tau_{1/2, S}$ = 550 h), but, above all, to advection ($D_{ADV, A}$ = 1.06E+06 mol h^{-1} Pa^{-1}), a process that does not exist for soil.

- The **bulk concentration** is higher in the soil compartment than in the air, due to the higher value of the bulk Z (Z_{STOT} = 6.83E-04 mol m^{-3} Pa^{-1}; Z_{ATOT} = 4.11E-04 mol m^{-3} Pa^{-1}), the fugacity value being similar; in particular, the increase in the Z_{STOT} is given by the soil water phase, which is 78.8% of the total.
- Looking at the **phases**, in air, the highest concentration is in aerosols. This could be determined by the value of the Z_Q, which is greater than the Z_A, thus, the greater capacity of the aerosol phase to retain benzene (Z_Q = 1.3E-02 mol m^{-3} Pa^{-1}; Z_A = 4.1E-04 mol m^{-3} Pa^{-1}). Such a high value of Z_Q is determined by the octanol-water partition coefficient of benzene K_{OW}, i.e. the tendency of the substance to partition into octanol, representative of the organic part of aerosols.

  However, it is only possible to predict concentrations on the basis of Z values when the partition is at equilibrium, as in the case of the gas phase and aerosol, both being part of the air compartment (internally in phase equilibrium). In fact, $K_{AQ} = Z_A/Z_Q = C_A/C_Q$.
- The **fish** compartment exhibits fugacity very close to those of water. At first glance, one might think that this is due to the fact that the fish only exchanges fluxes with water, but although the sediment is in the same condition, it has much lower fugacity values and concentrations. From the resolution of the matrix for the fish and sediment equations, it can be seen that it is, once again obviously, the D values involved, i.e. the flux of chemical per unit fugacity (mol h^{-1} Pa^{-1}), are the discriminating factor.

  The D values for the above equations are (Table 9):

Table 9 Equations coefficients for sediments and fish compartments in the local model

Compartment	Parameter	Value (mol $h^{-1}Pa^{-1}$)	Formula
Sediments	SEDSED	1.21E-02	$D_T + D_{DEG, SED} + D_B + D_R$
	WSED	3.64E-06	$D_D + D_T$
Fish	WF	5.83E-03	$D_{VWF} + D_{AF}$
	FF	6.18E-03	$D_{MF} + D_{EF} + D_{GF} + D_{VFW}$

Where SEDSED and FF represent the fluxes per unit of fugacity from sediment and fish, respectively. It can be seen that the flux per unit fugacity of the input water is 3 orders of magnitude higher for fish (WF) than for sediment (WSED). The latter also have a higher overall exit rate (SEDSED) than fish (FF).

As far as the input to the fish from the water is concerned, this is higher than for sediment mainly due to the component due to uptake through the gills (D_{VWF} = 5.83E-3 mol h^{-1} Pa^{-1}), where it is mainly the value of k_1 = 46.43 h^{-1}, which corresponds to a time of 2.15E-02 h, indicating a rapid intake process, compared to the exit time by respiration (0.13 h), the shortest time between fish losses, and halving by metabolism (28.8 h).

Assessing the exits from the two compartments, for the SEDSED parameter the most significant component is the degradation rate, which in sediments is two orders of magnitude higher ($D_{DEG, SED}$ = 1.21E-02 mol h^{-1} Pa^{-1}) compared, for example, to the metabolism of fish (D_{MF} = 3.20E-04 mol h^{-1} Pa^{-1}), for the greater volume of sediments (V_{SED} = 5.00E+03 m^3) compared to aquatic biota (V_F = 7E-02 m^3);

- **Vegetation** has higher fugacity than water. Although the deposition input from air to vegetation is comparable or, at most, lower than that to water and the degradation D rates are comparable between the two compartments ($D_{DEG, VEG}$ = 5.14E-01 mol h^{-1} Pa^{-1}; $D_{DEG, W}$ = 3.66E-01 mol h^{-1} Pa^{-1}), the result could be determined by the presence of an important outflow for the water compartment due to advection ($D_{ADV,W}$ = 3.23E+02 mol h^{-1} Pa^{-1}), absent for vegetation.

  Vegetation exchanges fluxes with air (diffusion and deposition, parameter AVEG = 5.33E-04 mol h^{-1} Pa^{-1}) and soil (roots uptake, D_{VEGS} = 5.24E-08 mol h^{-1} Pa^{-1}) and, analysing the values of D, per unit of fugacity, the largest flux is that relating to the exit from the vegetation compartment by degradation and diffusion (parameter VEGVEG = 5.14E-1 mol h^{-1} Pa^{-1}):

  The VEGVEG parameter is governed almost entirely by the degradation reaction ($D_{DEG, VEG}$ = 5.14E-01 mol h^{-1} Pa^{-1}, due to the high volume of vegetation V_{VEG} = 9.90E+03 m^3.

  The most relevant input phenomenon is wet deposition from the air (D_{MAVEG} = 5.33E-04 mol h^{-1} Pa^{-1}), followed by root uptake from the soil (D_{VEGS} = 5.24E-08 mol h^{-1} Pa^{-1}), mainly due to the higher wet deposition rate compared to the uptake rate (U_M = 6E-05 m h^{-1}; $U_{UPTAKEROOTS}$ = 5.90E-07 m h^{-1}) and for the greater contact area between air and vegetation than that of the vegetation stems absorbing from the soil (A_{AVEG} = 4.95E+03 m^2; $A_{STEMVEG}$ = 49.5 m^2).
- The compartment with one of the lowest fugacities and concentrations is **groundwater**: the only input is due to soil leaching and two removal phenomena are namely advection and degradation. Analysing the values of D, i.e. the flux per unit fugacity, the removal processes (parameter GWGW = 3.23E+01 mol h^{-1} Pa^{-1}) are higher than the input ones (D_L = 1.40E-04 mol h^{-1} Pa^{-1}). In particular, advection provides the greatest contribution to removing (D_{GW} = 3.23E+01 mol h^{-1} Pa^{-1}).

Analyzing the **water emitting scenario** (1 mol h^{-1}) (Table 10):

Table 10 Fugacities and concentration results for benzene emission in water in the local model

Compartments (emitting = E)	Fugacity (Pa)	C_{bulk} (mol m^{-3})	Phase	C_{phase} (mol m^{-3})	Phase	C_{phase} (mol m^{-3})	Phase	C_{phase} (mol m^{-3})
Air	2.63E-10	1.08E-13	Agas	1.08E-13	Aaerosol	3.41E-12	-	-
Water (E)	3.09E-03	5.55E-06	Wdiss	5.55E-06	Wsusps	1.84E-05	-	-
Soil	2.30E-08	1.57E-11	Ssolid	6.86E-11	Swater	4.14E-11	Sair	9.46E-12
Sediments	9.26E-07	-	SED	5.51E-09	-	-	-	-
Ground water	9.98E-14	-	GW	1.79E-16	-	-	-	-
Fish	2.92E-03	-	F	3.39E-05	-	-	-	-
Vegetation	2.75E-13	-	VEG	6.65E-16	-	-	-	-

- **Fugacity** is highest in the water compartment, followed by the fish compartment, while soil has fugacity that is 5 orders of magnitude smaller and 7 for air. This difference with the other compartments is determined by the D

values of degradation and advection for water that are significantly smaller than for air (-4 orders of magnitude for both processes); soil has a fugacity two orders of magnitude greater than air, despite the contribution of water to soil represented by irrigation (D_{IRRIG} = 1.05E-03 mol h^{-1} Pa^{-1}) is lower than the diffusion rate from water to air (D_{VAW} = 8.98E-02 mol h^{-1} Pa^{-1}), insufficient to balance the processes of degradation and advection.

- **Bulk concentration** is similarly higher in the water compartment. Both phases of the water compartment report high concentrations, but the highest concentration is in the suspended solids. This could be determined by the fact that the Z_P is higher than Z_W, therefore greater ability of the suspended solids phase to retain benzene (Z_P = 5.6E-03 mol m^{-3} Pa^{-1}; Z_W = 1.8E-03 mol m^{-3} Pa^{-1}). However, it is only possible to predict concentrations on the basis of Z values when the partition is at equilibrium, such as between the dissolved water phase and the suspended solids, both being part of the water compartment (within the equilibrium between its phases). In fact, $K_{WP} = Z_W/Z_P = C_W/C_P$. Such a high value of Z_P is determined by the octanol-water partition coefficient K_{OW} of benzene, or the tendency of the substance to partition into octanol, representing the organic part of suspended solids.
- **Fish** has a slightly lower fugacity than water, but a higher concentration, as in the case of emission to air. The higher concentration is therefore given by the Z_F (1.16E-02 mol m^{-3} Pa^{-1}) higher than Z_W (1.8E-03 mol m^{-3} Pa^{-1}). The former is determined on the basis of the latter by multiplication with the K_{FW}, that is equal to 6.48. This suggests that if the two compartments were in equilibrium, the fish would have a higher concentration than the latter. Such a high value is determined by the octanol-water partition coefficient K_{OW} of benzene, i.e. the tendency of the substance to partition into octanol, representative of the lipid part of the fish.
- **Vegetation** presents fugacity and concentrations among the lowest compared to the other compartments. There is, in fact, no direct connection with water, but only with soil and air, the processes of which were analysed for the emitting compartment described above.
- The compartment with the lowest fugacity is **groundwater**, for which the same considerations made for emission to air apply, as there is no direct connection with water.

Analysing the scenario for **soil emission** (1 mol h^{-1}) (Table 11):

Table 11 Fugacities and concentration results for benzene emission in soil in the local model

Compartments (emitting = E)	Fugacity (Pa)	C_{bulk} (mol m^{-3})	Phase	C_{phase} (mol m^{-3})	Phase	C_{phase} (mol m^{-3})	Phase	C_{phase} (mol m^{-3})
Air	9.31E-07	3.82E-10	Agas	3.82E-10	Aaerosol	1.21E-08	-	-
Water	1.51E-06	2.70E-09	Wdiss	2.70E-09	Wsusps	8.97E-09	-	-
Soil (E)	7.03E-03	4.80E-06	Ssolid	2.09E-05	Swater	1.26E-05	Sair	2.89E-06
Sediments	4.51E-10	-	SED	2.69E-12	-	-	-	-
Ground water	3.04E-08	-	GW	5.46E-11	-	-	-	-
Fish	1.42E-06	-	F	1.65E-08	-	-	-	-
Vegetation	1.68E-09	-	VEG	4.07E-12	-	-	-	-

- **Fugacity** is highest in the soil compartment, followed by water and fish and lastly air, but the latter does not differ much from the former. The reasons why air has a lower fugacity than water, despite the volatilisation rate D (D_{VAS} = 1.41E+02 mol h^{-1} Pa^{-1}) is greater than the runoff rates ($D_{RUNOFF, W+S}$ = 6.93E-02 mol h^{-1} Pa^{-1}) which connects soil with water, may again lie in the higher degradation and advection rates of air compared to water.

  The fugacity occurring in the air compartment is slightly lower than that occurring for an emission into the air compartment: this result may be attributed to the high soil-air diffusion rate (D_{VAS} = 1.41E+02 mol h^{-1} Pa^{-1}).

- The **bulk concentration** is highest in the soil compartment, all phases of the soil compartment report high concentrations, but the highest concentration is in the solid phase (organic carbon). This could be determined by the fact that the Z_S is higher than Z_W and Z_A, therefore greater ability of the organic carbon phase to retain benzene (Z_A = 4.1E-04 mol m^{-3} Pa^{-1}; Z_W = 1.8E-03 mol m^{-3} Pa^{-1}; Z_S = 2.98E-03 mol m^{-3} Pa^{-1}). However, it is only possible to predict concentrations on the basis of Z values when the partition is at equilibrium, such as between the different phases of the same compartment. Such a high value of Z_S is determined by the octanol-water partition coefficient K_{OW} of benzene, i.e. the tendency of the substance to partition into the octanol, representative of the organic part of the solid.
- The **fish** compartment has slightly lower fugacity than water, but a higher concentration, as for the emitter scenarios illustrated above.
- **Sediment** is the compartment with the lowest fugacity and concentration values, due to the absence of direct connection to the soil.
- **Vegetation** has a higher fugacity and concentration than sediment due to the uptake rate with roots.
- The **groundwater** compartment shows non-negligible concentrations for the first time and is also higher than other receiving compartments, such as vegetation, due to the direct connection to the soil by leaching, which is four orders of magnitude higher than the uptake with roots by vegetation.

Summarising, the fugacity analysis shows that the emitting compartment is also the compartment with the highest fugacity after dispersion. This is possible due to the vector of the emission (i.e. of known terms), which will be zero everywhere except for the emitting compartment.

Mass fluxes and masses results

Table 12 Mass fluxes results for each emitting compartment in the local model

Processes	Formula f x D	Fluxes (mol h^{-1}) E_A = 1 mol h^{-1}	Fluxes (mol h^{-1}) E_W = 1 mol h^{-1}	Fluxes (mol h^{-1}) E_S = 1 mol h^{-1}
Diffusion A-W	f_A x D_{VAW}	8.41E-08	2.36E-11	8.36E-08
Deposition A-W	f_A x (D_{MAW} + D_{CAW} + D_{QAW})	1.01E-09	2.83E-13	1.00E-09
Diffusion A-S	f_A x D_{VAS}	1.32E-04	3.72E-08	1.32E-04
Deposition A-S	f_A x (D_{MAS} + D_{CAS} + D_{QAS})	9.98E-08	2.80E-11	9.92E-08
Diffusion W-A	f_W x D_{VAW}	4.16E-11	2.78E-04	1.35E-07
Diffusion S-A	f_S x D_{VAS}	1.32E-04	3.26E-06	**9.94E-01**
Irrigation W-S	f_W x D_{IRRIG}	4.85E-13	3.24E-06	1.58E-09
Runoff S-W	f_S x ($D_{RUNOFFS}$ + $D_{RUNOFFW}$)	6.46E-08	1.60E-09	4.87E-04
Advection A	f_A x $D_{ADV,A}$	**9.96E-01**	2.80E-04	9.90E-01
Advection W	f_W x $D_{ADV,W}$	1.49E-07	**9.99E-01**	4.87E-04
Degradation A	f_A x $D_{DEG,A}$	3.76E-03	1.06E-06	3.74E-03
Degradation W	f_W x $D_{DEG,W}$	1.69E-10	1.13E-03	5.51E-07
Degradation S	f_S x $D_{DEG,S}$	7.29E-07	1.80E-08	5.50E-03
Degradation SED	f_{SED} x $D_{DEG,SED}$	1.68E-15	1.12E-08	5.48E-12
Degradation GW	f_{GW} x $D_{DEG,GW}$	1.47E-13	3.65E-15	1.11E-09
Degradation F	f_F x $D_{DEG,F}$	1.50E-13	1.01E-06	4.90E-10
Degradation VEG	f_{VEG} x $D_{DEG,VEG}$	4.99E-10	1.41E-13	8.65E-10

A preliminary analysis of the process flow categories shows, for each emitting scenario, having indicated in green input processes and in orange output processes for the emitting compartment itself (Table 12):

- all the most relevant flows are related to output processes from the compartment under consideration (highlighted in bold);
- the most relevant output flow for air and water is advection, for soil volatilisation; for all three, degradation follows;
- The most relevant input flux is volatilisation from soil for air, adsorption for water and soil.
- The air and soil scenarios result in very similar mass fluxes leaving the air compartment, as the calculated fugacity for the air compartment is very close in the two scenarios.

It is possible to calculate the masses permanently stationary in the compartments after emissions and in steady state, according to the general formula (Eq. 124), where the subscript i is used to denote the receiving compartment (Table 13):

$$M_i\ (mol) = f_i\ (Pa) \times Z_i\ (mol\ m^{-3} Pa^{-1}) \times V_i\ (m^3) \qquad \text{(Eq. 124)}$$

Table 13 Masses results for each emitting compartment in the local model

Receiving compartment *i*	**M_i (mol) $E_{A,LOC}$ = 1 mol h^{-1}**	**M_i (mol) E_{WLOC} = 1 mol h^{-1}**	**M_i (mol) $E_{S,LOC}$ = 1 mol h^{-1}**
Air_{bulk}	**9.22E-02**	2.59E-05	9.17E-02
$Water_{bulk}$	4.15E-08	**2.77E-01**	1.35E-04
$Soil_{bulk}$	6.32E-03	1.56E-04	**4.77E+01**
Sediments	4.13E-12	2.76E-05	1.34E-08
Ground water	3.62E-11	8.95E-13	2.73E-07
Fish	3.55E-13	2.37E-06	1.16E-09
Vegetation	2.32E-08	6.59E-12	4.03E-08
Total	9.86E-02	2.78E-01	4.78E+01

The largest mass is always in the emitting compartment and there are more significant differences between those compartments showing similar or at least the same order of magnitude fugacities, attributable to the different volumes of the compartments. In the soil-emitting scenario, the greatest mass "storage" of benzene occurs (row Total of Table 13), almost all of which resides in the soil, while in the air-emitting scenario the least "storage" occurs: in both cases, the results are related to the advective process, absent for the former, present and high for the latter. In the latter case, in fact, since the advective rate is much higher ($D_{ADV,A}$ = 1.06E+06 mol h^{-1} Pa^{-1}) compared to the other compartment exchange rates, the dispersion of benzene in the local world unit is more limited than in the other emitter scenarios.

Analogous to the USEtox fate matrix, these masses can also be interpreted as the residence times in the individual receiving compartments under steady-state conditions, which take into account all processes occurring in each compartment.

3.2.4 Fate factors

The resulting concentrations, converted into mg using the molecular weight of benzene, were used to calculate the Fate factors, one for each receiving compartment.

For compartments made of different phases. i.e. air, water and soil, the selected concentration was that of the prevailing phase for air and water, and water phase for soil, according to the following general Eq. 125:

$$FF_{x,i} = C_{x,i} \times 10^{-6} \times V_{x,i} \quad \text{(Eq. 125)}$$

Where $FF_{x,i}$ $(kg_{comp}\ h\ kg^{-1}\ or\ h)$ is the fate factor for the x phase of compartment i, $C_{x,i}$ $(mg\ m^{-3}\ mg_E^{-1}\ h)$ is the concentration in the x phase of compartment i for a hourly unit emission, $10^{-6}\ kg\ mg^{-1}$ is a conversion factor, $V_{x,i}$ (m^3) is the volume of the x phase of compartment i.

The fate factors results for each compartment and each emitting scenario are reported in Table 14:

Table 14 FF results for emission of benzene for each emitting compartment in the local model

Compartment	Formula	FF_i (h) (E_A = 1 kg h^{-1})	FF_i (h) (E_W = 1 kg h^{-1})	FF_i (h) (E_S = 1 kg h^{-1})
Air	$FF_{g,A} = C_{g,A} \times 10^{-6} \times V_{g,A}$	7.21E-03	2.02E-06	7.16E-03
Freshwater	$FF_{w,W} = C_{w,W} \times 10^{-6} \times V_{w,W}$	3.24E-09	2.17E-02	1.06E-05
Soil	$FF_{w,S} = C_{w,S} \times 10^{-6} \times V_{w,S}$	3.89E-04	9.63E-06	2.94E+00
Groundwater	$FF_{GW} = C_{GW} \times 10^{-6} \times V_{GW}$	3.62E-11	8.95E-13	2.73E-07
Fish	$FF_F = C_F \times 10^{-6} \times V_F$	2.78E-14	1.85E-07	9.04E-11
Sediments	$FF_{SED} = C_{SED} \times 10^{-6} \times V_{SED}$	3.22E-13	2.15E-06	1.05E-09
Vegetation	$FF_{VEG} = C_{VEG} \times 10^{-6} \times V_{VEG}$	1.82E-09	5.14E-13	3.15E-09

The choice of using for multi-phase compartments a phase concentration rather than the bulk one is driven by the need of expressing, in the following steps, the bioavailable mass of chemical, i.e. the mass of chemical to which the living beings are exposed to, as better reported in the following sections.

The FFs of groundwater and sediments are no longer used in this work, since the following steps of evaluation of ecotoxicology are focused on air, freshwater and soil, only. In fact, a simplifying assumption is made, stating that life is only present in the above-mentioned compartments, so the assessment of biodiversity loss is limited to them.

3.2.5 Exposure factors

The purpose of the exposure factor is to quantify the uptake by living beings exposed to a certain concentration. This concentration is calculated with the fate model as the bioavailable concentration.

The calculation for the exposure factor XF is differentiated between man and ecosystem, similarly to the USEtox model, since the subsequent steps of the analysis consider the dose for man and the bioavailable environmental concentration for the ecosystem as the starting point for determining the effect, respectively. The quantification of human exposure therefore takes place on the basis of the intake mass, for the ecosystem on the basis of the bioavailable concentration.

Since the bioavailable concentration was already included in the FFs in this model, the XF for the ecosystem becomes superfluous, so only the procedure for calculating the XF for humans is given below (Table 15).

The exposure calculation must take into account the exposure pattern, related to a certain environmental concentration, by the entire population at the local scale. In the present study, the value considered by USEtox on the urban scale (8333 persons km^{-2}, result of 2 x 10^6 people over 240 km^2), which is comparable to the local scale due to its small size, was taken as a reference for the number of people present, and halved to take into account a certain distance existing between the emitting point and the beginning of the built-up area, as illustrated in chapter 5.

The exposure modes envisaged in this study, similar to the USEtox model, are inhalation and ingestion, of water and food.

With regard to the ingestion of food, two separate XFs were defined for the ingestion of fish and vegetation. These two foods were chosen because they represented the two compartments included in the present study and of which the concentration that could be used for intake quantification had therefore been calculated. Vegetation is assumed to represent the entire intake of fruit and vegetables.

The general formula for quantifying chemical exposure in a medium via an exposure route ***j*** is (Eq. 126):

$$XF_j = \frac{G_j \times Pop_{loc}}{V_i} \qquad \text{(Eq. 126)}$$

where XF_j (h^{-1}) is the exposure factor via j, G_j $(m^3 h^{-1})$ is the volume of the medium taken up in the unit of time through the exposure route ***j***, Pop_{loc} is the number of people on the local scale, V_i (m^3) is the volume of the compartment.

An intake rate is therefore made explicit with respect to the total medium containing the mass of chemical. The route of exposure to food is quantified by mass rather than volume, according to the formulas detailed below based on Eq. 126:

Table 15 XF results for the local model

Exposure route *j*	Formula	Parameters	XF_j (h^{-1})
$Inhalation_A$	$XF_{inh} = \frac{G_{Breath} \times Pop_{loc}}{V_{g,A}}$	$G_{Breath} = 0.54\ m^3 h^{-1}$ human breathing rate	9.40E-06
$Ingestion_W$	$XF_{ing,w} = \frac{G_{Drink} \times Pop_{loc}}{V_{w,W}}$	$G_{Drink} = 1.67E-03\ m^3 h^{-1}$ hourly water ingestion rate	1.39E-04
$Ingestion_F$	$XF_{ing,F} = \frac{G_{Ing,F} \times Pop_{loc}}{V_F} \times \frac{1}{Dens.F}$	$G_{Ing,F} = 1.19E-03\ kg\ h^{-1}$ hourly fish ingestion rate (estimated) $Dens.F = 1.3\ t\ m^{-3} \times 10^3\ kg\ t^{-1}$ fish density (estimated)	5.45E-02
$Ingestion_{VEG}$	$XF_{ing,VEG} = \frac{G_{Ing,VEG} \times Pop_{loc}}{V_{VEG}} \times \frac{1}{Dens.Veg}$	$G_{Ing,VEG} = 3.3E-02\ kg\ h^{-1}$ hourly vegetation ingestion rate (estimated) $Dens.Veg = 1.2\ t\ m^{-3} \times 10^3\ kg\ t^{-1}$ vegetation density (estimated)	1.17E-05

The exposure factors calculated so far do not depend on the emitting compartment, so the values proposed are constant.

3.2.6 Effect factors

The purpose of the effect factor (EF) is to correlate the calculated intake mass with the corresponding toxicological effect. The definition of EFs for human health was made in accordance with the values reported by USEtox v.2.12 for benzene according to Eq. 24 and are summarised in Table 16.

Table 16 EF results of benzene for human toxicity from USEtox v.2.12 (Fantke et al. 2017)

Type of parameter	Name	Value	Unit of measure
Lifetime inhalation dose inducing non-cancer disease in 50% of population	$ED50_{inh,noncanc}$	1.35E+02	kg_{intake} $lifetime^{-1}$
Lifetime ingestion dose inducing non-cancer disease in 50% of population	$ED50_{ing,noncanc}$	1.35E+02	kg_{intake} $lifetime^{-1}$
Lifetime inhalation dose inducing cancer in 50% of population	$ED50_{inh,canc}$	3.41E+01	kg_{intake} $lifetime^{-1}$
Lifetime ingestion dose inducing cancer in 50% of population	$ED50_{ing,canc}$	3.41E+01	kg_{intake} $lifetime^{-1}$
Multiplier non cancer	0.5		-
Multiplier cancer	0.5		-
Effect factor non-cancer via inhalation	$EFhum_{inh,noncanc}$	3.72E-03	cases kg_{intake}^{-1}
Effect factor non-cancer via ingestion	$EFhum_{ing,noncanc}$	3.72E-03	cases kg_{intake}^{-1}
Effect factor cancer via inhalation	$EFhum_{inh,canc}$	1.47E-02	cases kg_{intake}^{-1}
Effect factor cancer via ingestion	$EFhum_{ing,canc}$	1.47E-02	cases kg_{intake}^{-1}

The assessment of biodiversity loss for the ecosystem is the basis for the definition of the effect factor. This is assessed by considering the most common species for the three main receiving compartments, namely air, water and soil. The eco-toxicity of air and soil is currently absent in USEtox, because as reported in chapter 2.3, a large number of reliable toxicological test results and appropriate extrapolation factors, specific to each compartment, are required.

In the present study, in order to also include air and soil toxicity, several approximations are made; in particular, the absence of specific extrapolation factors is filled by adopting water factors (Posthuma et al. 2019) and the data basket used is rather limited.

Aware of the limitations present, a preliminary model is proposed below for the assessment of ecotoxicity in all major environmental compartments (air, water and soil). The quantification of EF for the freshwater compartment is also repeated in order to obtain factors in a consistent manner, since they are affected by the same limitations and are the result of the same procedure.

The definition of the effect factors, in accordance with the USEtox framework as outlined in chapter 2.3, is based on a number of toxicological test data required for each compartment. In particular, as also reported in chapter 2.3, at least three species groups are required for each compartment in order to represent a sufficiently broad biodiversity. The three species groups were selected by attempting to reconstruct the food chain for each compartment, with each group feeding on the previous one:

$$I\ group \rightarrow II\ group \rightarrow III\ group$$

Within each group, at least three species were identified whenever possible, based on the availability of toxicological data and giving preference to species of increasing size (e.g. a low garden plant, a medium-sized bushy plant and a tree). When there were not at least three different species present, more data belonging to the same species were used.

Selected species groups (Table 17) may be exposed to the concentrations of more than one compartment, as is the case for vegetation, which receives the chemical by deposition and diffusion from the air and soil through uptake with the roots of the water phase; others, however, are only exposed to the concentration of one compartment, as they are considered to live permanently in it: this is the case for worms and microorganisms inhabiting the soil and the species selected for the water compartment, i.e. vegetation, crustaceans and fish.

In addition to the three groups of species, a fourth is selected in the present study to consider the damage due to the concentration of the chemical in water following exposure by ingestion by a terrestrial vertebrate animal. For this purpose, the corresponding toxicity compartment was called "Water+Oral ingestion" in the table below.

The species selected for each group could be expanded, especially in the air, where an important absence is birds and bees, due to their delicate role in ensuring ecosystem balance, and the soil, due to the absence of rodents, such as moles, or larger insects. The implementation of these species is reserved for future development.

Table 17 Selected species for ecosystem toxicity assessment in the local model. Species accompanied by (*) indicate that the exact name was not specified in the source.

Species group	Air species	Soil species	Freshwater species
I - Vegetation	Cabbage (*brassica oleracea*)	Lettuce	Green algae (*scenedesmus abundans*)
	Tobacco plant	Yellow lupin	Green algae (*chlamydomonas angulosa*)
	Terrestrial plants (*)	Spring rape (*Brassica Napus* var. *oleifera*)	Green algae (*chlorella vulgaris*)
	-	Salix	Green algae (*ankistrodesmus falcatus var. acicularis*)
II – Insects (A) / microorganisms (S) / crustaceans (W)	Fruit fly (*drosophila*)	Actinomycetes	Calanoid Copepod (*diaptomus forbesi*)
	Insect (*)	Fungi	Water Flea (*ceriodaphnia dubia*)
	Grass beetle (*tribolium castaneum*)	Nitrogen immobilizing bacteria	Water Flea (*daphnia magna*)
III – Terrestrial vertebrates (A) / worms (S) / fishes (W)	Mouse	Worm	Fathead Minnow (*pimephales promelas*)
	Rat	Collembola	Bluegill (*lepomis macrochirus*)
	-	-	Rainbow trout (*oncorhynchus mykiss*)
IV – Terrestrial vertebrates (W)	-	-	Red fox

For each selected species, at least three chronic EC_{50} data should be collected and, on these, a geometric mean should be performed at individual species level. The geometric averages of the individual species are again to be further geometrically averaged, therefore, the procedure followed first involved the calculation of the $\log_{10}$ of the EC_{50}s of the individual species, which was then arithmetically averaged at the compartment level to obtain the HC_{50} as shown in Eq. 25.

In the present study, due to limited data availability, hardly any EC_{50} data were collected at the level of each individual species, with a few exceptions in order to make up for the absence of an adequate number of species for each group, such as for the third group for air and soil. Only in these cases, therefore, was a geometric mean performed at species level.

The data found in the literature were rarely chronic EC_{50}s, so extrapolation factors had to be used, both for the duration of the test and for the type of working point available. The operations performed are shown below (Table 18) were applied as reported by (Posthuma et al. 2019):

Table 18 Extrapolation factors for aquatic toxicity from Posthuma et al. (2019)

Working point	Test duration	Treated as	Extrapolation factors to chronic EC_{50}
NOAEC	chronic	-	10 (chronic NOAEC to acute EC_{50}) 0.33 (acute EC_{50} to chronic EC_{50})
EC_0, LOAEC, EC_{10}	acute	acute NOAEC	0.33 (acute NOAEC to chronic NOAEC) 10 (chronic NOAEC to acute EC_{50}) 0.33 (acute EC_{50} to chronic EC_{50})
EC_{50}	acute	-	0.33 (acute EC_{50} to chronic EC_{50})
EC_{70}, EC_{80}, LC_{25}, LC_{50}, LC_{70}, LC_{75}	acute/chronic	acute EC_{50}	0.33 (acute EC_{50} to chronic EC_{50})

When the starting concentration data was expressed in ppb or ppm by volume, this was converted to kg m^{-3}, taking into account that 24.45 dm^3 mol^{-1} is the molar volume of an ideal gas at 25°C and 1 atm, as shown in Table 19.

For many studies, the working point was not made explicit, but concentration values and effects in % or absolute terms on individuals of the species were given. To fill this and other gaps, several assumptions were made.

In particular, for the fruit fly (*drosophila*) the reported concentration value is taken as EC_{10} because 3 out of 28 fruit flies tested have 1 chromosome with mutation, i.e. about 10% of the entire species considered.

For spring rape, the reported soil concentration value of petrol, taken as a proxy for benzene, is taken as EC_{70} (10 cm^3 kg^{-1} of soil) because a reduction in the mass of the vegetation from 448 g to 122 g was noted, assuming that the loss of mass equals the reduction in the number of plants.

For yellow lupin, the reported soil concentration value of diesel oil, taken as a proxy for benzene, for the above ground parts, 6.76 g kg^{-1} of soil affects the yield from 100% to 20%, thus assuming it to be an EC_{80}.

For actinomycetes, unleaded petrol is assumed as a proxy for benzene and the damage is assessed by taking the dose of 2 cm^3 kg^{-1} of soil for the scenario where the soil is not fertilised, as this is the concentration that causes the most damage. This is determined to be an LC_{70} because the number of microorganisms present without pollution (dose 0) is approximately 10 and is reduced to 3 after the 2 cm^3 kg^{-1} soil dose.

For fungi, unleaded petrol is taken as a proxy for benzene and the damage is assessed by taking the 2 cm^3 kg^{-1} soil dose for the scenario in which the soil is not fertilised as this is the concentration that causes the most damage. This is determined to be an LC_{75} because the number of microorganisms present without pollution (dose 0) is approximately 14 and is reduced to 3.5 after the 2 cm^3 kg^{-1} soil dose.

For nitrogen immobilising bacteria, unleaded petrol is taken as a proxy for benzene and the damage is assessed by taking the 2 cm^3 kg^{-1} soil dose for the scenario where the soil is not fertilised as this is the concentration that causes the most damage. This is determined to be an LC_{70} because the number of microorganisms present without pollution (dose 0) is approximately 11 and is reduced to 3.5 after the 2 cm^3 kg^{-1} soil dose.

For collembolas, the LC_{50} value of 300 mg kg^{-1} of soil is obtained by considering the 50 mg kg^{-1} of soil for each of the six PAHs considered, taken as a proxy for benzene, since this is a mortality test with a rate of around 50%. Similarly, to obtain the second value for collembolas (LC_{25} of 81 mg kg^{-1}), an average was taken between the two values reported for coarse soil (63 mg kg^{-1}) and fine soil (99 mg kg^{-1}).

Average concentration values were assumed for cabbage, tobacco plant and grass beetle as a range of 150-3000 Pb, 17.2-32.4 g m^{-3} and 10000-210000 mg m^{-3}, respectively, was reported.

Regarding the duration of the tests, when not explicit, this was assumed to be acute if the reported duration was between 1 and 24 hours (Posthuma et al. 2019) and if there was a single administration, in all other cases it was assumed to be chronic.

For aquatic species, the database consulted for each of them is EPA ECOTOX Knowledgebase (Olker et al. 2022; United States Environmental Protection Agency (US EPA) 2022), for the other compartments, scientific articles and governmental reports reporting several national studies were consulted, when the single source could not be traced.

Below are the data, the procedures for the calculation, the main parameters used and the results of the HC_{50}s, contained in the "Substance data sheet" of the calculation tool, as well as the result of the EFs (Table 19), contained in the "Effect factors sheet" of the calculation tool, which are constant irrespective of the emitting scenario, similar to the XFs.

Table 19 Ecotoxicity data of benzene and calculation of HC_{50S} for benzene in each compartment

	Air			Soil			Water		
Species group	**Type of data**	**Value**	**Source**	**Type of data**	**Value**	**Source**	**Type of data**	**Value**	**Source**
I - Vegetation	Terrestrial plants: acute LC_{50} (mg m^{-3})	10000	(Government of Canada et al. 1993)	Springrape: acute EC_{70} (cm^3 kg^{-1})	10	(Wyszkowski and Ziólkowska 2009)	Green algae: chronic EC_{50} (mg L^{-1})	1360	(Olker et al. 2022; United States Environmental Protection Agency (US EPA) 2022)
	Brassica oleracea: acute LOAEC (ppb)	1500	(Dumez et al. 2015)	Yellowlupin: acute EC_{80} (g kg^{-1})	6.76	(Wyszkowski et al. 2004)	Green algae: chronic EC_{50} (mg L^{-1})	461	
	Tobacco plant: acute EC_0 (g m^{-3})	24.8	(European Chemicals Agency (ECHA) 2008)	Salix: chronic EC_{50} (mg L^{-1})	292	(Clausen and Trapp 2017)	Green algae: chronic EC_{50} (mg L^{-1})	312.5	
	-	-	-	Lettuce: acute EC_{50} (mol m^{-3})	1	(Olker et al. 2022; United States Environmental Protection Agency (US EPA) 2022)	Green algae: chronic EC_{50} (mg L^{-1})	310	
II - insect/microorg.	Drosophila: acute EC_{10} (ppm)	27000	(Kale and Kale 1995)	Actinomycetes: acute LC_{70} (cm^3 kg^{-1})	2	(Wyszkowska and Kucharski 2001)	Calanoid Copepod: acute EC_{50} (mg L^{-1})	710	
	Insect: acute LC_{50} (mg m^{-3})	15500	(Government of Canada et al. 1993)	Fungi: acute LC_{75} (cm^3 kg^{-1})	2	(Wyszkowska and Kucharski 2001)	Water Flea: acute EC_{50} (mg L^{-1})	31.25	
	Tribolium castaneum: acute LC_{50} (mL L^{-1})	115.9	(Pajaro-Castro et al. 2017)	Nitrogen immobilizing bacteria: acute LC_{70} (cm^3 kg^{-1})	2	(Wyszkowska and Kucharski 2001)	Water Flea: acute EC_{50} (mg L^{-1})	10.15	
III - vertebrates/worm/fish	Mouse: chronic NOAEC (mg m^{-3})	960	(Olker et al. 2022; United States Environmental Protection Agency (US EPA) 2022)	Worm: chronic LC_{50} (mg kg^{-1})	1.9	(Doherty et al. 2019)	Fathead Minnow: acute EC_{50} (mg L^{-1})	2300	
	Mouse: chronic NOAEC (mg m^{-3})	32	(Olker et al. 2022; United States Environmental Protection Agency (US EPA) 2022)	-	-		Blue gill: acute EC_{50} (mg L^{-1})	1520.1	
	Rat: chronic LOAEC (ppm)	10	(European Chemicals Agency (ECHA) 2008)	Collembola: acute LC_{50} (mg kg^{-1})	300	(Leonardi 2008)	Rainbow trout: acute EC_{50} (mg L^{-1})	1038.911	
	-	-	-	Collembola: acute LC_{25} (mg kg^{-1})	81	(Canadian Council of Ministers of the Environment 2004)	Red fox: chronic NOAEC (µg L^{-1})	3.00E+05	

Compartment	Species group	Conversions in EC_{50} (kg m^{-3}) formulas	Geom. mean	log_{10}	$logHC_{50}$	HC_{50}
Air	I - Vegetation	**Terrestrial plants**	-	-2.48	-2.48	3.3E-03
		= 10000 mg m^{-3} x 10^{-6} kg mg^{-1} x 0.33 = 3.33E-03 kg m^{-3}				
		Cabbage		-4.8		
		= 1500 ppb x 10^{-3} ppm ppb^{-1} x 10^{-3} m^3 dm^{-3} / 24.45 dm^3 mol^{-1} x 7.81E-02 kg mol^{-1} x 10 x 0.33 = 1.60E-05 kg m^{-3} (24.45 dm^3 mol^{-1} is ideal gas molar volume; 7.81E-02 kg mol^{-1} is benzene molecular weight)				
		Tobacco plant		-1.08		
		= 24.8 g m^{-3} x 10^{-3} kg g^{-1} x 10 x 0.33 = 8.27E-02 kg m^{-3}				
	II - Insects	**Fruit fly**	-	-0.54		
		= 27000 ppm x 10^{-3} m^3 dm^{-3} / 24.45 dm^3 mol^{-1} x 7.81E-02 kg mol^{-1} x 10 x 0.33 = 0.29 kg m^{-3} (24.45 dm^3 mol^{-1} is ideal gas molar volume; 7.81E-02 kg mol^{-1} is benzene molecular weight)				
		Insects		-2.29		
		= 15500 mg m^{-3} x 10^{-6} kg mg^{-1} x 0.33 = 5.17E-03 kg m^{-3}				
		Grass beetle		-1.47		
		= 115.9 µL L^{-1} x 10^{-6} L $µL^{-1}$ x 10^3 L m^{-3} x 876.5 kg m^{-3} x 0.33 = 3.39E-02 kg m^{-3} (876.5 kg m^{-3} is benzene density)				
	III - Vertebrates	**Mouse I**	5.84E-04	-3.23		
		= 960 mg m^{-3} x 10^{-6} kg mg^{-1} x 10 x 0.33 = 1.07E-04 kg m^{-3}				
		Mouse II				
		= 32 mg m^{-3} x 10^{-6} kg mg^{-1} x 10 x 0.33 = 3.20E-03 kg m^{-3}				
		Rat		-3.97		
		= 10 ppm x 10^{-3} m^3 dm^{-3} / 24.45 dm^3 mol^{-1} x 7.81E-02 kg mol^{-1} x 10 x 0.33 = 1.06E-04 kg m^{-3} (24.45 dm^3 mol^{-1} is ideal gas molar volume; 7.81E-02 kg mol^{-1} is benzene molecular weight)				
Soil	I - Vegetation	**Spring rape**	-	0.64	-5.38	0.26
		= 10 cm^3 kg^{-1} x 10^{-3} dm^3 cm^{-3} x 876.5 g dm^{-3} x 10^{-3} kg g^{-1} x 1500 kg m^{-3} x 0.33 = 4.38 kg m^{-3} (1500 kg m^{-3} is soil density; 876.5 g dm^{-3} is benzene density)				
		Salix		-0.53		
		= 292 g m^{-3} x 10^{-3} kg g^{-1} = 0.292 kg m^{-3}				
		Yellow lupin		0.53		
		= 6.76 g kg^{-1} x 10^{-3} kg g^{-1} x 1500 kg m^{-3} x 0.33 = 3.38 kg m^{-3} (1500 kg m^{-3} is soil density)				
		Lettuce		-1.59		
		= 1 mol m^{-3} x 7.81E-02 kg mol^{-1} x 0.33 = 2.6E-02 kg m^{-3} (7.81E-02 kg mol^{-1} is benzene molecular weight)				
	II - Microorg.	**Actynomycetes**	-	-0.057		

		= 2 cm^3 kg^{-1} x 10^{-6} m^3 cm^{-3} x 876.5 g dm^{-3} x 1500 kg m^{-3} x 0.33 = 0.88 kg m^{-3} (1500 kg m^{-3} is soil density; 876.5 g dm^{-3} is benzene density)				
		Nitrogen immobilizing bacteria		-0.057		
		= 2 cm^3 kg^{-1} x 10^{-6} m^3 cm^{-3} x 876.5 g dm^{-3} x 1500 kg m^{-3} x 0.33 = 0.88 kg m^{-3} (1500 kg m^{-3} is soil density; 876.5 g dm^{-3} is benzene density)				
		Fungi		-0.057		
		= 2 cm^3 kg^{-1} x 10^{-6} m^3 cm^{-3} x 876.5 g dm^{-3} x 1500 kg m^{-3} x 0.33 = 0.88 kg m^{-3} (1500 kg m^{-3} is soil density; 876.5 g dm^{-3} is benzene density)				
	III - Big worm	**Worm**	-	-3.02		
		= 1.9 mg kg^{-1} x 10^{-6} kg mg^{-1} x 1500 kg m^{-3} x 0.33 = 9.5E-04 kg m^{-3} (1500 kg m^{-3} is soil density)				
		Collembola I	7.8E-02	-1.11		
		= 300 mg kg^{-1} x 10^{-6} kg mg^{-1} x 1500 kg m^{-3} x 0.33 = 0.15 kg m^{-3} (1500 kg m^{-3} is soil density)				
		Collembola II				
		= 81 mg kg^{-1} x 10^{-6} kg mg^{-1} x 1500 kg m^{-3} x 0.33 = 4.1E-02 kg m^{-3} (1500 kg m^{-3} is soil density)				
Water+Oral ingestion	**I - Algae**	**Green algae I**	-	0.13	-0.65	0.22
		= 1360 g m^{-3} x 10^{-3} kg g^{-1} = 1.36 kg m^{-3}				
		Green algae II		-0.34		
		= 461 g m^{-3} x 10^{-3} kg g^{-1} = 0.46 kg m^{-3}				
		Green algae III		-0.51		
		= 312.5 g m^{-3} x 10^{-3} kg g^{-1} = 0.31 kg m^{-3}				
		Green algae IV		-0.51		
		= 310 g m^{-3} x 10^{-3} kg g^{-1} = 0.31 kg m^{-3}				
	II - Crustacean	**Calanoid copepod**	-	-0.63		
		= 710 g m^{-3} x 10^{-3} kg g^{-1} x 0.33 = 0.24 kg m^{-3}				
		Water flea I		-1.98		
		= 31.25 g m^{-3} x 10^{-3} kg g^{-1} x 0.33 = 1.04E-02 kg m^{-3}				
		Water flea II		-2.47		
		= 10.15 g m^{-3} x 10^{-3} kg g^{-1} x 0.33 = 3.38E-03 kg m^{-3}				
	III - Fish	**Fathead minnow**	-	-0.12		
		= 2300 g m^{-3} x 10^{-3} kg g^{-1} x 0.33 = 7.67E-01 kg m^{-3}				
		Bluegill		-0.3		
		= 1520.1 g m^{-3} x 10^{-3} kg g^{-1} x 0.33 = 5.07E-01 kg m^{-3}				

		Rainbow trout		-0.46		
		= 1038.911 g m^{-3} x 10^{-3} kg g^{-1} x 0.33 = 3.64E-01 kg m^{-3}				
	IV- Red fox	**Red fox**	-	0		
		= 3E05 mg m^{-3} x 10^{-6} kg g^{-1} x 10 x 0.33 = 1 kg m^{-3}				

The calculation of the EF effect factors produced the following results (Table 20), based on the model of Eq. 28, which is designed to determine the angular coefficient of the straight line passing through the origin and the 50% fraction of potentially affected species (PAF) due to the hazardous concentration of the HC_{50} compartment to which the species considered in it are exposed.

Table 20 Calculation of EFs for ecotoxicity

Compartments	EF_i (PAF m^3 kg^{-1})
Air	$EF_A = \frac{0.5\ PAF}{3.3\text{E}-03\ \text{kg}\ m^{-3}} = 151.74$
Water	$EF_W = \frac{0.5\ PAF}{0.22\ \text{kg}\ m^{-3}} = 2.24$
Soil	$EF_S = \frac{0.5\ PAF}{0.26\ \text{kg}\ m^{-3}} = 1.92$

The factor obtained for the water compartment EF_W calculated *ex novo* in this study is one order of magnitude lower than that calculated by USEtox v. 2.12 for the same compartment (EF_{eco}(frw) = 15.4 PAF m^3 kg^{-1}). The reason is under investigation and will be deepened in a future development. The inclusion of a terrestrial animal, red fox, has a marginal impact, since excluding the concentration for this species results in $EF_W = 2.6\ PAF\ m^3 kg^{-1}$.

The factor obtained for soil is comparable to that for water. In other calculation methods, e.g. IMPACT 2002+ (Jolliet et al. 2003), the calculation of the soil HC_{50} from that of water is proposed, thus exploiting the presence of the soil pore water phase, according to Eq. 127:

$$HC_{50,S} = HC_{50,W} \times \left(K_f \times \rho_{solid} + v_{w,S}\right) \qquad \text{(Eq. 127)}$$

where K_f $(L\ kg^{-1})$ is the soil solid-water benzene partition coefficient, ρ_{solid} $(kg\ m^{-3})$ is the density of the soil solid and $v_{w,S}$ is the volume fraction of the water phase in the soil.

Assigning these parameters values from the literature, respectively $K_f = 2.97\ L\ kg^{-1}$ (Zytner 1994), $\rho_{solid} = 2.17\ kg\ m^{-3}$ and $v_{w,S} = 0.3$, it is obtained $HC_{50,S} = 1.5\ kg\ m^{-3}$ and, as consequence, $EF_S = 0.33\ PAF\ m^3 kg^{-1}$, with an 83% reduction in EF_S. However, it is decided not to use this second illustrated method for the calculation of the soil factor, which might be suitable in the case of a total lack of soil toxicity data.

The effect factor obtained for air has the highest level of damage for the plant and animal species that inhabit it, especially cabbage has the lowest EC_{50}, and is therefore the most affected species.

Below are the EFs, i.e. the angular coefficients of the straight lines connecting the origin with the co-ordinate point (HC_{50}; 0.5) of the concentration-fraction diagram of affected species, constructed for benzene for the 3 eco-toxicities, i.e. air eco-toxicity (Figure 12a), aquatic eco-toxicity (Figure 12b) and terrestrial eco-toxicity (Figure 12c).

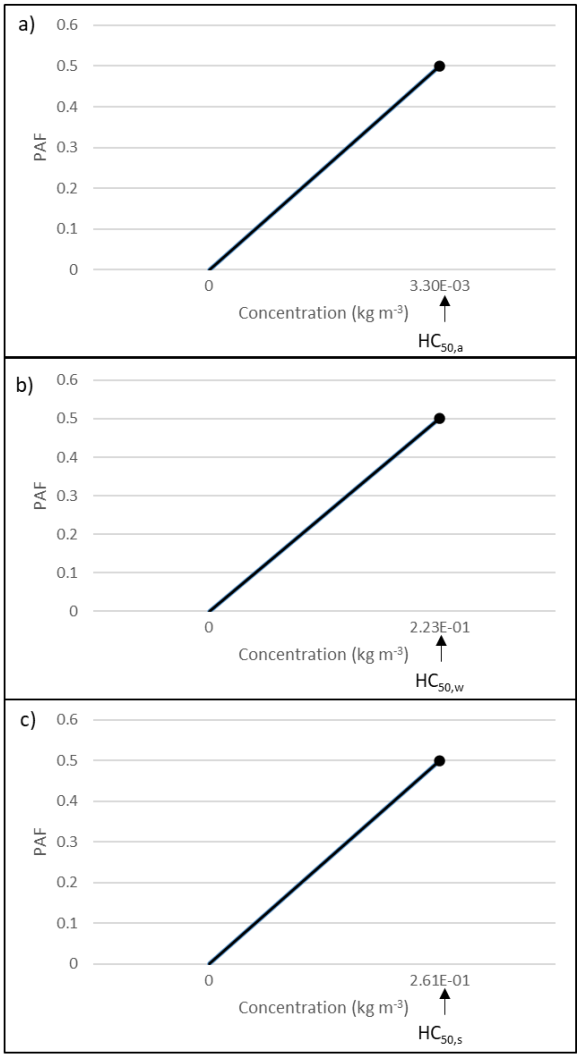

Figure 12 Linear extrapolation proposals for ecosystem EFs. a) air EF; b) water EF; c) soil EF

Since the pollutant dispersion model also allowed the concentration to be assessed for the vegetation and fish compartments, this intake concentration could be correlated with the damage with additional literature data. This second way of assessing eco-toxicity, therefore, directly considers the damage on biomass and is considered an alternative to the one proposed in this paper: considering both could lead to double counting of damage on vegetation and fish, for example. The second mode, to be sufficiently complete, should include additional types of biomass, such as terrestrial animals, birds, insects, etc., in order to be truly representative of ecosystems.

3.2.7 Characterization factors

The calculation of characterisation factors takes place in separate homonym sheets, one per emitting compartment, and only return the calculation when the emission vector $\vec{E}$, in "World unit data sheet", is non-zero for the relevant compartment.

Below are the formulas for calculating CFs at mid-point level, depending on the emitting compartment and the area of protection (HH or ECO).

Human toxicity (cancer/non cancer effects)

In general, for human health, CFs are obtained for each emitting compartment by summing up all contributions from concentrations in receiving compartments, depending on the different exposure modes and effect (Eq. 128 and Eq. 129).

$$CF_{LOC,HH,cancer,x} = FF_{g,A} \times XF_{inh} \times EF_{inh,cancer} + FF_{w,W} \times XF_{ing,w} \times EF_{ing,cancer} + FF_{veg} \times XF_{ing,veg} \times EF_{ing,cancer} + FF_{f} \times XF_{ing,f} \times EF_{ing,cancer} \quad \text{(Eq. 128)}$$

$$CF_{LOC,HH,non\ cancer,x} = FF_{g,A} \times XF_{inh} \times EF_{inh,non\ \ cancer} + FF_{w,W} \times XF_{ing,w} \times EF_{ing,non\ cancer} + FF_{veg} \times XF_{ing,veg} \times EF_{ing,non\ cancer} + FF_{f} \times XF_{ing,f} \times EF_{ing,non\ \ cancer} \quad \text{(Eq. 129)}$$

Where:

- $CF_{LOC,HH,cancer,x}$ (cases kg^{-1}) and $CF_{LOC,HH,non\ cancer,x}$ (cases kg^{-1}) are the characterisation factors for a local emission in compartment x causing carcinogenic and non-carcinogenic effects per kg emitted;
- $FF_{g,A}$ ($kg_{g,A}\ kg^{-1}\ h$) is the mass increase in the local air compartment, particularly in the gas phase, for an hourly, unitary emission in the compartment x;
- XF_{inh} ($m^3_{inh}\ h^{-1}\ pop.loc\ m^{-3}_{g,A}$) is the volume of air inhaled per hour by the local population relative to the volume of the total gas phase of the local air compartment;
- $EF_{inh,cancer}$ ($cases\ cancer\ lifetime\ dose^{-1}$) and $EF_{inh,non\ cancer}$ ($cases\ non\ cancer\ lifetime\ dose^{-1}$) are the lifetime probabilities of having a carcinogenic or non-carcinogenic effect relative to inhalation of a reference dose from toxicological studies;
- $FF_{w,W}$ ($kg_{w,W}\ kg^{-1}\ h$) is the mass increase that occurs in the local water compartment, particularly in the dissolved water phase, for an hourly, unitary emission in the compartment x;
- $XF_{ing,w}$ ($m^3_{ing,w}\ h^{-1}\ pop.loc\ m^{-3}_{w,W}$) is the volume of water ingested per hour by the local population compared to the volume of the total dissolved water phase of the local water compartment;
- $EF_{ing,cancer}$ ($cases\ cancer\ lifetime\ dose^{-1}$) and $EF_{ing,non\ cancer}$ ($cases\ non\ cancer\ lifetime\ dose^{-1}$) are the lifetime probabilities of having a carcinogenic or non-carcinogenic effect relative to ingestion of a reference dose from toxicological studies;
- FF_{veg} ($kg_{veg}\ kg^{-1}\ h$) is the mass increase in the local vegetation compartment for an hourly, unitary emission in the compartment x;
- $XF_{ing,veg}$ ($kg_{ing,veg}\ h^{-1}\ pop.loc\ kg^{-1}_{veg}$) is the mass of vegetation ingested per hour by the local population compared to the total mass of the local vegetation compartment;
- FF_{f} ($kg_{f}\ kg^{-1}\ h$) is the mass increase in the local fish compartment for an hourly, unitary emission in the compartment x;
- $XF_{ing,f}$ ($kg_{ing,f}\ h^{-1}\ pop.loc\ kg^{-1}_{f}$) is the mass of fish ingested per hour by the local population compared to the total mass of the local fish compartment.

Eco-toxicity (air/water/soil)

In general, for the health of the ecosystem, CFs are obtained for each emitting compartment x separating the effects in terms of fractions of PAF-affected species occurring in the receiving compartments, thus expressing air (Eq. 130), water (Eq. 131) and soil (Eq. 132) toxicities separately.

$$CF_{LOC,A-ECO,x} = FF_{g,A} \times EF_{eco,A} \quad \text{(Eq. 130)}$$

$$CF_{LOC,W-ECO,x} = FF_{w,W} \times EF_{eco,W} \quad \text{(Eq. 131)}$$

$$CF_{LOC,S-ECO,x} = FF_{w,S} \times EF_{eco,S} \quad \text{(Eq. 132)}$$

Where:

- $CF_{LOC,A-ECO,x}$ (PAF m^3 h kg^{-1}), $CF_{LOC,W-ECO,x}$ (PAF m^3 h kg^{-1}) and $CF_{LOC,S-ECO,x}$ (PAF m^3 h kg^{-1}) are, respectively, the local characterisation factor of air, water and soil ecotoxicity, i.e. for a local release of 1 kg in compartment x causing a fraction of affected species integrated in compartment volume and time in the receiving air, water and soil compartments;
- $FF_{g,A}$ ($kg_{g,A}\ kg^{-1}\ h$) is the mass increase in the local air compartment, particularly in the gas phase, for an hourly, unitary emission in the compartment x;
- $EF_{eco,A}$ ($PAF\ m^3 kg_A^{-1}$) is the fraction of species potentially affected due to a reference concentration established in the local air compartment by toxicological studies;
- $FF_{w,W}$ ($kg_{w,W}\ kg^{-1}\ h$) is the mass increase that occurs in the local water compartment, particularly in the dissolved water phase, for an hourly, unitary emission in the compartment x;
- $EF_{eco,W}$ ($PAF\ m^3 kg_W^{-1}$) is the fraction of species potentially affected due to a reference concentration established in the local water compartment by toxicological studies;
- $FF_{w,S}$ ($kg_{w,S}\ kg^{-1}\ h$) is the mass increase that occurs in the local soil compartment, particularly in the pore water phase, for an hourly, unitary emission in the compartment x;
- $EF_{eco,S}$ ($PAF\ m^3 kg_S^{-1}$) is the fraction of species potentially affected due to a reference concentration established in the local soil compartment by toxicological studies.

As already mentioned, in the case of eco-toxicity, a specific XF is not used, as the FF only considers the mass of chemical present in the phase that is bioavailable.

Mid-point CFs

The CFs results for a local emission are summarised in Table 21 and Table 22.

Table 21 Mid-point CFs for benzene for human toxicity in the local model

Effect	$CF_{LOC,HH}$ (cases kg^{-1}) E_{ALOC} = 1 kg h^{-1}	$CF_{LOC,HH}$ (cases kg^{-1}) E_{WLOC} = 1 kg h^{-1}	$CF_{LOC,HH}$ (cases kg^{-1}) E_{SLOC} = 1 kg h^{-1}
Cancer	9.96E-10	4.44E-08	1.01E-09
Non cancer	2.52E-10	1.12E-08	2.56E-10

Table 22 Mid-point CFs for benzene for eco-toxicity in the local model

Receiving compartment *i*	$CF_{LOC,ECO}$ (PAF m^3 h kg^{-1}) E_{ALOC} = 1 kg h^{-1}	$CF_{LOC,ECO}$ (PAF m^3 h kg^{-1}) E_{WLOC} = 1 kg h^{-1}	$CF_{LOC,ECO}$ (PAF m^3 h kg^{-1}) E_{SLOC} = 1 kg h^{-1}
Air	1.09	3.07E-04	1.09
Water	7.27E-09	4.86E-02	2.37E-05
Soil	7.46E-04	1.85E-05	5.63

At mid-point, no single toxicity values are derived for each emitting compartment, as for human health the effects are different and for the ecosystem the toxicities of the receiving compartments are defined separately.

When analysing the contributions to CF for human toxicity, the largest effects occur for a local water emission, while the effects for a local air and soil emission are comparable. The largest effect for a release to water is mainly determined by the fact that in this emitting scenario the concentrations in fish and water itself are maximised compared to the other scenarios (Table 14) and for these compartments the exposure modes (ingestion of water and fish) are the most relevant (Table 15).

Analysing the contributions to the CF for eco-toxicity, the largest effect to species, expressed in terms of PAF m^3 h, occurs in the same emitting compartment, where the concentration is highest, as shown in chapter 3.2.3. In particular, the scenario of an emission in the soil has the greatest effect on species, due to the high concentration occurring in this compartment due to the absence of advective outflow processes, and where the effect occurring in the air compartment is also significant. The latter is mainly determined by the high value of $EF_{ECO,A}$, rather than for the concentration in air, which is lower than in other compartments due to the important process of degradation and removal by advection.

Unlike the calculation of human toxicity, where the number of people present is taken into account, in the calculation of eco-toxicity the impact is calculated for a fraction of affected species, without assessing the total number of species involved. This approximation is necessary because, in general, it is very difficult to know the number of species present in an ecosystem. However, if it is possible and of interest to the analyst, it is possible to estimate the number of species affected on a local scale by extrapolating the value of PAFs from the unit of measurement considered in the CF and multiplying it by the number of species present, if known. Alternatively, the calculated PAF value alone can be used to express the magnitude of the impact generated on the total number of species present in each compartment.

The calculation of the PAFs alone for each emitter scenario on each compartment and scale is reported below (Table 23), where the graph of the SSD curve approximated by the straight line with the EF as its angular coefficient is used (Eq. 33).

Table 23 PAF results for each emitting compartment in the local model

Receiving compartment *i*	PAF E_{ALOC} = 1 kg h^{-1}	PAF E_{WLOC} = 1 kg h^{-1}	PAF E_{SLOC} = 1 kg h^{-1}
Air	4.56E-09	1.28E-12	4.53E-09
Water	1.45E-13	9.71E-07	4.73E-10
Soil	2.50E-10	6.19E-12	1.89E-06

For each emitting compartment, the highest PAF is always on the same compartment, as it is characterised by the highest concentration.

The value of PAFs could also be derived by dividing the value of $PAF\ m^3 h\ kg^{-1}$ for the volume of the compartment whose eco-toxicity is to be assessed, the emission time being 1 h.

The CFs for local emissions calculated so far could be included in a calculation method for evaluating damage caused by local emissions of benzene on a local world unit.

End-point CFs

According to USEtox 2.12 model, damage factors (DFs) (Table 24), based on Huijbregts et al. (2005) for human toxicity and on based on Jolliet et al. (2003) for freshwater eco-toxicity, are applied to mid-point results to obtain end-point CFs, expressed for human health (HH) in Disability Adjusted Life Years (DALYs) per kg emitted (Table 25), and for eco-toxicity in Potentially Disappeared Fraction of Species (PDF) integrated in volume and time, that are reported both in disaggregated and aggregated forms on receiving compartments (Table 26).

Table 24 DFs for human and eco-toxicity from Huijbregts et al. (2005)

Toxicity	DF
HH - Cancer	11.5 DALY cases^{-1}
HH - Non cancer	2.7 DALY cases^{-1}
ECO	0.5 PDF PAF^{-1}

Table 25 End-point CFs for benzene on human toxicity in the local model

$CF_{LOC,HH}$ (DALY kg^{-1}) E_{ALOC} = 1 kg h^{-1}	$CF_{LOC,HH}$ (DALY kg^{-1}) E_{WLOC} = 1 kg h^{-1}	$CF_{LOC,HH}$ (DALY kg^{-1}) E_{SLOC} = 1 kg h^{-1}
1.21E-08	5.41E-07	1.23E-08

As shown for mid-point results, the greatest damage occurs for a water emission, followed by the soil and air emission scenario.

Table 26 End-point CFs for benzene on eco-toxicity in the local model

Receiving compartment *i*	$CF_{LOC,ECO}$ (PDF m^3 h kg^{-1}) E_{ALOC} = 1 kg h^{-1}	$CF_{LOC,ECO}$ (PDF m^3 h kg^{-1}) E_{WLOC} = 1 kg h^{-1}	$CF_{LOC,ECO}$ (PDF m^3 h kg^{-1}) E_{SLOC} = 1 kg h^{-1}
Loc. Air	5.47E-01	1.54E-04	5.43E-01
Loc. Water	3.63E-09	2.43E-02	1.18E-05
Loc. Soil	3.73E-04	9.23E-06	2.82E+00
Total	5.47E-01	2.44E-02	3.36E+00

The same considerations made for the mid-point results also apply at the end-point level for eco-toxicity, as the reported values were only halved.

The CFs for local emissions calculated so far could be included in a calculation method for evaluating damage caused by local emissions of benzene on a local world unit.

3.3 The local - continental model

A model in which a local scale is communicated with a larger continental scale was built (Figure 13), while maintaining the constraint of the local scale as the only emitting scale. This variant represents a first step towards a more comprehensive model that will also include the global scale.

As a preliminary example for the two scales, only 3 compartments have been considered instead of 7, i.e. air, water and soil, both emitters (in the case of the local) and receivers.

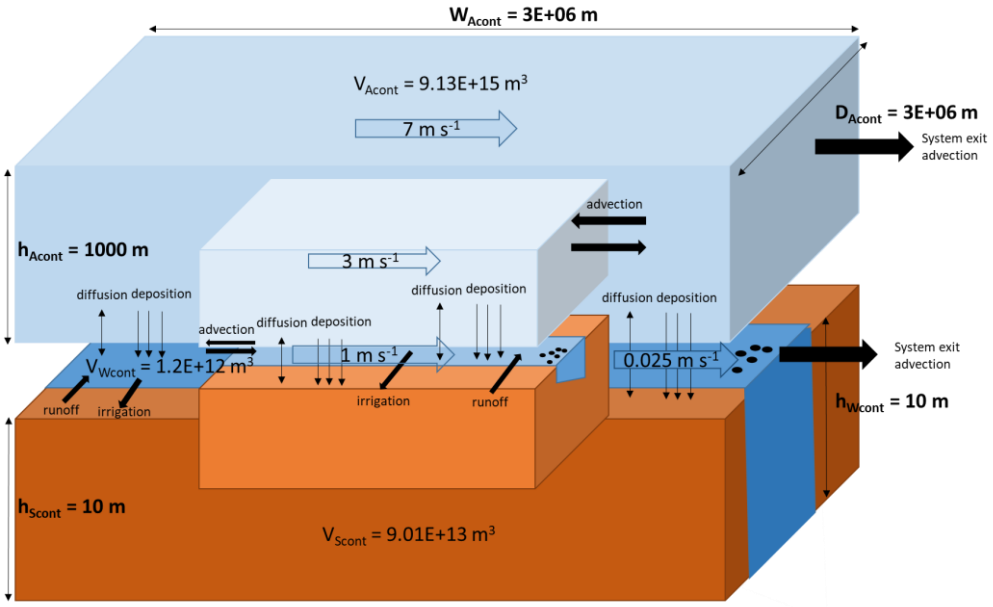

Figure 13 Local-continental world unit

The size of the local scale was differentiated from the continental one, especially for the latter a surface extent of land and water was set to have the same order of magnitude as the European extent, i.e. of the order of E+12 km^2. The surface water is schematised with data for the Volga River, taken as reference, which has an average depth of 10 m, an average width of 40000 m and a flow velocity of 0.025 m s^{-1}, calculated with the average flow rate of 8000 m^3 s^{-1} (Wikipedia 2022). The continental wind speed over Europe is assumed to average 7 m s^{-1} (Four Wind s.r.l. 2009). The soil is assumed to be of the same height as the local soil, but with an extension compatible with that of Europe.

When defining composite dimensional parameters, such as volumes, a calculation was set up to take into account only the 3 compartments considered, i.e:

- the soil volume was not reduced by the volume of sediment and groundwater, but only by the volume of surface water, leading to a higher local soil volume than the local model;
- the volume of water has not been reduced by the volume of fish, as fish are not present.

For the local scale, the D-rate values are, therefore, equal to the local-only model, considering the second decimal place as significant, with the exception of the value of $D_{DEG,S}$ = 7.84E-01 mol h^{-1} Pa^{-1}, increased compared to the previous model due to the larger volume of soil considered. Furthermore, it is noted that the D values for the sediment, groundwater, fish and vegetation compartments are no longer present.

Downstream, the D-values for the continental scale were also differentiated and are shown in Table 27, where it can be seen that all continental values are larger than local values, due to the larger size of the continental scale.

Table 27 D rates for benzene for each environmental process of the local-continental model

Continental	D diffusion (mol h^{-1} Pa^{-1})	Formula (k = mass transfer coeff., m h^{-1})
D_{VA}	3.35E+06	$k_A \times A_{AW} \times Z_A$
D_{VW}	8.07E+09	$k_W \times A_{AW} \times Z_W$
D_E	1.39E+10	$k_V \times A_{AS} \times Z_A$
D_{AS}	1.42E+09	$B_{AS}\ Y^{-1} \times A_{AS} \times Z_A$
D_{WS}	2.48E+06	$B_{WS}\ Y^{-1} \times A_{AS} \times Z_W$
D_{OCS}	1.26E-02	$B_{OCS}\ Y^{-1} \times A_{AS} \times Z_S$
D_{VAW}	3.35E+06	$(1/D_{VA} + 1/D_{VW})^{-1}$
D_{VAS}	1.29E+09	$(1/D_E + 1/(D_{AS} + D_{WS} + D_{OCS}))^{-1}$

Continental	D degradation (mol h^{-1} Pa^{-1})	Formula (k = rate constant, h^{-1})
$D_{DEG,\ A}$	1.53E+11	$k_A \times V_A \times v_{g,A} \times Z_A$
$D_{DEG,\ W}$	8.78E+06	$k_W \times V_W \times v_{w,W} \times Z_W$
$D_{DEG,\ S}$	7.10E+06	$k_S \times V_S \times v_{oc,S} \times Z_S$

Continental	D advection (mol h^{-1} Pa^{-1})	Formula
$D_{ADV,\ A}$	3.15E+10	$G_A \times Z_A$
$D_{ADV,\ W}$	6.86E+04	$G_W \times Z_W + G_{PW} \times Z_P$
D_{QAW}	3.11E-01	$U_Q \times v_{q,A} \times A_{AW} \times Z_Q$
D_{MAW}	1.29E+04	$U_M \times A_{AW} \times Z_W$
D_{CAW}	3.74E-01	$U_M \times A_{AW} \times Q \times v_{q,A} \times Z_Q$
D_{QAS}	2.34E+01	$U_Q \times v_{q,A} \times A_{AS} \times Z_Q$
D_{MAS}	9.70E+05	$U_M \times A_{AS} \times Z_W$
D_{CAS}	2.81E+01	$U_M \times A_{AS} \times Q \times v_{q,A} \times Z_Q$
$D_{RUNOFF,S}$	6.17E+02	$A_S \times U_{Solid} \times Z_S$
$D_{RUNOFF,W}$	6.31E+05	$A_S \times U_W \times Z_W$
D_{IRRIG}	9.55E+03	$U_{IRRIG} \times A_S \times Z_W$

Local	D diffusion (mol h^{-1} Pa^{-1})	Formula (k = mass transfer coeff., m h^{-1})
D_{VA}	8.99E-02	$k_A \times A_{AW} \times Z_A$
D_{VW}	3.56E+02	$k_W \times A_{AW} \times Z_W$
D_E	1.53E+03	$k_V \times A_{AS} \times Z_A$
D_{AS}	1.56E+02	$B_{AS}\ Y^{-1} \times A_{AS} \times Z_A$
D_{WS}	2.73E-01	$B_{WS}\ Y^{-1} \times A_{AS} \times Z_W$
D_{OCS}	1.39E-09	$B_{OCS}\ Y^{-1} \times A_{AS} \times Z_S$
D_{VAW}	8.98E-02	$(1/D_{VA} + 1/D_{VW})^{-1}$
D_{VAS}	1.41E+02	$(1/D_E + 1/(D_{AS} + D_{WS} + D_{OCS}))^{-1}$

Local	D degradation (mol h^{-1} Pa^{-1})	Formula (k = rate constant, h^{-1})
$D_{DEG,\ A}$	4.02E+03	$k_A \times V_A \times v_{g,A} \times Z_A$
$D_{DEG,\ W}$	3.66E-01	$k_W \times V_W \times v_{w,W} \times Z_W$
$D_{DEG,\ S}$	7.84E-01	$k_S \times V_S \times v_{oc,S} \times Z_S$

Local	D advection (mol h^{-1} Pa^{-1})	Formula
$D_{ADV,\ A}$	1.06E+06	$G_A \times Z_A$
$D_{ADV,\ W}$	3.23E+02	$G_W \times Z_W + G_{PW} \times Z_P$
D_{QAW}	2.59E-08	$U_Q \times v_{q,A} \times A_{AW} \times Z_Q$
D_{MAW}	1.08E-03	$U_M \times A_{AW} \times Z_W$
D_{CAW}	3.11E-08	$U_M \times A_{AW} \times Q \times v_{q,A} \times Z_Q$
D_{QAS}	2.57E-06	$U_Q \times v_{q,A} \times A_{AS} \times Z_Q$
D_{MAS}	1.07E-01	$U_M \times A_{AS} \times Z_W$
D_{CAS}	3.08E-06	$U_M \times A_{AS} \times Q \times v_{q,A} \times Z_Q$
$D_{RUNOFF,S}$	6.78E-05	$A_S \times U_{Solid} \times Z_S$
$D_{RUNOFF,W}$	6.93E-02	$A_S \times U_W \times Z_W$
D_{IRRIG}	1.05E-03	$U_{IRRIG} \times A_S \times Z_W$

3.3.1 Excel calculation tool and resolution matrix

An Excel spreadsheet (Local-continental model.xlsx) was created for collecting all required data and calculating fate dispersion. It contains all the required types of parameters, organized in sheets as follows:

- World unit data (highlighted in red in the Excel file): this sheet contains landscape parameters of local and continental scales and compartments details, such as specific processes velocities and phases composition. These parameters are adaptable to specific situations to represent the world unit under study. The emission vector $\vec{E}$ [E_A; E_W; E_S] is present in this sheet in cells B24:B27 (highlighted in red in the Excel file);
- Substance data: this sheet contains physico-chemical properties and toxicity data. These parameters are adaptable to the specific chemical under study;
- Partition coefficients $\boldsymbol{K}$ sheet: this sheet is automatically filled in on the basis of the information in Substance data sheet;
- Capacity of fugacities $\boldsymbol{Z}$: this sheet is automatically filled in on the basis of the information in Substance data sheet;
- Diffusivities $\boldsymbol{B}$ and mass transfer coefficients $\boldsymbol{k}$ sheet: this sheet presents fixed parameters and other parameters that are automatically filled in on the basis of the information in Substance data and World unit data sheets;
- D values sheet: this sheet is automatically filled in on the basis of the information in Substance data and World unit data sheets;
- Fugacities and concentrations: this sheet contains the equations, the matrix resolution, fugacities vector $\vec{f}$ (cells K50:K55), masses $\vec{M}$ (cells L50:L55) and concentrations $\boldsymbol{C}$, as well as a synthetic world unit mass balance (cells B79 and B81) and mass fluxes results (cells C85:C112). It is automatically filled in on the basis of the information in Substance data and World unit data sheets;
- Fate factors $\boldsymbol{FF}$: this sheet is automatically filled on the basis of the information in Substance data and World unit data sheets;
- Exposure factors $\boldsymbol{XF}$: this sheet contains the population parameters (adaptable to specific conditions) and is automatically filled on the basis of the information in World unit data sheet;
- Effect factors $\boldsymbol{EF}$: this sheet and is automatically filled on the basis of the information in Substance data sheet;
- Mid-point characterization factors for local air emissions $\boldsymbol{CF_{LOC,A}}$: this sheet and is automatically filled for emission vector $\vec{E}$ = [1;0;0] in World unit data sheet;
- Mid-point characterization factors for local water emissions $\boldsymbol{CF_{LOC,W}}$: this sheet and is automatically filled for emission vector $\vec{E}$ = [0;1;0] in World unit data sheet;
- Mid-point characterization factors for local soil emissions $\boldsymbol{CF_{LOC,S}}$: this sheet and is automatically filled for emission vector $\vec{E}$ = [0;0;1] in World unit data sheet;
- End-point characterization factors for local air emissions $\boldsymbol{CF_{LOC,A}}$: this sheet is connected with the mid-point $\boldsymbol{CF_{LOC,A}}$;
- End-point characterization factors for local water emissions $\boldsymbol{CF_{LOC,W}}$: this sheet is connected with the mid-point $\boldsymbol{CF_{LOC,W}}$;

- End-point characterization factors for local soil emissions $\boldsymbol{CF_{LOC,S}}$: this sheet is connected with the mid-point $\boldsymbol{CF_{LOC,S}}$.

There are 6 linear equations to solve, one for each compartment for each scale. In writing the equations, the relationships between the compartments of the different scales were taken into account, and in particular, in addition to the processes already known between the compartments of the same scale:

- local air advection towards continental air and *vice versa*;
- local water advection towards continental water and *vice versa*.

These advections represent, in fact, the outflows from the local scale and the subsequent 'return' by advection from the continental scale. These return fluxes are characterised by the continental scale fugacities, but by local scale advection D values, since, like a bottleneck, the local scale imposes its own dimensions on the incoming flux, not being large enough to receive a volume of air and water from a larger scale.

Inputs due to continental emissions continue to be considered zero, as done for the local model only, since, as already explained, it is a prerequisite that the emission occurs only at the local scale.

Below are the equations for the local-continental model (from Eq. 133 to Eq. 144), similar to those described for the local 7-compartment model, in a first extended form in which the input fluxes to the compartment under consideration have a positive sign and the output fluxes a negative sign. These signs are modified in a subsequent rewriting of the equations, in which the known term C is made explicit and the values of D referring to the same unknown are aggregated into coefficients whose names are made up of two letters XY, X indicating the compartment of departure, Y the one of arrival. The subscripts LOC and CONT mark the unknowns and the specific coefficients of each scale.

LOCAL AIR:

$$E_{A,LOC} + f_{W,LOC} \times D_{VAW,LOC} - f_{A,LOC} \times D_{VAW,LOC} - f_{A,LOC} \times D_{MAW,LOC} - f_{A,LOC} \times D_{QAW,LOC} - f_{A,LOC} \times D_{CAW,LOC} - f_{A,LOC} \times D_{MAS,LOC} - f_{A,LOC} \times D_{QAS,LOC} - f_{A,LOC} \times D_{CAS,LOC} - f_{A,LOC} \times D_{DEGA,LOC} - f_{A,LOC} \times D_{ADV,A,LOC} + f_{S,LOC} \times D_{VAS,LOC} - f_{A,LOC} \times D_{VAS,LOC} + f_{A,CONT} \times D_{ADV,A,LOC} = 0 \quad \text{(Eq. 133)}$$

$$f_{A,LOC} \times AA_{LOC} - f_{W,LOC} \times D_{VAW,LOC} - f_{S,LOC} \times D_{VAS,LOC} - f_{A,CONT} \times D_{ADV,A,LOC} = C_{A,LOC} \quad \text{(Eq. 134)}$$

Where:

- $AA_{LOC}\ (mol\ h^{-1}Pa^{-1}) = D_{VAW,LOC} + D_{MAW,LOC} + D_{QAW,LOC} + D_{CAW,LOC} + D_{MAS,LOC} + D_{QAS,LOC} + D_{CAS,LOC} + D_{DEGA,LOC} + D_{ADV,A,LOC} + D_{VAS,LOC}$
- $C_{A,LOC}\ (mol\ h^{-1}) = E_{A,LOC}$

LOCAL WATER:

$$E_{W,LOC} - f_{W,LOC} \times D_{VAW,LOC} + f_{A,LOC} \times D_{VAW,LOC} + f_{A,LOC} \times D_{MAW,LOC} + f_{A,LOC} \times D_{QAW,LOC} + f_{A,LOC} \times D_{CAW,LOC} - f_{W,LOC} \times D_{DEGW,LOC} - f_{W,LOC} \times D_{ADV,W,LOC} + f_{S,LOC} \times D_{RUNOFF,LOC} - f_{W,LOC} \times D_{IRRIG,LOC} + f_{W,CONT} \times D_{ADV,W,LOC} = 0 \quad \text{(Eq. 135)}$$

$$-f_{A,LOC} \times AW_{LOC} + f_{W,LOC} \times WW_{LOC} - f_{S,LOC} \times D_{RUNOFF,LOC} - f_{W,CONT} \times D_{ADV,W,LOC} = C_{W,LOC} \quad \text{(Eq. 136)}$$

where:

- $WW_{LOC}\ (mol\ h^{-1}Pa^{-1}) = D_{VAW,LOC} + D_{DEGW,LOC} + D_{ADV,W,LOC} + D_{IRRIG,LOC}$
- $AW_{LOC}\ (mol\ h^{-1}Pa^{-1}) = D_{VAW,LOC} + D_{MAW,LOC} + D_{QAW,LOC} + D_{CAW,LOC}$
- $C_{W,LOC}\ (mol\ h^{-1}) = E_{W,LOC}$

LOCAL SOIL:

$$E_{S,LOC} - f_{S,LOC} \times D_{VAS,LOC} + f_{A,LOC} \times D_{VAS,LOC} + f_{A,LOC} \times D_{MAS,LOC} + f_{A,LOC} \times D_{QAS,LOC} + f_{A,LOC} \times D_{CAS,LOC} - f_{S,LOC} \times D_{DEGS,LOC} - f_{S,LOC} \times D_{RUNOFF,LOC} + f_{W,LOC} \times D_{IRRIG,LOC} = 0 \quad \text{(Eq. 137)}$$

$$-f_{A,LOC} \times AS_{LOC} - f_{W,LOC} \times D_{IRRIG,LOC} + f_{S,LOC} \times SS_{LOC} = C_S \quad \text{(Eq. 138)}$$

where:

- $SS_{LOC}\ (mol\ h^{-1}Pa^{-1}) = D_{VAS,LOC} + D_{DEGS,LOC} + D_{RUNOFF,LOC}$
- $AS_{LOC}\ (mol\ h^{-1}Pa^{-1}) = D_{VAS,LOC} + D_{MAS,LOC} + D_{QAS,LOC} + D_{CAS,LOC}$
- $C_{S,LOC}\ (mol\ h^{-1}) = E_{S,LOC}$

CONTINENTAL AIR:

$$f_{W,CONT} \times D_{VAW,CONT} - f_{A,CONT} \times D_{VAW,CONT} - f_{A,CONT} \times D_{MAW,CONT} - f_{A,CONT} \times D_{QAW,CONT} - f_{A,CONT} \times D_{CAW,CONT} - f_{A,CONT} \times D_{MAS,CONT} - f_{A,CONT} \times D_{QAS,CONT} - f_{A,CONT} \times D_{CAS,CONT} - f_{A,CONT} \times D_{DEGA,CONT} - f_{A,CONT} \times D_{ADV,A,CONT} + f_{S,CONT} \times D_{VAS,CONT} - f_{A,CONT} \times D_{VAS,CONT} + f_{A,LOC} \times D_{ADV,A,LOC} = 0 \quad \text{(Eq. 139)}$$

$$f_{A,CONT} \times AA_{CONT} - f_{W,CONT} \times D_{VAW,CONT} - f_{S,CONT} \times D_{VAS,CONT} - f_{A,LOC} \times D_{ADV,A,LOC} = 0 \quad \text{(Eq. 140)}$$

Where:

$$AA_{CONT}\ (mol\ h^{-1}Pa^{-1}) = D_{VAW,CONT} + D_{MAW,CONT} + D_{QAW,CONT} + D_{CAW,CONT} + D_{MAS,CONT} + D_{QAS,CONT} + D_{CAS,CONT} + D_{DEGA,CONT} + D_{ADV,A,CONT} + D_{VAS,CONT}$$

CONTINENTAL WATER:

$$-f_{W,CONT} \times D_{VAW,CONT} + f_{A,CONT} \times D_{VAW,CONT} + f_{A,CONT} \times D_{MAW,CONT} + f_{A,CONT} \times D_{QAW,CONT} + f_{A,CONT} \times D_{CAW,CONT} - f_{W,CONT} \times D_{DEGW,CONT} - f_{W,CONT} \times D_{ADV,W,CONT} + f_{S,CONT} \times D_{RUNOFF,CONT} - f_{W,CONT} \times D_{IRRIG,CONT} + f_{W,LOC} \times D_{ADV,W,LOC} = 0 \quad \text{(Eq. 141)}$$

$$-f_{A,CONT} \times AW_{CONT} + f_{W,CONT} \times WW_{CONT} - f_{S,CONT} \times D_{RUNOFF,CONT} - f_{W,LOC} \times D_{ADV,W,LOC} = 0 \quad \text{(Eq. 142)}$$

where:

- $WW_{CONT}\ (mol\ h^{-1}Pa^{-1}) = D_{VAW,CONT} + D_{DEGW,CONT} + D_{ADV,W,CONT} + D_{IRRIG,CONT}$
- $AW_{CONT}\ (mol\ h^{-1}Pa^{-1}) = D_{VAW,CONT} + D_{MAW,CONT} + D_{QAW,CONT} + D_{CAW,CONT}$

CONTINENTAL SOIL:

$$-f_{S,CONT} \times D_{VAS,CONT} + f_{A,CONT} \times D_{VAS,CONT} + f_{A,CONT} \times D_{MAS,CONT} + f_{A,CONT} \times D_{QAS,CONT} + f_{A,CONT} \times D_{CAS,CONT} - f_{S,CONT} \times D_{DEGS,CONT} - f_{S,CONT} \times D_{RUNOFF,CONT} + f_{W,CONT} \times D_{IRRIG,CONT} = 0 \quad \text{(Eq. 143)}$$

$$-f_{A,CONT} \times AS_{CONT} - f_{W,CONT} \times D_{IRRIG,CONT} + f_{S,CONT} \times SS_{CONT} = 0 \quad \text{(Eq. 144)}$$

where:

- $SS_{CONT}\ (mol\ h^{-1}Pa^{-1}) = D_{VAS,CONT} + D_{DEGS,CONT} + D_{RUNOFF,CONT}$
- $AS_{CONT}\ (mol\ h^{-1}Pa^{-1}) = D_{VAS,CONT} + D_{MAS,CONT} + D_{QAS,CONT} + D_{CAS,CONT}$

Within the air and water equations of both scales there is now a further unknown represented by the fugacity of the same compartment of the opposite scale, due to the advective phenomena described above.

The presence of the advective flow "back" from the continental scale towards the local scale also determines an advective exit from the system for continental water and air towards, presumably, a global scale: in fact, there is a residual quota of pollutant flow which, net of what "returns" from the continental to the local scale, will exit from the former towards the outside of the system $F_{A,OUTSYSTEM}\ (mol\ h^{-1})$ and $F_{W,OUTSYSTEM}\ (mol\ h^{-1})$, according to Eq. 149 and Eq. 150:

$$F_{A,OUTSYSTEM} = f_{A,CONT} \times D_{ADV,A,CONT} - f_{A,CONT} \times D_{ADV,A,LOC} \quad \text{(Eq. 145)}$$

$$F_{W,OUTSYSTEM} = f_{W,CONT} \times D_{ADV,W,CONT} - f_{W,CONT} \times D_{ADV,W,LOC} \quad \text{(Eq. 146)}$$

The quantification of these flows for each emitting scenario is shown in Table 32.

The system was again solved by the product of the inverse matrix of the coefficients of the unknowns $-\overline{D}^{-1}$ and the vector of known terms $\vec{E}$, listed below for completeness (Table 28 and Table 29).

Table 28 Resolution matrix with equations coefficients of the local-continental model

	Contributing compartment					
Analyzed compartment	**A,LOC**	**W,LOC**	**S,LOC**	**A,CONT**	**W,CONT**	**S,CONT**
A,LOC	AA_{LOC}	$-D_{VAW,LOC}$	$-D_{VAS,LOC}$	$-D_{ADV,A,LOC}$	0	0
W,LOC	$-AW_{LOC}$	WW_{LOC}	$-D_{RUNOFF,LOC}$	0	0	0
S,LOC	$-AS_{LOC}$	$-D_{IRRIG,LOC}$	SS_{LOC}	0	0	0
A,CONT	$-D_{ADV,A,LOC}$	0	0	AA_{CONT}	$-D_{VAW,CONT}$	$-D_{VAS,CONT}$
W,CONT	0	$-D_{ADV,W,LOC}$	0	$-AW_{CONT}$	WW_{CONT}	$-D_{RUNOFF,CONT}$
S,CONT	0	0	0	$-AS_{CONT}$	$-D_{IRRIG,CONT}$	SS_{CONT}

The rows of Table 28 represent the individual compartments for which the balance equation is written, the columns represent the compartments that interact with the compartments under analysis. When there is no process connecting two compartments, a value of zero is entered. Similarly to the previous model, the columns also do not represent all emitting compartments, unlike the USEtox framework, where the columns can also be interpreted as the emitting compartments and the rows as the receiving compartments.

The diagonal cells represent the output of the compartment represented by the row, with a positive sign for all compartments as their sign has been changed to isolate the emitting vector.

Table 29 Vector of known terms C (emission vector $\vec{E}$) in the local-continental model

Emitting compartment	
A,LOC	$C_{A,LOC}$
W,LOC	$C_{W,LOC}$
S,LOC	$C_{S,LOC}$
A,CONT	0
W,CONT	0
S,CONT	0

The vector of known terms $\vec{E}$ is structured so as to have as many rows as there are sub-funds in the system and a single column, in which the direct and continuous emission (Table 29) is present.

In order to obtain the characterisation factors for each individual emitting compartments, the known terms must be equal to 1 mol h^{-1} only for the compartment for which the CF is to be calculated.

However, it is also possible to model the dispersion according to different emitting scenarios, in which case the purpose is to assess the damage due to emissions and not to calculate CFs for an LCA analysis.

The result of the multiplication returns the vector $\vec{f}$ of unknowns (Table 30):

Table 30 Vector of unknown terms (fugacity vector $\vec{f}$) in the local-continental model

Compartment	
A_{LOC}	f_{ALOC}
W_{LOC}	f_{WLOC}
S_{LOC}	f_{SLOC}
A_{CONT}	f_{ACONT}
W_{CONT}	f_{WCONT}
S_{CONT}	f_{SCONT}

The concentrations are derived C (mol m^{-3}), either bulk ones, i.e. by compartments consisting of several phases, or by single phase, through the product of the Z_{ibulk} and of Z_x, namely (Eq. 122 and Eq. 123).

Through multiplication with volume V (m^3) masses M (mol) are obtained, converted into kg in molecular weight.

3.3.2 Fugacities and concentrations results

Below, Table 31, are the fugacity and concentration results in the local-continental model compartments for each emitter scenario.

Table 31 Fugacities and concentration results for benzene emission in each compartment in the local-continental model. Symbol ↑ indicates fugacity increase compared to the local model

Compartments (emitting = E)	**Fugacity (Pa)**	**C_{bulk} (mol m^{-3})**	**Phase**	**C_{phase} (mol m^{-3})**	**Phase**	**C_{phase} (mol m^{-3})**	**Phase**	**C_{phase} (mol m^{-3})**
AirLoc (E)	9.36E-07	3.84E-10	Agas	3.84E-10	Aaerosol	1.21E-08	-	-
WaterLoc	4.63E-10	8.31E-13	Wdiss	8.30E-13	Wsusps	2.76E-12	-	-
SoilLoc	9.31E-07	6.36E-10	Ssolid	2.77E-09	Swater	1.67E-09	Sair	3.82E-10
AirCont	5.40E-12	2.22E-15	Agas	2.22E-15	Aaerosol	2.22E-15	-	-
WaterCont	1.78E-12	3.19E-15	Wdiss	3.19E-15	Wsusps	3.19E-15	-	-
SoilCont	5.38E-12	3.67E-15	Ssolid	1.60E-14	Swater	9.65E-15	Sair	2.21E-15
Compartments (emitting = E)	**Fugacity (Pa)**	**C_{bulk} (mol m^{-3})**	**Phase**	**C_{phase} (mol m^{-3})**	**Phase**	**C_{phase} (mol m^{-3})**	**Phase**	**C_{phase} (mol m^{-3})**
AirLoc	**2.65E-10 ↑** (Loc. 2.63E-10)	1.09E-13	Agas	1.09E-13	Aaerosol	3.43E-12	-	-
WaterLoc (E)	3.09E-03	5.55E-06	Wdiss	5.55E-06	Wsusps	1.84E-05	-	-
SoilLoc	2.30E-08	1.57E-11	Ssolid	6.86E-11	Swater	4.14E-11	Sair	9.46E-12
AirCont	1.49E-12	6.13E-16	Agas	6.13E-16	Aaerosol	6.13E-16	-	-
WaterCont	8.18E-08	1.47E-10	Wdiss	1.47E-10	Wsusps	1.47E-10	-	-
SoilCont	2.09E-12	1.43E-15	Ssolid	6.21E-15	Swater	3.75E-15	Sair	8.57E-16
Compartments (emitting = E)	**Fugacity (Pa)**	**C_{bulk} (mol m^{-3})**	**Phase**	**C_{phase} (mol m^{-3})**	**Phase**	**C_{phase} (mol m^{-3})**	**Phase**	**C_{phase} (mol m^{-3})**
AirLoc	9.31E-07	3.82E-10	Agas	3.82E-10	Aaerosol	1.21E-08	-	-
WaterLoc	1.51E-06	2.70E-09	Wdiss	2.70E-09	Wsusps	8.97E-09	-	-
SoilLoc (E)	7.03E-03	4.80E-06	Ssolid	2.09E-05	Swater	1.26E-05	Sair	2.89E-06
AirCont	5.37E-12	2.21E-15	Agas	2.21E-15	Aaerosol	2.21E-15	-	-
WaterCont	4.16E-11	7.47E-14	Wdiss	7.47E-14	Wsusps	7.47E-14	-	-
SoilCont	5.35E-12	3.65E-15	Ssolid	1.59E-14	Swater	9.59E-15	Sair	2.19E-15

The analysis of the results below focuses mainly on the differences between scales and between the local and local-continental models, having already commented on the peculiarities of the processes within the same scale in the local model.

An analysis of the resulting fugacities and concentrations for an emission of 1 mol h^{-1} in each local compartment, obtained by multiplying the fugacities by the respective Z-values, shows that these at the local scale are several orders of magnitude greater than those at the continental scale. The fugacity result is motivated by the presence of the emission vector $\vec{E}$ in the local scale and the smaller local scale, which maximise concentrations. An analysis of the masses is given below.

The fugacity results for the local scale are the same as those obtained with the local model, with one exception occurring in the local air for an emission into the local water: here the fugacity is higher (2.65E-10 Pa) than in the previous model (2.63E-10 Pa). This increase in fugacity can be attributed to the presence of advective flow from the continental scale, which was absent in the previous model, as explained below.

Mass fluxes and masses results

Analysing, in fact, the magnitude of the fluxes, shown in Table 32, for a local water emission, the advective flux from local air to continental air turns out to be 3 orders of magnitude smaller than for the other emission scenarios. The similarity between the advective air fluxes for an emission in air and in soil can be attributed to the similar fugacities of the local air in the two scenarios, as already pointed out in Chapter 3.3.2. Since the local air outflow is smaller for an emission in water, the advective input from continental air assumes greater relevance and weight, compared to the other emitter scenarios, leading only for this scenario to an increase in air fugacity compared to the local model.

Table 32 Mass fluxes results for each emitting compartment in the local-continental model

Processes	Formula f x D	Fluxes (mol h^{-1}) $E_{A,LOC}$ = 1 mol h^{-1}	Fluxes (mol h^{-1}) $E_{W,LOC}$ = 1 mol h^{-1}	Fluxes (mol h^{-1}) $E_{S,LOC}$ = 1 mol h^{-1}
Loc. Diffusion A-W	$f_{A,LOC}$ x $D_{VAW,LOC}$	8.41E-08	2.38E-11	8.36E-08
Loc. Deposition A-W	$f_{A,LOC}$ x ($D_{MAW,LOC}$ + $D_{CAW,LOC}$ + $D_{QAW,LOC}$)	1.01E-09	2.85E-13	1.00E-09
Loc. Diffusion A-S	$f_{A,LOC}$ x $D_{VAS,LOC}$	1.32E-04	3.74E-08	1.32E-04
Loc. Deposition A-S	$f_{A,LOC}$ x ($D_{MAS,LOC}$ + $D_{CAS,LOC}$ + $D_{QAS,LOC}$)	9.98E-08	2.82E-11	9.92E-08
Loc. Diffusion W-A	$f_{W,LOC}$ x $D_{VAW,LOC}$	4.16E-11	2.78E-04	1.35E-07
Loc. Diffusion S-A	$f_{S,LOC}$ x $D_{VAS,LOC}$	1.32E-04	3.26E-06	**9.94E-01**
Loc. Irrigation W-S	$f_{W,LOC}$ x $D_{IRRIG,LOC}$	4.85E-13	3.24E-06	1.58E-09
Loc. Runoff S-W	$f_{S,LOC}$ x ($D_{RUNOFFS,LOC}$ + $D_{RUNOFFW,LOC}$)	6.46E-08	1.60E-09	4.87E-04
Loc. Advection A_{LOC}-A_{CONT}	$f_{A,LOC}$ x $D_{AIRADV,LOC}$	**9.96E-01**	2.81E-04	9.90E-01
Loc. Advection W_{LOC}-W_{CONT}	$f_{W,LOC}$ x $D_{WATERADV,LOC}$	1.49E-07	**9.99E-01**	4.87E-04
Loc. Degradation A	$f_{A,LOC}$ x $D_{DEGA,LOC}$	3.76E-03	1.06E-06	3.74E-03
Loc. Degradation W	$f_{W,LOC}$ x $D_{DEGW,LOC}$	1.69E-10	1.13E-03	5.51E-07
Loc. Degradation S	$f_{S,LOC}$ x $D_{DEGS,LOC}$	7.30E-07	1.81E-08	5.51E-03
Cont. Diffusion A-W	$f_{A,CONT}$ x $D_{VAW,CONT}$	1.81E-05	5.00E-06	1.80E-05
Cont. Deposition A-W	$f_{A,CONT}$ x ($D_{MAW,\ CONT}$ + $D_{CAW,\ CONT}$ + $D_{QAW,\ CONT}$)	6.99E-08	1.93E-08	6.95E-08
Cont. Diffusion A-S	$f_{A,\ CONT}$ x $D_{VAS,\ CONT}$	6.96E-03	1.92E-03	6.92E-03
Cont. Deposition A-S	$f_{A,\ CONT}$ x ($D_{MAS,\ CONT}$ + $D_{CAS,\ CONT}$ + $D_{QAS,\ CONT}$)	5.25E-06	1.45E-06	5.21E-06
Cont. Diffusion W-A	$f_{W,\ CONT}$ x $D_{VAW,\ CONT}$	5.96E-06	2.74E-01	1.39E-04
Cont. Diffusion S-A	$f_{S,\ CONT}$ x $D_{VAS,\ CONT}$	6.92E-03	2.69E-03	6.88E-03
Cont. Irrigation W-S	$f_{W,\ CONT}$ x $D_{IRRIG,\ CONT}$	1.70E-08	7.81E-04	3.98E-07
Cont. Runoff S-W	$f_{S,\ CONT}$ x ($D_{RUNOFFS,\ CONT}$ + $D_{RUNOFFW,\ CONT}$)	3.39E-06	1.32E-06	3.37E-06
Cont. Advection A_{CONT}-A_{LOC}	$f_{A,\ CONT}$ x $D_{AIRADV,\ LOC}$	5.75E-06	1.59E-06	5.72E-06
Cont. Advection W_{CONT}-W_{LOC}	$f_{W,\ CONT}$ x $D_{WATERADV,\ LOC}$	5.75E-10	2.64E-05	1.34E-08
Cont. Degradation A	$f_{A,\ CONT}$ x $D_{DEGA,\ CONT}$	**8.26E-01**	2.28E-01	**8.21E-01**
Cont. Degradation W	$f_{W,\ CONT}$ x $D_{DEGW,\ CONT}$	1.56E-05	**7.19E-01**	3.66E-04
Cont. Degradation S	$f_{S,\ CONT}$ x $D_{DEGS,\ CONT}$	3.82E-05	1.48E-05	3.80E-05
Cont. Advection A_{CONT}-OUT	$f_{A,\ CONT}$ x ($D_{AIRADV,\ CONT}$ - $D_{AIRADV,\ LOC}$)	1.70E-01	4.70E-02	1.69E-01
Cont. Advection W_{CONT}-OUT	$f_{W,\ CONT}$ x ($D_{WATERADV,\ CONT}$ - $D_{WATERADV,\ LOC}$)	1.14E-07	5.26E-03	2.68E-06

The most relevant fluxes for each scale and emitting compartment are shown in bold text in Table 32 and are all related to processes exiting the compartment under consideration.

The local air- and water-emitting scenarios have the same types of most relevant processes, i.e. the most relevant flux occurring on the same scale is advection to the corresponding continental compartment, while on the continental scale the most relevant flux is degradation in the same compartment.

For a local soil emission, on the other hand, the most relevant flux occurring on the same scale is diffusion to the local air (volatilisation), while on the continental scale the most relevant flux is degradation in air. In the soil, in fact, there is no advective process involving the whole volume of the same compartment and the most relevant degradation occurs in the continental air compartment as this has higher degradation rates for benzene and a larger volume.

Accordingly, it is possible to calculate the bulk masses permanently stationary in the compartments after emissions and in steady state, according to the general formula (Eq. 126).

The resulting bulk masses in the compartments of both scales for each emission scenario are summarised below:

Table 33 Masses results for each emitting scenario in the local-continental model. Symbol ↑ indicates mass increase compared to the local model

Receiving compartment	**M_x (mol) $E_{A,Loc}$ = 1 mol h^{-1}**	**M_x (mol) $E_{W,Loc}$ = 1 mol h^{-1}**	**M_x (mol) $E_{S,Loc}$ = 1 mol h^{-1}**
Loc. Air_{bulk}	9.22E-02	2.61E-05	9.17E-02
Loc. $Water_{bulk}$	4.15E-08	2.77E-01	1.35E-04
Loc. $Soil_{bulk}$	6.33E-03	1.57E-04	4.78E+01
Loc. Total	9.86E-02	2.78E-01	**4.79E+01** ↑ (Loc. mod. 4.78E+01)
Cont. Air_{bulk}	2.03E+01	5.59E+00	2.01E+01
Cont. $Water_{bulk}$	3.83E-03	1.76E+02	8.97E-02
Cont. $Soil_{bulk}$	3.31E-01	1.28E-01	3.29E-01
Cont. Total	2.06E+01	1.82E+02	2.06E+01

The total masses that reside at the local scale (row Loc. Total of Table 33) are almost unchanged compared to the local model, the only emitting scenario that shows a small increase is the local soil, where the same compartment, due to the increase in volume, hosts more benzene masses.

While concentrations were higher at the local scales, the results on the masses show that it is the continental compartments that have the highest values, due to their high volume. Consequently, continental FFs are also expected to be higher than local FFs, as analysed in the following sections.

In general, the largest mass is always in the continental compartment corresponding to the local emitting one, with the exception of the local soil emitting scenario, where the largest mass occurs in the same local compartment, due to the absence of significant advective phenomena, present for air and water, connecting the two different scales. The local water emitting scenario creates the largest "storage" of benzene at the continental level (Cont. Total row), higher than the other two scenarios by an order of magnitude, which is mainly concentrated in continental water. In fact, the continental water compartment receives a large amount of benzene through advection and, due to the low degradation rate of the substance in water, a high accumulation of the chemical occurs in it. For a local air and soil release, the same mass stored on the continental scale is determined, for both cases it resides more in the continental air compartment.

3.3.3 Fate factors

The resulting concentrations, converted into mg using the molecular weight of benzene, were used to calculate the Fate factors, one for each i compartment.

For compartments made of different phases. i.e. air, water and soil, the selected concentration was that of the prevailing phase for air and water, and water phase for soil, according to the following general Eq. 125.

The fate factors results for each compartment and scale and each emitting scenario are reported in Table 34.

Table 34 FF results for each local emitting scenario in the local-continental model. Symbol ↑ indicates FF increase compared to the local model

Compartment	Formula	$FF_i(h)$ ($E_{A,Loc}$ = 1 kg h^{-1})	$FF_i(h)$ ($E_{W,Loc}$ = 1 kg h^{-1})	$FF_i(h)$ ($E_{S,Loc}$ = 1 kg h^{-1})
Loc. Air	$FF_{g,ALOC} = C_{g,ALOC} \times 10^{-6} \times V_{g,ALOC}$	7.21E-03	**2.04E-06** ↑ (Loc. mod.: 2.02E-06)	7.16E-03
Loc. Freshwater	$FF_{w,WLOC} = C_{w,WLOC} \times 10^{-6} \times V_{w,WLOC}$	3.24E-09	2.17E-02	1.06E-05
Loc. Soil	$FF_{w,SLOC} = C_{w,SLOC} \times 10^{-6} \times V_{w,SLOC}$	**1.30E-03** ↑ (Loc. mod.: 3.89E-04)	**3.21E-05** ↑ (Loc. mod.: 9.63E-06)	**9.8** ↑ (Loc. mod.: 2.94)
Cont. Air	$FF_{g,ACONT} = C_{g,ACONT} \times 10^{-6} \times V_{g,ACONT}$	1.58	4.37E-01	1.57
Cont. Freshwater	$FF_{w,WCONT} = C_{w,WCONT} \times 10^{-6} \times V_{w,WCONT}$	2.99E-04	1.38	7.01E-03
Cont. Soil	$FF_{w,SCONT} = C_{w,SCONT} \times 10^{-6} \times V_{w,SCONT}$	6.79E-02	2.64E-02	6.75E-02

Some increased results are present on local compartments compared to the local model, in particular, for local soil for each emitting scenario and local air for local water emission. In the first case the increase can be attributed to the increased volume of local soil, thanks to the absence of sediments and groundwater, in the second case it can be attributed to the presence of continental advective flux into local air.

The general behaviour of the FFs in this model follows the masses results (Table 33), in which continental air and water present the highest values for an emission in the corresponding local compartments, while local soil shows the highest FF for an emission in the compartment itself.

The choice of using for multi-phase compartments a phase concentration rather than the bulk one is driven by the need of expressing, in the following steps, the bioavailable mass of chemical, i.e. the mass of chemical to which the living beings are exposed to.

3.3.4 Exposure factors

As with the local model, the calculation for the exposure factor XF is diversified between man and ecosystem, similar to the USEtox model. In addition, in the present model, the XF for human health is also diversified according to scale, to account for the different number of people present.

Since the bioavailable concentration was already included in the FFs of the present model, the XF for the ecosystem becomes superfluous, therefore, only the procedure for calculating the XF for humans is given below.

The exposure calculation must take into account the exposure pattern, related to a certain environmental concentration, by the entire population at the local scale. In the present study, for the number of people present, the value considered by USEtox on the urban scale (8333 persons km^{-2}), which is comparable to the local scale due to its small size, was taken as a reference, and halved to take into account a certain distance existing between the emitting point and the beginning of the built-up area, as illustrated in chapter 5. The number of people on the continental scale was calculated taking into account the population density considered by USEtox on the continental scale (111 persons km^{-2}, result of 9.98 x 10^8 people over 9013369.73 km^2).

The exposure modes in this study, similar to the USEtox model, are inhalation and ingestion, of water and food.

With regard to ingestion of food, similarly to the local model, two separate XFs were defined for ingestion of fish and vegetation. Unlike the local model, in which the fish and vegetation compartments were present and formed part of the resolution matrix, in the present study, the bioaccumulation factors (BAFs) calculated in the local model were used to compensate for the lack of specific FFs.

Bioaccumulation factors are defined as the ratio between the concentration determined in the biomass and the concentration of the medium to which it is exposed, according to the following formula (Eq. 147):

$$BAF_{BIOM.MEDIUM} = \frac{C_{biom.}(kg_{chem.}/m^3{}_{biom.})}{C_{x,medium}(kg_{chem.}/m^3{}_{x,medium})} \quad \text{(Eq. 147)}$$

where BAF has unit of measure ($m^3{}_{biom.}\, m^{-3}_{medium}$), $C_{biom.}(kg_{chem.}\, m^{-3}_{biom.})$ is the concentration of chemical per unit mass of biomass, $C_{x,medium}$ $(kg_{chem.}\, m^{-3}_{medium})$ is the concentration of chemical per unit mass of medium. In particular, the concentration relative to the phase of the medium to which the biomass is exposed, i.e. the dissolved water for fish and the gas phase for vegetation, was assumed as the concentration of the medium. In the calculation of the CFs, in fact, the FF used will be that relative to the two mentioned phases. The BAF is, therefore, used as a proportionality factor between the concentrations, returning the concentration in the biomass of interest in the local-continental model from the concentration in the medium of the local-continental model.

This approximation is more uncertain for vegetation, whose concentration value is due to the exposure of both air and soil concentrations, but in the present study, the concentration value with respect to air was taken as the reference, since as shown in chapter 3.2.3, the most relevant flux to vegetation is deposition from it. Specifically, the gas phase of the air is taken as the reference since, for each emitting scenario, the concentration value for vegetation is more similar to that of the gas phase than aerosols.

BAFs were included in the formulae for calculating XFs for human health in Table 35. Vegetation is assumed to represent all fruit and vegetable requirements.

The general formula for quantifying chemical exposure in a medium via an exposure route ***j*** is Eq. 126, declined according to the two different populations.

An intake rate is then made explicit with respect to the total medium containing the mass of chemical. The food exposure pathway is quantified by mass rather than volume (Table 35):

Table 35 XF results for the local-continental model. Symbol ↓ indicates XF decrease compared to the local model

Exposure route *j* (LOC/CONT)	**Formula**	**Parameters**	XF_j (h^{-1})
$Inhalation_{ALOC/CONT}$	$XF_{inhLOC/CONT} = \frac{G_{Breath} \times Pop_{LOC/CONT}}{V_{g,ALOC/CONT}}$	$G_{Breath} = 0.54\ m^3h^{-1}$ human breathing rate	L: 9.40E-06 C: 6.01E-08
$Ingestion_{WLOC/CONT}$	$XF_{ing,wLOC/CONT} = \frac{G_{Drink} \times Pop_{LOC/CONT}}{V_{w,WLOC/CONT}}$	$G_{Drink} = 1.67E-03\ m^3h^{-1}$ water ingestion rate	L: 1.39E-04 C: 1.41E-06
$Ingestion_{FLOC/CONT}$	$XF_{ing,FLOC/CONT} = BAF_{F,W} \times \frac{G_{Ing,F} \times Pop_{LOC/CONT}}{V_{w,WLOC/CONT}} \times \frac{1}{Dens.F}$	$G_{Ing,F} = 1.19E-03\ kg\ h^{-1}$ fish ingestion rate (estimated) $Dens.F = 1.3\ t\ m^{-3} \times 10^3\ kg\ t^{-1}$ fish density (estimated) $BAF_{F,W} = 6.11 \frac{kg\ m^{-3}_{FLOC}}{kg\ m^{-3}_{w,WLOC}}$ fish bioaccumulation factor versus dissolved water concentration (from local model for E_W = 1 kg)	**L: 4.66E-07 ↓** (Loc mod.: 5.45E-02) C: 4.72E-09
$Ingestion_{VEGLOC/CONT}$	$XF_{ing,VEGLOC/CONT} = BAF_{VEG,A} \times \frac{G_{Ing,VEG} \times Pop_{LOC/CONT}}{V_{w,SLOC/CONT}} \times \frac{1}{Dens.Veg}$	$G_{Ing,VEG} = 3.3E-02\ kg\ h^{-1}$ vegetation ingestion rate (estimated) $Dens.Veg = 1.2\ t\ m^{-3} \times 10^3\ kg\ t^{-1}$ vegetation density (estimated) $BAF_{VEG,A} = 6.11E-03\ \frac{kg\ m^{-3}_{VEGLOC}}{kg\ m^{-3}_{g,ALOC}}$ bioaccumulation factor of vegetation versus air gas phase concentration (from local model for E_A = 1 kg)	**L: 2.95E-12 ↓** (Loc mod.: 1.17E-05) C: 1.88E-14

Fish bioaccumulation factor $BAF_{F,W} = 6.11\ \frac{kg\ m^{-3}_{FLOC}}{kg\ m^{-3}_{w,WLOC}} = 4.7\ \frac{kg\ kg^{-1}_{FLOC}}{kg\ L^{-1}_{w,WLOC}}$ obtained in the local model is very similar to the BAF for fish reported in the USEtox database (BAF_{fish} = 4.27 L kg_F^{-1}) and are both referred to dissolved water, but this similarity does not occur for vegetation, which in the USEtox database is broken down into roots and leaves, both reported with respect to soil (BAF_{root} = 0 kg_{veg} kg_{soil}^{-1}; BAF_{leaf} = 0 kg_{veg} kg_{soil}^{-1}). In the local model, the bioaccumulation value with respect to the bulk soil is very small, but not zero ($BAF_{VEG,S} = 8.47E-07\ \frac{kg\ m^{-3}_{VEGLOC}}{kg\ m^{-3}_{SLOC}}$), however, as mentioned above, the vegetation concentration used in the calculation of this BAF still takes the exposure to air concentration into account.

In the USEtox model and the local model, a different schematisation of vegetation and fish is applied. In USEtox, these do not form a compartment, as in the local-continental model, and the BAF values are derived from the literature for fish and by means of a more elaborate modelling for vegetation, respectively, which considers separately the processes involved in the part of the vegetation above the ground (leaves) and the part of the vegetation below the ground (roots). On the former, contributions are considered by diffusion from the gas phase of the air, by deposition from aerosols and by transpiration from the soil. As the latter process is not included in the Mackay modelling, it is not considered in the local model. Other assumptions made on the parameters, e.g. with regard to leaf area and mass transfer coefficient for diffusion, as discussed in chapter 3.2, may also contribute to this difference in BAF for vegetation.

As a future development of this work, the process of soil transpiration could be included, in order to obtain a more complete and consistent representation of the processes.

The exposure factors calculated so far do not depend on the emitting compartment, so the proposed values are constant.

The new XFs for the local scale for fish and vegetation ingestion (highlighted in bold) are smaller than those calculated for the local model, due to the presence of BAFs, however the function of BAFs will be exercised in the multiplication with water and air FFs, so these reductions in XFs are not of real significance at present.

The values are higher for local exposure than for continental exposure. This result may seem counterintuitive, since the continental population is larger than the local one, however, it can be explained by considering that the volume of the continental compartments, which divides the exposure, is far greater than the local ones. The presence of the volume at the denominator, in fact, has the role of returning a concentration, after multiplication with the FF representing the mass in the receiving compartment. In this sense, it is understandable that the local concentration is higher than the continental one, as already shown in Table 31.

3.3.5 Effect factors

The definition of the effect factors follows what has already been reported for the local model.

A clarification is necessary with regard to the health of the ecosystem: using the same EFs for both the local and continental ecosystem, it is, therefore, assumed that the compartments at different scales are characterised by the same biodiversity, in terms of the types of species present. Of course, this is unrealistic, as a larger scale will contain a greater variety of species, however, this assumption is necessary in the present study due to the limited availability of data, but it could be overcome in a further development of the study by conducting a more in-depth analysis on this issue.

3.3.6 Characterization factors

The calculation of characterisation factors takes place in separate homonym sheets, one per local emitting compartment, and only return the calculation when the emission vector $\vec{E}$, placed in the "World unit data sheet", is non-zero for the local compartment considered.

In this model, the effect due to local emissions will occur on both the local and continental scales. Generally, a characterisation factor returns a single value of damage due to an emission, summing all the effects that occur. However, it is considered necessary to keep the effects on the scales separate in order to ensure transparency and knowledge of the damage occurring on the local scale, consistent with the objective of this paper. Therefore, CFs values disaggregated on the receiving scales and by type of effect will be reported.

Below are the formulas for calculating CFs at mid-point level, depending on the emitting compartment x and the protection area (HH or ECO).

Human toxicity (cancer/non cancer effects)

In general, for human health, CFs are obtained for each emitting compartment x by summing up all contributions from concentrations in the receiving compartments, depending on the different exposure modes and effect (Eq. 148 and Eq. 149).

As mentioned in chapter 3.3.4, in order to assess the effect from ingestion of fish and vegetation, as the FFs for fish and vegetation were not available in this model, those for water and soil were taken as proxies, respectively, adjusted to represent the two missing compartments by multiplication with the relevant BAFs.

$$CF_{LOC,HH,cancer,x} = FF_{g,ALOC} \times XF_{inhLOC} \times EF_{inh,cancer} + FF_{w,WLOC} \times XF_{ing,wLOC} \times EF_{ing,cancer} + FF_{g,ALOC} \times XF_{ing,vegLOC} \times EF_{ing,cancer} + FF_{w,WLOC} \times XF_{ing,fLOC} \times EF_{ing,cancer} + FF_{g,ACONT} \times XF_{inhCONT} \times EF_{inh,cancer} + FF_{w,WCONT} \times XF_{ing,wCONT} \times EF_{ing,cancer} + FF_{g,ACONT} \times XF_{ing,vegCONT} \times EF_{ing,cancer} + FF_{w,WCONT} \times XF_{ing,fCONT} \times EF_{ing,cancer} \quad \text{(Eq. 148)}$$

$$CF_{LOC,HH,non-cancer,x} = FF_{g,ALOC} \times XF_{inhLOC} \times EF_{inh,non-cancer} + FF_{w,WLOC} \times XF_{ing,wLOC} \times EF_{ing,non-cancer} + FF_{g,ALOC} \times XF_{ing,vegLOC} \times EF_{ing,non-cancer} + FF_{w,WLOC} \times XF_{ing,fLOC} \times EF_{ing,non-cancer} + FF_{g,ACONT} \times XF_{inhCONT} \times EF_{inh,non-cancer} + FF_{w,WCONT} \times XF_{ing,wCONT} \times EF_{ing,non-cancer} + FF_{g,ACONT} \times XF_{ing,vegCONT} \times EF_{ing,non-cancer} + FF_{w,WCONT} \times XF_{ing,fCONT} \times EF_{ing,non-cancer} \quad \text{(Eq. 149)}$$

Where:

- $CF_{LOC,HH,cancer,x}$ (cases kg^{-1}) and $CF_{LOC,HH,non\ cancer,x}$ (cases kg^{-1}) are the characterisation factors for a local emission in compartment x causing carcinogenic and non-carcinogenic effects per kg emitted;
- $FF_{g,ALOC/CONT}$ ($kg_{g,ALOC/CONT}\ kg^{-1}\ h$) is the mass increase that occurs in the local and continental air compartments, respectively, in the gas phase, for an hourly, unitary emission in the local compartment x;
- $XF_{inhLOC/CONT}$ ($m^3_{inh}\ h^{-1}\ pop.loc/cont\ m^{-3}_{g,ALOC/CONT}$) is the volume of air inhaled per hour by the local and continental population, respectively, compared to the volume of the total gas phase of the local and continental air compartment;
- $EF_{inh,cancer}$ ($cases\ cancer\ lifetime\ dose^{-1}$) and $EF_{inh,non\ cancer}$ ($cases\ non\ cancer\ lifetime\ dose^{-1}$) are the lifetime probabilities of having a carcinogenic or non-carcinogenic effect relative to inhalation of a reference dose from toxicological studies;
- $FF_{w,WLOC/CONT}$ ($kg_{w,WLOC/CONT}\ kg^{-1}\ h$) is the mass increase that occurs in the local and continental water compartments, respectively, in the dissolved water phase, for an hourly, unitary emission in the local compartment x;
- $XF_{ing,wLOC/CONT}$ ($m^3_{ing,w}\ h^{-1}\ pop.loc/cont\ m^{-3}_{w,WLOC/CONT}$) is the volume of water ingested per hour by the local and continental population, respectively, compared to the volume of the total dissolved water phase of the local and continental water compartment;
- $EF_{ing,cancer}$ ($cases\ cancer\ lifetime\ dose^{-1}$) and $EF_{ing,non\ cancer}$ ($cases\ non\ cancer\ lifetime\ dose^{-1}$) are the lifetime probabilities of having a carcinogenic or non-carcinogenic effect relative to ingestion of a reference dose from toxicological studies;
- $XF_{ing,vegLOC/CONT}$ ($kg_{ing,veg}\ h^{-1}\ pop.loc/cont\ kg^{-1}_{vegLOC/CONT}$) is the mass of vegetation ingested per hour by the local and continental population, respectively, compared to the total mass of the hypothetical local and continental vegetation compartments;

- $XF_{ing,fLOC/CONT}$ $(kg_{ing,f}\ h^{-1}\ pop.loc/cont\ kg_{fLOC/CONT}^{-1})$ is the mass of fish ingested per hour by the local and continental population respectively, compared to the total mass of the hypothetical local and continental fish compartments.

Eco-toxicity (air/water/soil)

In general, for ecosystem health, CFs are obtained for each emitting compartment x by separating the effects in terms of fractions of PAF-affected species occurring in the receiving compartments, thus expressing air (Eq. 150), water (Eq. 151) and soil (Eq. 152) toxicities separately on both scales.

$$CF_{LOC,A-ECO,x} = FF_{g,ALOC} \times EF_{eco,A} + FF_{g,ACONT} \times EF_{eco,A} \quad \text{(Eq. 150)}$$

$$CF_{LOC,W-ECO,x} = FF_{w,WLOC} \times EF_{eco,W} + FF_{w,WCONT} \times EF_{eco,W} \quad \text{(Eq. 151)}$$

$$CF_{LOC,S-ECO,x} = FF_{w,SLOC} \times EF_{eco,S} + FF_{w,SCONT} \times EF_{eco,S} \quad \text{(Eq. 152)}$$

Where:

- $CF_{LOC,A-ECO,x}$ $(\text{PAF}\ m^3\ \text{h}\ kg^{-1})$, $CF_{LOC,W-ECO,x}$ $(\text{PAF}\ m^3\ \text{h}\ kg^{-1})$ and $CF_{LOC,S-ECO,x}$ $(\text{PAF}\ m^3\ \text{h}\ kg^{-1})$ are, respectively, the local characterisation factor of air, water and soil ecotoxicity, i.e. for a local release of 1 kg in compartment x causing a fraction of affected species integrated in compartment volume and time in the receiving air, water and soil compartments;
- $FF_{g,ALOC/CONT}$ $(kg_{g,ALOC/CONT}\ kg^{-1}\ h)$ is the mass increase that occurs in the local and continental air compartments, respectively, in the gas phase, for an hourly, unitary emission in the local compartment;
- $EF_{eco,A}$ $(PAF\ m^3 kg_A^{-1})$ is the fraction of species potentially affected due to a reference concentration established in the local air compartment by toxicological studies;
- $FF_{w,WLOC/CONT}$ $(kg_{w,WLOC/CONT}\ kg^{-1}\ h)$ is the increase in mass that occurs in the local and continental water compartment, respectively, in the dissolved water phase, for an hourly, unitary emission in the local compartment x;
- $EF_{eco,W}$ $(PAF\ m^3 kg_W^{-1})$ is the fraction of species potentially affected due to a reference concentration established in the local water compartment by toxicological studies;
- $FF_{w,SLOC/CONT}$ $(kg_{w,SLOC/CONT}\ kg^{-1}\ h)$ is the mass increase that occurs in the local and continental soil compartment, respectively, in the pore water phase, for an hourly, unitary emission in the local compartment x;
- $EF_{eco,S}$ $(PAF\ m^3 kg_S^{-1})$ is the fraction of species potentially affected due to a reference concentration established in the local soil compartment from toxicological studies.

As already mentioned in ch. x, in the case of eco-toxicity, a specific XF is not used, as the FF only considers the mass of chemical present in the phase that is bioavailable.

Mid-point CFs

The CFs results for a local emission are summarised in the Table 36 and Table 37.

Table 36 Mid-point CFs for local emissions of benzene on human toxicity in the local-continental model

Effect	$CF_{LOC,HH}$ (cases kg^{-1}) E_{ALOC} = 1 kg h^{-1}	$CF_{LOC,HH}$ (cases kg^{-1}) E_{WLOC} = 1 kg h^{-1}	$CF_{LOC,HH}$ (cases kg^{-1}) E_{SLOC} = 1 kg h^{-1}
Loc. Cancer	9.96E-10	4.44E-08	1.01E-09
Loc. Non cancer	2.52E-10	1.12E-08	2.56E-10
Cont. Cancer	1.41E-09	2.86E-07	1.54E-09
Cont. Non cancer	3.56E-10	7.24E-08	3.89E-10

With regard to human health (Table 36), the CFs disaggregated on the local scale show the same results as those obtained with the local model. In the local-continental model, the effects are highest on the continental scale, with an increase over the local scale of no more than an order of magnitude. The largest increase occurs for an emission in local water, as for this emitter scenario the mass of intake through water ingestion, which has the largest XF, is maximised due to the peak FF reached in continental water compared to the other emitter scenarios.

Table 37 Mid-point CFs for local emissions of benzene on eco-toxicity in the local-continental model. Symbol ↑ indicates CF increase compared to the local model

Receiving compartment *i*	$CF_{LOC,ECO}$ (PAF m^3 h kg^{-1}) E_{ALOC} = 1 kg h^{-1}	$CF_{LOC,ECO}$ (PAF m^3 h kg^{-1}) E_{WLOC} = 1 kg h^{-1}	$CF_{LOC,ECO}$ (PAF m^3 h kg^{-1}) E_{SLOC} = 1 kg h^{-1}
Loc. Air	1.09	**3.09E-04** ↑ (Loc. mod.: 3.07E-04)	1.09
Loc. Water	7.27E-09	4.86E-02	2.37E-05
Loc. Soil	**2.49E-03** ↑ (Loc. mod.: 7.46E-4)	**6.16E-05** ↑ (Loc. mod.: 1.85E-05)	**18.79** ↑ (Loc. mod.: 5.63)
Cont. Air	240.19	66.31	238.78
Cont. Water	6.71E-04	30.9	1.57E-02
Cont. Soil	0.13	0.05	0.13

As shown for FFs, that in the present work already include the bioavailable mass of chemical, for ecotoxicity results (Table 37) some increased values are present on local compartments compared to the local model, in particular local soil for each emitting scenario and local air for local water emission. In the first case the increase can be attributed to the increased volume of local soil, thanks to the absence of sediments and groundwater, in the second case it can be attributed to the presence of continental advective flux into local air.

For each emitting scenario, the continental compartment with the greatest impact (PAF m^3 h) is air, a result attributable to the high value that the FF, and thus mass, takes on in this compartment, characterised by the largest volume, as well as for the calculated EF, the greatest compared to the other eco-toxicities. On the local scale, however, the greatest effect occurs on the same emitting compartment, consistent with the results of the dispersion model, expressed by the FFs.

The general behaviour of the FFs in this model follows the masses results (Table 33), in which continental air and water present the highest values for an emission in the corresponding local compartments, while local soil shows the highest FF for an emission in the compartment itself.

Unlike the results on human health, for emissions to air and water, the damage occurring on the continental scale is more significant than on the local scale, by at least two orders of magnitude. Several differences are present in the calculation of eco-toxicity compared to human toxicity.

First of all, the calculation of human toxicity takes into account the number of people on each scale, so although the concentration on the continental scale is lower than on the local scale, its reduced effect on a single individual, extended to a larger number of people involved, results in greater damage.

In the calculation of eco-toxicity, on the other hand, the impact is calculated for a fraction of affected species, without considering the total number of species involved. Furthermore, as illustrated in chapter 2.4.1, a change of variable in the cause-effect relationship of ecotoxicity being made, moving from concentration to mass in the compartment as cause (x-axis) and from PAFs to PAF m^3 as effect (y-axis), the greater volume of the continental scale returns an amplified impact on it, in terms of PAF m^3, compared to the local scale.

The calculation of the PAFs alone for each emitting scenario on each compartment and scale is reported below (Table 38), in which the graph of the SSD curve approximated by the straight line with the EF as its angular coefficient is used (Eq. 33).

Table 38 PAF results for local emissions of benzene in the local-continental model

Receiving compartment *i*	**PAF E_{ALOC} = 1 kg h^{-1}**	**PAF E_{WLOC} = 1 kg h^{-1}**	**PAF E_{SLOC} = 1 kg h^{-1}**
Loc. Air	4.56E-09	1.29E-12	4.53E-09
Loc. Water	1.45E-13	9.71E-07	4.73E-10
Loc. Soil	2.50E-10	6.19E-12	1.89E-06
Cont. Air	2.63E-14	7.26E-15	2.61E-14
Cont. Water	5.59E-16	2.57E-11	1.31E-14
Cont. Soil	1.44E-15	5.61E-16	1.44E-15

For each local emitting compartment, the highest PAF is always on the same local compartment, as it is characterised by the highest concentration. Continental compartments have concentrations that are at least 3 orders of magnitude lower than the corresponding local compartment. Looking at the continental scale alone, the greatest effect is in the continental compartment corresponding to the local emitter compartment, with the exception of the local soil emitter scenario, where, due to the absence of advective phenomena connecting the local emitter compartment with the continental soil, the greatest concentration occurs in continental air.

The PAF value could also be derived by dividing the value of $PAF\ m^3 h\ kg^{-1}$ for the volume of the compartment whose eco-toxicity is to be assessed, the emission time being 1 h.

As with the local model, no single mid-point toxicity values are derived for each emitting compartment, since for human health the effects are different and for the ecosystem the toxicities of the receiving compartments are defined separately.

End-point CFs

According to USEtox 2.12 model, damage factors (DFs) (Table 24), based on Huijbregts et al. (2005) for human toxicity and on based on Jolliet et al. (2003) for freshwater eco-toxicity, are applied to mid-point results to obtain end-point CFs, expressed for human health (HH) in Disability Adjusted Life Years (DALYs) per kg emitted, that are reported both in disaggregated and aggregated forms on scales (Table 39), and for eco-toxicity in Potentially Disappeared Fraction of Species (PDF) integrated in volume and time, that are reported both in disaggregated and aggregated forms on scales and receiving compartments (Table 40).

Table 39 End-point CFs for local emissions of benzene on human toxicity in the local-continental

Receiving scale S	**$CF_{LOC,HH}$ (DALY kg^{-1}) E_{ALOC} = 1 kg h^{-1}**	**$CF_{LOC,HH}$ (DALY kg^{-1}) E_{WLOC} = 1 kg h^{-1}**	**$CF_{LOC,HH}$ (DALY kg^{-1}) E_{SLOC} = 1 kg h^{-1}**
Local	1.21E-08	5.41E-07	1.23E-08
Continental	1.71E-08	3.49E-06	1.87E-08
Total	2.93E-08	4.03E-06	3.10E-08

As shown for the mid-point results, in the local-continental model the effects are highest at the continental scale, with the increase over the local scale not exceeding an order of magnitude, and the largest increase occurs for a local water emission.

Table 40 End-point CFs for local emissions of benzene on eco-toxicity in the local-continental

Receiving compartment *i*	**$CF_{LOC,ECO}$ (PDF m^3 h kg^{-1}) E_{ALOC} = 1 kg h^{-1}**	**$CF_{LOC,ECO}$ (PDF m^3 h kg^{-1}) E_{WLOC} = 1 kg h^{-1}**	**$CF_{LOC,ECO}$ (PDF m^3 h kg^{-1}) E_{SLOC} = 1 kg h^{-1}**
Loc. Air	5.47E-01	1.54E-04	5.43E-01
Loc. Water	3.63E-09	2.43E-02	1.18E-05
Loc. Soil	1.24E-03	3.08E-05	9.39E+00
Loc. Total	5.48E-01	2.45E-02	9.94E+00
Cont. Air	1.20E+02	3.32E+01	1.19E+02
Cont. Water	3.36E-04	1.54E+01	7.85E-03
Cont. Soil	6.51E-02	2.53E-02	6.47E-02
Cont. Total	1.20E+02	4.86E+01	1.19E+02
Total	1.21E+02	4.86E+01	1.29E+02

The same considerations made for the mid-point results also apply at the end-point level for eco-toxicity, as the reported values were only halved.

4 Testing the local model on the fate modelling

4.1 Comparison with Plume modelling

A comparison was made between the application of a box model for the air compartment, where the concentration is uniformly distributed at every point, and a model that evaluates the dispersion of a pollutant according to a Gaussian distribution. For both models, the only environmental process considered is that determined by the advective effect of the wind alone.

The purpose of this comparison is to check whether, under appropriate conditions, there can be a similarity in the concentration results. The Plume model, as already specified for EUSES, was used to describe the distribution of pollutants near the emission points. The reference document for Plume modelling is by Allen and Durrenberger (Allen and Durrenberger, 2003).

The Gaussian Plume model is a semi-empirical stationary model based on the following assumptions:

- the territory being considered has no significant orography and is morphologically uniform;
- the sources emitting the pollutant are sufficiently high chimneys;
- the emission is continuous;
- the pollutants are chemically non-reactive (the degradation process is not considered);
- the meteorological conditions vary very slowly in space and time (they are constant);
- dispersion along the x-axis is negligible;
- dispersion along the y- and z-axis are Gaussian;
- the plume reactions with soil surface are not considered (soil deposition processes are not considered).

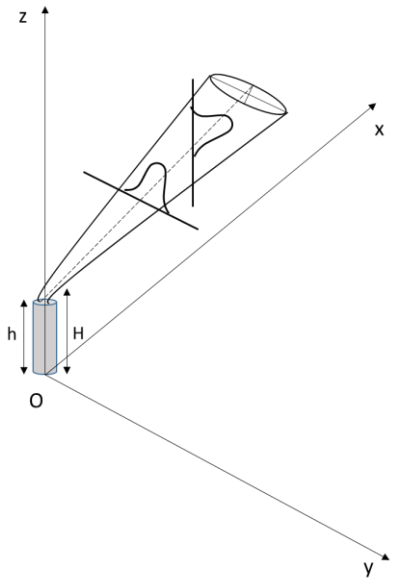

Figure 14 Plume modelling dispersion profiles. Image adapted from Allen and Durrenberger (2003)

The processes involved in plume modelling are (Figure 14):

- advection, i.e. wind transport along the x-axis;
- diffusion in the air compartment, i.e. Gaussian dispersion along the y and z axes.

The equation of the concentration measured in a generic point of co-ordinates (x, y, z) following an emission of height H, located at the origin of the Cartesian axes, in general form is (Eq. 153):

$$C(x,y,z,H) = \frac{Q\times10^6}{2\,\pi\,U\,\sigma_y\sigma_z}\,\exp[-\frac{y^2}{2{\sigma_y}^2}]\left\{\exp[-\frac{(z-H)^2}{2{\sigma_z}^2}]+\exp[-\frac{(z+H)^2}{2{\sigma_z}^2}]\right\} \quad \text{(Eq. 153)}$$

When z = 0 the equation is written as follow (Eq. 154):

$$C(x,y,0,H) = \frac{Q\times10^6}{\pi\,U\,\sigma_y\sigma_z}\,\exp[-\frac{y^2}{2{\sigma_y}^2}]\,\exp[-\frac{H^2}{2{\sigma_z}^2}] \quad \text{(Eq. 154)}$$

where:

- Q (g s^{-1}) is the constant chemical emission rate;
- 10^6 (μg g^{-1}) is mass conversion factor;
- U (m s^{-1}) is the emission velocity;
- σ_y and σ_z (m) are the standard deviations of concentration distribution on y and z axes;
- H (m) is the effective height, given by the sum of the stack height and the height of the plume rise;
- x (m) is the downwind distance from the emitting point;
- y (m) is the distance perpendicular to the wind from the emitting point;
- z (m) is the vertical distance from ground level.

The calculation of σ_y and σ_z (Eq. 155 and Eq. 156) is made according to the stability class, defined according to surface wind speed (3 m s^{-1}) and reported in the EPA guidelines ("Procedures for Evaluation Air Quality Impact of New Stationary Sources"). Considering a surface wind speed of 3 m s^{-1} and assuming a moderate insolation, the corresponding stability class is B.

$$\sigma_y = c \times x^d \quad \text{(Eq. 155)}$$

$$\sigma_z = a \times x^b \quad \text{(Eq. 156)}$$

Where coefficients a,b,c and d are obtained assuming that the emissive source is located at the origin of the cartesian plane (0 m x 0 m), and the wanted concentration is at the half plane and at a height of H=100 m (500 m x 500 m x 100 m) therefore:

- a = 0.1393;
- b = 0.9467;
- c = 0.31;
- d = 0.897.

Therefore:

- σ_z= $0.1393 \times 500^{0.9467}$= 50.01 m;
- σ_y = $0.31 \times 500^{0.897}$ = 81.72 m.

The Plume model allows the calculation of the concentration at a precise point, but as mentioned, this concentration follows a Gaussian distribution along the y and z axes. Therefore, the maximum concentration will be on the x-axis (x, y=0, z=0).

Therefore, to calculate C_{max}, the concentration along the x-axis is calculated using the following formula (Eq. 157):

$$C_{max}(x_{max}, 0,0, H) = \frac{Q \times 10^6}{\pi\, U \sigma_{y_{max}} \sigma_{z_{max}}} \exp[-\frac{H^2}{2\sigma_{z_{max}}{}^2}] \quad \text{(Eq. 157)}$$

Q is equal to 2.17E-02 g s^{-1}, converted obtained according to (Eq. 158):

$$Q = \frac{E_A \times MW \times 10^3}{3600} \quad \text{(Eq. 158)}$$

Where $E_A = 1\ mol\ h^{-1}$ is the emission vector for air compartment, $MW = 0.78\ kg\ mol^{-1}$ is benzene molecular weight and $10^3\ g\ kg^{-1}$is a conversion factor, $3600\ s\ h^{-1}$is a conversion factor.

It is possible to calculate the point on the x-axis where the concentration will be maximum, x_{max} (Eq. 159):

$$x_{max} = [\frac{b \times H^2}{a^2(d+b)}]^{\frac{1}{2b}} \quad \text{(Eq. 159)}$$

x_{max} is equal to 731.07 m, so the maximum ground level concentration falls within the local air compartment considered.

If it did not fall within the local context, unless of constraints on the positioning of the local context to be considered, the local scale under analysis could be moved so that the point of maximum concentration fell within the considered compartment. In the simulation proposed below the emitting point is considered positioned in the middle of one of the sides that forms the boundaries of the local area.

Then, all the mentioned parameter must be calculated according to the x_{max}:

- a_{max} = 0.04936;
- b_{max} = 1.114;
- c_{max} = 0.31;
- d_{max} = 0.897;
- $\sigma_{z_{max}}$= 114.9 m;
- $\sigma_{y_{max}}$ = 76.53 m.

Then, C_{max} = 0.11 μg m^{-3}.

To calculate the average concentration C_{mean} in the air compartment, 6 points were assumed, two located along the x-axis (y = 0 m) and where C is maximum (x_{max}) and C is mean (x_{mean}), two located at the same altitude but for y = 250 m and two for y = 500 m (Eq. 160 and Figure 15).

$$C_{mean} = \frac{C\ (x_{mean},y=0,z=0) + C\ (x_{mean},y=250,z=0) + C\ (x_{mean},y=500,z=0) + C\ (x_{max},y=0,z=0) + C\ (x_{max},y=250,z=0) + C\ (x_{max},y=500,z=0)}{6}$$

(Eq. 160)

An assumption is made about the calculation of $C\ (x_{mean}, y = 0, z = 0)$ that the minimum concentration is 0 µg m^{-3} and occurs immediately at the base of the emissive point, when the plume has maximum height (Eq. 161):

$$C\ (x_{mean}, y = 0, z = 0) = \frac{0.11\ \mu g\ m^{-3} + 0\ \mu g\ m^{-3}}{2} \qquad \text{(Eq. 161)}$$

To determine the crosswind concentration at a distance y from the centerline (x axis), multiply the centerline concentration by a factor (Eq. 162):

$$K_y = \exp[-\frac{y^2}{2\sigma_y{}^2}] \qquad \text{(Eq. 162)}$$

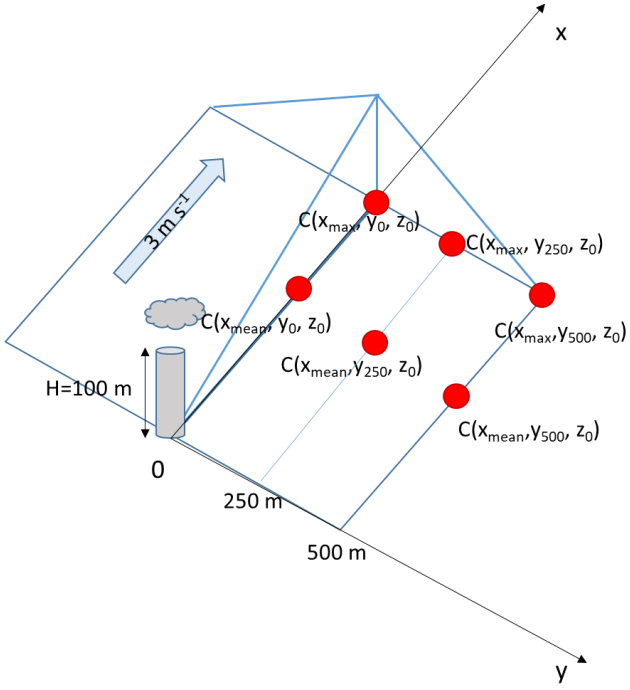

Figure 15 Selected points for Cs calculation in Plume modelling

All points considered are at ground level (z = 0 m) since the scope is to determine the concentration to which humans and biota are exposed to. Just half of the local area was taken into account, as a starting assumption, improvable in future developments.

Therefore, when calculating the average concentration, only the ground level values are taken into account and the resulting number is compared with the value obtained with the well-mixed box approach with fugacity.

The average concentration at ground level is therefore deliberately extended to the entire air compartment, although this is of course not true and is an assumption.

The results of concentrations and parameters are reported in Table 41.

Table 41 Concentrations results in the selected point with Plume modelling

Parameter	Value
$C_{max}\ (x_{max}, y_0, z_0)$ (µg m^{-3})	0.11
$C\ (x_{mean}, y_0, z_0)$ (µg m^{-3})	5.57E-02
$K_y\ (y_{500})$	7.73E-05
$C\ (x_{max}, y_{500}, z_0)$ (µg m^{-3}) = $C_{max}\ (x_{mean}, y_0, z_0) \times K_y\ (y_{500})$	8.62E-06
$C\ (x_{mean}, y_{500}, z_0)$ (µg m^{-3}) = $C\ (x_{mean}, y_0, z_0) \times K_y\ (y_{500})$	4.31E-06
$K_y\ (y_{250})$	9.37E-02
$C\ (x_{max}, y_{250}, z_0)$ (µg m^{-3}) = $C_{max}\ (x_{mean}, y_0, z_0) \times K_y\ (y_{250})$	1.1E-02
$C\ (x_{mean}, y_{250}, z_0)$ (µg m^{-3}) = $C\ (x_{mean}, y_0, z_0) \times K_y\ (y_{250})$	5.23E-03
C_{mean} (µg m^{-3})	3.05E-02

In the case of the concentration calculation with the box model using the fugacity approach, in order to respect the similarities with the Gaussian Plume model, only advection in the air compartment is considered. All other processes between with other compartments are omitted.

Under the assumption of the well mixed box, diffusion within the same compartment is never represented, so only advection is considered in this simulation.

Moreover, the concentration calculated by the box model is homogeneous and well mixed in the air compartment and it is therefore the concentration to which humans and biota are exposed to.

Therefore, the equation for the air compartment becomes (Eq. 163):

$$f_A \times AA = C_A \qquad \text{(Eq. 163)}$$

where:

- $AA\ (mol\ h^{-1} Pa^{-1}) = D_{ADV,A}$
- $C_A\ (mol\ h^{-1}) = E_A$

By inversion of the formula, $f_A = 9.39E-07\ Pa$ and, after multiplication with Z_A and MW, $C_A = 3.01E-02\ \mu g\ m^{-3}$

The results show that, if the concentration obtained with Plume modelling is averaged on several values, in particular in this case study 6 ground points were considered, similar results were obtained with the well mixed box assumption. Even if the well-mixed box assumption could not show the most sensitive points where the highest values of concentration are present, since the spatial resolution is not embedded, anyway the homogeneous concentration resulted to be higher for 4 of the 6 points analyzed, extending a principle of caution to the entire air compartment.

4.2 Comparison with the model of Trent University (CA)

In order to test the robustness of the local model and the correctness of the tool created, the results of the fate model are compared with the model built by Canadian Environmental Modelling Centre of the Trent University in Canada (CA) (Canadian Environmental Modelling Centre (CEMC) 2022), adapting some landscape parameters.

It is a spreadsheet for pollutant dispersion based on level III described in Mackay (2001).

This model considers 4 compartments, both emitting and receiving, and each is composed of phases:

- Air (bulk, air vapour, aerosol);
- Water (bulk, air, susp. particles, fish);
- Soil (bulk, air, water, solids);
- Sediment (bulk, water, solids).

All the environmental processes foreseen by the local model are present, with an important exception, since the irrigation process from water to soil is not considered in the model developed by the CEMC.

A fugacity is calculated for each of the reported compartments and by multiplication with the Z-values of the phases the concentration in each phase is calculated.

This sheet does not allow to assess the effect of the calculated concentration, but only the distribution, so the test is done by comparing the resulting fugacities.

The sheet is constructed considering mainly a section devoted to the substance and its physico-chemical properties, a section devoted to the description of the world unit and a section with the results, in which the fugacities and resulting concentrations are reported. There are two further sections showing graphs useful for understanding the results.

There is a database of substances, which is much more limited than USEtox, but in which the substance 'benzene' under study is also included.

Solving the system of equations is done by substitution, first obtaining the fugacity of the air, and with this the fugacities of the other compartments are obtained by substitution.

The sheet considers the input data of emission rate in kg h^{-1}, therefore, in order to equate the input condition to the sheet constructed in this work (1 mol h^{-1}), the corresponding 0.078 kg h^{-1} are considered as emissions for all compartments, except for sediment, since in the local model, sediment is not an emission compartment.

The input data modified from the original version of the CEMC sheet are shown below (Table 42).

Table 42 Adapted parameters in the calculation tool on Mackay's III level dispersion model by CEMC

Emission Rate (kg h^{-1})	
Into Air	0.078
Into Water	0.078
Into Soil	0.078
Into Sediment	0
Advective Inflow Concentrations	
Concentration in Air	0 ng m^{-3}
Concentration in Water	0 ng L^{-1}
Area (m^2)	
Air	1.00E+06
Water	1.00E+04
Soil	9.90E+05
Sediment	1.00E+04
Depth (m)	
Air	240
Water	5
Soil	10
Sediment	0.5
Advective Flow Residence Times (h)	
Air (obtained by dividing the volume of the compartment by the flow rate, i.e. the speed, considered for the compartment)	9.23E-02
Water (obtained by dividing the volume of the compartment by the flow rate, i.e. the speed, considered for the compartment)	0.28
Sediment (burial) (obtained by dividing sediments height by the burial velocity suggested by Mackay 4.6E-8 m h^{-1})	6.52E+07
Transport velocities (m h^{-1})	
Air-side air-water MTC	1.98E+01
Water-side air-water MTC	2.19E-02
Rain rate	6E-05
Aerosol dry deposition	10
Soil-air phase diffusion MTC	3.35E-04
Soil-water phase diffusion MTC	2.68E-06
Soil-air boundary layer MTC	3.77
Water-side sed.-water diffusion MTC	1E-07
Sediment deposition	4.6E-08
Sediment resuspension	1.1E-08
Soil-water runoff rate	3.9E-05
Soil-solids runoff rate	2.3E-08

The fugacities results are reported in Table 43, in comparison with those of the local model developed in the present study.

Table 43 Fugacities results of the adapted model on Mackay's III level spreadsheet by CEMC

	E_A = 1 mol h^{-1}		E_W = 1 mol h^{-1}		E_S = 1 mol h^{-1}	
Receiving compartment	**Trent University**	**Local model (present study)**	**Trent University**	**Local model (present study)**	**Trent University**	**Local model (present study)**
Air	9.50E-07	9.36E-07	2.59E-10	2.63E-10	7.47E-07	9.31E-07
Water	4.23E-10	4.63E-10	3.09E-03	3.09E-03	1.22E-06	1.51E-06
Soil	7.48E-07	9.31E-07	2.04E-10	2.30E-08	5.67E-03	7.03E-03
Sediment	1.41E-12	1.39E-13	1.03E-05	9.26E-07	4.08E-09	4.51E-10

Compared to the local model developed in the present study and previously described in section 3.2, significant similarities in the results for air, water and soil fugacity for each emitting compartment are present, while the sediment fugacity value is always about 1 order of magnitude smaller (differences in results are highlighted in orange).

For a water emission, the fugacity values in the soil differ by two orders of magnitude, this result could be attributed to the absence of the irrigation process, that reduces the chemical mass in the soil.

The sediments highest result of the Trent University model could be attributed to the absence of fish compartment in the water: fish is considered only as a phase and so all removal processes due to fish presence from water are not considered, probably increasing mass flux towards sediments.

In conclusion, this test shows the robustness of the local model and that the processes were constructed correctly, according to Mackay's instructions.

5 Implementation of the local scale in a current calculation model

Thanks to the collaboration with Prof. Peter Fantke of Quantitative Sustainability Assessment Division, Department of Management Engineering, Technical University of Denmark (DTU), it was possible to deepen and explore the characteristics of the local scale by its inclusion within a widely-used calculation model for LCIA, i.e. the global scientific consensus model USEtox 2.12 (Fantke et al. 2017).

The scope of this part of the study is to assess the relevance of the local scale made of 4 ground-level emitting compartments (air, freshwater, natural soil and agricultural soil), nesting a small scale box within a continental scale environment, in terms of differences and distributions of damages on human and environmental health due to the exposure to all the receiving compartments.

The damage calculation passes through the definition of local characterization factors (CFs), the main output of calculation methods that allow to identify and quantify damage related to the inventory data of an LCA analysis, therefore the introduction of the local environment into the fate and exposure assessment framework of a current calculation model was the first objective pursued. The scientific consensus model USEtox 2.12 model (Fantke et al. 2017) was chosen as the reference model for assessing toxicity of local emissions.

The inclusion of a local environment into the fate and exposure assessment framework of the mentioned model as an Excel spreadsheet (USEtox2.12-local.xlsm) was preparatory for the achievement of the other set objectives, i.e. to derive and compare a set of human health and freshwater ecosystem impact characterization factors per unit emission of an exploration chemical at local and continental scale of the newly built model with the local environment, and, in a following step, to couple them with a set of defined ground-level emissions in a case study for a broader range of chemicals, in order to find drivers of differences in impact scores (ISs) across the model with the local environment and a current model without the local environment and provide recommendations when local scale environments are relevant in LCA.

5.1 Methods

In the calculation method with the local dimension, the introduced local scale, consisting of 4 ground-level emitting and receiving compartments (air, freshwater, natural and agricultural soil), nested in the continental box (Figure 16), was linked with continental and urban scales via advective transport processes, in particular:

- for air compartment, the advective local flow towards the mentioned scales was shared, namely, for 3/4 and 1/4, based on the number of sides of the local air boundary in communication with each scale, that, in turn, exchanges air with the local scale;
- for freshwater compartment, one-way advective flow was foreseen towards continental freshwater.

Intermedia partition processes between local compartments were included as well, respecting the structure of processes and rate constants described in USEtox, for consistency reasons.

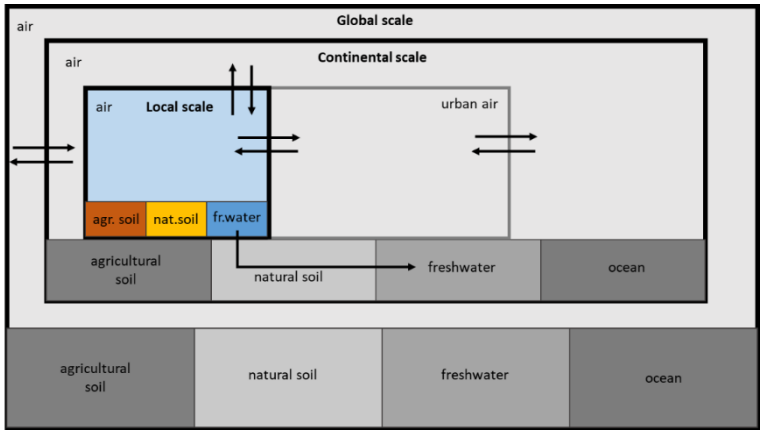

Figure 1 Introduction of the local scale in USEtox, with focus on airflows and water flow. Image adapted from Rosenbaum et al. (2008)

The area of the local scale is 1 x 1 km^2 and it was identified by means of Google Maps on the territory of the Emilia-Romagna region, taken as reference since it is one of the most industrialised regions in Italy. It includes the point of emission into air, water and soil and the consequent intake by people through the exposure pathways already present in USEtox.

It was verified that the distance between densely populated centres and production sites of companies in the ceramic sector, typical of this region, can be as short as 400-500 m, thus estimating a population density at the local scale of about half that of the urban scale (8333 pers km^{-2}) in the USEtox model.

This check was carried out for the sole purpose of verifying the possible proximity of densely populated centres to plants and defining the population density accordingly. The local scale, in fact, represents a generic standard environment, where each compartment could hypothetically be affected by an emission. Human intake through ingestion of water by local population was considered, as better described in chapter 5.2.2, as well as ingestion of food cultivated near a generic point of emission.

Since the well-mixed box model is not able to investigate very local phenomena, like distances between pollutant source and target populations and the evaluation of spatial distances would require appropriately spatialized model, the assumption of steady-state model with instantaneous and homogeneous mixing in every compartment of a local scale was used to provide an estimate of the magnitude of local impacts compared to larger emitting scales, in particular the continental one, but it was not intended to provide realistic concentration distribution within the so defined small scale, that would be better represented by properly spatialized models or non-homogeneous mixing models.

The introduced scale added 4 new mass balance equations and related dimensions in the K-matrix, which, in a previous step of the work, were written with the fugacity approach according to the III type Mackay model, as reported in chapter 3.3. Later, the equations were translated into masses and rate constants, for consistency with USEtox approach, as reported in Table 63 and Table 64 of Appendix – A.4. The calculation is performed in the Excel spreadsheet Mass-based local-continental model.xlsx, in particular, in the sheets “Conversion Local” and “Conversion Continental”.

Two approaches were used into translations and they gave the same results. The first one converts D_i values directly into mass-based rates dividing the by fugacity-based parameters, specific for the contributing compartment, as follows (Eq. 164):

$$k_i = \frac{D_i}{V_i \times Z_{ibulk}} \quad \text{(Eq. 164)}$$

Where k_i (h^{-1}) is the mass-based rate constant for an environmental process originated from i compartment, D_i $(mol\ h^{-1}Pa^{-1})$ is the fugacity-based rate constant for the i compartment, V_i (m^3) is the volume of the i compartment, Z_{ibulk} $(mol\ m^{-3}Pa^{-1})$ is the fugacity capacity of the *i* compartment.

The second approach used required sometimes time-consuming translation procedures, starting from the entire mass flux N_i $(mol\ h^{-1})$ for each environmental process, then the D_i values were unpacked and each parameter contained was translated. In this case, the followed procedure was (from Eq. 165 to Eq. 167):

1. the calculation of the concentration in the phase of the compartment responsible for the process $C_{x,i}$, according to Eq. 165:

$$C_{x,i} = f_i \times Z_x \quad \text{(Eq. 165)}$$

Where $C_{x,i}$ $(mol\ m^{-3})$ is the concentration in the x phase, f_i (m^3) is the fugacity of the i compartment, Z_x $(mol\ m^{-3}Pa^{-1})$ is the fugacity capacity of the x phase.

2. the calculation of the mass in the phase $M_{x,i}$, according to Eq. 166:

$$C_{x,i} = \frac{M_{x,i}}{V_{x,i}} \quad \text{(Eq. 166)}$$

Where $C_{x,i}$ $(mol\ m^{-3})$ is the concentration in the x phase, $M_{x,i}$ (mol) is the mass in the x phase of the i compartment, $V_{x,i}$ (m^3) is the volume of the x phase.

3. the calculation of the mass in the compartment M_i (Eq. 168) starting from the phase applying the equilibrium principle between a compartment and its phases, according to Eq. 167:

$$K_{x,itot} = \frac{C_{x,i}}{C_i} = \frac{\frac{M_{x,i}}{V_{x,i}}}{\frac{M_i}{V_i}} \quad \text{(Eq. 167)}$$

Where $K_{x,itot}$ is the partition coefficient between the x phase and the i compartment, $M_{x,i}$ (mol) is the mass in the x phase, of the i compartment, $V_{x,i}$ (m^3) is the volume of the x phase, M_i (mol) is the mass in the i compartment, V_i (m^3) is the volume of the i-th compartment (Eq. 168).

$$M_i = M_{x,i} \times \frac{V_{x,i}}{V_i} \times K_{x,itot} = M_{x,i} \times v_{x,i} \times K_{x,itot} \quad \text{(Eq. 168)}$$

Where $v_{x,i}$ (m^3) is the volume fraction of the x phase.

The following equation (Eq. 169) was added in defined conditions:

$$fr\_m_{x,i} = v_{x,i} \times K_{x,itot} \quad \text{(Eq. 169)}$$

Where $fr\_m_{x,i}$ is the chemical mass fraction in the x phase of the i compartment.

The unknown M_i was separated from the remaining parameters, that were riunited in mass-based rates k_i (h^{-1}).

A third translation process was considered for diffusive and deposition processes from air to water and soil, according to the procedure suggested by McKone and Bennett (2003), similar to the first one, in which the D_i $(mol\ h^{-1}Pa^{-1})$ were divided by the contact area A_{ij} (m^2) between compartments i and j in order to obtain an intermediate parameter Y_i $(mol\ h^{-1}Pa^{-1}m^{-2})$, that, in turn, was divided by the compartment depth d_i (m) and fugacity capacity Z_{ibulk} $(mol\ m^{-3}Pa^{-1})$. A difference in the final result was observed compared to the previous approaches, since the contact area is lower than the horizontal section of the air compartment.

The correspondence between the equations with fugacity and mass was verified by comparing the fate results of the local-continental model with a copy of the same model in which the new mass-based rates were implemented. The rates and fate results of the new model, called "mass based local-continental model", are reported from Table 63 to Table 65 of Appendix – A.4.

Compared to USEtox rate constants, some differences were present at the end of the translation procedures, due to additional processes considered in USEtox, and they are explicited below each analytical derivation.

For the purpose of applicability in the USEtox model, in a following step, the moles were converted to kg and the time unit became the day, d and additional processes included in USEtox, such as intermittent rain process (Jolliet and Hauschild 2005) and additional soil and sediments diffusion parameters, were integrated into the local scale rates in order to obtain the same rate structure already used in USEtox.

Moreover, landscape parameters of the local scale were aligned with the USEtox ones, in the following way:

- surface area distributed among the compartments as follows: 3% freshwater, 97% soil (48.5% natural soil, 48.5% agricultural soil);
- height of the compartments: 240 m for air, 2.5 m for freshwater, 0.03 m for sediment, 0.1 m for soil;
- local water width: 5 m;
- wind speed: 2.5 m s^{-1};
- water velocity defined by considering the water flow as generated only by rain and, consequently, also by runoff (eq. 28 of USEtox). The latter leads to a lower water flow rate compared to the developed models in this study, as the contribution of mountain springs, for example, would not be taken into account, but this was a necessary modification as otherwise a volume of runoff would have been generated that would have led the sedimentation rate to be negative (USEtox eq. 33);
- soil phase composition: air 20%, water 20%, solid 60%.

Compared to the USEtox model, two differences are included, in particular about the implementation of the corrected formula for the calculation of the chemical mass fraction associated to the gas phase of air compartment FRg, according to Holmquist et al. (2020), that replaces the current version of eq. 8 of USEtox for every scale, and about the calculation

of the local irrigation velocity, where only the local agricultural soil area is considered, according to the following (Eq. 170), that replaces eq. 118 of USEtox:

$$v_{fw[L]} = \frac{v_{[L]}}{A_{[L]} \times fr_{A_{asl\,[L]}}} \times \frac{0.6}{3600 \times 24 \times 365} \quad \text{(Eq. 170)}$$

with $v_{fw[L]}$ is the irrigation from local fresh water to agricultural soil (m s^{-1}), $v_{[L]}$ is the irrigation at local scale (km^3), $A_{[L]}$ is the local system area (km^2), $fr_{A_{asl\,[L]}}$ is the area fraction local agricultural soil, 0.6 is a constant (y), 3600 × 24 × 365 is a conversion factor (s y^{-1}).

The introduction of the corrected formula for FRg for the 10 chemicals investigated, as better illustrated in the following sections, did not produce significant changes, with the exception of two chemicals, Di-(2-ethyl hexyl) phthalate and, at a lesser extent, 2,3,7,8-Tetra CDD. In particular, an increase (respectively, +162.5%, from $FRg_{aC,\,USEtox}$ = 3.60E-01 to $FRg_{aC,\,w/L}$ = 9.45E-01, and +0.2%, from $FRg_{aC,\,USEtox}$ = 9.98E-01 to $FRg_{aC,\,w/L}$ = 1) was observed. The variation is more pronounced for these chemicals as they have the highest octanol-water partition coefficient (respectively, Kow = 3.98E+07 L L^{-1} and Kow = 6.31E+06 L L^{-1}) among the selected chemicals, fundamental property for the calculation of the chemical fraction associated with the aerosol phase of the air compartment. The characteristics and dimensions of the local scale are reported in Table 44, where the changes in dimensional parameters of the other scales are included, too (Table 45), as a consequence of the introduction of the local scale in the "Default USEtox" region.

Table 44 Scale parameters of the local environment

Local scale	Value	Unit
Landscape data		
Area local system	1.00E+06	m^2
Area fraction fresh water	5.00E-03	-
Area fraction natural/agricultural soil	4.98E-01	-
Temperature	2.85E+02	K
Surface wind speed	2.50E+00	$m.s^{-1}$
Average precipitation	2.22E-08	$m.s^{-1}$
Soil erosion	9.51E-13	$m.s^{-1}$
Irrigation	7.79E+03	m^3
Local environment		
Volume air compartment	2.40E+08	m^3
Mixed height air compartment	2.40E+02	m
Volume fraction gas air	1.00E+00	-
Volume fraction water air	2.46E-13	-
Volume fraction aerosols air	2.00E-11	-
Volume fresh water compartment	1.25E+04	m^3
Mixed depth fresh water compartment	2.50E+00	m
Volume fresh water sediment compartment	1.50E+02	m^3
Mixed depth fresh water sediment compartment	3.00E-02	m
Volume fraction water in sediment	8.00E-01	-
Volume fraction solids in sediment	2.00E-01	-
Volume natural soil compartment	4.98E+04	m^3
Volume agricultural soil compartment	4.98E+04	m^3
Depth natural/agricultural soil compartment	1.00E-01	m
Volume fraction air natural/agricultural soil	2.00E-01	-
Volume fraction water natural/agricultural soil	2.00E-01	-
Volume fraction solids natural/agricultural soil	6.00E-01	-
Human population	4.17E+03	

Table 45 Modified scale parameters in the other environments

Other environments	Modified formula	Value
Urban environment		
Transfer air - continental scale	$k.aU.aC = \frac{1}{TAU.aU} - k.aU.aL$	1.74E+01 d^{-1}
Continental environment		
Area continental system	$SYSTEMAREA.C = \frac{(\mathrm{AREAland.C} + \mathrm{AREAsea.C} - \mathrm{SYSTEMAREA.U} - \mathrm{SYSTEMAREA.L})}{1000000}$	1.00E+13 m^2
Area fraction natural soil	$AREAFRAC.s1C = \frac{((\mathrm{AREAland.C} \times \mathrm{FRACnatsoil.C}) - \mathrm{SYSTEMAREA.U} - \mathrm{SYSTEMAREA.L})}{SYSTEMAREA.C}$	4.37E-01
Transfer air - global scale	$k.aC.aG = \frac{1}{TAU.aC} - k.aC.aU - k.aC.aL$	2.42E-01 d^{-1}
Human population	$9.98\mathrm{E}+08 - 4.17\mathrm{E}+03$	9.98E+08

5.2 Assessment of the magnitude of local and continental CFs in the model with the local dimension for a unit emission of benzene

Benzene was designated as a reference substance to explore the behaviour of the newly introduced scale, since it is one of the most commonly studied organic chemicals.

First of all the K-matrix rate constants were derived for the local and continental compartments. Concentration results were obtained dividing the elements of the fate factor FF-matrix (d), provided by the inversion of the K-matrix and representing the mass increase in a receiving compartment for a unit emission in an emitting compartment, and the corresponding receiving compartment volume.

The calculation of the corresponding CFs went through the following definition of exposure for the two considered scales, adopting for the local scale the same factor structure used in USEtox, varying only the populations for the calculation of damage to human health according to the values reported in Table 44 and Table 45. The overall damage expressed by the CFs was broken down into the contributions on the different receiving scales by disaggregating the exposure matrix and the subsequent matrices. For the damage on the aquatic ecosystem, the disaggregation took place at the level of the effect factor matrix, since aquatic ecosystems do not take into account species richness across regions.

5.2.1 Damage comparison between model with the local dimension and a current LCA model for 10 chemicals

In order to assess the relevance of the presence of local scale in the model with the local dimension, the latter was compared with a current LCA model, i.e. USEtox model, through the assessment of the Impact Score (IS) change for human health and freshwater toxicity, defined as Eq. 171:

$$\Delta\%\mathrm{IS}_{x,i} = \frac{IS_{x,i\,(w/\,L)} - IS_{x,i\,(w/o\,L)}}{IS_{x,i\,(w/o\,L)}} \times 100 \qquad \text{(Eq. 171)}$$

with $\Delta\%\mathrm{IS}_{x,i}$ is the percentage damage change across the models for an emission of a chemical x in a compartment i, $IS_{x,i\,(w/L)}$ is the impact score resulting from the model with the local dimension for an emission of a chemical x in a local compartment i according to Eq. 172 below, $IS_{x,i\,(w/o\,L)}$ is the impact score resulting from the Model without the local dimension for an emission of a chemical x in a continental compartment i according to (Eq. 173) below.

$$\mathrm{IS}_{x,i(w/L)} = CF_{x,i,L\ (w/L)} \times E_{x,i,L\ (w/L)} + CF_{x,i,C\ (w/L)} \times E_{x,i,C\ (w/L)} \quad \text{(Eq. 172)}$$

$$\mathrm{IS}_{x,i(w/o\ L)} = CF_{x,i,C\ (w/o\ L)} \times E_{x,i,Ctot\ (w/o\ L)} \quad \text{(Eq. 173)}$$

with $CF_{x,i,L\ (w/\ L)}$ is the characterization factor (DALY kg_{em}^{-1} or PDF m^3 d kg_{em}^{-1}) for an emission of a chemical x in a local compartment i in the model with the local dimension, $E_{x,i,L\ (w/L)}$ is emission (kg) of a chemical x in a local compartment i in the model with the local dimension, $CF_{x,i,C\ (w/L)}$ is the characterization factor (DALY kg_{em}^{-1} or PDF m^3 d kg_{em}^{-1}) for an emission of a chemical x in a continental compartment i in the model with the local dimension, $E_{x,i,C\ (w/L)}$ is emission (kg) of a chemical x in a continental compartment i in the model with the local dimension, $CF_{x,i,C\ (w/o\ L)}$ is the characterization factor (DALY kg_{em}^{-1} or PDF m^3 d kg_{em}^{-1}) for an emission of a chemical x in a continental compartment i in the model without the local dimension, $E_{x,i,Ctot\ (w/o\ L)}$ is emission (kg) of a chemical x in a continental compartment i in the model without the local dimension.

In order to obtain comparable results, the following correlation shall be respected (Eq. 174):

$$E_{x,i,Ctot\ (w/o\ L)} = E_{x,i,L\ (w/\ L)} + E_{x,i,C\ (w/\ L)} \quad \text{(Eq. 174)}$$

Since damage variation is potentially driven by concentration variation, Eq. 175 was employed to show differences in fate between the two models:

$$\Delta C_{x,i} = \frac{C_{x,i,tot\ (w/\ L)} - C_{x,i,tot\ (w/o\ L)}}{C_{x,i,tot\ (w/o\ L)}} \quad \text{(Eq. 175)}$$

with $\Delta C_{x,i}$ is the concentration change across the models for an emission of a chemical x in a compartment i, $C_{x,i,tot\ (w/\ L)}$ is the sum of the concentrations in local and continental i compartments from the model with the local dimension for an emission of a chemical x in the same compartments, $C_{x,i,tot\ (w/o\ L)}$ is the concentration resulting from the model without the local dimension for an emission of chemical x in a continental compartment i, according to eq. Eq. 173.

The proposed model was then applied to 10 chemicals, to include a sufficiently large number of chemicals covered by both the USEtox and E-PRTR databases (EEA 2017) with different physico-chemical properties, on which the simulation with real emitting scenarios, developed in chapter 5.2.2, was based. The main physico-chemical properties of the selected chemicals are reported in Table 46.

Table 46 Physico-chemical properties of the selected chemicals

Chemicals	kdega (s^{-1})	kdegw (s^{-1})	kdegs (s^{-1})	Koc (L kg^{-1})	K_{H25C} (Pa m^3 mol^{-1})
2,3,7,8 -TetraCDD	9.63E-07	4.81E-08	2.14E-10	3.16E+06	5.05E+00
Fluoranthene	2.19E-05	3.23E-08	1.62E-08	6.31E+04	1.33E+00
Anthracene	3.00E-05	5.29E-08	2.64E-08	2.04E+04	5.06E+00
Di-(2-ethyl hexyl) phthalate	1.65E-05	5.35E-07	2.67E-07	8.71E+04	2.73E-02
Atrazine	2.05E-05	1.34E-07	2.77E-07	1.74E+02	2.38E-04
Dichloromethane	1.07E-07	2.14E-07	1.07E-07	2.75E+01	3.28E+02
1,2-dichloroethane (DCE)	1.86E-07	2.14E-07	1.07E-07	3.31E+01	1.19E+02
Naphthalene	1.62E-05	2.54E-06	1.27E-06	9.12E+02	4.62E+01
Benzene	9.23E-07	2.14E-07	1.07E-07	5.62E+01	5.61E+02
1,1,1-trichloroethane	7.01E-09	1.34E-07	6.69E-08	8.91E+01	1.74E+03

For ISs calculation unit emissions are considered for the selected chemicals to show damage results on both local and continental scale of the model with the local dimension ($E_{x,i,L\ (w/\ L)}$ = $E_{x,i,C\ (w/\ L)}$ = 1 kg) and, consequently, 2 kg in the continental scale of the model without the local dimension, according to Eq. 174.

The mentioned quantities considered in this section are not intended to represent realistic emitting conditions, but only to assess at first glance the presence of a possible common trend to all selected chemicals in the transition from one model to another.

5.2.2 Sensitivity analysis: simulation of real European amounts emitted for 10 chemicals

For ISs calculation realistic emissions were considered for the selected chemicals from E-PRTR data for whole Europe. In particular, for each chemical, the total yearly continental emissions were calculated by summing reported emissions in each emitting compartment, from every facility or plant from every activity sector. The selected emission year was the most recent with the highest number of emitting point reported, taking care to avoid accidental releases as local emissions, identified as large amounts emitted that are not repeated in adjacent years to the one considered. Then, the total amount of the chemical x for the emitting compartment i of the model without the local dimension was referred to daily emissions and called $E_{x,i,Ctot\ (w/o\ L)}$.

The quantities considered for the model with the local dimension were determined according 3 emitting scenarios as follows:

- the local emissions of chemical x for air and soils compartments $E_{x,a/ns/as,L\ (w/\ L)}$were defined in turn as the daily maximum/mean/minimum value among those reported for chemical industry sector. The mean value was calculated as the arithmetic mean of the admissible values;
- the local emissions of chemical x for water compartment $E_{x,w,L\ (w/\ L)}$were defined in turn as the daily maximum/mean/minimum value among those reported for urban wastewater treatment effluents. The mean value was calculated as the arithmetic mean of the admissible values;
- the continental emissions of chemical x for every i emitting compartment $E_{x,i,C\ (w/\ L)}$ were calculated according to Eq. 174.

Local emissions were supposed to coincide with emissions from a facility or plant that had the above-mentioned characteristics.

The constraint of the activity sectors for the local emissions was necessary in order to provide a realistic representation about types of emitting sources that could be found on a local environment and to which local population could be exposed to. In fact, the local surface area was supposed to include the point of emission into air, water and soil and the consequent intake by people living in the proximity of the emitting point. Air emissions and soil emissions were supposed to be generated by chemical industries, whose presence in 1 x 1 km^2 was documented by means of Google Maps on the territory of the Emilia-Romagna region in Italy, as reported in chapter 5. Drinking water consumption in 1 x 1 km^2 was considered compatible with the presence of urban wastewater treatment plants in a local scale since the Italian regulation currently governing safeguard areas for surface and groundwater intended for human consumption (Italian Ministry of the Environment and Protection of and territory 2006) distributed through aqueduct systems

stipulates that safeguard areas are to be identified, divided into absolute protection zones and protection zones, in which the dispersion of wastewater, even if purified, is prohibited for a radius of 10 m and 200 m respectively from the point of capture.

It is important to emphasise that the considerations reported above are intended only to identify the possible types of emitting sources near densely inhabited centres, since the simple box model is not able to investigate very local phenomena, like distances between pollutant source and target populations.

The entity of local emission over the total continental emission is reported in Table 47. Generally, for air compartment, the percentage on local scale ranges from 0.17% to 15.13% and for water compartment from 0.02% to 25% of total continental emissions.

Table 47 Percentage of local emission over total continental emission according to the 3 emitting scenarios. n/a for the mean emission scenario indicates that there is no existing location emitting the reported quantity

Chemical x	**Emitting compartment i (year data)**	$\mathbf{E}_{x,i,\mathrm{L}\,(\mathrm{w/\,L})} = \mathbf{MAX}\ \mathbf{E}_{x,i,\mathrm{Ctot}\,(\mathrm{w/o\,L})}$ **(country of local emission)**	$\mathbf{E}_{x,i,\mathrm{L}\,(\mathrm{w/\,L})} = \mathbf{MEAN}\ \mathbf{E}_{x,i,\mathrm{Ctot}\,(\mathrm{w/o\,L})}$ **(country of local emission)**	$\mathbf{E}_{x,i,\mathrm{L}\,(w/\,\mathrm{L})} = \mathbf{MIN}\ \mathbf{E}_{x,i,\mathrm{Ctot}\,(\mathrm{w/o\,L})}$ **(country of local emission)**
2,3,7,8 -TetraCDD	Air (2016)	0.94% (Poland)	0.07% (n/a)	0.01% (Poland)
	Water (2016)	2.16% (Italy)	0.63% (n/a)	0.19% (U.K.)
Fluoranthene	Air (2017)	1.52% (Norway)	0.78% (n/a)	0.03% (Norway)
	Water (2017)	0.59% (Italy)	0.22% (n/a)	0.09% (Sweden)
Anthracene	Water (2013)	4.75% (U.K.)	0.68% (n/a)	0.25% (U.K.)
Di-(2-ethyl hexyl) phthalate	Air (2015)	2.24% (U.K.)	1.63% (n/a)	1.51% (Czech Republic)
	Water (2015)	4.64% (Sweden)	0.25% (n/a)	0.01% (Spain)
Atrazine	Water (2016)	50.70% (Italy)	25% (n/a)	6.89% (Germany)
Dichloromethane	Air (2016)	15.13% (Italy)	0.96% (n/a)	0.03% (Switzerland)
	Water (2016)	12.85% (Italy)	0.89% (n/a)	0.13% (U.K.)
	Nat. Soil (2009)	100% (Czech Republic)	100% (Czech Republic)	100% (Czech Republic)
1,2-dichloroethane (DCE)	Air (2016)	12.48% (France)	1% (n/a)	0.19% (France)
	Water (2016)	9.86% (Italy)	2.94% (n/a)	0.15% (Poland)
	Nat. Soil (2009)	100% (France)	100% (France)	100% (France)
Naphthalene	Air (2016)	0.17% (Spain)	0.12% (n/a)	0.04% (Portugal)
	Water (2016)	0.3% (U.K.)	0.02% (n/a)	0.01% (U.K.)
Benzene	Air (2016)	5.14% (U.K.)	0.47% (n/a)	0.03% (Germany)
	Water (2016)	0.05% (Italy)	0.05% (Italy)	0.05% (Italy)
1,1,1-trichloroethane	Air (2016)	12.53% (France)	3.16% (n/a)	1.29% (Belgium)

For some chemicals not all the emitting compartments were considered for local emissions due to the absence of the identified type of sources in E-PRTR database.

Since none of the selected chemicals, for which soil emission data were available from E-PRTR data, were pesticides, agricultural soil was never considered as emitting compartment. Moreover, for natural soil emissions, only one emission value is available for Dichloromethane and 1,2-Dichloroethane (DCE), thus for every emitting scenario $\mathbf{E}_{x,i,\mathrm{L}\,(\mathrm{w/\,L})} =$

$\mathbf{E}_{x,i,\mathrm{Ctot\ (w/o\ L)}} = \mathbf{100}\%$. For benzene water emissions, only one value was available for urban wastewater treatment plant, thus for every emitting scenario $\mathbf{E}_{x,i,\mathrm{L\ (w/\ L)}} = \mathbf{0.5}\%\ \mathbf{E}_{x,i,\mathrm{Ctot\ (w/o\ L)}}$.

5.3 Results

5.3.1 Analysis of rate constants of the K-matrix for benzene from model with the local dimension

The variation of the rate constants between the main scales of the model with the local dimension are reported in Table 48 for benzene.

Table 48 Rate constants of the K-matrix (d^{-1}) of the model modified with the local dimension. The added compartments to the USEtox framework are: airL = local air, fr.waterL = local freshwater, nat.soilL = local natural soil, agr.soilL = local agricultural soil.

Loss processes	**Emitting compartment**								
	airU	airL	fr.waterL	nat.soilL	agr.soilL	airC	fr.waterC	nat.soilC	agr.soilC
removal	3.55E-04	3.17E-05	**8.32E-05**	2.85E-03	2.85E-03	3.17E-05	**5.33E-05**	2.85E-03	2.85E-03
degradation	7.97E-02	7.97E-02	1.85E-02	9.24E-03	9.24E-03	7.97E-02	1.85E-02	9.24E-03	9.24E-03
Receiving compartment	**Emitting compartment**								
	airU	airL	fr.waterL	nat.soilL	agr.soilL	airC	fr.waterC	nat.soilC	agr.soilC
airU	-1.87E+01	7.20E+01	0	0	0	1.07E-04	0	0	0
airL	1.20E+00	-2.88E+02	1.78E-01	7.84E-02	7.84E-02	6.91E-06	0	0	0
fr.waterL	0	8.22E-05	-2.37E-01	2.85E-03	2.85E-03	0	0	0	0
nat.soilL	0	2.77E-04	0	-9.34E-02	0	0	0	0	0
agr.soilL	0	2.77E-04	1.02E-03	0	-9.34E-02	0	0	0	0
airC	1.74E+01	2.16E+02	0	0	0	-3.23E-01	2.08E-01	7.84E-02	7.84E-02
fr.waterC	1.78E-04	0	3.89E-02	0	0	1.25E-04	-2.34E-01	2.85E-03	2.85E-03
sea.waterC	0	0	0	0	0	1.29E-04	6.97E-03	0	0
nat.soilC	0	0	0	0	0	5.83E-05	0	-9.33E-02	0
agr.soilC	0	0	0	0	0	5.83E-05	6.55E-05	0	-9.33E-02
airG	0	0	0	0	0	2.42E-01	0	0	0
fr.waterG	0	0	0	0	0	0	0	0	0
nat.soilG	0	0	0	0	0	0	0	0	0
agr.soilG	0	0	0	0	0	0	0	0	0

The soils volatilization rates (highlighted in yellow) are the same between the two scales for soil since they do not depend on the size of the compartments. For water the value of the local volatilization rate (highlighted in light blue) is lower because of the dependence of the partial mass transfer coefficients on the wind speed, lower (2.5 m s^{-1}) compared to the continental one (3 m s^{-1}). The soils partial mass transfer coefficients, on the other hand, are constant, according to USEtox model.

These similarities are not preserved for the absorption rates (to water, in dark green, and to soils, in pink) since they depend on the respective area fractions, resulting in opposite tendences between absorption rate to water, lower at the local scale than the continental scale for smaller freshwater area fraction (0.005 for local freshwater and 0.0272 for continental water), and absorption to soils, higher at the local scale than the continental one for greater soil area fraction (0.498 for each local soil and 0.437 for each continental soil).

The irrigation rate from water to agricultural soil (highlighted in orange) is greater for the local scale than for continental soil because of the difference described above (Eq. 170).

The local removal rate for freshwater (in bold font) is higher than the continental one since the net sediment accumulation rate, described in eq. 33 of USEtox, is directly proportional to the area fractions of soils.

The advection rates from local and continental freshwater compartments are highlighted in light green, showing that the first one is higher of about one order of magnitude, because of the inverse proportionality with the size of the compartment.

The dominant processes for each emitting compartment are of the same type between the scales, in particular advection for air and volatilization for freshwater and soils. In the case of local air emitting compartment, advection rates towards bigger environments like continental and urban air are significantly high compared to continental rate (+3 orders of magnitude, highlighted in dark blue) towards global air, because of the direct proportionality between the residence time in air and the size of the compartment.

5.3.2 Analysis of concentrations and CFs for local and continental emissions of benzene

Considering an emission of 1 kg d^{-1} of benzene, the local scale always has higher concentrations (Table 49) for an emission in the same scale compared to those found on the continental scale. This result can undoubtedly be attributed to the greater volume of the continental scale, which lowers the concentration of the incoming mass.

Urban air shows a higher concentration compared to the continental air compartment for reasons related to the compartment volume, too, and 2 orders of magnitude separate local and urban air for each emitting compartment.

Local air registers similar values of concentration for each local emitting compartment, since the main process for water and soils is represented by volatilization, but lower values compared to those found in local water and soils for an emission in the same compartments, due to the relevance of advective process in air.

For an emission in the continental scale, different behaviours can be observed on the local compartments, in particular local air shows a concentration of the same order of magnitude of the continental and urban air, while local freshwater and soils always show lower concentrations compared to the corresponding continental compartments. These results can be explained taking into account that a direct link via advection is present only between air compartments.

In particular, for a continental air emission, the local air shows a concentration that is twice as high as the former, partly due to the additional contribution from the urban scale.

Table 49 Concentration results (kg m^{-3}) of the model with the local dimension for 1 kg d^{-1} of benzene emitted

	Emitting compartment			
Receiving compartment	**airL**	**fr.waterL**	**nat.soilL**	**agr.soilL**
airU	2.37E-13	1.79E-13	2.04E-13	2.04E-13
airL	1.47E-11	1.11E-11	1.27E-11	1.27E-11
fr.waterL	1.18E-10	3.38E-04	1.03E-05	1.03E-05
nat.soilL	2.10E-10	1.59E-10	2.15E-04	1.82E-10
agr.soilL	2.11E-10	9.32E-07	2.86E-08	2.15E-04
airC	3.25E-16	2.94E-16	2.82E-16	2.82E-16
fr.waterC	2.65E-15	1.04E-12	3.41E-14	3.41E-14
nat.soilC	4.64E-15	4.20E-15	4.03E-15	4.03E-15
agr.soilC	4.65E-15	5.33E-15	4.07E-15	4.07E-15
Receiving compartment	**airC**	**fr.waterC**	**nat.soilC**	**agr.soilC**
airU	3.34E-16	3.00E-16	2.90E-16	2.90E-16
airL	6.59E-16	5.91E-16	5.72E-16	5.72E-16
fr.waterL	5.30E-15	4.76E-15	4.60E-15	4.60E-15
nat.soilL	9.43E-15	8.46E-15	8.18E-15	8.18E-15
agr.soilL	9.44E-15	8.47E-15	8.19E-15	8.19E-15
airC	3.25E-16	2.92E-16	2.82E-16	2.82E-16
fr.waterC	2.64E-15	6.33E-12	1.96E-13	1.96E-13
nat.soilC	4.65E-15	4.17E-15	2.45E-11	4.03E-15
agr.soilC	4.65E-15	1.10E-14	4.25E-15	2.45E-11

The damages calculated for unit emissions on both scales (Table 50) are always higher for local compartments, ranging from twice (air emission) to + 2 orders of magnitude for human health, while the increase of the factors for the quality of the ecosystem remains more limited on the local scale (one order of magnitude is never reached).

Table 50 Characterization factors (CFs) results for 1 kg d^{-1} of benzene emitted

	Emitting compartment			
Endpoint toxicity potential	**airL**	**fr.waterL**	**nat.soilL**	**agr.soilL**
Human health (DALY kg_{em}^{-1})	2.26E-06	3.67E-04	1.31E-05	5.87E-05
Freshwater ecosystem (PDF m^3 d kg_{em}^{-1})	2.58E-02	3.80E+01	1.18E+00	1.18E+00
Endpoint toxicity potential	**airC**	**fr.waterC**	**nat.soilC**	**agr.soilC**
Human health (DALY kg_{em}^{-1})	1.02E-06	2.55E-06	9.34E-07	2.18E-06
Freshwater ecosystem (PDF m^3 d kg_{em}^{-1})	2.58E-02	3.30E+01	1.03E+00	1.03E+00

5.3.3 Analysis of the damage distribution on the receiving scales

For human toxicity (Table 51), the combination between high concentration and high population broadly determines the extent of damage on each receiving scale.

For this reason, for an emission of 1 kg d^{-1} in the local compartments, the highest contribution to human toxicity can be found on the same emitting compartments, except for air emission, where urban air dominates the damage due to the higher population.

Considering an emission in the continental compartments, the local scale always shows the lowest damage.

Table 51 Disaggregated CFs on the receiving scales for endpoint human health toxicity potential (DALY kg_{em}^{-1}) for benzene

	Emitting compartment			
Receiving scale	**airL**	**fr.waterL**	**nat.soilL**	**agr.soilL**
Urban	1.10E-06	8.32E-07	9.49E-07	9.49E-07
Local	1.43E-07	3.65E-04	1.13E-05	5.68E-05
Continental	7.55E-07	9.52E-07	6.64E-07	6.64E-07
Global	2.61E-07	2.36E-07	2.26E-07	2.26E-07
Receiving scale	**airC**	**fr.waterC**	**nat.soilC**	**agr.soilC**
Urban	1.55E-09	1.39E-09	1.35E-09	1.35E-09
Local	6.40E-12	5.74E-12	5.55E-12	5.55E-12
Continental	7.56E-07	2.32E-06	7.06E-07	1.95E-06
Global	2.61E-07	2.34E-07	2.27E-07	2.27E-07

For freshwater ecotoxicity (Table 52), damage is driven by the bioavailable mass rather than intake mass. For this reason, for an emission of 1 kg d^{-1} in the local compartments, the highest contribution can be found on the same emitting scale, except for air emission.

In this case, in fact, the stored mass in local air (FF_{aL} = 3.53E-03 kg_{comp} d kg_{em}^{-1}) is very low compared to the continental and global mass in air ($FF_{aC,aL}$ = 1.92E+01 kg_{comp} d kg_{em}^{-1} and $FF_{aG,aL}$ = 6.95E+02 kg_{comp} d kg_{em}^{-1}), leading to an absorbed mass in freshwater dependent on the reported values, but even lowered for the local freshwater compartment by the smaller absorption rate, as shown in chapter 5.3.2 (respectively $FF_{wL,aL}$= 4.90E-07 kg_{comp} d kg_{em}^{-1}, $FF_{wC,aL}$ = 3.48E-03 kg_{comp} d kg_{em}^{-1}). The significant difference between the mentioned masses can be attributed to the high local advection rate towards the continental air, as shown in chapter 5.3.2.

For an emission in local freshwater, a non-negligible contribution could be found on the continental scale, thanks to the advective process.

For an emission in the continental scale, the highest contribution can be found on the same emitting scale, since advection is not present towards local freshwater.

Table 52 Disaggregated CFs on the receiving scales for ecotoxicity potential (PDF m^3 d kg_{em}^{-1}) for benzene

	Emitting compartment			
Receiving scale	**airL**	**fr.waterL**	**nat.soilL**	**agr.soilL**
Local	1.14E-05	3.26E+01	9.93E-01	9.93E-01
Continental+Global	2.58E-02	5.45E+00	1.88E-01	1.88E-01
Receiving scale	**airC**	**fr.waterC**	**nat.soilC**	**agr.soilC**
Local	5.11E-10	4.58E-10	4.43E-10	4.43E-10
Continental+Global	2.58E-02	3.30E+01	1.03E+00	1.03E+00

5.3.4 Analysis of the IS change between the two models for different chemicals for unit emission

Table 53 CFs resulting from the model with the local dimension for the 10 chemicals

Endpoint human health toxicity potential (DALY kg_{em}^{-1})	**2,3,7,8 - TetraCDD**	**Fluoranthene**	**Anthracene**	**Di-(2-ethyl hexyl) phthalate**	**Atrazine**	**Dichloromethane**	**1,2-dichloroethane (DCE)**	**Naphthalene**	**Benzene**	**1,1,1-trichloroethane**
$CF_{a,C}$	3.97E+02	5.26E-05	1.21E-04	1.50E-05	1.02E-05	1.44E-06	1.96E-06	1.03E-06	1.02E-06	4.02E-08
$CF_{a,L}$	4.74E+02	1.22E-04	3.61E-04	3.33E-05	1.22E-04	2.00E-06	3.10E-06	7.91E-06	2.26E-06	4.22E-08
$CF_{w,C}$	1.67E+03	1.01E-03	2.93E-03	4.08E-06	5.40E-05	2.25E-06	1.80E-05	8.16E-06	2.55E-06	4.00E-08
$CF_{w,L}$	7.02E+04	9.65E-02	4.63E-01	5.65E-04	4.45E-03	2.14E-04	3.58E-03	1.71E-03	3.67E-04	7.18E-07
$CF_{ns,C}$	1.78E+02	6.20E-06	2.82E-05	1.95E-09	2.12E-06	1.28E-06	2.68E-06	1.53E-07	9.34E-07	3.66E-08
$CF_{ns,L}$	1.84E+03	2.40E-04	1.71E-03	8.05E-08	1.75E-04	1.27E-05	2.59E-04	3.80E-06	1.31E-05	5.30E-08
$CF_{as,C}$	3.06E+02	4.13E-05	3.31E-04	3.38E-07	1.18E-05	1.81E-06	1.82E-05	2.11E-06	2.18E-06	3.88E-08
$CF_{as,L}$	5.32E+03	1.44E-03	1.25E-02	1.24E-05	5.29E-04	3.23E-05	8.28E-04	7.53E-05	5.87E-05	1.34E-07
Endpoint ecotoxicity potential (PDF m^3 d kg_{em}^{-1})	**2,3,7,8 - TetraCDD**	**Fluoranthene**	**Anthracene**	**Di-(2-ethyl hexyl) phthalate**	**Atrazine**	**Dichloromethane**	**1,2-dichloroethane (DCE)**	**Naphthalene**	**Benzene**	**1,1,1-trichloroethane**
$CF_{a,C}$	1.08E+05	2.12E+02	2.89E+02	1.35E+00	2.43E+03	4.15E-02	6.08E-02	3.50E-01	2.58E-02	9.44E-02
$CF_{a,L}$	1.14E+05	2.72E+02	3.33E+02	2.14E+00	4.05E+03	4.16E-02	6.08E-02	3.80E-01	2.58E-02	9.44E-02
$CF_{w,C}$	4.72E+06	5.70E+04	1.51E+05	1.61E+02	4.37E+04	7.30E+00	7.55E+00	4.53E+02	3.30E+01	1.08E+01
$CF_{w,L}$	1.47E+06	4.55E+04	1.57E+05	1.68E+02	4.87E+04	8.40E+00	8.68E+00	4.86E+02	3.80E+01	1.25E+01
$CF_{ns,C}$	1.80E+05	1.56E+02	5.94E+02	2.06E-02	1.71E+03	4.11E-01	5.86E-01	7.64E-01	1.03E+00	3.18E-01
$CF_{ns,L}$	9.00E+04	1.41E+02	6.16E+02	2.19E-02	1.91E+03	4.67E-01	6.66E-01	8.18E-01	1.18E+00	3.54E-01
$CF_{as,C}$	1.80E+05	1.56E+02	5.94E+02	2.06E-02	1.71E+03	4.11E-01	5.86E-01	7.64E-01	1.03E+00	3.18E-01
$CF_{as,L}$	9.00E+04	1.41E+02	6.16E+02	2.19E-02	1.91E+03	4.67E-01	6.66E-01	8.18E-01	1.18E+00	3.54E-01

In Table 54 the percentage IS change $\Delta\%IS$ for human health across the models is reported in the hypothesis of a unit emission for each scale of the model with the local dimension. The CFs used in Eq. 172 are reported in Table 53.

Table 54 Percentage IS change results ($\Delta\%IS_{x,i}$) according to Eq. 171 for endpoint human health toxicity potential ($\Delta\%$DALYs) for 10 chemicals with $E_{x,i,L\ (w/\ L)} = E_{x,i,C\ (w/L)} = 1$ kg and $E_{x,i,Ctot\ (w/o\ L)} = 2$ kg

	Emitting compartment *i*			
Chemical *x*	**air**	**fr.water**	**nat.soil**	**agr.soil**
2,3,7,8 -TetraCDD	+9.62%	+2051.44%	+467.10%	+818.58%
Fluoranthene	+65.643%	+4710.21%	+1883.84%	+1696.31%
Anthracene	+98.96%	+7846.34%	+2983.69%	+1841.75%
Di-(2-ethyl hexyl) phthalate	+61.15%	+6872.90%	+4136.62%	+3670.50%
Atrazine	+544.61%	+4071.52%	+8228.92%	+4486.61%
Dichloromethane	+19.32%	+4718.06%	+446.68%	+841.94%
1,2-dichloroethane (DCE)	+29.26%	+9900.66%	+4786.76%	+2225.03%
Naphthalene	+334.50%	+10397.30%	+1187.48%	+1732.03%
Benzene	+60.82%	+7148.70%	+651.21%	+1297.33%
1,1,1-trichloroethane	+2.53%	+847.78%	+22.41%	+122.85%

For every chemical and every emitting compartment a damage increase is observed, in particular for air emissions the range increase is more limited compared to the other compartments, due to the higher mass transferred from local scale to the continental one via advection, as shown by the transfer coefficients $f_{iL,iC}$, that express the mass fraction emitted in a i local compartment transferred to the corresponding i continental compartment (Table 55).

Table 55 Transfer coefficients $f_{iL,iC}$ from local to continental compartments of the selected chemicals resulting from the model with the local dimension

Chemical *x*	$f_{aL,aC} = FF_{aL,aC}/FF_{aC}$	$f_{wL,wC} = FF_{wL,wC}/FF_{wC}$	$f_{nsL,nsC} = FF_{nsL,nsC}/FF_{nsC}$	$f_{asL,asC} = FF_{asL,asC}/FF_{asC}$
2,3,7,8 -TetraCDD	9.93E-01	1.11E-01	4.10E-02	4.10E-02
Fluoranthene	9.66E-01	3.55E-01	1.80E-03	1.80E-03
Anthracene	9.59E-01	3.11E-01	5.47E-04	5.48E-04
Di-(2-ethyl hexyl) phthalate	9.55E-01	4.27E-01	2.30E-05	2.31E-05
Atrazine	6.36E-01	7.54E-01	2.98E-04	4.02E-04
Dichloromethane	1.00E+00	1.69E-01	2.83E-04	2.85E-04
1,2-dichloroethane (DCE)	1.00E+00	1.78E-01	4.20E-04	4.24E-04
Naphthalene	9.77E-01	9.71E-02	1.71E-04	1.71E-04
Benzene	9.99E-01	1.65E-01	1.64E-04	1.66E-04
1,1,1-trichloroethane	1.00E+00	1.87E-01	4.72E-04	4.73E-04

High transfer coefficients $f_{iL,iC}$ for air lead to a lower mass stored in the local compartment and, consequently, a lower concentration increase $\Delta C_{x,i}$, defined according to Eq. 175 in the hypothesis of a unit emission, between the two models compared to other emitting compartments, as depicted in Figure 17.

Even though soils transfer coefficients are lower compared to water compartment, the concentration increase is more significant for the latter for the smaller volume compared to soils (Table 44).

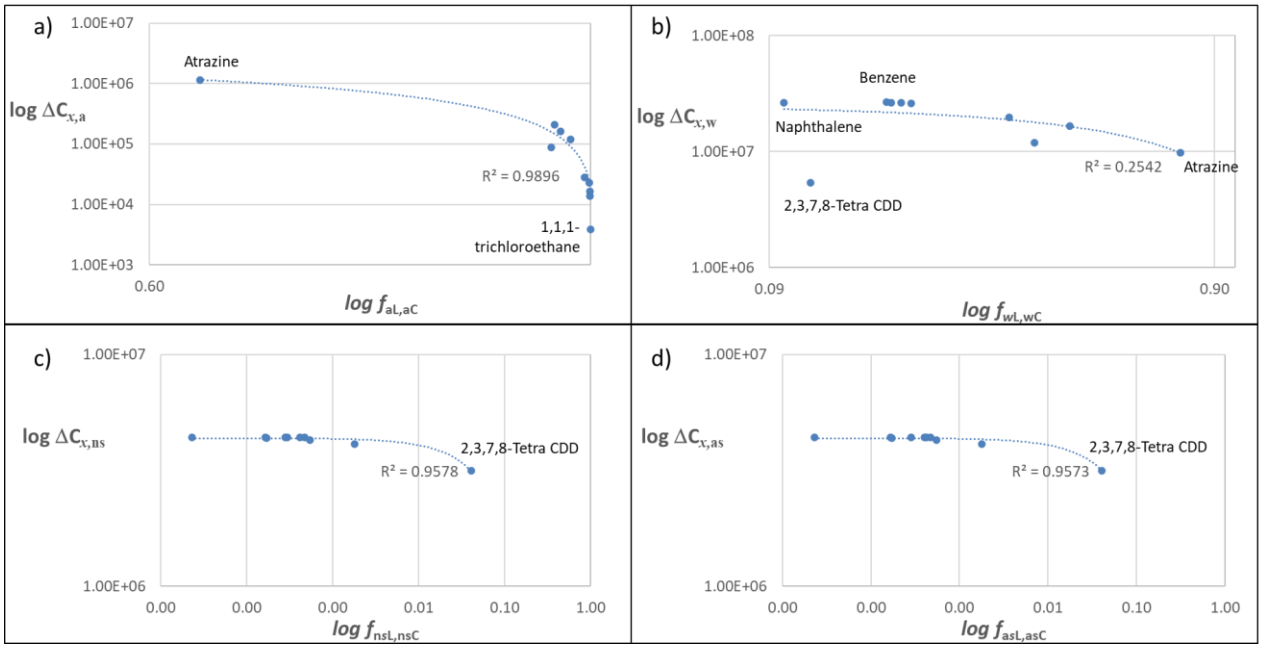

Figure 17 Concentration change (ΔC) for every emitting compartment - a) air, b) freshwater, c) natural soil, d) agricultural soil - respect to the transfer coefficients.

A strong correlation is present between $\Delta C_{x,i}$ and $f_{L,C}$ for air compartment (Figure 17a), where the chemical with the lowest $f_{aL,aC}$ is Atrazine and it is the chemical with the highest concentration and damage increase between the models. Atrazine is the chemical with the lowest air-water partition coefficient (Table 46), leading to a reduction of the mass flux displaced via advection towards continental air due to the significant water absorption.

On the other hand, 1,1,1-trichloroethane is characterized by the lowest degradation rate in air (Table 46), that allows a high transport to the continental scale, resulting in the lowest concentration (ΔC = 3.83E+03) and damage (Table 54) increase between the models.

A weaker correlation is present for water compartment (Figure 17b), where in particular 2,3,7,8-Tetra CDD (ΔC = 5.42E+06, $f_{wL,wC}$ = 1.11E-01) is not interpolated by the trend line. This chemical, due to its high Koc (Table 46) is characterized by the highest local removal for sedimentation process, that lowers the mass in the local compartment compared to the continental one (FF_{wL} = 2.85 kg_{comp} d kg_{em}^{-1}, FF_{wC} = 1.42E+01 kg_{comp} d kg_{em}^{-1}), producing a limited concentration increase compared to the other chemicals.

The chemicals with the highest ΔC are Benzene, Dichloromethane, Naphthalene and 1,2-Dichloroethane, because of different chemical and physical properties. In fact Naphthalene is characterized by the highest degradation rate (Table 46), thus reducing the mass transferred to the continental scale (i.e. the chemical does not have 'time' to reach the continental scale, FF_{wL} = 2.49 kg_{comp} d kg_{em}^{-1}, $FF_{wL,wC}$ = 2.48E-01 kg_{comp} d kg_{em}^{-1}), while the other mentioned chemicals are characterized by the highest air-water partition coefficients, reducing the chemicals persistence in water. Atrazine, the chemical with the highest water transfer coefficient thanks to its limited tendency to volatilize, has a low concentration increase.

Soil compartments (Figure 17c and Figure 17d) show a low variability of concentration with transfer coefficients change, with the exception of 2,3,7,8-Tetra CDD, which combines the highest transfer coefficient with the lowest

increase in concentration. This chemical is characterized by the lowest degradation rate in soil (Table 8), that allows a high transport to the continental scale.

Generally, all transfer coefficients of the soil compartments are much lower than the air and water compartments (up to - 4 orders of magnitude, Table 55), mainly due to the absence of advective process linking the different scales. For this reason, no significant concentration increases are appreciable between the two models across chemicals.

Since the IS is obtained by multiplication of three factors (FF, XF and EF), the correlations shown above between $\Delta C_{x,i}$ and $f_{iL,iC}$ are less pronounced, or even not found, when $\Delta\%IS_{x,i}$ is related to $f_{iL,iC}$, as reported in Figure 18.

Generally, a great variability in damage change across chemicals with similar transfer coefficients can be noticed for every emitting compartment. This result can be attributed mainly to differences in toxicity effects of different chemicals.

For example, for water emission scenario, the great variability in damage change among chemicals with low $f_{wL,wC\%}$ (9-20%) could be attributed mainly to the EFs, in fact for 2,3,7,8 TetraCDD, Dichloromethane and 1,1,1-trichloroethane lower values are present compared to the other chemicals with low transfer fractions (Table 56).

Table 56 Percentage IS change (Δ%IS) for endpoint human health toxicity potential (Δ%DALYs) and EFs for chemicals with low $f_{wL,wC}$

Chemical x	**$f_{wL,wC}$ (%)**	$\Delta\%IS_{x,i}$	**EF (Cancer) (cases kg_{intake}^{-1})**	**EF (Non cancer) (cases kg_{intake}^{-1})**
Naphthalene	9.71%	+207.95%	Inh.: 7.3E-2 Ing.: 7.3E-2	Inh.: 7.19E-2 Ing.: 1.29E-2
2,3,7,8 -TetraCDD	11.14%	+41.03%	Inh.: 4.88E-4 Ing.: 4.88E-4	Inh.: 0 Ing.: 0
Benzene	16.49%	+142.98%	Inh.: 1.47E-2 Ing.: 1.47E-2	Inh.: 3.72E-3 Ing.: 3.72E-3
Dichloromethane	16.89%	+94.36%	Inh.: 1.86E-3 Ing.: 2.62E-3	Inh.: 2.17E-2 Ing.: 2.17E-2
1,2-dichloroethane (DCE)	17.84%	+198.01%	Inh.: 1.42E-2 Ing.: 1.43E-1	Inh.: 0 Ing.: 0
1,1,1-trichloroethane	18.75%	+16.97%	Inh.: 0 Ing.: 0	Inh.: 1.08E-4 Ing.: 1.08E-4

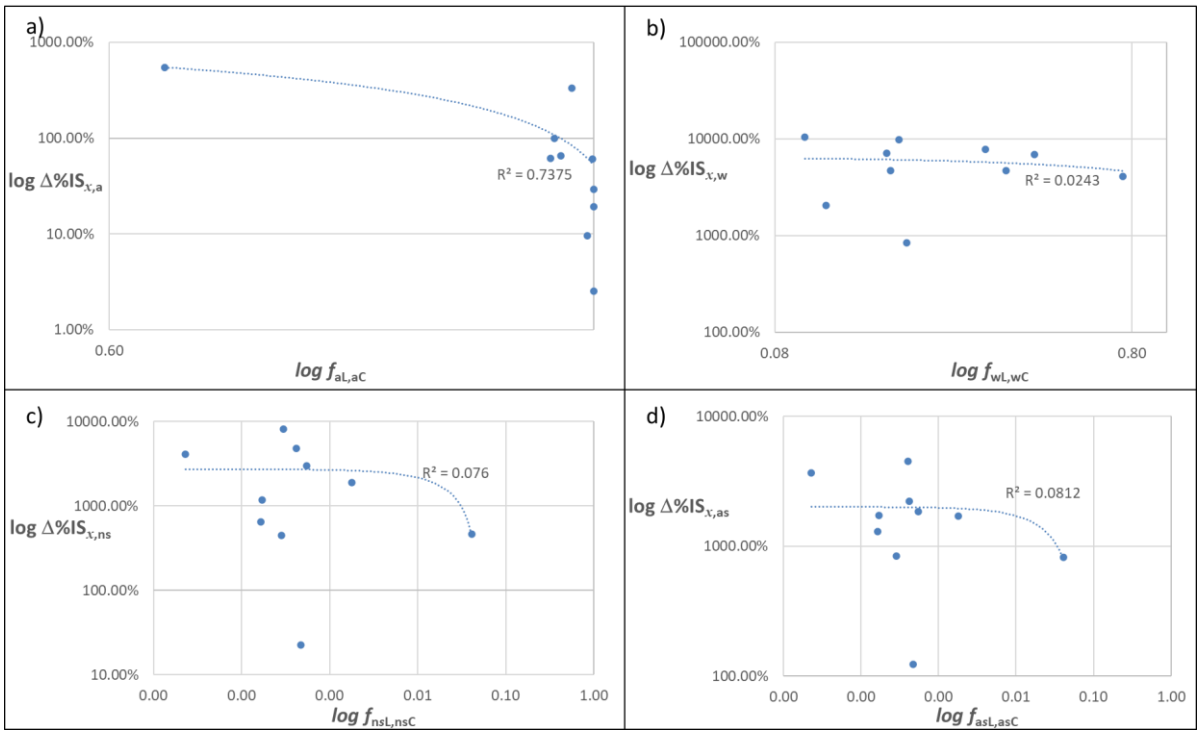

Figure 18 Percentage IS change (Δ%IS) for endpoint human health toxicity potential (Δ%DALYs) for every emitting compartment - a) air, b) freshwater, c) natural soil, d) agricultural soil - respect to the transfer coefficients

In Table 57 the percentage IS change Δ%IS for ecotoxicity across the models is reported in the hypothesis of a unit emission for each scale of the model with the local dimension.

For the endpoint ecotoxicity potential, the IS increase is not always detectable, depending on the emitting compartment and on the chemical. In particular, an IS decrease occurs for air emission of Di-2-ethyl hexyl phtalate and for water and soils emissions of 2,3,7,8 TetraCDD and Fluoranthene.

Table 57 Percentage IS change (Δ%IS) for endpoint ecotoxicity potential (Δ%PDF m³ d) for every emitting compartment for 10 chemicals with $E_{x,i,L\ (w/\ L)} = E_{x,i,C\ (w/\ L)} = 1$ kg and $E_{x,i,Ctot\ (w/o\ L)} = 2$ kg

	Emitting compartment *i*			
Chemical *x*	**air**	**water**	**nat. soil**	**agr. soil**
2,3,7,8 -TetraCDD	+2.40%	-34.40%	-25.08%	-25.08%
Fluoranthene	+14.152%	-10.10%	-4.85%	-4.85%
Anthracene	+7.46%	+2.21%	+1.92%	+1.92%
Di-(2-ethyl hexyl) phthalate	-12.70%	+2.15%	+2.85%	+2.84%
Atrazine	+33.48%	+5.79%	+5.85%	+5.86%
Dichloromethane	+0.02%	+7.57%	+6.91%	+6.91%
1,2-dichloroethane (DCE)	+0.03%	+7.47%	+6.86%	+6.86%
Naphthalene	+4.28%	+3.61%	+3.50%	+3.50%
Benzene	+0.11%	+7.62%	+7.41%	+7.41%
1,1,1-trichloroethane	+0.02%	+7.74%	+5.68%	+5.68%

For air emission, some CFs for continental air of the model with the local dimension (Table 53) are lower than those resulting for the same emitting compartment of the model without the local dimension. This result is always verified,

for every chemical, emitting compartment and type of damage (i.e. DALYs and PDFs) and it is probably attributable to the introduction of a new receiving scale from the continental environment that reduces chemical mass stored there.

But, in particular for Di-(2-ethyl hexyl) phthalate, a significant reduction is observed for CF_{aC} (from 2E-06 PDF m^3 d kg_{em}^{-1} of model without the local dimension to 1.35E-06 PDF m^3 d kg_{em}^{-1} of the model with the local dimension). This result is attributed to the update of the calculation formula for the fraction of chemical of the gas phase FRg in the model with the local dimension according to Holmquist et al. (2020), which was found to be very effective for this chemical, as explained in chapter 5.1.

A slight decrease is observed for $CF_{aC\ (USEtox\ L)}$ of 2,3,7,8 – TetraCDD, too (-0.3%) for the same reason, but damage reduction is not found for this emission condition.

The decrease in IS for 2,3,7,8 TetraCDD and Fluoranthene for water and soils emissions is, instead, due to a reduced CF for the local scale compared to the continental scale of the model with the local dimension.

This difference is attributed to a very lower mass stored in the local freshwater compartment compared to the continental one (for 2,3,7,8 TetraCDD FF_{wL} = 2.85, FF_{wC} = 1.42E+01; for Fluoranthene FF_{wL} = 9.1, FF_{wC} = 2.06E+01). The damage pathway for ecosystem, as reported in chapter 2.4, takes into account the bioavailable mass of chemical dissolved in the freshwater compartment.

For the mentioned chemicals the CFs reduction on the local scale was proven to depend on a higher local removal rate for sedimentation, that for these chemicals is the most relevant process in water compartments, compared to the continental scale, due to their high Koc (Table 46). Moreover, the fraction of chemical dissolved in the water phase is is negatively affected by the tendency of the chemical to be absorbed more into the organic carbon of the suspended solids. Di-(2-ethyl hexyl) phthalate, even if characterized by a high Koc, too, is mainly removed via degradation in water and soils.

5.3.5 Analysis of the results of the sensitivity analysis for real European amounts for 10 chemicals

The results reported in the following sections are highly dependent on the proportion between amounts at local and continental scale of chemical emitted, so the results will not be commented on too extensively. For more detailed information on the influence of chemicals characteristics on the results, please refer to the previous section.

In Figure 19 the results of human health toxicity change for air emissions are reported, in particular for each chemical the damage increase is reported according to the 3 scenarios of local emission.

If the maximum local scenario is considered, the damage increase does not exceed 8% (1,2-dichloroethane (DCE), 7.31%), if the mean local scenario is considered the damage increase does not exceed 2% (Di-(2-ethyl hexyl) phthalate, 1.99%).

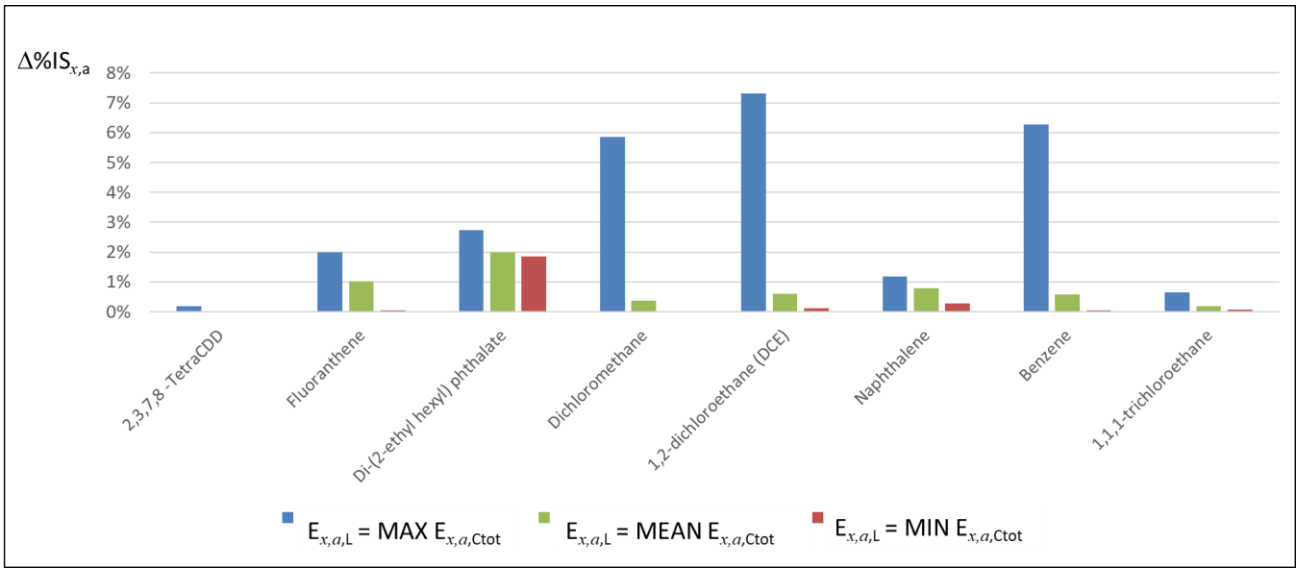

Figure 19 Percentage IS (Δ%IS) change for endpoint human health toxicity potential (Δ%DALYs) for every inventoried chemical emitted in air according to the 3 emitting scenarios

For water emissions (Figure 20), the highest IS increase is observed for Atrazine (+4128.58%) in the maximum scenario, while the IS increase for the mean emitting scenario ranges from +5.13% (Naphthalene) to +2035.76% (Atrazine).

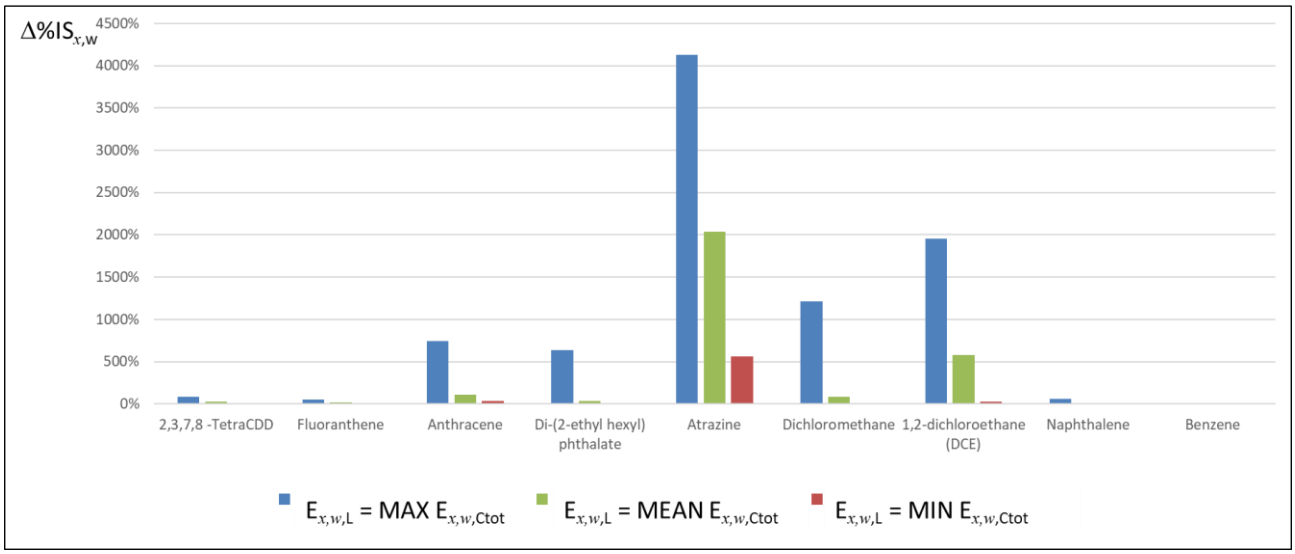

Figure 20 Percentage IS (Δ%IS) change for endpoint human health toxicity potential (Δ%DALYs) for every inventoried chemical emitted in water according to the 3 emitting scenarios

For natural soil emissions (Figure 21), only two chemicals emissions were available from E-PRTR database. Moreover, for Dichloromethane and 1,2-dichloroethane (DCE) only one emission value from chemical industry source was reported, thus the IS increase is the same for the 3 emitting scenarios, ranging from 893.35% to 9573.52%.

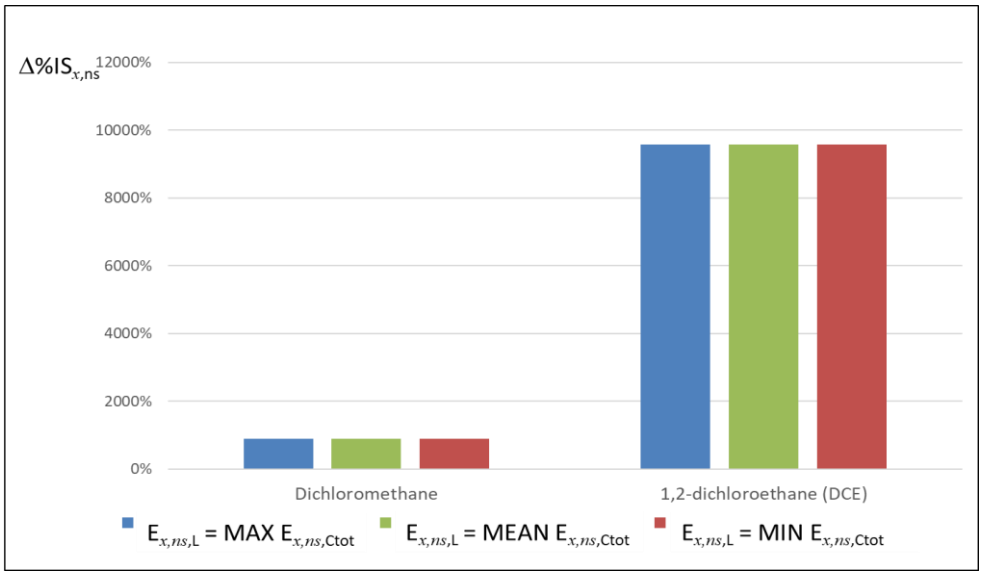

Figure 21 Percentage IS (Δ%IS) change for endpoint human health toxicity potential (Δ%DALYs) for every inventoried chemical emitted in natural soil according to the 3 emitting scenarios

The 3 realistic scenarios of local emission accentuate the trend highlighted in Table 56 for chemicals with damage decrease.

The results reported in Figure 22 show ecotoxicity change for each chemical emitted in air, where the highest damage increase is observed for Fluoranthene in the maximum emission scenario (+0.42%), and the highest decrease occurs for Di-(2-ethyl hexyl) phthalate (-31.78%) in the minimum emission scenario. Also 2,3,7,8-Tetra CDD shows a slight damage decrease (ranging from -0.31% to -0.26%, according to the emission scenario), unlike in the Table 56 for different emission conditions.

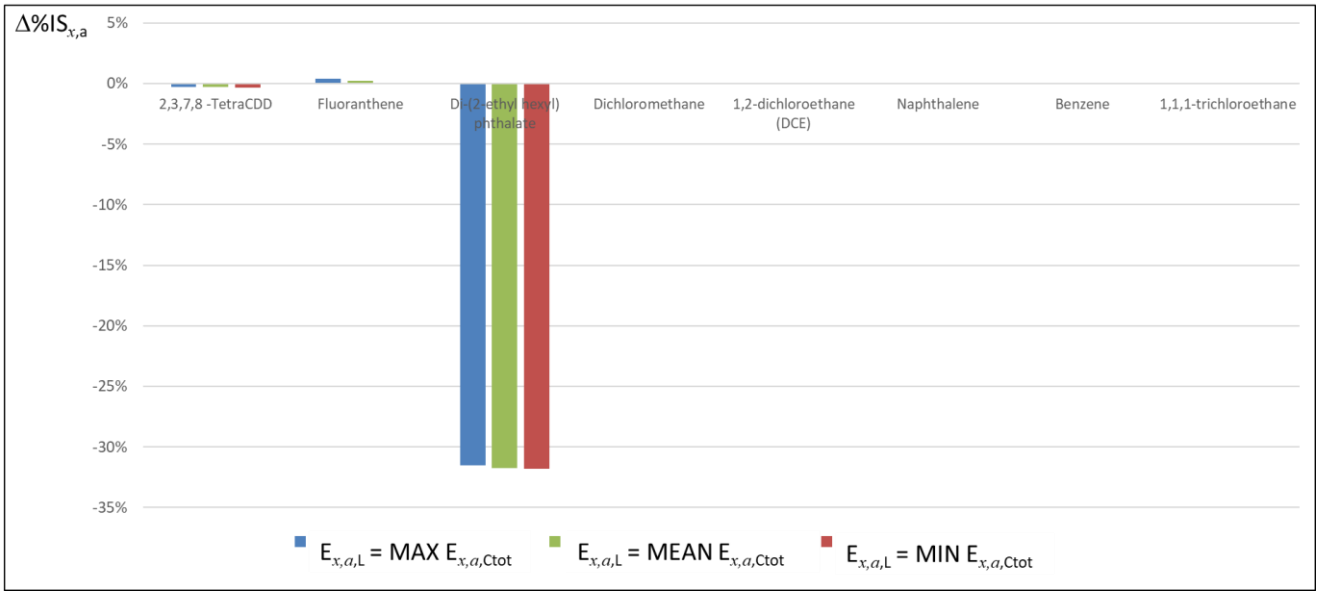

Figure 22 Percentage IS (Δ%IS) change for endpoint ecotoxicity potential (Δ%PDF m^3 d kg_{em}^{-1}) for every inventoried chemical emitted in air according to the 3 emitting scenarios

The results reported in Figure 23 for water emission show a more varied situation than in the previous emission compartment, where chemicals with the highest damage increase (Dichloromethane and 1,2-dichloroethane (DCE)) and

with the highest damage decrease (2,3,7,8-TetraCDD and Fluoranthene) in the model with the local dimension compared to USEtox are emphasised by the considerable masses emitted in the maximum emission scenario (Table 57).

For the average emission scenario, the highest damage increase is observed for 1,2-dichloroethane (DCE) (+0.44%) and the highest damage decrease for 2,3,7,8-TetraCDD (-0.43%).

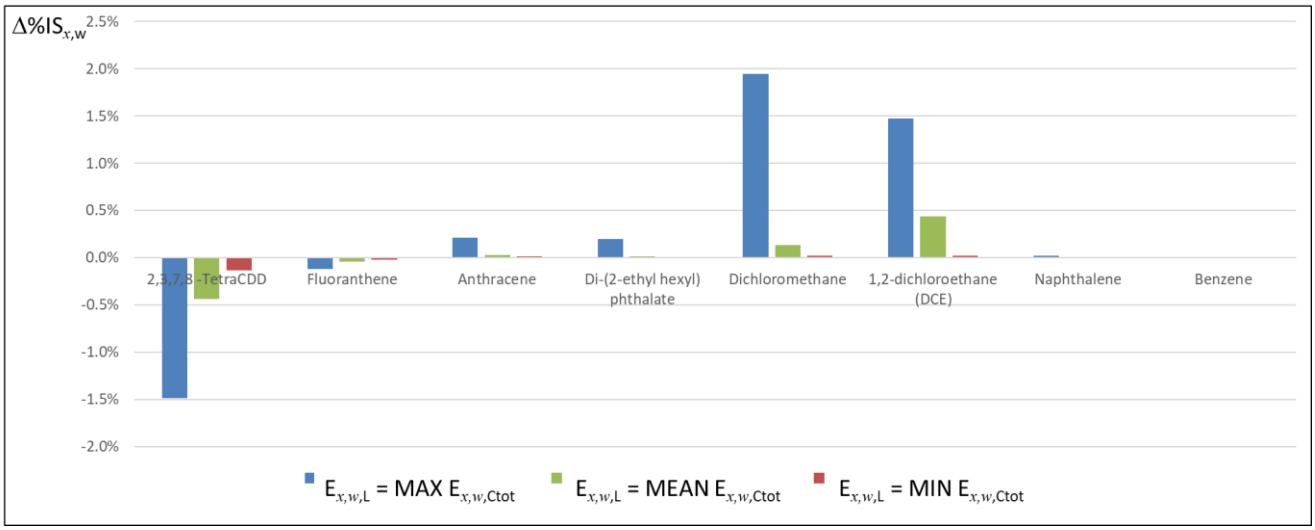

Figure 23 Percentage IS (Δ%IS) change for endpoint ecotoxicity potential (Δ%PDF m³ d kg$_{em}^{-1}$) for every inventoried chemical emitted in water according to the 3 emitting scenarios

For natural soil emissions (Figure 24) the IS increase is the same for the 3 emitting scenarios, ranging from 13.72% to 13.82%.

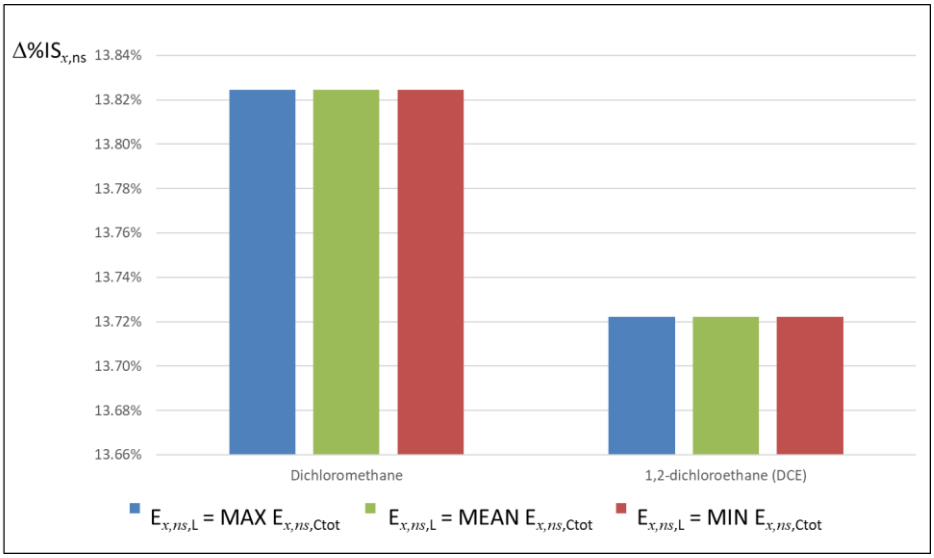

Figure 24 Percentage IS (Δ%IS) change for endpoint ecotoxicity potential (Δ%PDF m³ d kg$_{em}^{-1}$) for every inventoried chemical emitted in natural soil according to the 3 emitting scenarios

6 Comparison between the local-continental model and a current LCA model adapted with the local scale

A comparison between the local-continental model developed in the present study (see chapter 3.3) and a current LCA model adapted with the local scale is proposed below in order to analyse the results of the fate models. USEtox v. 2.12 was taken as reference. In our opinion, it is less meaningful to compare the final results in terms of effect, firstly because the focus for this comparison is the introduction of the local scale and fate results, and secondly, because the definition of the effect factors is either totally identical between the two models, as for human health, or analyses different eco-toxicities. Furthermore, the differences between the models in terms of human exposure and effect for the aquatic ecosystem were highlighted in chapter 3.2.6.

In order to make a meaningful comparison between the results of the two models at the local scale, certain parameters were adapted in the local-continental model in order to create the most similar conditions possible of the existing model adapted with local scale.

Below is a list of the landscape parameters of the local-continental model that were equated with those in use in the reference model, i.e. USEtox 2.12:

- local and continental soil height h_S = 0.1 m;
- local and continental h_W water height = 2.5 m;
- local and continental sediment height h_{SED} = 0.03 m;
- local water depth $Depth_W$ = 5 m;
- local sediment depth $Depth_{SED}$ = 5 m;
- local freshwater flow G_W = 2.03E+01 m^3 h^{-1};
- continental freshwater discharge G_W = 1.08E+08 m^3 h^{-1};
- volume fraction of water in soil = 0.2
- volume fraction of solid in soil = 0.6;
- local wind speed = 2.5 m s^{-1};
- continental wind speed = 3 m s^{-1}.

Landscape-related parameters such as volumes varied accordingly.

In addition, the influence of parameters related to degradation and diffusion processes was noted. In order to equate the models, USEtox values were assumed, in particular:

- degradation rate in air of benzene, which in the USEtox database has a lower value (k_{degA} = 9.2E-07 s^{-1}) than that reported in the Mackay volume (k_A = 1.13E-05 s^{-1});
- degradation rate in water of benzene, which in the USEtox database presents a lower value (k_{degW} = 2.1E-07 s^{-1}) from that reported in the Mackay volume (k_W = 1.13E-06 s^{-1});
- soil degradation rate of benzene, which in the USEtox database presents a lower value (k_{degSl} = 1.1E-07 s^{-1}) from that reported in the Mackay volume (k_S = 3.5E-07 s^{-1});

- penetration depth relative to the air-soil diffusion, soil side, PENdepth.sL = 0.849 m, calculated on the basis of the chemical, in use in USEtox, different from the thickness Y= 2E-03 m considered in the study as a proxy for the air-water situation;
- partial mass transfer coefficient for air-soil diffusion, air side, k_V = 18 m h^{-1} in USEtox, while the value suggested by Mackay is k_V = 3.77 m h^{-1};
- partition coefficient between gas phase and organic carbon phase used in USEtox K_{SA} = 21.51, while from Mackay equations it results to be K_{SA} = 7.25 for benzene.

The local-continental model - for comparison has, similar to the other models developed in this paper, an emission vector of $\vec{E}\ (mol\ h^{-1})$ while in USEtox source vector $\vec{S}\ (kg\ d^{-1})$. Thus, the comparison was performed considering 1 kg d^{-1} in the different local compartments of the adapted USEtox model and 0.53 mol h^{-1} in the local-continental model - by comparison, by converting units according to the general formula (Eq. 176):

$$\vec{E} = \frac{\vec{S}}{MW \times 24} \qquad \text{(Eq. 176)}$$

where $MW = 0.78\ kg\ mol^{-1}$ is benzene molecular weight and $24\ h\ d^{-1}$ is day-to hours conversion factor.

Below are the results in terms of benzene masses and bulk concentrations for each local emitter scenario (Table 58).

Table 58 Comparison of concentrations results between adapted USEtox model with the local scale and the local-continental model

	Receiving compartment *i*	**C_i (kg m^{-3}) $E_{A,LOC}$ = 1 kg d^{-1}**	**C_i (kg m^{-3}) $E_{W,LOC}$ = 1 kg d^{-1}**	**C_i (kg m^{-3}) $E_{NS,LOC}$ = 1 kg d^{-1}**	**C_i (kg m^{-3}) $E_{AS,LOC}$ = 1 kg d^{-1}**
USEtox 2.12 modified with the local scale	**A_{LOC}**	1.47E-11	1.11E-11	1.27E-11	1.27E-11
	W_{LOC}	1.18E-10	3.38E-04	1.03E-05	1.03E-05
	NS_{LOC}	2.10E-10	1.59E-10	2.15E-04	1.82E-10
	AS_{LOC}	2.11E-10	9.32E-07	2.86E-08	2.15E-04
	A_{CONT}	3.25E-16	2.94E-16	2.82E-16	2.82E-16
	W_{CONT}	2.65E-15	1.04E-12	3.41E-14	3.41E-14
	NS_{CONT}	4.64E-15	4.20E-15	4.03E-15	4.03E-15
	AS_{CONT}	4.65E-15	5.33E-15	4.07E-15	4.07E-15
Local-continental model	**Receiving compartment *i***	**C_i (kg m^{-3}) $E_{A,LOC}$ = 1 kg d^{-1}**	**C_i (kg m^{-3}) $E_{W,LOC}$ = 1 kg d^{-1}**	**C_i (kg m^{-3}) $E_{S,LOC}$ = 1 kg d^{-1}**	
	A_{LOC}	1.93E-11	8.92E-12	1.86E-11	
	W_{LOC}	6.10E-11	7.53E-04	3.01E-05	
	S_{LOC}	3.52E-11*	5.01E-07	4.72E-05*	
	A_{CONT}	6.59E-16	5.10E-16	6.43E-16	
	W_{CONT}	2.62E-15	6.92E-12	2.79E-13*	
	S_{CONT}	1.21E-15	5.56E-15	1.36E-15	

All emitting scenarios show a good correspondence in the concentration results between the two models.

Differences in the local-continental model compared to the modified USEtox that are equal to or exceed 1 order of magnitude are indicated with an *. These concern the local soil and continental water compartments. In particular, in the local-continental model local soil concentrations are smaller than in the modified USEtox model, while an opposite trend observed for continental water. The modified USEtox model includes additional removal processes from the compartments such as:

- air: escape to stratosphere;
- water: sedimentation and burial;
- soil: leaching.

These removal processes are not considered in the local-continental model, as only processes concerning the compartments included in the system have been included.

The absence of such processes in the local-continental system should lead the results to higher concentration values than in the USEtox model adapted with the local scale, and this is reflected only for continental water case. For local soil compartment, in the two reported emitter scenarios, the concentration is lower. The difference between the soil volumes in the two models (the sum of the agricultural and natural soil volumes of USEtox is equal to the soil volume of the local-continental model) is not sufficient to explain a difference of 1 order of magnitude, since, at most, doubling the volume of one of the two USEtox soils and minimising the other would halve the concentration.

The reasons for this could lie in the diffusive or deposition phenomena linking air and soil, however, to our current knowledge, all parameters relating to these processes were compared and equated. It is difficult to estimate the influence of the differences in terms of the overall framework between the two models (taking an indoor, urban and global scale as well as additional compartments such as seawater for USEtox).

7 Conclusive remarks and future perspectives

Two gaps currently present in the LCA were identified in this work and a preliminary model was proposed to at least partially fill them. The first one concerns the quantification of the potential damage occurring on human health and eco-system in a small scale near the emitting point through LCA methodology. The "local issue" was raised during a public debate of an Italian city council with the citizens worried about the fate and exposure to emissions from the municipal waste incinerator and, in that occasion, LCA researchers from University of Modena and Reggio Emilia, summoned to give their opinion to the local authority and citizenship, have found that the local scale is scarcely considered in the currently available methods.

The second challenge faced in this work was the evaluation of eco-toxicity in all environmental compartments. Nowadays, the most studied compartment is freshwater, so much so that it was included in the USEtox v. 2.12 evaluation framework, the UNEP/SETAC global scientific consensus model for characterizing human and ecotoxicological impacts of chemical emissions in life cycle assessment (Fantke et al. 2017). The lack of availability of reliable data about chronic EC_{50} has postponed the inclusion of soil and air toxicity, or partially addressed, as in the case of soil toxicity (Fantke, et al. 2018; Jolliet et al. 2003).

To overcome the reported limitations, two models were proposed within this study, characterized for one largely studied chemical, i.e. benzene. At the same time, the obtained results were analyzed in order to assess the relevance of the local damage.

Moreover, the relevance of the local issue was deepen also in the context of a current model for LCA, i.e. USEtox v. 2.12. The presence of a chemicals database gave the opportunity to study the behaviour of the local scale on additional chemicals, in order to provide indications on the recommended use of the local scale according to the physico-chemical properties of chemicals.

A discussion is reported below, analyzing results, application, limitations and future developments for the new proposed models and the current LCA model modified with the local scale.

Both new proposed models produce CFs for local emissions in air, water and soil, addressing human toxicity, expressed in DALYs per emitted kg of benzene, and full eco-toxicity, including soil and air effects on biodiversity, expressed in PDF m^3 d per emitted kg of benzene.

CFs were built according to the general framework of USEtox 2.12 (Fantke et al. 2017; Rosenbaum et al. 2008) thus including the quantification of the environmental concentration thanks to a fate model, that take into account all transport and removal processes according to chemical's properties, the quantification of the intake mass by targets – e.g. taking into account the exposure route, the number of people exposed - through exposure to the concentration, the calculation of adverse effect based on toxicological tests results.

CFs are intentionally left disaggregated on the different receiving scales (for human health and for eco-toxicity) and on the receiving compartments (for eco-toxicity), in order to allow the LCA practitioner to know distinctly the damage on the human population and on the biota, also distinguished by type of ecosystem, in the local scale. Aggregated value of

CFs are provided, too, at end-point level, since normally CFs provide the sum of damages occurring in each receiving compartment on each scale caused by a unit emission.

About the fate model, a local world unit was developed in the proposed models following Mackay type III evaluative environment for steady state conditions and homogeneous compartments with the fugacity-based approach, then converted in kg for consistency with USEtox model. 7 local compartments (air, freshwater, soil, sediments, groundwater, vegetation, fish) make the “local model” and a local scale made of 3 compartments (air, freshwater and soil) nested in a continental 3 compartments scale make the “local-continental model”.

The exposure model was developed for human intake considering the exposure routes to the compartments addressed in each model, starting from the calculated concentration in each of them. When not available, e.g. for fish and vegetation as indirect exposure route through food ingestion, BAFs were used. Two different population were considered in the scales of the local-continental model, defined according to USEtox 2.12 data. In particular, for the local scale half of the population density of urban scale of the cited model was supposed. Ecosystem exposure, consisting in the bioavailable mass, was not explicited as already included in fate results.

The effect model for human health is defined according to USEtox 2.12, so the same EFs were used. Ecotoxicity was evaluated thanks to the development of specific EFs, based on toxicity data retrieved from literature about species belonging to selected species group to reproduce the framework used by USEtox for aquatic toxicity. 3 species group were selected for each compartment and for each of them at least 3 species were included. EC_{50}s were obtained from toxicity data mainly retrieved on EPA’s CompTox database or on scientific literature applying extrapolations factors defined for aquatic toxicity (Posthuma et al. 2019).

The building of CFs for benzene gave the chance to analyze in detail the results of each calculation step, particularly the fate analysis gave the chance to understand the role of benzene’s physico-chemical properties and their interactions with compartments properties.

The local model was built as an exploratory model of the main environmental processes across the different compartments, then the acquired knowledge was transferred on the local-continental model, whose results were compared with those generated with the local model to highlight the relevance on the local scale results of a bigger scale.

The fate model analysis highlighted that, first of all, the behaviour of the local scale in terms of masses and concentrations of benzene between the two models is almost the same, suggesting that the introduction of the continental scale does not influence the fate results on the local one.

Considering the local scale only for both models, for each local emitting compartment, the highest mass is found in the same compartment. In the soil-emitting scenario, the greatest mass "storage" of benzene occurs in the local scale, and almost the totality resides in the soil, while in the air-emitting scenario the lowest "storage" occurs: in both cases the results are connected to the advective process, absent for the first one, present and high for the air.

Considering the continental scale of the local-continental model, the highest chemical mass is in the continental compartment corresponding to the local emitting one, with the exception of the local soil emitting scenario, where the

highest mass occurs in the same local compartment, due to the absence of significant advective process connecting the two scales. The local water emitting scenario creates the highest "storage" of benzene at the continental level, which is mainly concentrated in continental water. In fact, the continental water compartment receives a large amount of benzene through advection and, due to the low degradation rate of the substance in water, a high accumulation of the chemical occurs in it. For a local air and soil emission, the same mass stored on the continental scale is in the continental air compartment.

This result can be explained considering that for local soil emission, the most relevant exit mass flux is volatilization from soil to air, while for air and water emission the highest exits are represented by, namely, air advection and water advection.

In the local-continental model, the highest mass is traceable on the continental scale for transport processes from the local scale, but, looking at the concentration results, the local scale present the highest values, thanks to the lower volume.

Toxicity results (i.e. disaggregated CFs) show that for human health in the local-continental model the effects are slightly higher on the continental scale, since the higher concentration on the local scale is compensated by the higher population on the continental scale; consequently, in terms of potential damage per person, a higher value on the local scale is expected, depending on concentration.

Eco-toxicity results (i.e. disaggregated CFs) could be interpreted as the product between concentrations, EFs and compartments volume, thus, even if the highest PDF resulted to occur always on the same local compartment, as it is characterised by the highest concentration, the continental scale presents the highest damage because of the highest volumes. Since the PDFs are related to the different numbers of species on the scales, supposed depending on the size of the compartment, integrating them into the volume of the respective compartments would allow to take into account the differences of species richness across scales.

Some limitations are present in this work and some of the methodological choices made could be considered questionable from the scientific community.

First of all, the presence of the local scale is very controversial in LCA, for several reasons. A shared opinion in the scientific community is that in a LCA value chain the emitting point is often not known (Fantke et al. 2017) and that, by the very nature of LCA, the final result of damage is provided by aggregating in space and time all emissions that occur in the life cycle of a product. Symptom of this thinking was the removal of the local scale from the pollutant dispersion model SimpleBox v. 4.0 (Hollander et al. 2016), as the authors found that in multimedia fate modelling practice (e.g. at the Dutch Institute for Public Health and the Environment) little use was made of modelled concentrations in local environmental compartments. From the point of view of the LCIA, the toxicity assessment is based on chronic effects and at the local level there are conditions of higher exposure and thus acute effects (Larsen and Hauschild 2006a).

Moreover, the task of assessing damage on a local level is recognized to be addressed by the Health Risk Assessment (HRA) procedure, however the support in decision-making on broad issues that affect the whole community could be pursued only in a LCT prospective by the LCA methodology.

The main limitations of this study mainly concern the fate modelling and the calculated EFs for eco-toxicity.

The fate modelling presents some criticalities. First of all, the representation of pollutant dispersion near an emitting point can hardly be likened to a well-mixed box. Indeed, as the results of the present work also show, the great dominance of advective processes has addressed the fate modelling of tools and researches to local-scale modelling based on the single medium, as PLUME modelling (Allen and Durrenberger 2003) and EUSES (Lijzen and Rikken 2004). In the context of regulatory risk assessment the EUSES model, based on Simple Box, assesses chemical risk for high production volume chemicals in the European Union (Rosenbaum et al. 2007).

Very local phenomena and realistic concentration distribution within the so defined small scale would be better represented by properly spatialized or non-homogeneous mixing models. Logically speaking, any emission could always be defined as local, since, in relation to the chemistry of the chemical, it will have effects, more or less evident, on the local population first. From this point of view, spatially resolved models that identify as many neighbours 'local' cells provide a more truthful representation of reality. The advantage of using a simple box nested model is that it allows to analyze one local system at a time, assuming that all the amount emitted out of the single local cell identified occurs in a large box containing it.

Secondly, the use of the fugacity approach is not adopted in current calculation methods and this could represent a limitation in the use of the proposed models by LCA practitioners. Mackay's model was followed as it represents the basis of the fate modelling, as in the SimpleBox model, and, thus, in USEtox. The work by Mackay (Mackay 2001) provides a clear, comprehensive and detailed treatment of environmental processes, leading the reader to construction of the fate parameters, not found in other documentation, limitedly to my knowledge. Thanks to the conversion process from fugacity approach to mass, it was possible to fully understand the meaning and the origin of fate parameters currently used in calculation methods.

As a future development, both models will be maintained with mass-based approach in order to be easily used by LCA practitioners.

Thirdly, both proposed models are not supported by a chemical database and substance data, such as physico-chemical properties and toxicity data, are to be found in literature for each chemical, with time- and energy-consuming research. In the future, it will be necessary to link the built models with databases, in order to make them usable for every chemical. As best of our knowledge, a database comprehensive of all the required data does not exist. The USEtox chemical database (Huijbregts et al. 2005) is filled with data selected with prioritizing procedures towards different data sources. The databases mostly used in USEtox are: EPI Suite (United States Environmental Protection Agency (US EPA) 2012) for physico-chemical properties, Integrated Risk Information System IRIS (US EPA 2022) and World Health Organization (WHO) for human toxicity data, National Institute for Public Health and the Environment (RIVM) e-toxBase (Wintersen et al. 2004), ECOTOX (Olker et al. 2022) and IUCLID (European Chemicals Agency (ECHA) 2022) for ecotoxicity.

About the second issue, the use for air and soil toxicity of extrapolation factors developed for aquatic ecosystem in the conversion from different toxicity levels reported in literature to chronic EC_{50}s is approximate and not supported by scientific evidence, as well as freshwater DFs for conversion to end-point CFs. Anyway, the present work does not aim

in providing a robust framework in evaluating ecotoxicity for every receiving compartment. Considerable amount of test data as well as adequate protocols in data selection and modelling are to be found from the scientific community.

Two further methodological developments are foreseen for the proposed models. The first one is about the expansion of the considered compartments of the local-continental model, up to 7 compartments on each scale, thus adding sediments, groundwater, vegetation and fish, and nesting the continental scale in a global scale.

The second one is about a different way of addressing effects on the ecosystem. Since the chemicals fate model could allow to assess the concentration for the vegetation and fish compartments, too, it could be correlated with the damage with additional toxicity data from literature. Thus, the alternative way of assessing eco-toxicity linking directly the damage on the concentration in biomass could substitute the current one, but, to be sufficiently representative of whole ecosystem, it should include additional types of biomass, such as terrestrial animals, birds and insects.

Local CFs could be used in LCA whether the emitting point is known or not. In fact, in the first case, site-specific CFs could be obtained adapting the model with known local dimensional parameters. This condition usually occurs for the production phase if a product's LCA is performed or, for example, for the treatment process if a service LCA about waste management is performed, as they represent the core phase for which usually there is high data availability.

When the emitting point is not known, and this usually occurs for the upstream (e.g. raw materials extraction) and downstream (e.g. use phase and end of life) of a product's LCA, default (generic) local CFs could be adopted.

The current model modified with the local dimension took into account the introduction of a local scale sizing 1 x 1 km^2, consisting in 4 compartments (air, freshwater, natural soil and agricultural soil) and related processes, that includes a potential ground-level point of emission and target population and ecosystem, in a current LCA calculation model, i.e. USEtox 2.12.

The main output of the model with the local dimension are local CFs, that include damage on each receiving compartment for a unit emission in a local compartment. Local CFs, coupled with inventoried emitted amounts in LCA from known sources, allow to assess, first of all, damage on human and ecosystem health near the emitting point.

The proposed model could be adapted to represent specific environments and local population exposure conditions, shifting from the generic standard environment to site-specific environment, in relation to the ultimate purpose of the proposed model, i.e. reflecting the potential hazard that an emission could generate on the surrounding community and ecosystem first, expression of the high level of damage achieved by individuals exposed to high concentrations.

A limitation of this study is the absence of modelling of very local phenomena, that could not be represented by the well-mixed box assumption, as reported for the new proposed models. Very local phenomena and realistic concentration distribution within the so defined small scale would be better represented by properly spatialized or non-homogeneous mixing models.

Based on the results obtained for the model with the local dimension about the relevance of the local dimension, the author and the LCA WG research group (Unimore) suggest to use the local CFs, since, compared to the continental CFs, the local CFs highlight always higher damage, in particular for human health.

Moreover, the disaggregation of the CF for a unit emission of benzene in the various local compartments on the different receiving scales show that the greatest contribution to damage comes from the same local emitting scales for both human and ecosystem health, with the exception of local air, where, thanks to the high capacity of the air to be cleaned from pollutants by the wind, the greatest contribution to damage occurs on the urban scale for human toxicity and on the continental scale for ecotoxicity.

The relevance of advective process of local air determines lower mass and concentration values in the same compartment compared to other local compartments. On the other hand, water advective process, depending on rain rate rather than water flow, is not as effective in transporting the mass of chemical to the continental scale.

It is worth pointing out that this result depends of course on the chemical-physical properties of the chemical analysed. In particular, it was possible to verify the influence of the air degradation rate: for example, 1,1,1-trichloroethane, which has a lower degradation rate in air than benzene (- 2 orders of magnitude), causes the greatest damage to human health on the global local scale (3.29E-08 DALY kg^{-1} vs 1.81E-09 DALY kg^{-1} on the urban scale and 2.32E-10 DALY kg^{-1} on the local scale), while Anthracene (with a degradation rate + 2 orders of magnitude compared to benzene) affects the local scale more for a unit emission in air (4.48E-05 DALY kg^{-1} on the urban scale, 1.99E-04 DALY kg^{-1} on the local scale, 1.16E-04 DALY kg^{-1} on the continental scale and 1.30E-06 DALY kg^{-1} on the global scale).

Further considerations on the CF disaggregated on the receiving scales per person (DALY kg^{-1} $person^{-1}$) can lead to an assessment of the extent of potential damage irrespective of the populousness of the region considered. Since this result is directly linked with the concentration, it returns to the damages comparison between the two receiving scales the same distance between the respective concentrations (+ 5 orders of magnitude for local air, + 8 orders of magnitude for local freshwater and +7 orders of magnitude for local soils for benzene emission).

Guidance about the relevance of the local scale for 10 chemicals is reported below in terms of concentration increase between the two models for a unit emission, according to the chemical-physical characteristics, that make them more or less persistent at a local scale. Toxicity-related considerations could be added and evaluated case-by-case by the LCA practitioner.

For air emission, chemicals with lowest air-water partition coefficient (e.g. Atrazine) produce the highest concentration increase (ΔC_a > + 1E+06), even if concentration increase could not be considered negligible for none of the selected chemicals. 1,1,1-trichloroethane experiences the lowest increase in concentration (ΔC_a = + 3.85E+03) due to its high degradation rate. Both characteristics are well accounted by the air transfer coefficient, as shown in Figure 17a.

For water emissions, significant concentration increase between the two models are always observed. Generally, chemicals with the highest degradation rate (Naphthalene) and highest air-water partition coefficients (Benzene and Dichloromethane) show the most significant concentration increase, up to ΔC_w = + 2.67E+07 for Benzene.

The influence of the mentioned properties on the concentration increase is shown in Figure 17b, where the chemical does not have 'time' to reach the continental scale via advection, while the most transferred chemical, causing low concentration increase (ΔC_w = + 9.78E+06), is Atrazine, for its greater persistence in water determined by low air-water partition coefficient. The transfer coefficients for these chemicals are well fitted by the trend line with concentration

change, unlike 2,3,7,8-Tetra CDD that, due to its high Koc, is characterized by the highest local removal for sedimentation process, producing the most limited concentration increase compared to the other chemicals (ΔC_w = + 5.42E+06).

Soil compartments (Figure 17c and Figure 17d) show significant concentrations increase (+ 3.16E+06 $\leq \Delta C_{ns} \leq$ + 4.39E+06 across chemicals) and a low variability of concentration with transfer coefficients change, due to the small value of the fraction of the local mass transferred locally for soils, up to E-05. The chemical with the lowest degradation rate in soil (2,3,7,8-Tetra CDD) presents the lowest increase in concentration for both soils.

The unit emission scenario can be interpreted as the scenario in which 50% of the total continental emission is emitted on the local scale. By cross-referencing the results reported above with real amounts emitted in Europe from every activity sector from E-PRTR data, in which the local emissions were supposed to coincide with those reported from admissible types of sources in local contexts according to 3 levels of emissions (highest, average, lowest) depending on each chemical, an assumption made was that each of the identified local emitting points had the same population density and area size, in order to simplify the analysis which otherwise would have required a large amount of landscape data of each of the emitting points reported in the E-PRTR database.

The comparison between the model with the local dimension and the model without the local dimension shows mainly a significant relevance of the local scale for water and natural soil compartment for human health toxicity.

The consideration of average real amounts emitted in Europe shows that the neglecting local emissions leads to underestimating the damage for human health especially for water emissions of Atrazine (≈+2000%) and for soil emissions of 1,2-dichloroethane (DCE) (≈+9000%), while for air damage increase does not exceed 2% (Di-(2-ethyl hexyl) phthalate). Ecotoxicity shows a non-negligible damage significance only for the natural soil compartment, where the increase is around 14%.

The consideration of the average emitting scenario certainly provides an indicative trend of the behaviour of chemicals in the presence of a local emitting scale in relation to the amount usually emitted in the European context, but, from the point of view of the present author and of the LCA WG research group (Unimore), the relevance of the local scale cannot be established a priori with a cut-off, since the highest emitting scenarios, even if extreme, have actually occurred, affecting local communities more severely, even for the air emitting compartment (damage increase between the two models exceeds 7% for 1,2-dichloroethane (DCE)).

In conclusion, because of the relevance of the local damage, assessed with the building of a new model, the local-continental model, and by adapting a current LCA model (i.e. USEtox 2.12), local CFs are highly recommended for LCA, whether the emitting point is known or not.

The new proposed models (local and local-continental models) will be applied back to the *casus belli*, i.e. the matter concerning the discussion between citizens' committees and the municipality of Coriano (RN) on the emissions generated by the municipal incinerator, after collecting all the physico-chemical and toxicological data of the chemicals detected, in order to provide preliminary results.

Acknowledgements

I thank Prof. Anna Maria Ferrari, who has always had great faith in this work, getting excited at every result and strongly believing in the importance of research as a necessary guide, leading the LCA Working Group in the development of pioneering research topics.

I thank Eng. Paolo Neri, who strongly wanted this work, promoting the topic and working side by side with me every day for the past three years. I thank him for the patience and kindness and for the important scientist life lessons he has passed on to me: to always cultivate doubt, not to distrust, but to deepen and make one's own path of knowledge, with the awareness that one never arrives at a conclusion.

I thank Prof. Peter Fantke, that helped me with patience and kindness in deepening the topic of my research to a level that I would never have achieved without our valuable collaboration and conveying to me a great enthusiasm for research in modelling LCA methodology.

I thank Prof. Roberto Rosa, who very willingly provided me his suggestions and showed great interest in the research topic.

I thank Prof. Olivier Jolliet and Prof. Dik van de Meent for valuable comments on the inclusion of local compartment processes into USEtox.

Matteo, your support cannot be quantified or described in a few lines, because it is essential and vital. I simply borrow a song from The Cure, that is dear to you:

“Whenever I’m alone with you

You make me feel like I am home again

Whenever I’m alone with you

You make me feel like I am whole again”.

Mum, dad and Enzo, we are so different but I am so lucky that you are my family and that you love me, despite the way I am.

I would like to thank specially all the LCA Working Group, present and past (Anna Maria, Paolo, Roberto, Martina, Lucrezia, Vanessa, Micol, Devid, Marco, Chiara, Andrei, Rosangela) for taking me in over the past 6 years and making me feel important to them, searching for and listening to my opinion, even when, as a newcomer to the group, I had no skills.

The wonderful memories I have are due to the wonderful people in this group and I will always be grateful to them for this beautiful gift they gave me.

I hope with all my heart that I have given as much as I have received.

Hoping to meet again and hug each other again.

References

Agenzia Interregionale per il fiume Po (AIPo). (2011). Fiume Po da Cremona al Mare. https://www.agenziapo.it/idrovia/fiume-po-da-cremona-al-mare

Allen, D. T., & Durrenberger, C. J. (2003). Gaussian Plume Modeling.

Arpae Emilia-Romagna. (2022). Meteo - Mappe previsione vento Nord Italia. https://www.arpae.it/it/temi-ambientali/meteo/previsioni-meteo/previsioni-meteo-modellistiche/previsione-vento-10-metri

Bare, J. (2011). TRACI 2.0: The tool for the reduction and assessment of chemical and other environmental impacts 2.0. *Clean Technologies and Environmental Policy*, *13*(5), 687–696. https://doi.org/10.1007/S10098-010-0338-9

Brandt, J., Christensen, J. H., Frohn, L. M., Palmgren, F., Berkowicz, R., & Zlatev, Z. (2001). Operational air pollution forecasts from European to local scale. *Atmospheric Environment*, *35*(SUPPL. 1), S91–S98. https://doi.org/10.1016/S1352-2310(00)00415-5

Breivik, K., Eckhardt, S., McLachlan, M. S., & Wania, F. (2021). Introducing a nested multimedia fate and transport model for organic contaminants (NEM). *Environmental Science: Processes & Impacts*, *23*(8), 1146–1157. https://doi.org/10.1039/D1EM00084E

Buffoli, M., Odone, A., Leask, J., & Signorelli, C. (2016). Not In My Backyard (NIMBY), an endemic syndrome influencing Environmental Policies. *COMMENTARY Epidemiology Biostatistics and Public Health-2016*, *13*. https://doi.org/10.2427/11256

Bulle, C., Margni, M., Patouillard, L., Boulay, A. M., Bourgault, G., De Bruille, V., et al. (2019). IMPACT World+: a globally regionalized life cycle impact assessment method. *International Journal of Life Cycle Assessment*, *24*(9), 1653–1674. https://doi.org/10.1007/S11367-019-01583-0/FIGURES/6

Canadian Council of Ministers of the Environment. Canadian soil quality guidelines for the protection of environmental and human health: Benzene (2004). Canadian Council of Ministers of the Environment, Winnipeg.

Canadian Environmental Modelling Centre - Trent University (CA). (2022). Level III Model. https://www.trentu.ca/cemc/resources-and-models/level-iii-model. Accessed 3 December 2022

Clausen, L. P. W., & Trapp, S. (2017). Toxicity of 56 substances to trees. *Environmental Science and Pollution Research*, *24*(22), 18035–18047. https://doi.org/10.1007/S11356-017-9398-2/FIGURES/3

Cooter, E. J., Bash, J. O., Benson, V., & Ran, L. (2012). Linking agricultural crop management and air quality models for regional to national-scale nitrogen assessments. *Biogeosciences*, *9*(10), 4023–4035. https://doi.org/10.5194/BG-9-4023-2012

Crenna, E., Sala, S., Polce, C., & Collina, E. (2017). Pollinators in life cycle assessment: towards a framework for impact assessment. *Journal of Cleaner Production*, *140*, 525–536. https://doi.org/10.1016/J.JCLEPRO.2016.02.058

Den Hollander, H. A., Van Eijkeren, J. C. H., & Van De Meent, D. (2004). *SimpleBox 3.0: multimedia mass balance model for evaluating the fate of chemical in the environment*.

Dennis, R. L., Mathur, R., Pleim, J. E., & Walker, J. T. (2010). Fate of ammonia emissions at the local to regional scale as simulated by the Community Multiscale Air Quality model. *Atmospheric Pollution Research*, *1*(4), 207–214. https://doi.org/10.5094/APR.2010.027

Derognat, C., Beekmann, M., Baeumle, M., Martin, D., & Schmidt, H. (2003). Effect of biogenic volatile organic compound emissions on tropospheric chemistry during the Atmospheric Pollution Over the Paris Area (ESQUIF) campaign in the Ile-de-France region. *Journal of Geophysical Research:*

Atmospheres, *108*(D17), 8560. https://doi.org/10.1029/2001JD001421

Doherty, F. V., Aneyo, I., & Otitoloju, A. A. (2019). Histopathological and biochemical alterations in Eudrilus eugeniae (Kinberg 1867) as biomarkers of exposure to monocyclic aromatic hydrocarbons in oil impacted site. *The Journal of Basic and Applied Zoology 2019 80:1*, *80*(1), 1–15. https://doi.org/10.1186/S41936-019-0130-2

Dumez, S., Germain, S., Soubigou-Taconnat, L., Bernard, F., Garat, A., Co, B., et al. (2015). Conference: 25th Meeting of the Society of Environmental Toxicology And Chemistry (SETAC). In *Effects of atmospheric benzene exposures on plants*. Barcelona.

European Chemicals Agency (ECHA). (2008). *European Union Risk Assessment Report - BENZENE - RISK ASSESSMENT*.

European Chemicals Agency (ECHA). (2022). International Uniform ChemicaL Information Database (IUCLID). https://iuclid6.echa.europa.eu/. Accessed 3 December 2022

European Commission. COMMUNICATION FROM THE COMMISSION TO THE EUROPEAN PARLIAMENT, THE EUROPEAN COUNCIL, THE COUNCIL, THE EUROPEAN ECONOMIC AND SOCIAL COMMITTEE AND THE COMMITTEE OF THE REGIONS. The European Green Deal (2019).

European Environment Agency (EEA). (2017). European Pollutant Release and Transfer Register (E-PRTR).

Fagin, D. (2012). Toxicology: The learning curve. *Nature*, *490*(7421), 462–465. https://doi.org/10.1038/490462A

Fantke, P., Aylward, L., Chiu, W., Gouin, T., Jolliet, O., Judson, R., et al. (2019). Human toxicity. In *Frischknecht R, Jolliet O (eds) Global Guidance on Environmental Life Cycle Impact Assessment Indicators, vol 2.* (pp. 80–103).

Fantke, P., Aurisano, N., Bare, J., Backhaus, T., ecile Bulle, C., Chapman, P. M., et al. (2018). Toward Harmonizing Ecotoxicity Characterization in Life Cycle Impact Assessment. *SETAC Environmental Toxicology and Chemistry*, *37*(12), 2955–2971. https://doi.org/10.1002/etc.4261

Fantke, P., Aylward, L., Bare, J., Chiu, W. A., Dodson, R., Dwyer, R., et al. (2018). Advancements in Life Cycle Human Exposure and Toxicity Characterization. *Environmental Health Perspectives*, *126*(12). https://doi.org/10.1289/EHP3871

Fantke, P., Bijster, M., Guignard, C., Hauschild, M., Huijbregts, M., Jolliet, O., et al. (2017). *UNEP/SETAC scientific consensus model for characterizing human toxicological and ecotoxicological impacts of chemical emissions in life cycle assessment DOCUMENTATION (Version 1.1) USEtox ® 2.0 Documentation USEtox ® 2.0 Documentation USEtox ® 2.0 Documen*. https://doi.org/10.11581/DTU:00000011

Fantke, P., Chiu, W. A., Aylward, L., Judson, R., Huang, L., Jang, S., et al. (2021). Exposure and toxicity characterization of chemical emissions and chemicals in products: global recommendations and implementation in USEtox. *International Journal of Life Cycle Assessment*, *26*(5), 899–915. https://doi.org/10.1007/S11367-021-01889-Y/TABLES/2

Fantke, Peter, Gillespie, B. W., Juraske, R., & Jolliet, O. (2014). Estimating half-lives for pesticide dissipation from plants. *Environmental Science and Technology*, *48*(15), 8588–8602. https://doi.org/10.1021/ES500434P/SUPPL_FILE/ES500434P_SI_001.PDF

Fazio, S., Biganzioli, F., De Laurentiis, V., Zampori, L., Sala, S., & Diaconu, E. (2018). Supporting information to the characterisation factors of recommended EF Life Cycle Impact Assessment methods. https://doi.org/10.2760/002447

Ferrari, A. M., Volpi, L., Pini, M., Siligardi, C., García-Muiña, F. E., & Settembre-Blundo, D. (2019). Building a

Sustainability Benchmarking Framework of Ceramic Tiles Based on Life Cycle Sustainability Assessment (LCSA). *Resources*, *8*(1), 11. https://doi.org/10.3390/resources8010011

Four Wind s.r.l. (2009). *Stretto di Sicilia offshore wind farm in the Pantelleria and Banchi Avventura area - Environmental Assessments and Authorisations*.

Frischknecht, R., & Jolliet, O. (2016). *Global Guidance for Life Cycle Impact Assessment Indicators*.

Giannouli, M., Kalognomou, E. A., Mellios, G., Moussiopoulos, N., Samaras, Z., & Fiala, J. (2011). Impact of European emission control strategies on urban and local air quality. *Atmospheric Environment*, *45*(27), 4753–4762. https://doi.org/10.1016/J.ATMOSENV.2010.03.016

Goedkoop, M., & Spriemsma, R. (2000). *The Eco-indicator 99-A damage oriented method for Life Cycle Impact Assessment. Methodology Report.* https://doi.org/10.1007/bf02979347

Gold, L. S., Slone, T. H., Manley, N. B., Garfinkel, G. B., Hudes, E. S., Rohrbach, L., & Ames, B. N. (1991). The Carcinogenic Potency Database: Analyses of 4000 chronic animal cancer experiments published in the general literature and by the U.S. National Cancer Institute/National Toxicology Program. *Environmental Health Perspectives*, *96*, 11–15. https://doi.org/10.1289/EHP.919611

Golsteijn, L., van Zelm, R., Veltman, K., Musters, G., Jan Hendriks, A., & Mark Huijbregts, A. J. (2012). Including ecotoxic impacts on warm-blooded predators in life cycle impact assessment. *Integrated Environmental Assessment and Management*, *8*(2), 372–378. https://doi.org/10.1002/IEAM.269

Government of Canada, Environment Canada, & Health and Welfare Canada. (1993). *Canadian Environmental Protection Act - Priority Substances List Assessment Report - Benzene*.

Hollander, A., Sauter, F., den Hollander, H., Huijbregts, M., Ragas, A., & van de Meent, D. (2007). Spatial variance in multimedia mass balance models: Comparison of LOTOS–EUROS and SimpleBox for PCB-153. *Chemosphere*, *68*(7), 1318–1326. https://doi.org/10.1016/J.CHEMOSPHERE.2007.01.035

Hollander, A., Schoorl, M., & van de Meent, D. (2016). SimpleBox 4.0: Improving the model while keeping it simple…. *Chemosphere*, *148*, 99–107. https://doi.org/10.1016/J.CHEMOSPHERE.2016.01.006

Holmquist, H., Fantke, P., Cousins, I. T., Owsianiak, M., Liagkouridis, I., & Peters, G. M. (2020). An (Eco)Toxicity Life Cycle Impact Assessment Framework for Per-And Polyfluoroalkyl Substances. *Environmental Science and Technology*, *54*(10), 6224–6234. https://doi.org/10.1021/ACS.EST.9B07774/ASSET/IMAGES/LARGE/ES9B07774_0002.JPEG

Huijbregts, M. A. J., Struijs, J., Goedkoop, M., Heijungs, R., Jan Hendriks, A., & Van De Meent, D. (2005). Human population intake fractions and environmental fate factors of toxic pollutants in life cycle impact assessment. *Chemosphere*, *61*(10), 1495–1504. https://doi.org/10.1016/J.CHEMOSPHERE.2005.04.046

Humbert, S., Manneh, R., Shaked, S., Wannaz, C., Horvath, A., Deschênes, L., et al. (2009). Assessing regional intake fractions in North America. *Science of The Total Environment*, *407*(17), 4812–4820. https://doi.org/10.1016/J.SCITOTENV.2009.05.024

Italian Ministry of the Environment and Protection of, & territory. Italian Legislative Decree 152/2006, pt. III - REGULATIONS ON SOIL PROTECTION AND COMBATING DESERTIFICATION, PROTECTION OF WATER AGAINST POLLUTION AND WATER RESOURCE MANAGEMENT MANAGEMENT OF WATER RESOURCES (2006).

Jaworskal, J. S., Schowanek, D., & Feijtel, T. C. J. (1999). ENVIRONMENTAL RISK ASSESSMENT FOR TRISODIUM [S,S]-ETHYLENE DIAMINE DISUCCINATE, A BIODEGRADABLE CHELATOR USED IN DETERGENT APPLICATIONS. *Chemosphere*, *38*(15), 3591–3625.

Joint Research Center (JRC) European Commission. (2019). *EN 15804 reference package*.

Jolliet, O., & Hauschild, M. (2005). Modeling the Influence of Intermittent Rain Events on Long-Term Fate and Transport of Organic Air Pollutants. *Environmental Science and Technology*. https://doi.org/10.1021/ES049913

Jolliet, O., Margni, M., Charles, R., Humbert, S., Payet, J., Rebitzer, G., & Rosenbaum, R. (2003). IMPACT 2002+: A new life cycle impact assessment methodology. *The International Journal of Life Cycle Assessment*, *8*(324). https://doi.org/https://doi.org/10.1007/BF02978505

Jolliet, O., Rosenbaum, R., Chapman, P. M., McKone, T., Margni, M., Scheringer, M., et al. (2006). Corner: UNEP/SETAC Life Cycle Initiative Establishing a Framework for Life Cycle Toxicity Assessment Findings of the Lausanne Review Workshop. *Int J LCA*, *11*(3), 209–212. https://doi.org/10.1065/lca2006.03.002

Kale, P., & Kale, R. (1995). Induction of delayed mutations by benzene and ethylene dibromide in drosophila. *Environmental and Molecular Mutagenesis*, *25*(3), 211–215. https://doi.org/10.1002/em.2850250307

Kawamoto, K., Arey, J. S., & Gschwend, P. M. (2012). Emission and Fate Assessment of Methyl Tertiary Butyl Ether in the Boston Area Airshed Using a Simple Multimedia Box Model: Comparison with Urban Air Measurements. *http://dx.doi.org/10.1080/10473289.2003.10466320*, *53*(12), 1426–1435. https://doi.org/10.1080/10473289.2003.10466320

Klepper, O., & van de Meent, D. (1997). *Mapping the Potentially Affected Fraction (PAF) of species as an indicator of generic toxic stress*.

Larsen, H. F., & Hauschild, M. (2006a). Evaluation of Ecotoxicity Effect Indicators for Use in LCIA. *The International Journal of Life Cycle Assessment 2007 12:1*, *12*(1), 24–33. https://doi.org/10.1065/LCA2006.12.287

Larsen, H. F., & Hauschild, M. (2006b). GM-troph: A Low Data Demand Ecotoxicity Effect Indicator for Use in LCIA (13+3 pp). *The International Journal of Life Cycle Assessment 2007 12:2*, *12*(2), 79–91. https://doi.org/10.1065/LCA2006.12.288

Laurens J Brandes, Hollander H den, & D. Van de meent. (1996). *SimpleBox 2.0: a nested multimedia fate model for evaluating the environmental fate of chemicals*.

Leonardi, V. (2008). *Uso di agenti mobilizzanti nel micorisanamento di suoli sottoposti a contaminazione recente e storicamente contaminati da idrocarburi policiclici aromatici*. Università degli studi della Tuscia - Viterbo.

Lijzen, J. P. A., & Rikken, M. G. J. (2004). *European Union System for the Evaluation of Substances (EUSES)* (No. 601900005/2004).

Loiseau, E., Aissani, L., Feon, S. Le, Laurent, F., Cerceau, J., Sala, S., & Roux, P. (2018). Territorial Life Cycle Assessment (LCA): What exactly is it about? A proposal towards using a common terminology and a research agenda. *Journal of Cleaner Production*, (176), 474–485. https://doi.org/https://doi.org/10.1016/j.jclepro.2017.12.169

Mackay, D. (2001). Multimedia environmental models: The fugacity approach, second edition. *Multimedia Environmental Models: The Fugacity Approach, Second Edition*, 1–263. https://doi.org/10.1201/9781420032543/MULTIMEDIA-ENVIRONMENTAL-MODELS-DONALD-MACKAY

McKone, T. E., & Bennett, D. H. (2003). Chemical-specific representation of air-soil exchange and soil penetration in regional multimedia models. *Environmental Science and Technology*, *37*(14), 3123–3132. https://doi.org/10.1021/ES0258529/SUPPL_FILE/ES0258529SI20021126_022620.PDF

McKone, Thomas E., Kyle, A. D., Jolliet, O., Olsen, S. I., & Hauschild, M. (2006). Dose-Response Modeling for Life Cycle Impact Assessment - Findings of the Portland Review Workshop. *The International Journal of Life Cycle Assessment 2006 11:2*, *11*(2), 137–140. https://doi.org/10.1065/LCA2006.02.005

Municipality of Coriano and Riccione (RN). (2018). *Analisi di sostenibilità comparativa sulla gestione dei rifiuti in Emilia Romagna" rifiuti in Emilia Romagna*.

Musmeci, L., & Istituto Superiore di Sanità (ISS). (2007). Applicazione dell'Analisi di Rischio ai Siti Contaminati - Agenzia per la protezionedell'Ambiente e per i servizi tecnici (APAT). In *Nozioni base di tossicologia*.

Olker, J. H., Elonen, C. M., Pilli, A., Anderson, A., Kinziger, B., Erickson, S., et al. (2022). The ECOTOXicology Knowledgebase: A Curated Database of Ecologically Relevant Toxicity Tests to Support Environmental Research and Risk Assessment. *Environmental Toxicology and Chemistry*, *41*(6), 1520–1539. https://doi.org/10.1002/ETC.5324

Olsen, S. I., Christensen, F. M., Hauschild, M., Pedersen, F., Larsen, H. F., & Tørsløv, J. (2001). Life cycle impact assessment and risk assessment of chemicals — a methodological comparison. *Environmental Impact Assessment Review*, *21*(4), 385–404. https://doi.org/10.1016/S0195-9255(01)00075-0

Pajaro-Castro, N., Caballero-Gallardo, K., & Olivero-Verbel, J. (2017). Toxicity of naphthalene and benzene on Tribollium castaneum herbst. *International Journal of Environmental Research and Public Health*, *14*(6). https://doi.org/10.3390/ijerph14060667

Pennington, D., Wolf, M. A., Bersani, R., & Pretato, U. (2007). Overcoming barriers to the broader implementation of life cycle thinking in business and public administration. *The International Journal of Life Cycle Assessment 2007 12:7*, *12*(7), 458–460. https://doi.org/10.1065/LCA2007.07.355

Posthuma, L., van Gils, J., Zijp, M. C., van de Meent, D., & de Zwartd, D. (2019). Species sensitivity distributions for use in environmental protection, assessment, and management of aquatic ecosystems for 12 386 chemicals. *Environmental Toxicology and Chemistry*, *38*(4), 905–917. https://doi.org/10.1002/ETC.4373

PRé Consultants. (2021). SimaPro 9.3 Multi user. Amersfoort, The Netherlands.

Radomyski, A., Ciffroy, P., & Giubilato, E. (2016). The Fish MERLIN-Expo model V1.4.

Rosenbaum, R. K., Bachmann, T. M., Gold, L. S., Huijbregts, M. A. J., Jolliet, O., Juraske, R., et al. (2008). USEtox - The UNEP-SETAC toxicity model: Recommended characterisation factors for human toxicity and freshwater ecotoxicity in life cycle impact assessment. *International Journal of Life Cycle Assessment*, *13*(7), 532–546. https://doi.org/10.1007/S11367-008-0038-4/TABLES/2

Rosenbaum, R. K., Margni, M., & Jolliet, O. (2007). A flexible matrix algebra framework for the multimedia multipathway modeling of emission to impacts. *Environment International*, *33*(5), 624–634. https://doi.org/10.1016/J.ENVINT.2007.01.004

Sala, S., Amadei, A. M., Beylot, A., & Ardente, F. (2021). The evolution of life cycle assessment in European policies over three decades. *International Journal of Life Cycle Assessment*, *26*(12), 2295–2314. https://doi.org/10.1007/S11367-021-01893-2/FIGURES/6

Sala, S., Reale, F., Cristóbal-García, J., Marelli, L., & Rana, P. (2016). Life cycle assessment for the impact assessment of policies. Life thinking and assessment in the European policies and for evaluating policy options. *Joint Research Centre*, *28380*, 53. https://doi.org/10.2788/318544

Sanyé-Mengual, E., & Sala, S. (2022). Life Cycle Assessment support to environmental ambitions of EU policies and the Sustainable Development Goals. *Integrated Environmental Assessment and Management*, *18*(5), 1221–1232. https://doi.org/10.1002/IEAM.4586

Schaap, M., Timmermans, R. M. A., Roemer, M., Boersen, G. A. C., Builtjes, P. J. H., Sauter, F. J., et al. (2008). The LOTOS-EUROS model: Description, validation and latest developments. *International Journal of Environment and Pollution*, *32*(2), 270–290. https://doi.org/10.1504/IJEP.2008.017106

Seigneur, C., Vijayaraghavan, K., Lohman, K., Karamchandani, P., & Scott, C. (2004). Modeling the atmospheric fate and transport of mercury over North America: power plant emission scenarios. *Fuel Processing Technology*, *85*(6–7), 441–450. https://doi.org/10.1016/J.FUPROC.2003.11.001

Smyrnova, Y., Kang, J., Blackford, C., & Cheal, C. (2012). Diffusion coefficient of vegetation: measurements and simulation.

Sonnemann, G., Gemechu, E. D., Sala, S., Schau, E. M., Allacker, K., Pant, R., et al. (2017). Life cycle thinking and the use of LCA in policies around the world. In *Life Cycle Assessment: Theory and Practice* (pp. 429–463). Springer International Publishing. https://doi.org/10.1007/978-3-319-56475-3_18/COVER

UNI EN ISO. UNI EN ISO 14040:2021 - Environmental management — Life cycle assessment — Principles and framework (2021).

UNI EN ISO. UNI EN ISO 14044:2021 - Environmental management — Life cycle assessment — Requirements and guidelines (2021).

United Nations (UN). Convention on Biological Diversity. , United Nations Publications (1992). https://doi.org/10.1016/B978-0-12-384719-5.00418-4

United States Environmental Protection Agency (US EPA). (2012). EPI Suite™-Estimation Program Interface. https://www.epa.gov/tsca-screening-tools/epi-suitetm-estimation-program-interface. Accessed 3 December 2022

United States Environmental Protection Agency (US EPA). (2022). CompTox Chemicals Dashboard - Benzene - Hazard.

US EPA. (2022). Integrated Risk Information System. https://www.epa.gov/iris. Accessed 2 December 2022

Van De Meent, D., Hollander, A., Comber, M., & Parkerton, T. (2010). Environmental fate factors and human intake fractions for risk assessment of petroleum products. *Integrated environmental assessment and management*, *6*(1), 135–144. https://doi.org/10.1897/IEAM_2009-035.1

Van Zelm, R., Huijbregts, M. A. J., Van Jaarsveld, H. A., Reinds, G. J., De Zwart, D., Struijs, J., & Van De Meent, D. (2007). Time horizon dependent characterization factors for acidification in life-cycle assessment based on forest plant species occurrence in Europe. *Environmental Science and Technology*, *41*(3), 922–927. https://doi.org/10.1021/ES061433Q/SUPPL_FILE/ES061433QSI20061114_055220.PDF

Verones, F., Hellweg, S., Antón, A., Azevedo, L. B., Chaudhary, A., Cosme, N., et al. (2020). LC-IMPACT: A regionalized life cycle damage assessment method. *Journal of Industrial Ecology*, *24*(6), 1201–1219. https://doi.org/10.1111/JIEC.13018

Wannaz, C., Fantke, P., & Jolliet, O. (2018). Multiscale Spatial Modeling of Human Exposure from Local Sources to Global Intake. *Environmental Science and Technology*, *52*(2), 701–711. https://doi.org/10.1021/ACS.EST.7B05099/ASSET/IMAGES/LARGE/ES-2017-05099D_0005.JPEG

Whitman, W. G. (1923). A Preliminary Experimental Conjirmation of THE TWO-FILM THEORY OF GAS ABSORPTION. *International Journal of Heat Mass Transfer*, *5*, 429–433.

Wikipedia. (2022). Volga. https://it.wikipedia.org/wiki/Volga. Accessed 3 December 2022

Wintersen, A., Posthuma, L., & De Zwart, D. (2004). *The RIVM e-toxBase. A database for storage, Retrieval Environment, and export of ecotoxicity data.*

Wold Health Organization (WHO). (2020). *Methods and data sources for global burden of disease estimates 2000-2011*.

Wyszkowska, J., & Kucharski, J. (2001). Correlation between number of microbes and degree of soil

contamination by petrol. *Polish Journal of Environmental Studies*, *10*(3), 175–181.

Wyszkowski, M., Wyszkowska, J., & Ziółkowska, A. (2004). Effect of soil contamination with diesel oil on yellow lupine yield and macroelements content. *Plant, Soil and Environment*, *50*(5), 218–226. https://doi.org/10.17221/4025-PSE

Wyszkowski, Mirosław, & Ziólkowska, A. (2009). Role of compost, bentonite and calcium oxide in restricting the effect of soil contamination with petrol and diesel oil on plants. *Chemosphere*, *74*(6), 860–865. https://doi.org/10.1016/J.CHEMOSPHERE.2008.10.035

Zannetti, P. (1990). Gaussian Models. *Air Pollution Modeling*, 141–183. https://doi.org/10.1007/978-1-4757-4465-1_7

Zytner, R. G. (1994). Sorption of benzene, toluene, ethylbenzene and xylenes to various media. *Journal of Hazardous Materials*, *38*(1), 113–126. https://doi.org/10.1016/0304-3894(94)00027-1

Appendix

A.1 Derivation of intermedia partitioning processes

Each calculation is based on the mass balance between the i-th total m_{itot} and the individual masses contained in the phases x, y and z (Eq. 177):

$$m_{itot} = m_x + m_y + m_z \quad \text{(Eq. 177)}$$

Mass fraction in the gas phase of air (ref. eq. 8 USEtox v2.12 – modified by Holmquist et al. (2020))

$$m_{atot} = m_{gas} + m_{ae} + m_{cldw} \quad \text{(Eq. 178)}$$

$$\frac{m_{atot}}{m_{atot}} = \frac{m_{gas} + m_{ae} + m_{cldw}}{m_{atot}}$$

$$1 = fr\_m_{gas} + fr\_m_{ae} + fr\_m_{cldw}$$

$$\frac{1}{fr\_m_{gas}} = \frac{fr\_m_{gas} + fr\_m_{ae} + fr\_m_{cldw}}{fr\_m_{gas}}$$

$$\frac{1}{fr\_m_{gas}} = 1 + \frac{fr\_m_{ae}}{fr\_m_{gas}} + \frac{fr\_m_{cldw}}{fr\_m_{gas}}$$

$$fr\_m_{gas} = \frac{1}{1 + \frac{fr\_m_{ae}}{fr\_m_{gas}} + \frac{fr\_m_{cldw}}{fr\_m_{gas}}}$$

$$= \frac{1}{1 + \frac{\frac{m_{ae}}{m_{atot}}}{\frac{m_{gas}}{m_{atot}}} + \frac{\frac{m_{cldw}}{m_{atot}}}{\frac{m_{gas}}{m_{atot}}}}$$

$$= \frac{1}{1 + \frac{\frac{C_{ae} \times V_{ae}}{C_a \times V_a}}{\frac{C_{gas} \times V_{gas}}{C_a \times V_a}} + \frac{\frac{C_{cldw} \times V_{cldw}}{C_a \times V_a}}{\frac{C_{gas} \times V_{gas}}{C_a \times V_a}}}$$

$$= \frac{1}{1 + \frac{\frac{C_{ae}}{C_a} \times fr\_V_{ae}}{\frac{C_{gas}}{C_a} \times fr\_V_{gas}} + \frac{\frac{C_{cldw}}{C_a} \times fr\_V_{cldw}}{\frac{C_{gas}}{C_a} \times fr\_V_{gas}}}$$

$$= \frac{1}{1 + \frac{C_{ae}}{C_a} \times \frac{C_a}{C_{gas}} \times \frac{fr\_V_{ae}}{fr\_V_{gas}} + \frac{C_{cldw}}{C_a} \times \frac{C_a}{C_{gas}} \times \frac{fr\_V_{cldw}}{fr\_V_{gas}}}$$

$$= \frac{1}{1 + \frac{C_{ae}}{C_{gas}} \times \frac{fr\_V_{ae}}{fr\_V_{gas}} + \frac{C_{cldw}}{C_{gas}} \times \frac{fr\_V_{cldw}}{fr\_V_{gas}}}$$

$$= \frac{1}{1 + K_{ae,gas} \times \frac{fr\_V_{ae}}{fr\_V_{gas}} + K_{w,gas} \times \frac{fr\_V_{cldw}}{fr\_V_{gas}}}$$

Assuming that $V_{gas} \approx V_a$, $fr\_V_{gas} \approx 1$

$$fr\_m_{gas} = \frac{1}{1 + K_{ae,gas} \times fr\_V_{ae} + K_{w,gas} \times fr\_V_{cldw}}$$

Mass fraction in the dissolved water phase (ref. eq. 20 USEtox v2.12)

$$m_{wtot} = m_{wdiss} + m_{doc} + m_{susp} + m_{fish} \quad \text{(Eq. 179)}$$

$$\frac{m_{wtot}}{m_{wtot}} = \frac{m_{wdiss} + m_{doc} + m_{susp} + m_{fish}}{m_{wtot}}$$

$$1 = fr\_m_{wdiss} + fr\_m_{doc} + fr\_m_{susp} + fr\_m_{fish}$$

$$\frac{1}{fr\_m_{wdiss}} = \frac{fr\_m_{wdiss} + fr\_m_{doc} + fr\_m_{susp} + fr\_m_{fish}}{fr\_m_{wdiss}}$$

$$\frac{1}{fr\_m_{wdiss}} = 1 + \frac{fr\_m_{doc}}{fr\_m_{wdiss}} + \frac{fr\_m_{susp}}{fr\_m_{wdiss}} + \frac{fr\_m_{fish}}{fr\_m_{wdiss}}$$

$$fr\_m_{wdiss} = \frac{1}{1 + \frac{fr\_m_{doc}}{fr\_m_{wdiss}} + \frac{fr\_m_{susp}}{fr\_m_{wdiss}} + \frac{fr\_m_{fish}}{fr\_m_{wdiss}}}$$

$$= \frac{1}{1 + \frac{\frac{m_{doc}}{m_{wtot}}}{\frac{m_{wdiss}}{m_{wtot}}} + \frac{\frac{m_{susp}}{m_{wtot}}}{\frac{m_{wdiss}}{m_{wtot}}} + \frac{\frac{m_{fish}}{m_{wtot}}}{\frac{m_{wdiss}}{m_{wtot}}}}$$

$$= \frac{1}{1 + \frac{\frac{C_{doc} \times V_{doc}}{C_w \times V_w}}{\frac{C_{wdiss} \times V_{wdiss}}{C_w \times V_w}} + \frac{\frac{C_{susp} \times V_{susp}}{C_w \times V_w}}{\frac{C_{wdiss} \times V_{wdiss}}{C_w \times V_w}} + \frac{\frac{C_{fish} \times V_{fish}}{C_w \times V_w}}{\frac{C_{wdiss} \times V_{wdiss}}{C_w \times V_w}}}$$

$$= \frac{1}{1 + \frac{\frac{C_{doc}}{C_w} \times fr\_V_{doc}}{\frac{C_{wdiss}}{C_w} \times fr\_V_{wdiss}} + \frac{\frac{C_{susp}}{C_w} \times fr\_V_{susp}}{\frac{C_{wdiss}}{C_w} \times fr\_V_{wdiss}} + \frac{\frac{C_{fish}}{C_w} \times fr\_V_{fish}}{\frac{C_{wdiss}}{C_w} \times fr\_V_{wdiss}}}$$

$$= \frac{1}{1 + \frac{C_{doc}}{C_w} \times \frac{C_w}{C_{wdiss}} \times \frac{fr\_V_{doc}}{fr\_V_{wdiss}} + \frac{C_{susp}}{C_w} \times \frac{C_w}{C_{wdiss}} \times \frac{fr\_V_{susp}}{fr\_V_{wdiss}} + \frac{C_{fish}}{C_w} \times \frac{C_w}{C_{wdiss}} \times \frac{fr\_V_{fish}}{fr\_V_{wdiss}}}$$

$$= \frac{1}{1 + \frac{C_{doc}}{C_{wdiss}} \times \frac{fr\_V_{doc}}{fr\_V_{wdiss}} + \frac{C_{susp}}{C_{wdiss}} \times \frac{fr\_V_{susp}}{fr\_V_{wdiss}} + \frac{C_{fish}}{C_{wdiss}} \times \frac{fr\_V_{fish}}{fr\_V_{wdiss}}}$$

$$= \frac{1}{1 + K_{doc,w} \times \frac{fr\_V_{doc}}{fr\_V_{wdiss}} + K_{susp,w} \times \frac{fr\_V_{susp}}{fr\_V_{wdiss}} + BAF_{fish,w} \times \frac{fr\_V_{fish}}{fr\_V_{wdiss}}}$$

Assuming that $V_{wdiss} \approx V_w$, $fr\_V_{wdiss} \approx 1$

$$fr\_m_{wdiss} = \frac{1}{1 + K_{doc,w} \times fr\_V_{doc} + K_{susp,w} \times fr\_V_{susp} + BAF_{fish,w} \times fr\_V_{fish}}$$

Where:

- fr_m_w is the chemical mass fraction into water phase;
- fr_V_w is the water phase volume fraction;
- $K_{gas,w}$ is the partition coefficient between gas phase and water phase;
- fr_V_{gas} is the gas phase volume fraction;
- $K_{solid,w}$ $(L\ kg_{solid}^{-1})$ is the solid-water partition coefficient;
- ρ_{solid} $(kg\ m^{-3})$ is the soil density;
- $1000\ L\ m^{-3}$ is the unit conversion;
- fr_V_{solid} is the solid phase volume fraction.

Mass fraction in the solid phase (organic carbon) of the soil (ref. eq. 46 USEtox v2.12)

$$m_{stot} = m_{solid} + m_{gas} + m_w \qquad \text{(Eq. 180)}$$

$$\frac{m_{stot}}{m_{stot}} = \frac{m_{solid} + m_{gas} + m_w}{m_{stot}}$$

$$1 = fr\_m_{solid} + fr\_m_{gas} + fr\_m_w$$

$$\frac{1}{fr\_m_{solid}} = \frac{fr\_m_{solid} + fr\_m_{gas} + fr\_m_w}{fr\_m_{solid}}$$

$$\frac{1}{fr\_m_{solid}} = 1 + \frac{fr\_m_{gas}}{fr\_m_{solid}} + \frac{fr\_m_w}{fr\_m_{solid}}$$

$$fr\_m_{solid} = \frac{1}{1 + \frac{fr\_m_{gas}}{fr\_m_{solid}} + \frac{fr\_m_w}{fr\_m_{solid}}}$$

$$= \frac{1}{1 + \frac{\frac{m_{gas}}{m_{stot}}}{\frac{m_{solid}}{m_{stot}}} + \frac{\frac{m_w}{m_{stot}}}{\frac{m_{solid}}{m_{stot}}}}$$

$$= \frac{1}{1 + \frac{\frac{C_{gas} \times V_{gas}}{C_s \times V_s}}{\frac{C_{solid} \times V_{solid}}{C_s \times V_s}} + \frac{\frac{C_w \times V_w}{C_s \times V_s}}{\frac{C_{solid} \times V_{solid}}{C_s \times V_s}}}$$

$$= \frac{1}{1 + \frac{\frac{C_{gas}}{C_s} \times fr\_V_{gas}}{\frac{C_{solid}}{C_s} \times fr\_V_{solid}} + \frac{\frac{C_w}{C_s} \times fr\_V_w}{\frac{C_{solid}}{C_s} \times fr\_V_{solid}}}$$

$$= \frac{1}{1 + \frac{C_{gas}}{C_s} \times \frac{C_s}{C_{solid}} \times \frac{fr\_V_{gas}}{fr\_V_{solid}} + \frac{C_w}{C_s} \times \frac{C_s}{C_{solid}} \times \frac{fr\_V_w}{fr\_V_{solid}}}$$

$$= \frac{1}{1 + \frac{C_{gas}}{C_{solid}} \times \frac{fr\_V_{gas}}{fr\_V_{solid}} + \frac{C_w}{C_{solid}} \times \frac{fr\_V_w}{fr\_V_{solid}}}$$

$$= \frac{1}{1 + K_{gas,solid} \times \frac{fr\_V_{gas}}{fr\_V_{solid}} + \frac{\frac{K_{w,solid}}{\rho_{solid}}}{1000} \times \frac{fr\_V_w}{fr\_V_{solid}}}$$

$$= \frac{fr\_V_{solid}}{fr\_V_{solid} + K_{gas,solid} \times fr\_V_{gas} + \frac{\frac{K_{w,solid}}{\rho_{solid}}}{1000} \times fr\_V_w}$$

Where

- fr_m_{solid} is the chemical mass fraction into solid phase;
- fr_V_w is the water phase volume fraction;
- $K_{gas,solid}$ is the partition coefficient between gas phase and solid phase;
- fr_V_{gas} is the gas phase volume fraction;
- $K_{w,solid}$ $(kg_{solid}\ L^{-1})$ is the water-solid partition coefficient;
- ρ_{solid} $(kg\ m^{-3})$ is the soil density;
- $1000\ L\ m^{-3}$ is the unit conversion;
- fr_V_{solid} is the solid phase volume fraction.

Mass fraction in the soil water phase (ref. eq. 48 USEtox v2.12)

$$m_{stot} = m_{solid} + m_{gas} + m_w \quad \text{(Eq. 181)}$$

$$\frac{m_{stot}}{m_{stot}} = \frac{m_{solid} + m_{gas} + m_w}{m_{stot}}$$

$$1 = fr\_m_{solid} + fr\_m_{gas} + fr\_m_w$$

$$\frac{1}{fr\_m_w} = \frac{fr\_m_{solid} + fr\_m_{gas} + fr\_m_w}{fr\_m_w}$$

$$\frac{1}{fr\_m_w} = 1 + \frac{fr\_m_{gas}}{fr\_m_w} + \frac{fr\_m_{solid}}{fr\_m_w}$$

$$fr\_m_w = \frac{1}{1 + \frac{fr\_m_{gas}}{fr\_m_w} + \frac{fr\_m_{solid}}{fr\_m_w}}$$

$$= \frac{1}{1 + \frac{\frac{m_{gas}}{m_{stot}}}{\frac{m_w}{m_{stot}}} + \frac{\frac{m_{solid}}{m_{stot}}}{\frac{m_w}{m_{stot}}}}$$

$$= \frac{1}{1 + \frac{\frac{C_{gas} \times V_{gas}}{C_s \times V_s}}{\frac{C_w \times V_w}{C_s \times V_s}} + \frac{\frac{C_{solid} \times V_{solid}}{C_s \times V_s}}{\frac{C_w \times V_w}{C_s \times V_s}}}$$

$$= \frac{1}{1 + \frac{\frac{C_{gas}}{C_s} \times fr\_V_{gas}}{\frac{C_w}{C_s} \times fr\_V_w} + \frac{\frac{C_{solid}}{C_s} \times fr\_V_{solid}}{\frac{C_w}{C_s} \times fr\_V_w}}$$

$$= \frac{1}{1 + \frac{C_{gas}}{C_s} \times \frac{C_s}{C_w} \times \frac{fr\_V_{gas}}{fr\_V_w} + \frac{C_{solid}}{C_s} \times \frac{C_s}{C_w} \times \frac{fr\_V_{solid}}{fr\_V_w}}$$

$$= \frac{1}{1 + \frac{C_{gas}}{C_w} \times \frac{fr\_V_{gas}}{fr\_V_w} + \frac{C_{solid}}{C_w} \times \frac{fr\_V_{solid}}{fr\_V_w}}$$

$$= \frac{1}{1 + K_{gas,w} \times \frac{fr\_V_{gas}}{fr\_V_w} + K_{solid,w} \times \frac{\rho_{solid}}{1000} \times \frac{fr\_V_{solid}}{fr\_V_w}}$$

$$= \frac{fr\_V_w}{fr\_V_w + K_{gas,w} \times fr\_V_{gas} + K_{solid,w} \times \frac{\rho_{solid}}{1000} \times fr\_V_{solid}}$$

Where:

- fr_m_w is the chemical mass fraction into water phase;
- fr_V_w is the water phase volume fraction;
- $K_{gas,w}$ is the partition coefficient between gas phase and water phase;
- fr_V_{gas} is the gas phase volume fraction;
- $K_{solid,w}$ $(L\ kg_{solid}^{-1})$ is the solid-water partition coefficient;
- ρ_{solid} $(kg\ m^{-3})$ is the soil density;
- $1000\ L\ m^{-3}$ is the unit conversion;
- fr_V_{solid} is the solid phase volume fraction.

<u>Soil density (ref. eq. 53 USEtox v2.12)</u>

$$m_{stot} = m_{solid} + m_{gas} + m_w \qquad \text{(Eq. 182)}$$

$$\rho_{stot} \times V_{stot} = \rho_{solid} \times V_{solid} + \rho_{gas} \times V_{gas} + \rho_{water} \times V_{water}$$

$$\rho_{stot} = \rho_{solid} \times \frac{V_{solid}}{V_{stot}} + \rho_{gas} \times \frac{V_{gas}}{V_{stot}} + \rho_{water} \times \frac{V_{water}}{V_{stot}}$$

$$\rho_{stot} = \rho_{solid} \times fr\_V_{solid} + \rho_{gas} \times fr\_V_{gas} + \rho_{water} \times fr\_V_{water}$$

Where:

- fr_V_w is the water phase volume fraction;
- fr_V_{solid} is the solid phase volume fraction;
- fr_V_{gas} is the gas phase volume fraction;
- ρ_{solid} $(kg\ m^{-3})$ is the soil density.

A.2 Derivation of intermedia transfer processes

In this chapter parameters related to transfer processes between compartments are analyzed, in particular interpretations on their building are proposed, also doing parallelism with Mackay (x) equations.

The mass balance among phases within the same compartment is used, too, for processes that involve all the phases of a compartment.

Penetration depth in soil (ref. eq. 54 USEtox v2.12)

$$h_{sl,penetr} = \frac{v_{eff,adv,sl} + \sqrt{v_{eff,adv,sl}^2 + 4 \times \frac{k_{deg,sl}}{(3600 \times 24)} \times D_{eff,sl}}}{2 \times \frac{k_{deg,sl}}{(3600 \times 24)}} \quad \text{(Eq. 183)}$$

Where:

- $h_{sl,penetr}$ (m) is the penetration depth of continental and global natural and agricultural soil;
- $v_{eff,adv,sl}$ $(m\ s^{-1})$ is the effective advective transport in continental and global natural and agricultural soil;
- $D_{eff,sl}$ $(m^2\ s^{-1})$ is the effective diffusion coefficient in continental and global natural and agricultural soil;
- $k_{deg,sl}$ (d^{-1}) is the degradation rate in continental and global natural and agricultural soil;
- 3600×24 $(s\ d^{-1})$ is the unit conversion factor.

The hypothesis to motivate this equation is a solution of a second-degree equation, where the starting equation could be (Eq. 184):

$$k_{deg,sl} \times {h_{sl,penetr}}^2 + v_{eff,adv,sl} \times h_{sl,penetr} + D_{eff,sl} = 0 \quad \text{(Eq. 184)}$$

The generic quadratic solution could be (Eq. 185):

$$h_{sl,penetr} = \frac{-b \times (b^2 - 4 \times a \times c)}{2 \times a} \quad \text{(Eq. 185)}$$

Where $v_{eff,adv,sl} = -b$.

The complete discussion of the origin of this equation was reported by McKone and Bennett (2003).

Diffusion in soil (ref. eq. 57 USEtox v2.12)

$$D_{eff,sl} = D_{gas} + D_{water} + D_{solid} \quad \text{(Eq. 186)}$$

Where:

- $D_i = \frac{B_i \times A_i \times C_i}{Y_i}$
- $C_i = \frac{M_i}{V_i}$

$$\frac{B_{sl} \times A_{sl} \times C_{sl}}{Y_{sl}} = \frac{B_{gas} \times A_{gas} \times C_{gas}}{Y_{gas}} + \frac{B_{water} \times A_{water} \times C_{water}}{Y_{water}} + \frac{B_{solid} \times A_{solid} \times C_{solid}}{Y_{solid}}$$

$$\frac{B_{sl} \times A_{sl}}{Y_{sl}} \times \frac{M_{sl}}{V_{sl}} = \frac{B_{gas} \times A_{gas}}{Y_{gas}} \times \frac{M_{gas}}{V_{gas}} + \frac{B_{water} \times A_{water}}{Y_{water}} \times \frac{M_{water}}{V_{water}} + \frac{B_{solid} \times A_{solid}}{Y_{solid}} \times \frac{M_{solid}}{V_{solid}}$$

$$\frac{B_{sl} \times A_{sl}}{Y_{sl}} = \frac{B_{gas} \times A_{gas}}{Y_{gas}} \times \frac{M_{gas}}{M_{sl}} \times \frac{V_{sl}}{V_{gas}} + \frac{B_{water} \times A_{water}}{Y_{water}} \times \frac{M_{water}}{M_{sl}} \times \frac{V_{sl}}{V_{water}} + \frac{B_{solid} \times A_{solid}}{Y_{solid}} \times \frac{M_{solid}}{M_{sl}} \times \frac{V_{sl}}{V_{solid}}$$

$$\frac{B_{sl} \times A_{sl}}{Y_{sl}} = \frac{B_{gas} \times A_{gas}}{Y_{gas}} \times fr\_m_{gas} \times \frac{1}{fr\_V_{gas}} + \frac{B_{water} \times A_{water}}{Y_{water}} \times fr\_m_{water} \times \frac{1}{fr\_V_{water}} + \frac{B_{solid} \times A_{solid}}{Y_{solid}} \times fr\_m_{solid} \times \frac{1}{fr\_V_{solid}}$$

$$B_{sl} = B_{gas} \times \frac{A_{gas}}{A_{sl}} \times \frac{Y_{sl}}{Y_{gas}} \times \frac{fr\_m_{gas}}{fr\_V_{gas}} + B_{water} \times \frac{A_{water}}{A_{sl}} \times \frac{Y_{sl}}{Y_{water}} \times \frac{fr\_m_{water}}{fr\_V_{water}} + B_{solid} \times \frac{A_{solid}}{A_{sl}} \times \frac{Y_{sl}}{Y_{solid}} \times \frac{fr\_m_{solid}}{fr\_V_{solid}}$$

Where:

- $\frac{A_{gas}}{A_{sl}} = F_a$, the void fraction according to Mackay
- $\frac{Y_{gas}}{Y_{sl}} = F_Y$, the tortuosity factor according to Mackay
- $B_E = \sum_i \frac{B_i \times F_a}{F_Y} \cong \sum_i B_i \times fr\_V_i^{1.33}$, the diffusivity in the porous medium (soil) according to Mackay

$$B_{sl} = B_{gas} \times fr\_V_{gas}^{1.5} \times \frac{fr\_m_{gas}}{fr\_V_{gas}} + B_{water} \times fr\_V_{water}^{1.5} \times \frac{fr\_m_{water}}{fr\_V_{water}} + B_{solid} \times fr\_V_{solid}^{1.5} \times \frac{fr\_m_{solid}}{fr\_V_{solid}}$$

Where:

$$fr\_m_{gas} = 1 - fr_{m_{water}} - fr\_m_{solid}$$

and

- $D_{eff,sl}$ $(m^2\ s^{-1})$ is the effective diffusion coefficient in continental and global natural and agricultural soil;

- D_{gas} $(m^2\ s^{-1})$ is the gas phase diffusion coefficient;
- D_{water} $(m^2\ s^{-1})$ is the water phase diffusion coefficient;
- D_{solid} $(m^2\ s^{-1})$ is the solid phase diffusion coefficient;
- fr_V_w is the water phase volume fraction;
- fr_V_{solid} is the solid phase volume fraction;
- fr_V_{gas} is the gas phase volume fraction;
- fr_m_{water} is the chemical mass fraction into water phase;
- fr_m_{gas} is the chemical mass fraction into gas phase;
- fr_m_{solid} is the chemical mass fraction into solid phase;
- B_{gas} $(m^2\ s^{-1})$ is the gas diffusivity;
- B_{water} $(m^2\ s^{-1})$ is the water diffusivity;
- B_{solid} $(m^2\ s^{-1})$ is the solid (organic carbon) diffusivity.

A.3 Mass balance check on the local model

Compliance with the mass balance per compartment and for the whole system was verified for each individual emitting compartment and for the sum of the emitting compartments. Below are tables (from Table 59 to Table 62) with the results, in which the mass flows in mol h^{-1} for each process are quantified.

Table 59 Mass balance of the local model for a unit emission of benzene in air

WORLD UNIT EMISSION RATE E (mol h^{-1})		
AIR	WATER	SOIL
1	0	0

INPUT (mol h^{-1})			
AIR			
VOLATILIZATION W	4.16E-11	DIFFUSIONtot	1.32E-04
VOLATILIZATION S	1.32E-04		
VOLATILIZATION VEG	2.50E-19		

OUTPUT (mol h^{-1})			
AIR			
DIFFUSION (ABSORPTION) S	1.32E-04	DIFFUSIONtot	1.33E-04
DIFFUSION (ABSORPTION) W	8.41E-08	ADVECTIONtot (excl. exit)	1.01E-07
DIFFUSION (ABSORPTION) VEG	2.41E-16		
WET DEP. W	1.01E-09		
DRY PART. DEP W	2.43E-14		
WET PART. DEP. W	2.91E-14		
WET DEP. S	9.98E-08		
DRY PART. DEP S	2.40E-12		
WET PART. DEP. S	2.88E-12		
WET DEP. VEG	4.99E-10		
DRY PART. DEP VEG	1.20E-14		
WET PART. DEP. VEG	1.44E-14		
REACTION	3.76E-03		

INPUT (mol h^{-1})			
WATER			
DIFFUSION A	8.41E-08	DIFFUSIONtot	8.41E-08
WET DEP. A	1.01E-09	ADVECTIONtot	6.56E-08
DRY PART. DEP A	2.43E-14		
WET PART. DEP. A	2.91E-14		
RUNOFF S	6.46E-08		
DIFFUSION SED	1.24E-19		
RESUSP. SED	9.08E-20		
DIFFUSION F	2.55E-12		

OUTPUT (mol h^{-1})			
WATER			
VOLATILIZATION A	4.16E-11	DIFFUSIONtot	4.43E-11
REACTION	1.69E-10	ADVECTIONtot (excl. exit)	4.87E-13
ADVECTION (W+P)	1.49E-07		
IRRIGATION S	4.85E-13		
DEPOSITION SED	1.27E-15		
DIFFUSION SED	4.15E-16		
UPTAKE F	2.43E-16		

ADVECTION	9.96E-01

AIR	
INPUT TOT	**OUTPUT TOT**
1.00E+00	1.00E+00

INPUT (mol h^{-1})			
SOIL			
DIFFUSION A	1.32E-04	DIFFUSIONtot	1.32E-04
WET DEP. A	9.98E-08	ADVECTIONtot	9.98E-08
DRY PART. DEP A	2.40E-12		
WET PART. DEP. A	2.88E-12		
IRRIGATION W	4.85E-13		

OUTPUT (mol h^{-1})			
SOIL			
VOLATILIZATION A	1.32E-04	DIFFUSIONtot	1.32E-04
REACTION	7.29E-07	ADVECTIONtot	6.47E-08
RUNOFF(W+P)	6.46E-08		
LEACHING GW	1.30E-10		
UPTAKE VEG	4.88E-14		

SOIL	
INPUT TOT	**OUTPUT TOT**
1.33E-04	1.33E-04

INPUT (mol h^{-1})	
VEGETATION	
DIFFUSION A	2.41E-16

DIFFUSION F	2.70E-12

WATER	
INPUT TOT	**OUTPUT TOT**
1.50E-07	1.50E-07

INPUT (mol h^{-1})	
SEDIMENT	
DIFFUSION W	4.15E-16
DEPOSITION W	1.27E-15

OUTPUT (mol h^{-1})	
SEDIMENT	
RESUSPENSION W	9.08E-20
REACTION	1.68E-15
BURIAL	3.80E-19
DIFFUSION W	1.24E-19

SEDIMENT	
INPUT TOT	**OUTPUT TOT**
1.68E-15	1.68E-15

INPUT (mol h^{-1})	
FISH	
UPTAKE W	2.43E-16
DIFFUSION W	2.70E-12

OUTPUT (mol h^{-1})	
FISH	
DIFFUSION W	2.55E-12

WET DEP. A	4.99E-10
DRY PART. DEP A	1.44E-14
WET PART. DEP. A	1.20E-14
UPTAKE S	4.88E-14

OUTPUT (mol h^{-1})	
VEGETATION	
VOLATILIZATION A	2.50E-19
REACTION	4.99E-10

VEGETATION	
INPUT TOT	**OUTPUT TOT**
4.99E-10	4.99E-10

INPUT (mol h^{-1})	
GROUNDWATER	
LEACHING S	1.30E-10

OUTPUT (mol h^{-1})	
GROUNDWATER	
REACTION	1.47E-13
ADVECTION (W+P)	1.30E-10
GROUNDWATER	
INPUT TOT	**OUTPUT TOT**
1.30E-10	1.30E-10

GROWTH	1.05E-14
METABOLISM	1.40E-13
EJECTION	5.73E-17

FISH	
INPUT TOT	**OUTPUT TOT**
2.70E-12	2.70E-12

WORLD UNIT INPUT (mol h^{-1})	WORLD UNIT OUTPUT (mol h^{-1})
1.00E+00	1.00E+00

Table 60 Mass balance of the local model for a unit emission of benzene in water

WORLD UNIT EMISSION RATE E (mol h^{-1})		
AIR	**WATER**	**SOIL**
0	1	0

INPUT (mol h^{-1})			
AIR			
VOLATILIZATION W	2.78E-04	DIFFUSIONtot	2.81E-04
VOLATILIZATION S	3.26E-06		
VOLATILIZATION VEG	7.08E-23		

OUTPUT (mol h^{-1})			
AIR			
DIFFUSION (ABSORPTION) S	3.72E-08	DIFFUSIONtot	3.72E-08
DIFFUSION (ABSORPTION) W	2.36E-11	ADVECTIONtot (excl. exit)	2.85E-11
DIFFUSION (ABSORPTION) VEG	6.78E-20		
WET DEP. W	2.83E-13		
DRY PART. DEP W	6.82E-18		
WET PART. DEP. W	8.19E-18		
WET DEP. S	2.80E-11		
DRY PART. DEP S	6.75E-16		
WET PART. DEP. S	8.10E-16		
WET DEP. VEG	1.40E-13		
DRY PART. DEP VEG	3.38E-18		
WET PART. DEP. VEG	4.05E-18		
REACTION	1.06E-06		
ADVECTION	2.80E-04		

AIR	
INPUT TOT	**OUTPUT TOT**

INPUT (mol h^{-1})			
WATER			
DIFFUSION A	2.36E-11	DIFFUSIONtot	1.70E-05
WET DEP. A	2.83E-13	ADVECTIONtot	1.60E-09
DRY PART. DEP A	6.82E-18		
WET PART. DEP. A	8.19E-18		
RUNOFF S	1.60E-09		
DIFFUSION SED	8.31E-13		
RESUSP. SED	6.06E-13		
DIFFUSION F	1.70E-05		

OUTPUT (mol h^{-1})			
WATER			
VOLATILIZATION A	2.78E-04	DIFFUSIONtot	2.96E-04
REACTION	1.13E-03	ADVECTIONtot (excl. exit)	3.25E-06
ADVECTION (W+P)	9.99E-01		
IRRIGATION S	3.24E-06		
DEPOSITION SED	8.47E-09		
DIFFUSION SED	2.77E-09		
UPTAKE F	1.62E-09		
DIFFUSION F	1.80E-05		

WATER	
INPUT TOT	**OUTPUT TOT**

2.81E-04	2.81E-04

INPUT (mol h^{-1})			
SOIL			
DIFFUSION A	3.72E-08	DIFFUSIONtot	3.72E-08
WET DEP. A	2.80E-11	ADVECTIONtot	3.24E-06
DRY PART. DEP A	6.75E-16		
WET PART. DEP. A	8.10E-16		
IRRIGATION W	3.24E-06		

OUTPUT (mol h^{-1})			
SOIL			
VOLATILIZATION A	3.26E-06	DIFFUSIONtot	3.26E-06
REACTION	1.80E-08	ADVECTIONtot	1.60E-09
RUNOFF(W+P)	1.60E-09		
LEACHING GW	3.23E-12		
UPTAKE VEG	1.21E-15		

SOIL	
INPUT TOT	**OUTPUT TOT**
3.28E-06	3.28E-06

INPUT (mol h^{-1})	
VEGETATION	
DIFFUSION A	6.78E-20
WET DEP. A	1.40E-13
DRY PART. DEP A	4.05E-18
WET PART. DEP. A	3.38E-18
UPTAKE S	1.21E-15

1.00E+00	1.00E+00

INPUT (mol h^{-1})	
SEDIMENT	
DIFFUSION W	2.77E-09
DEPOSITION W	8.47E-09

OUTPUT (mol h^{-1})	
SEDIMENT	
RESUSPENSION W	6.06E-13
REACTION	1.12E-08
BURIAL	2.54E-12
DIFFUSION W	8.31E-13

SEDIMENT	
INPUT TOT	**OUTPUT TOT**
1.12E-08	1.12E-08

INPUT (mol h^{-1})	
FISH	
UPTAKE W	1.62E-09
DIFFUSION W	1.80E-05

OUTPUT (mol h^{-1})	
FISH	
DIFFUSION W	1.70E-05
GROWTH	7.03E-08
METABOLISM	9.35E-07
EJECTION	3.83E-10

OUTPUT (mol h^{-1})	
VEGETATION	
VOLATILIZATION A	7.08E-23
REACTION	1.41E-13

VEGETATION	
INPUT TOT	**OUTPUT TOT**
1.41E-13	1.41E-13

INPUT (mol h^{-1})	
GROUNDWATER	
LEACHING S	3.23E-12

OUTPUT (mol h^{-1})	
GROUNDWATER	
REACTION	3.65E-15
ADVECTION (W+P)	3.22E-12
GROUNDWATER	
INPUT TOT	**OUTPUT TOT**
3.23E-12	3.23E-12

FISH	
INPUT TOT	**OUTPUT TOT**
1.80E-05	1.80E-05

WORLD UNIT INPUT (mol h^{-1})	WORLD UNIT OUTPUT (mol h^{-1})
1.00E+00	1.00E+00

Table 61 Mass balance of the local model for a unit emission of benzene in soil

WORLD UNIT EMISSION RATE E (mol h^{-1})		
AIR	WATER	SOIL
0	0	1

INPUT (mol h^{-1})			
AIR			
VOLATILIZATION W	1.35E-07	DIFFUSIONtot	9.94E-01
VOLATILIZATION S	9.94E-01		
VOLATILIZATION VEG	4.33E-19		

OUTPUT (mol h^{-1})			
AIR			
DIFFUSION (ABSORPTION) S	1.32E-04	DIFFUSIONtot	1.32E-04
DIFFUSION (ABSORPTION) W	8.36E-08	ADVECTIONtot (excl. exit)	1.01E-07
DIFFUSION (ABSORPTION) VEG	2.40E-16		
WET DEP. W	1.00E-09		
DRY PART. DEP W	2.41E-14		
WET PART. DEP. W	2.90E-14		
WET DEP. S	9.92E-08		
DRY PART. DEP S	2.39E-12		
WET PART. DEP. S	2.87E-12		
WET DEP. VEG	4.96E-10		
DRY PART. DEP VEG	1.19E-14		
WET PART. DEP. VEG	1.43E-14		
REACTION	3.74E-03		
ADVECTION	9.90E-01		

AIR

INPUT (mol h^{-1})			
WATER			
DIFFUSION A	8.36E-08	DIFFUSIONtot	9.19E-08
WET DEP. A	1.00E-09	ADVECTIONtot	4.87E-04
DRY PART. DEP A	2.41E-14		
WET PART. DEP. A	2.90E-14		
RUNOFF S	4.87E-04		
DIFFUSION SED	4.05E-16		
RESUSP. SED	2.96E-16		
DIFFUSION F	8.30E-09		

OUTPUT (mol h^{-1})			
WATER			
VOLATILIZATION A	1.35E-07	DIFFUSIONtot	1.44E-07
REACTION	5.51E-07	ADVECTIONtot (excl. exit)	1.59E-09
ADVECTION (W+P)	4.87E-04		
IRRIGATION S	1.58E-09		
DEPOSITION SED	4.13E-12		
DIFFUSION SED	1.35E-12		
UPTAKE F	7.90E-13		
DIFFUSION F	8.79E-09		

WATER

INPUT TOT	OUTPUT TOT
9.94E-01	9.94E-01

INPUT (mol h^{-1})			
SOIL			
DIFFUSION A	1.32E-04	DIFFUSIONtot	1.32E-04
WET DEP. A	9.92E-08	ADVECTIONtot	1.01E-07
DRY PART. DEP A	2.39E-12		
WET PART. DEP. A	2.87E-12		
IRRIGATION W	1.58E-09		

OUTPUT (mol h^{-1})			
SOIL			
VOLATILIZATION A	9.94E-01	DIFFUSIONtot	9.94E-01
REACTION	5.50E-03	ADVECTIONtot	4.88E-04
RUNOFF(W+P)	4.87E-04		
LEACHING GW	9.84E-07		
UPTAKE VEG	3.69E-10		

SOIL	
INPUT TOT	OUTPUT TOT
1.00E+00	1.00E+00

INPUT (mol h^{-1})	
VEGETATION	
DIFFUSION A	2.40E-16
WET DEP. A	4.96E-10
DRY PART. DEP A	1.43E-14
WET PART. DEP. A	1.19E-14

INPUT TOT	OUTPUT TOT
4.88E-04	4.88E-04

INPUT (mol h^{-1})	
SEDIMENT	
DIFFUSION W	1.35E-12
DEPOSITION W	4.13E-12

OUTPUT (mol h^{-1})	
SEDIMENT	
RESUSPENSION W	2.96E-16
REACTION	5.48E-12
BURIAL	1.24E-15
DIFFUSION W	4.05E-16

SEDIMENT	
INPUT TOT	OUTPUT TOT
5.48E-12	5.48E-12

INPUT (mol h^{-1})	
FISH	
UPTAKE W	7.90E-13
DIFFUSION W	8.79E-09

OUTPUT (mol h^{-1})	
FISH	
DIFFUSION W	8.30E-09
GROWTH	3.43E-11
METABOLISM	4.56E-10
EJECTION	1.87E-13

UPTAKE S	3.69E-10

OUTPUT (mol h^{-1})	
VEGETATION	
VOLATILIZATION A	4.33E-19
REACTION	8.65E-10

VEGETATION	
INPUT TOT	**OUTPUT TOT**
8.65E-10	8.65E-10

INPUT (mol h^{-1})	
GROUNDWATER	
LEACHING S	9.84E-07

OUTPUT (mol h^{-1})	
GROUNDWATER	
REACTION	1.11E-09
ADVECTION (W+P)	9.83E-07
GROUNDWATER	
INPUT TOT	**OUTPUT TOT**
9.84E-07	9.84E-07

FISH	
INPUT TOT	**OUTPUT TOT**
8.79E-09	8.79E-09

WORLD UNIT INPUT (mol h^{-1})	**WORLD UNIT OUTPUT (mol h^{-1})**
1.00E+00	1.00E+00

Table 62 Mass balance of the local model for a unit emission of benzene in air, water and soil

WORLD UNIT EMISSION RATE E (mol h^{-1})		
AIR	WATER	SOIL
1	1	1

INPUT (mol h^{-1})			
AIR			
VOLATILIZATION W	2.78E-04	DIFFUSIONtot	9.95E-01
VOLATILIZATION S	9.94E-01		
VOLATILIZATION VEG	6.83E-19		

OUTPUT (mol h^{-1})			
AIR			
DIFFUSION (ABSORPTION) S	2.64E-04	DIFFUSIONtot	2.64E-04
DIFFUSION (ABSORPTION) W	1.68E-07	ADVECTIONtot (excl. exit)	2.02E-07
DIFFUSION (ABSORPTION) VEG	4.81E-16		
WET DEP. W	2.01E-09		
DRY PART. DEP W	4.84E-14		
WET PART. DEP. W	5.81E-14		
WET DEP. S	1.99E-07		
DRY PART. DEP S	4.79E-12		
WET PART. DEP. S	5.75E-12		
WET DEP. VEG	9.95E-10		
DRY PART. DEP VEG	2.40E-14		
WET PART. DEP. VEG	2.88E-14		
REACTION	7.50E-03		
ADVECTION	1.99E+00		

AIR	
INPUT TOT	OUTPUT TOT

INPUT (mol h^{-1})			
WATER			
DIFFUSION A	1.68E-07	DIFFUSIONtot	1.72E-05
WET DEP. A	2.01E-09	ADVECTIONtot	4.88E-04
DRY PART. DEP A	4.84E-14		
WET PART. DEP. A	5.81E-14		
RUNOFF S	4.87E-04		
DIFFUSION SED	8.31E-13		
RESUSP. SED	6.07E-13		
DIFFUSION F	1.70E-05		

OUTPUT (mol h^{-1})			
WATER			
VOLATILIZATION A	2.78E-04	DIFFUSIONtot	2.96E-04
REACTION	1.13E-03	ADVECTIONtot (excl. exit)	3.25E-06
ADVECTION (W+P)	9.99E-01		
IRRIGATION S	3.24E-06		
DEPOSITION SED	8.47E-09		
DIFFUSION SED	2.77E-09		
UPTAKE F	1.62E-09		
DIFFUSION F	1.80E-05		

WATER	
INPUT TOT	OUTPUT TOT

1.99E+00	1.99E+00

INPUT (mol h^{-1})			
SOIL			
DIFFUSION A	2.64E-04	DIFFUSIONtot	2.64E-04
WET DEP. A	1.99E-07	ADVECTIONtot	3.44E-06
DRY PART. DEP A	4.79E-12		
WET PART. DEP. A	5.75E-12		
IRRIGATION W	3.24E-06		

OUTPUT (mol h^{-1})			
SOIL			
VOLATILIZATION A	9.94E-01	DIFFUSIONtot	9.94E-01
REACTION	5.50E-03	ADVECTIONtot	4.88E-04
RUNOFF(W+P)	4.87E-04		
LEACHING GW	9.84E-07		
UPTAKE VEG	3.69E-10		

SOIL	
INPUT TOT	**OUTPUT TOT**
1.00E+00	1.00E+00

INPUT (mol h^{-1})	
VEGETATION	
DIFFUSION A	4.81E-16
WET DEP. A	9.95E-10
DRY PART. DEP A	2.88E-14
WET PART. DEP. A	2.40E-14
UPTAKE S	3.69E-10

1.00E+00	1.00E+00

INPUT (mol h^{-1})	
SEDIMENT	
DIFFUSION W	2.77E-09
DEPOSITION W	8.47E-09

OUTPUT (mol h^{-1})	
SEDIMENT	
RESUSPENSION W	6.07E-13
REACTION	1.12E-08
BURIAL	2.54E-12
DIFFUSION W	8.31E-13

SEDIMENT	
INPUT TOT	**OUTPUT TOT**
1.12E-08	1.12E-08

INPUT (mol/h)	
FISH	
UPTAKE W	1.62E-09
DIFFUSION W	1.80E-05

OUTPUT (mol h^{-1})	
FISH	
DIFFUSION W	1.70E-05
GROWTH	7.04E-08
METABOLISM	9.35E-07
EJECTION	3.83E-10

OUTPUT (mol h^{-1})	
VEGETATION	
VOLATILIZATION A	6.83E-19
REACTION	1.36E-09

VEGETATION	
INPUT TOT	**OUTPUT TOT**
1.36E-09	1.36E-09

INPUT (mol h^{-1})	
GROUNDWATER	
LEACHING S	9.84E-07

OUTPUT (mol h^{-1})	
GROUNDWATER	
REACTION	1.11E-09
ADVECTION (W+P)	9.83E-07
GROUNDWATER	
INPUT TOT	**OUTPUT TOT**
9.84E-07	9.84E-07

FISH	
INPUT TOT	**OUTPUT TOT**
1.80E-05	1.80E-05

WORLD UNIT INPUT (mol h^{-1})	WORLD UNIT OUTPUT (mol h^{-1})
3.00E+00	3.00E+00

A.4 Analytic conversion of mass-based rate constants *k* from fugacity-based rates *D*

Air Degradation

$$N_{DEG,A} = f_A \times D_{DEGA} \quad \text{(Eq. 187)}$$

$$= f_A \times k_A \times V_{g,A} \times Z_A$$

$$= C_{g,A} \times V_{g,A} \times k_A$$

$$= \frac{M_{g,A}}{V_{g,A}} \times V_{g,A} \times k_A$$

$$= M_{g,A} \times k_A$$

$$= M_A \times k_A \times v_{g,A} \times K_{g,Atot}$$

$$= M_A \times k_{DEGA}$$

Where:

- $k_{DEGA}(h^{-1}) = k_A \times v_{g,A} \times K_{g,Atot}$ is the mass-based rate for air degradation;
- $M_A\ (kg)$ is the mass in air compartment;
- $M_{g,A}\ (kg\ m^{-3})$ is the chemical mass in the gas phase;
- $v_{g,A}$ is the gas volume fraction in air compartment;
- $K_{g,Atot}$ is the partition coefficient between gas phase and air compartment;
- $V_{g,A}\ (m^3)$ is the volume of the gas phase;
- $k_A\ (h^{-1})$ is the rate constant for air degradation;
- $C_{g,A}\ (kg\ m^{-3})$ is the chemical concentration in the gas phase;
- $Z_A\ (kg\ Pa^{-1}m^{-3})$ is the fugacity capacity of gas phase;
- $D_{DEGA}\ (kg\ Pa^{-1}h^{-1})$ is the fugacity-based rate D for air degradation;
- $f_A\ (Pa)$ is the air fugacity;
- $N_{DEG,A}\ (kg\ h^{-1})$ is the air degradation mass flux.

Water Degradation

$$N_{DEG,W} = f_W \times D_{DEGW} \quad \text{(Eq. 188)}$$

$$= f_W \times k_W \times V_{w,W} \times Z_W$$

$$= C_{w,W} \times V_{w,W} \times k_W$$

$$= \frac{M_{w,W}}{V_{w,W}} \times V_{w,W} \times k_W$$

$$= M_{w,W} \times k_W$$

$$= M_W \times k_W \times v_{w,W} \times K_{w,Wtot}$$

$$= M_W \times k_{DEGW}$$

Where:

- $k_{DEGW}(h^{-1}) = k_W \times v_{w,W} \times K_{w,Wtot}$ is the mass-based rate for water degradation;
- $M_W\ (kg)$ is the mass in water compartment;
- $v_{w,W}$ is the dissolved water volume fraction in water compartment;
- $K_{w,Wtot}$ is the partition coefficient between dissolved water phase and water compartment;
- $V_{w,W}\ (m^3)$ is the volume of the dissolved water phase;
- $k_W\ (h^{-1})$ is the rate constant for water degradation;
- $C_{w,W}\ (kg\ m^{-3})$ is the chemical concentration in the dissolved water phase;
- $Z_W\ (kg\ Pa^{-1}m^{-3})$ is the fugacity capacity of dissolved water phase;
- $D_{DEGW}\ (kg\ Pa^{-1}h^{-1})$ is the fugacity-based rate D for water degradation;
- $f_W\ (Pa)$ is the water fugacity
- $N_{DEG,W}\ (kg\ h^{-1})$ is the water degradation mass flux.

Soil Degradation

$$N_{DEG,S} = f_S \times D_{DEGS} \quad \text{(Eq. 189)}$$

$$= f_S \times k_S \times V_{oc,S} \times Z_S$$

$$= C_{oc,S} \times V_{oc,S} \times k_S$$

$$= \frac{M_{oc,S}}{V_{oc,S}} \times V_{oc,S} \times k_S$$

$$= M_{oc,S} \times k_S$$

$$= M_S \times k_S \times v_{oc,S} \times K_{oc,Stot}$$

$$= M_S \times k_{DEGS}$$

Where:

- $k_{DEGS}(h^{-1}) = k_S \times v_{oc,S} \times K_{oc,Stot}$ is the mass-based rate for soil degradation;
- $M_S\ (kg)$ is the mass in soil compartment;
- $v_{oc,S}$ is the organic carbon volume fraction in soil compartment;
- $K_{oc,Stot}$ is the partition coefficient between organic carbon phase and soil compartment;
- $V_{oc,S}\ (m^3)$ is the volume of the organic carbon phase;
- $k_S\ (h^{-1})$ is the rate constant for soil degradation;
- $C_{oc,S}\ (kg\ m^{-3})$ is the chemical concentration in the organic carbon phase;
- $Z_S\ (kg\ Pa^{-1}m^{-3})$ is the fugacity capacity of organic carbon phase;
- $D_{DEGS}\ (kg\ Pa^{-1}h^{-1})$ is the fugacity-based rate D for soil degradation;

- $f_S\ (Pa)$ is the soil fugacity
- $N_{DEG,S}\ (kg\ h^{-1})$ is the soil degradation mass flux.

Air Advection

$$N_{ADV,A} = f_A \times D_{ADVA} \quad \text{(Eq. 190)}$$

$$= f_A \times G_A \times Z_A$$

$$= C_{g,A} \times G_A$$

$$= \frac{M_{g,A}}{V_{g,A}} \times G_A$$

$$= M_A \times v_{g,A} \times K_{g,Atot} \times \frac{G_A}{V_{g,A}}$$

$$= M_A \times K_{g,Atot} \times \frac{G_A}{V_A}$$

$$= M_A \times k_{ADVA}$$

Where:

- $k_{ADVA}(h^{-1}) = K_{g,Atot} \times \frac{G_A}{V_A}$ is the mass-based rate for air advection;
- $M_A\ (kg)$ is the mass in air compartment;
- $M_{g,A}\ (kg\ m^{-3})$ is the chemical mass in the gas phase;
- $v_{g,A}$ is the gas volume fraction in air compartment;
- $K_{g,Atot}$ is the partition coefficient between gas phase and air compartment;
- $V_{g,A}\ (m^3)$ is the volume of the gas phase;
- $G_A\ (m^3\ h^{-1})$ is the air flow rate;
- $V_A\ (m^3)$ is the volume of air compartment;
- $C_{g,A}\ (kg\ m^{-3})$ is the chemical concentration in the gas phase;
- $Z_A\ (kg\ Pa^{-1}m^{-3})$ is the fugacity capacity of gas phase;
- $D_{ADVA}\ (kg\ Pa^{-1}h^{-1})$ is the fugacity-based rate D for air advection;
- $f_A\ (Pa)$ is the air fugacity;
- $N_{ADV,A}\ (kg\ h^{-1})$ is the air advection mass flux.

Water Advection

$$N_{ADV,W} = f_W \times D_{ADVW} \quad \text{(Eq. 191)}$$

$$= f_W \times (G_W \times Z_W + G_{PW} \times Z_{PW})$$

$$= f_W \times (G_W \times Z_W + G_{PW} \times K_{PW} \times Z_W)$$

$$= f_W \times G_W \times Z_W \times (1 + v_{PW} \times K_{PW})$$

$$= C_{w,W} \times G_W \times (1 + v_{PW} \times K_{PW})$$

$$= \frac{M_{w,W}}{V_{w,W}} \times G_W \times (1 + v_{PW} \times K_{PW})$$

$$= M_W \times \ v_{w,W} \times K_{w,Wtot} \times \frac{G_W}{V_{w,W}} \times (1 + v_{PW} \times K_{PW})$$

$$= M_W \times K_{w,Wtot} \times \frac{G_W}{V_W} \times (1 + v_{PW} \times K_{PW})$$

$$= M_W \times k_{ADVW}$$

Where:

- $k_{ADVW}(h^{-1}) = K_{w,Wtot} \times \frac{G_W}{V_W} \times (1 + v_{PW} \times K_{PW})$ is the mass-based rate for water advection;
- $M_W\ (kg)$ is the mass in water compartment;
- $v_{w,W}$ is the dissolved water volume fraction in water compartment;
- $v_{p,W}$ is the suspended solids volume fraction in water compartment;
- $K_{w,Wtot}$ is the partition coefficient between dissolved water phase and water compartment;
- K_{PW} is the partition coefficient between suspended solids phase and dissolved water phase;
- $V_{w,W}\ (m^3)$ is the volume of the dissolved water phase;
- $G_W\ (m^3\ h^{-1})$ is the water flow rate;
- $G_{PW}\ (m^3\ h^{-1})$ is the suspended solids flow rate;
- $V_W\ (m^3)$ is the volume of water compartment;
- $C_{w,W}\ (kg\ m^{-3})$ is the chemical concentration in the dissolved water phase;
- $Z_W\ (kg\ Pa^{-1}m^{-3})$ is the fugacity capacity of dissolved water phase;
- $D_{ADVW}\ (kg\ Pa^{-1}h^{-1})$ is the fugacity-based rate D for water advection;
- $f_W\ (Pa)$ is the water fugacity;
- $N_{ADV,W}\ (kg\ h^{-1})$ is the water advection mass flux.

Air-water diffusion

$$N_{DIFF,AW} = f_A \times D_{VAW} \qquad \text{(Eq. 192)}$$

$$= f_A \times (\frac{1}{k_A \times A_{AW} \times Z_A} + \frac{1}{k_W \times A_{AW} \times Z_W})^{-1}$$

$$= f_A \times (\frac{1}{k_A \times A_{AW} \times Z_A} + \frac{1}{k_W \times A_{AW} \times K_{AW} \times Z_A})^{-1}$$

$$= f_A \times Z_A \times A_{AW} \times (\frac{1}{k_A} + \frac{1}{k_W \times K_{AW}})^{-1}$$

$$= C_{g,A} \times A_{AW} \times \frac{k_{OW}}{K_{AW}}$$

$$= \frac{M_{g,A}}{V_{g,A}} \times A_{AW} \times \frac{k_{OW}}{K_{AW}}$$

$$= \frac{M_A}{V_{g,A}} \times v_{g,A} \times K_{g,Atot} \times A_{AW} \times \frac{k_{OW}}{K_{AW}}$$

Assuming that $V_{g,A} \approx V_A$:

$$= M_A \times v_{g,A} \times K_{g,Atot} \times \frac{A_{AW}}{V_A} \times \frac{k_{OW}}{K_{AW}}$$

$$= M_A \times fr\_m_g \times \frac{areafractW \times A_A}{V_A} \times \frac{k_{OW}}{K_{AW}}$$

$$= M_A \times k_{VAW}$$

Where:

- $k_{VAW}(h^{-1}) = fr\_m_g \times areafractW \times \frac{1}{h_A} \times \frac{k_{OW}}{K_{AW}}$ is the mass-based rate for air-water diffusion;
- $M_A\ (kg)$ is the mass in air compartment;
- $M_{g,A}\ (kg\ m^{-3})$ is the chemical mass in the gas phase;
- $fr\_m_g = v_{g,A} \times K_{g,Atot}$ is the fraction of chemical in the gas phase;
- $v_{g,A}$ is the gas volume fraction in air compartment;
- $K_{g,Atot}$ is the partition coefficient between gas phase and air compartment;
- K_{AW} is the partition coefficient between gas phase and dissolved water phase;
- $V_{g,A}\ (m^3)$ is the volume of the gas phase;
- $A_{AW}(m^2) = areafractW \times A_A$ is the contact area between water and air;
- $areafractW$ is the fraction of area occupied by water;
- $A_A(m^2)$ is the surface area of air;
- $V_A\ (m^3)$ is the volume of air compartment;
- $k_{OW} = (\frac{1}{k_W} + \frac{1}{k_A \times K_{AW}})^{-1}$ is the overall mass transfer coefficient for air-water diffusion;
- $k_A\ (m\ h^{-1})$ is the partial mass transfer rate air side for diffusion;
- $k_W\ (m\ h^{-1})$ is the partial mass transfer rate water side for diffusion;
- $C_{g,A}\ (kg\ m^{-3})$ is the chemical concentration in the gas phase;
- $Z_A\ (kg\ Pa^{-1}m^{-3})$ is the fugacity capacity of gas phase;
- $D_{VAW}\ (kg\ Pa^{-1}h^{-1})$ is the fugacity-based rate D for air-water diffusion;
- $f_A\ (Pa)$ is the air fugacity;
- $N_{DIFF,AW}\ (kg\ h^{-1})$ is the air-water diffusion mass flux.

Water-air diffusion

$$N_{DIFF,WA} = f_W \times D_{VAW} \quad \text{(Eq. 193)}$$

$$= f_W \times (\frac{1}{k_A \times A_{AW} \times Z_A} + \frac{1}{k_W \times A_{AW} \times Z_W})^{-1}$$

$$= f_W \times (\frac{1}{k_A \times A_{AW} \times Z_W \times K_{AW}} + \frac{1}{k_W \times A_{AW} \times Z_W})^{-1}$$

$$= f_W \times Z_W \times A_{AW} \times (\frac{1}{k_A \times K_{AW}} + \frac{1}{k_W})^{-1}$$

$$= C_{w,W} \times A_{AW} \times k_{OW}$$

$$= \frac{M_{w,W}}{V_{w,W}} \times A_{AW} \times k_{OW}$$

$$= \frac{M_W}{V_{w,W}} \times v_{w,W} \times K_{w,Wtot} \times A_{AW} \times k_{OW}$$

Assuming that $V_{w,W} \approx V_W$:

$$= M_W \times v_{w,W} \times K_{w,Wtot} \times \frac{A_{AW}}{V_W} \times k_{OW}$$

$$= M_W \times fr\_m_w \times \frac{A_{AW}}{V_W} \times k_{OW}$$

$$= M_W \times k_{VWA}$$

Where:

- $k_{VWA}(h^{-1}) = fr\_m_w \times areafractW \times \frac{1}{h_W} \times k_{OW}$ is the mass-based rate for water-air diffusion;
- $M_W\ (kg)$ is the mass in water compartment;
- $fr\_m_w = v_{w,W} \times K_{w,Wtot}$ is the fraction of chemical in the dissolved water phase;
- $v_{w,W}$ is the dissolved water volume fraction in water compartment;
- $K_{w,Wtot}$ is the partition coefficient between dissolved water phase and water compartment;
- K_{AW} is the partition coefficient between gas phase and dissolved water phase;
- $V_{w,W}\ (m^3)$ is the volume of the dissolved water phase;
- $A_{AW}(m^2) = A_W(m^2)$ is the surface area of water compartment;
- $V_W\ (m^3)$ is the volume of water compartment;
- $k_{OW} = (\frac{1}{k_W} + \frac{1}{k_A \times K_{AW}})^{-1}$ is the overall mass transfer coefficient for air-water diffusion;
- $k_A\ (m\ h^{-1})$ is the partial mass transfer rate air side for diffusion;
- $k_W\ (m\ h^{-1})$ is the partial mass transfer rate water side for diffusion;
- $C_{w,W}\ (kg\ m^{-3})$ is the chemical concentration in the dissolved water phase;
- $Z_W\ (kg\ Pa^{-1}m^{-3})$ is the fugacity capacity of dissolved water phase;

- D_{VAW} $(kg\ Pa^{-1}h^{-1})$ is the fugacity-based rate D for air-water diffusion;
- f_W (Pa) is the water fugacity;
- $N_{DIFF,WA}$ $(kg\ h^{-1})$ is the water-air diffusion mass flux.

Air-soil diffusion

$$N_{DIFF,AS} = f_A \times D_{VAS} \quad \text{(Eq. 194)}$$

$$= f_A \times (\frac{1}{k_V \times A_{AS} \times Z_A} + \frac{1}{(\frac{B_{EA} \times Z_A + B_{EW} \times Z_W + B_{EOC} \times Z_S}{Y}) \times A_{AS}})^{-1}$$

$$= f_A \times (\frac{1}{k_V \times A_{AS} \times Z_A} + \frac{1}{(\frac{B_{EA} \times Z_A + B_{EW} \times K_{WA} \times Z_A + B_{EOC} \times K_{SA} \times Z_A}{Y}) \times A_{AS}})^{-1}$$

$$= f_A \times Z_A \times A_{AS} \times (\frac{1}{k_V} + \frac{1}{\frac{B_{EA} + B_{EW} \times K_{WA} + B_{EOC} \times K_{SA}}{Y}})^{-1}$$

$$= C_{g,A} \times A_{AS} \times (\frac{1}{k_V} + \frac{1}{\frac{B_{EA} + B_{EW} \times K_{WA} + B_{EOC} \times K_{SA}}{Y}})^{-1}$$

$$= \frac{M_{g,A}}{V_{g,A}} \times A_{AS} \times (\frac{1}{k_V} + \frac{1}{\frac{B_{EA} + B_{EW} \times K_{WA} + B_{EOC} \times K_{SA}}{Y}})^{-1}$$

$$= \frac{M_A}{V_{g,A}} \times v_{g,A} \times K_{g,Atot} \times A_{AS} \times (\frac{1}{k_V} + \frac{1}{\frac{B_{EA} + B_{EW} \times K_{WA} + B_{EOC} \times K_{SA}}{Y}})^{-1}$$

Assuming that $V_{g,A} \approx V_A$:

$$= M_A \times v_{g,A} \times K_{g,Atot} \times \frac{A_{AS}}{V_A} \times (\frac{1}{k_V} + \frac{1}{\frac{B_{EA} + B_{EW} \times K_{WA} + B_{EOC} \times K_{SA}}{Y}})^{-1}$$

$$= M_A \times fr\_m_g \times \frac{areafractS \times A_A}{V_A} \times (\frac{1}{k_V} + \frac{1}{\frac{B_{EA} + B_{EW} \times K_{WA} + B_{EOC} \times K_{SA}}{Y}})^{-1}$$

$$= M_A \times k_{VAS}$$

Where:

- $k_{VAS}(h^{-1}) = fr\_m_g \times areafractS \times \frac{1}{h_A} \times (\frac{1}{k_V} + \frac{1}{\frac{B_{EA}+B_{EW}\times K_{WA}+B_{EOC}\times K_{SA}}{Y}})^{-1}$ is the mass-based rate for air-soil diffusion;
- M_A (kg) is the mass in air compartment;
- $M_{g,A}$ $(kg\ m^{-3})$ is the chemical mass in the gas phase;
- $fr\_m_g = v_{g,A} \times K_{g,Atot}$ is the fraction of chemical in the gas phase;

- $v_{g,A}$ is the gas volume fraction in air compartment;
- $K_{g,Atot}$ is the partition coefficient between gas phase and air compartment;
- K_{WA} is the partition coefficient between dissolved water phase and gas phase;
- K_{SA} is the partition coefficient between organic carbon phase and gas phase;
- $V_{g,A}$ (m^3) is the volume of the gas phase;
- A_{AS} (m^2) $= areafractS \times A_A$ is the contact area between soil and air;
- $areafractS$ is the fraction of area occupied by soil;
- $A_A(m^2)$ is the surface area of air;
- V_A (m^3) is the volume of air compartment;
- Y (m) is the penetration depth in soil;
- B_{EA} $(m^2\ h^{-1})$ is the gas phase diffusivity soil side;
- B_{EW} $(m^2\ h^{-1})$ is the pore water phase diffusivity soil side;
- B_{EOC} $(m^2\ h^{-1})$ is the organic carbon phase diffusivity soil side;
- k_V $(m\ h^{-1})$ is the partial mass transfer rate air side for air-soil diffusion;
- $C_{g,A}$ $(kg\ m^{-3})$ is the chemical concentration in the gas phase;
- Z_A $(kg\ Pa^{-1}m^{-3})$ is the fugacity capacity of gas phase;
- D_{VAS} $(kg\ Pa^{-1}h^{-1})$ is the fugacity-based rate D for air-soil diffusion;
- f_A (Pa) is the air fugacity;
- $N_{DIFF,AS}$ $(kg\ h^{-1})$ is the air-soil diffusion mass flux.

Compared to eq. 105 of USEtox, effective advective transport Veff is not considered here.

Soil-air diffusion

$$N_{DIFF,SA} = f_S \times D_{VAS} \qquad \text{(Eq. 195)}$$

$$= f_S \times \left(\frac{1}{k_V \times A_{AS} \times Z_A} + \frac{1}{\left(\frac{B_{EA} \times Z_A + B_{EW} \times Z_W + B_{EOC} \times Z_S}{Y}\right) \times A_{AS}}\right)^{-1}$$

$$= f_A \times \left(\frac{1}{k_V \times A_{AS} \times K_{AS} \times Z_S} + \frac{1}{\left(\frac{B_{EA} \times K_{AS} \times Z_S + B_{EW} \times K_{WS} \times Z_S + B_{EOC} \times Z_S}{Y}\right) \times A_{AS}}\right)^{-1}$$

$$= f_S \times Z_S \times A_{AS} \times \left(\frac{1}{k_V \times K_{AS}} + \frac{1}{\frac{B_{EA} \times K_{AS} + B_{EW} \times K_{WS} + B_{EOC}}{Y}}\right)^{-1}$$

$$= C_{oc,S} \times A_{AS} \times \left(\frac{1}{k_V \times K_{AS}} + \frac{1}{\frac{B_{EA} \times K_{AS} + B_{EW} \times K_{WS} + B_{EOC}}{Y}}\right)^{-1}$$

$$= \frac{M_{oc,S}}{V_{oc,S}} \times A_{AS} \times \left(\frac{1}{k_V \times K_{AS}} + \frac{1}{\frac{B_{EA} \times K_{AS} + B_{EW} \times K_{WS} + B_{EOC}}{Y}}\right)^{-1}$$

$$= \frac{M_S}{V_{oc,S}} \times v_{oc,S} \times K_{oc,Stot} \times A_{AS} \times \left(\frac{1}{k_V \times K_{AS}} + \frac{1}{\frac{B_{EA} \times K_{AS} + B_{EW} \times K_{WS} + B_{EOC}}{Y}}\right)^{-1}$$

$$= M_S \times K_{oc,Stot} \times \frac{A_{AS}}{V_S} \times \left(\frac{1}{k_V \times K_{AS}} + \frac{1}{\frac{B_{EA} \times K_{AS} + B_{EW} \times K_{WS} + B_{EOC}}{Y}}\right)^{-1}$$

$$= M_S \times K_{oc,Stot} \times K_{AS} \times \frac{A_{AS}}{V_S} \times \left(\frac{1}{k_V} + \frac{1}{\frac{B_{EA} + B_{EW} \times K_{WS}/K_{AS} + B_{EOC}/K_{AS}}{Y}}\right)^{-1}$$

$$= M_S \times K_{oc,Stot} \times K_{AS} \times \frac{A_{AS}}{V_S} \times \left(\frac{1}{k_V} + \frac{1}{\frac{B_{EA} + B_{EW} \times K_{WA} + B_{EOC} \times K_{SA}}{Y}}\right)^{-1}$$

$$= M_S \times k_{VSA}$$

Where:

- $k_{VSA}(h^{-1}) = K_{oc,Stot} \times K_{AS} \times \frac{1}{h_S} \times \left(\frac{1}{k_V} + \frac{1}{\frac{B_{EA}+B_{EW} \times K_{WA}+B_{EOC} \times K_{SA}}{Y}}\right)^{-1}$ is the mass-based rate for soil-air diffusion;
- $M_S\ (kg)$ is the mass in soil compartment;
- $v_{oc,S}$ is the organic carbon volume fraction in soil compartment;
- $K_{oc,Stot}$ is the partition coefficient between organic carbon phase and soil compartment;
- $K_{WA} = K_{WS}/K_{AS}$ is the partition coefficient between dissolved water phase and gas phase;
- $K_{SA} = 1/K_{AS}$ is the partition coefficient between organic carbon phase and gas phase;
- K_{AS} is the partition coefficient between gas phase and organic carbon phase;
- $V_{oc,S}\ (m^3)$ is the volume of the organic carbon phase;
- $A_{AS}\ (m^2) = A_S\ (m^2)$ is the surface area of soil;
- $V_S\ (m^3)$ is the volume of soil compartment;
- $Y\ (m)$ is the penetration depth in soil;
- $B_{EA}\ (m^2\ h^{-1})$ is the gas phase diffusivity soil side;
- $B_{EW}\ (m^2\ h^{-1})$ is the pore water phase diffusivity soil side;
- $B_{EOC}\ (m^2\ h^{-1})$ is the organic carbon phase diffusivity soil side;
- $k_V\ (m\ h^{-1})$ is the partial mass transfer rate air side for air-soil diffusion;
- $C_{oc,S}\ (kg\ m^{-3})$ is the chemical concentration in the organic carbon phase;
- $Z_S\ (kg\ Pa^{-1}m^{-3})$ is the fugacity capacity of organic carbon phase;
- $D_{VAS}\ (kg\ Pa^{-1}h^{-1})$ is the fugacity-based rate D for air-soil diffusion;
- $f_S\ (Pa)$ is the soil fugacity;
- $N_{DIFF,SA}\ (kg\ h^{-1})$ is the soil-air diffusion mass flux.

Compared to eq. 113 of USEtox, effective advective transport Veff is not considered here.

Aerosol dry deposition towards water

$$N_{DRYDEP,Q,AW} = f_A \times D_{QAW} \quad \text{(Eq. 196)}$$

$$= f_A \times U_Q \times v_{q,A} \times A_{AW} \times Z_Q$$

$$= f_A \times U_Q \times v_{q,A} \times A_{AW} \times K_{QA} \times Z_A$$

$$= C_{g,A} \times U_Q \times v_{q,A} \times A_{AW} \times K_{QA}$$

$$= \frac{M_{g,A}}{V_{g,A}} \times U_Q \times v_{q,A} \times A_{AW} \times K_{QA}$$

$$= M_A \times v_{g,A} \times K_{g,Atot} \times \frac{U_Q \times v_{q,A} \times A_{AW} \times K_{QA}}{V_{g,A}}$$

Assuming that $V_{g,A} \approx V_A$:

$$= M_A \times v_{g,A} \times K_{g,Atot} \times \frac{U_Q \times v_{q,A} \times AreafractW \times A_A \times K_{QA}}{V_A}$$

$$= M_A \times v_{g,A} \times K_{g,Atot} \times K_{QA} \times \frac{U_Q \times v_{q,A} \times AreafractW \times A_A}{V_A}$$

$$= M_A \times v_{g,A} \times K_{q,Atot} \times v_{q,A} \times \frac{U_Q \times AreafractW \times A_A}{V_A}$$

$$= M_A \times v_{g,A} \times fr\_m_{q,Atot} \times \frac{U_Q \times AreafractW \times A_A}{V_A}$$

$$= M_A \times v_{g,A} \times fr\_m_{q,Atot} \times U_Q \times AreafractW \times \frac{A_A}{V_A}$$

$$= M_A \times k_{QAW}$$

Where:

- $k_{QAW}(h^{-1}) = v_{g,A} \times fr\_m_{q,Atot} \times U_Q \times AreafractW \times \frac{1}{h_A}$ is the mass-based rate for aerosol dry deposition to water;
- M_A (kg) is the mass in air compartment;
- $M_{g,A}$ $(kg\ m^{-3})$ is the chemical mass in the gas phase;
- $v_{g,A}$ is the gas volume fraction in air compartment;
- $v_{q,A}$ is the aerosol volume fraction in air compartment;
- $K_{g,Atot}$ is the partition coefficient between gas phase and air compartment;
- K_{QA} is the partition coefficient between aerosol phase and gas phase;

- $K_{q,Atot} = K_{g,Atot} \times K_{QA}$ is the partition coefficient between aerosol phase and air compartment;
- $fr\_m_{q,Atot} = K_{q,Atot} \times v_{q,A}$ is the mass fraction of chemical in aerosol phase;
- $V_{g,A}\ (m^3)$ is the volume of the gas phase;
- $A_{AW}(m^2)\ = areafractW \times A_A$ is the contact area between water and air;
- $areafractW$ is the fraction of area occupied by water;
- $A_A(m^2)$ is the surface area of air;
- $U_Q\ (m\ h^{-1})$ is the aerosol deposition rate;
- $V_A\ (m^3)$ is the volume of air compartment;
- $C_{g,A}\ (kg\ m^{-3})$ is the chemical concentration in the gas phase;
- $Z_A\ (kg\ Pa^{-1}m^{-3})$ is the fugacity capacity of gas phase;
- $D_{QAW}\ (kg\ Pa^{-1}h^{-1})$ is the fugacity-based rate D for aerosol dry deposition to water;
- $f_A\ (Pa)$ is the air fugacity;
- $N_{DRYDEP,Q}\ (kg\ h^{-1})$ is the aerosol dry deposition mass flux.

Compared to eq. 93 of USEtox, here there is also the gas volume fraction.

Rain dissolution (gas washout)

$$N_{RAINDISS,AW} = f_A \times D_{MAW} \qquad \text{(Eq. 197)}$$

$$= f_A \times U_M \times A_{AW} \times Z_W$$

$$= f_A \times U_M \times A_{AW} \times K_{WA} \times Z_A$$

$$= C_{g,A} \times U_M \times A_{AW} \times K_{WA}$$

$$= \frac{M_{g,A}}{V_{g,A}} \times U_M \times A_{AW} \times K_{WA}$$

$$= M_A \times v_{g,A} \times K_{g,Atot} \times \frac{U_M \times A_{AW} \times K_{WA}}{V_{g,A}}$$

Assuming that $V_{g,A} \approx V_A$:

$$= M_A \times v_{g,A} \times K_{g,Atot} \times \frac{U_M \times Areafract W \times A_A \times K_{WA}}{V_A}$$

$$= M_A \times v_{g,A} \times K_{g,Atot} \times K_{WA} \times \frac{U_M \times Areafract W \times A_A}{V_A}$$

$$= M_A \times fr\_m_{g,Atot} \times K_{WA} \times \frac{U_M \times Areafract W \times A_A}{V_A}$$

$$= M_A \times fr\_m_{g,Atot} \times K_{WA} \times U_M \times Areafract W \times \frac{A_A}{V_A}$$

$$= M_A \times k_{MAW}$$

Where:

- $k_{MAW}(h^{-1}) = fr\_m_{g,Atot} \times K_{WA} \times U_M \times AreafractW \times \frac{1}{h_A}$ is the mass-based rate for rain dissolution of gas to water;
- $M_A\ (kg)$ is the mass in air compartment;
- $M_{g,A}\ (kg\ m^{-3})$ is the chemical mass in the gas phase;
- $v_{g,A}$ is the gas volume fraction in air compartment;
- $K_{g,Atot}$ is the partition coefficient between gas phase and air compartment;
- K_{WA} is the partition coefficient between dissolved water phase and gas phase;
- $fr\_m_{g,Atot} = K_{q,Atot} \times v_{q,A}$ is the mass fraction of chemical in gas phase;
- $V_{g,A}\ (m^3)$ is the volume of the gas phase;
- $A_{AW}(m^2) = areafractW \times A_A$ is the contact area between water and air;
- $areafractW$ is the fraction of area occupied by water;
- $A_A(m^2)$ is the surface area of air;
- $V_A\ (m^3)$ is the volume of air compartment;
- $U_M\ (m\ h^{-1})$ is the rain rate;
- $C_{g,A}\ (kg\ m^{-3})$ is the chemical concentration in the gas phase;
- $Z_A\ (kg\ Pa^{-1}m^{-3})$ is the fugacity capacity of gas phase;
- $D_{MAW}\ (kg\ Pa^{-1}h^{-1})$ is the fugacity-based rate D for aerosol rain dissolution of gas to water;
- $f_A\ (Pa)$ is the air fugacity;
- $N_{RAINDISS,AW}\ (kg\ h^{-1})$ is the rain dissolution mass flux.

Compared to eq. 97 of USEtox, fr_mcldw is not present here, as well as the intermittent rain model.

Wet aerosol deposition

$$N_{WETDEP,Q,AW} = f_A \times D_{CAW} \quad \text{(Eq. 198)}$$

$$= f_A \times U_M \times v_{q,A} \times A_{AW} \times Q \times Z_Q$$

$$= f_A \times U_M \times v_{q,A} \times A_{AW} \times Q \times K_{QA} \times Z_A$$

$$= C_{g,A} \times U_M \times v_{q,A} \times A_{AW} \times Q \times K_{QA}$$

$$= \frac{M_{g,A}}{V_{g,A}} \times U_M \times v_{q,A} \times A_{AW} \times Q \times K_{QA}$$

$$= M_A \times v_{g,A} \times K_{g,Atot} \times \frac{U_M \times v_{q,A} \times A_{AW} \times Q \times K_{QA}}{V_{g,A}}$$

Assuming that $V_{g,A} \approx V_A$:

$$= M_A \times v_{g,A} \times K_{g,Atot} \times \frac{U_M \times v_{q,A} \times AreafractW \times A_A \times Q \times K_{QA}}{V_A}$$

$$= M_A \times v_{g,A} \times K_{g,Atot} \times K_{QA} \times \frac{U_M \times v_{q,A} \times AreafractW \times Q \times A_A}{V_A}$$

$$= M_A \times v_{g,A} \times K_{q,Atot} \times v_{q,A} \times \frac{U_M \times AreafractW \times Q \times A_A}{V_A}$$

$$= M_A \times v_{g,A} \times fr\_m_{q,Atot} \times \frac{U_M \times AreafractW \times Q \times A_A}{V_A}$$

$$= M_A \times v_{g,A} \times fr\_m_{q,Atot} \times U_M \times AreafractW \times Q \times \frac{A_A}{V_A}$$

$$= M_A \times k_{CAW}$$

Where:

- $k_{CAW}(h^{-1}) = v_{g,A} \times fr\_m_{q,Atot} \times U_M \times AreafractW \times Q \times \frac{1}{h_A}$ is the mass-based rate for aerosol wet deposition to water;
- $M_A\ (kg)$ is the mass in air compartment;
- $M_{g,A}\ (kg\ m^{-3})$ is the chemical mass in the gas phase;
- $v_{g,A}$ is the gas volume fraction in air compartment;
- $v_{q,A}$ is the aerosol volume fraction in air compartment;
- $K_{g,Atot}$ is the partition coefficient between gas phase and air compartment;
- K_{QA} is the partition coefficient between aerosol phase and gas phase;
- $K_{q,Atot} = K_{g,Atot} \times K_{QA}$ is the partition coefficient between aerosol phase and air compartment;
- $fr\_m_{q,Atot} = K_{q,Atot} \times v_{q,A}$ is the mass fraction of chemical in aerosol phase;
- $V_{g,A}\ (m^3)$ is the volume of the gas phase;
- $A_{AW}(m^2) = areafractW \times A_A$ is the contact area between water and air;
- $areafractW$ is the fraction of area occupied by water;
- $A_A(m^2)$ is the surface area of air;
- Q is the scavenging ratio of aerosol by rain;
- $U_M\ (m\ h^{-1})$ is the rain rate;
- $V_A\ (m^3)$ is the volume of air compartment;
- $C_{g,A}\ (kg\ m^{-3})$ is the chemical concentration in the gas phase;
- $Z_A\ (kg\ Pa^{-1}m^{-3})$ is the fugacity capacity of gas phase;
- $D_{CAW}\ (kg\ Pa^{-1}h^{-1})$ is the fugacity-based rate D for aerosol wet deposition to water;
- $f_A\ (Pa)$ is the air fugacity;
- $N_{WETDEP,Q,AW}\ (kg\ h^{-1})$ is the aerosol wet deposition mass flux.

Compared to eq. 98 of USEtox, gas volume fraction v_g is not present here, as well as the intermittent rain model.

Irrigation

$$N_{IRRIG,WS} = f_W \times D_{IRRIG} \quad \text{(Eq. 199)}$$

$$= f_W \times U_{IRRIG} \times A_S \times Z_W$$

$$= C_{w,W} \times U_{IRRIG} \times A_S$$

$$= \frac{M_{w,W}}{V_{w,W}} \times U_{IRRIG} \times A_S$$

$$= M_W \times v_{w,W} \times K_{w,Wtot} \times U_{IRRIG} \times \frac{A_S}{V_{w,W}}$$

$$= M_W \times K_{w,Wtot} \times U_{IRRIG} \times \frac{A_S}{V_W}$$

Assuming that all the water compartment is used, not only dissolved water:

$$= M_W \times U_{IRRIG} \times \frac{A_S}{V_W}$$

$$= M_W \times U_{IRRIG} \times \frac{areafractS \times A_A}{\frac{areafractW \times A_A}{h_w}}$$

$$= M_W \times U_{IRRIG} \times \frac{areafractS}{\frac{areafractW}{h_w}}$$

$$= M_W \times k_{IRRIG}$$

Where:

- $k_{IRRIG}(h^{-1}) = U_{IRRIG} \times \frac{areafractS}{\frac{areafractW}{h_w}}$ is the mass-based rate for irrigation;
- $M_W\ (kg)$ is the mass in water compartment;
- $v_{w,W}$ is the dissolved water volume fraction in water compartment;
- $K_{w,Wtot}$ is the partition coefficient between dissolved water phase and water compartment;
- $V_{w,W}\ (m^3)$ is the volume of the dissolved water phase;
- $U_{IRRIG}\ (m\ h^{-1})$ is the irrigation rate;
- $V_W\ (m^3)$ is the volume of water compartment;
- $A_W(m^2) = areafractW \times A_A$ is the surface area of water compartment;
- $areafractW$ is the fraction of area occupied by water;
- $A_A(m^2)$ is the surface area of air;
- $A_S(m^2) = areafractS \times A_A$ is the surface area of soil compartment;
- $areafractS$ is the fraction of area occupied by soil;
- $h_w\ (m)$ is the water compartment height;
- $C_{w,W}\ (kg\ m^{-3})$ is the chemical concentration in the dissolved water phase;

- Z_W $(kg\ Pa^{-1}m^{-3})$ is the fugacity capacity of dissolved water phase;
- D_{IRRIG} $(kg\ Pa^{-1}h^{-1})$ is the fugacity-based rate D for irrigation;
- f_W (Pa) is the water fugacity;
- $N_{IRRIG,WS}$ $(kg\ h^{-1})$ is the water advection mass flux.

Compared to eq. 118 of USEtox, U_{IRRIG} is not shared among different scales.

Leaching

$$N_{LEACH,S} = f_S \times D_{LEACH} \quad \text{(Eq. 200)}$$

$$= f_S \times U_L \times A_S \times Z_W$$

$$= f_S \times U_L \times A_S \times K_{WS} \times Z_S$$

$$= C_{oc,S} \times U_L \times A_S \times K_{WS}$$

$$= \frac{M_{oc,S}}{V_{oc,S}} \times U_L \times A_S \times K_{WS}$$

$$= M_{oc,S} \times U_L \times A_S \times \frac{K_{WS}}{V_{oc,S}}$$

$$= M_S \times v_{oc,S} \times K_{oc,Stot} \times U_L \times A_S \times \frac{K_{WS}}{V_{oc,S}}$$

$$= M_S \times K_{oc,Stot} \times U_L \times A_S \times \frac{K_{WS}}{V_S}$$

$$= M_S \times K_{oc,Stot} \times K_{WS} \times U_L \times \frac{A_S}{V_S}$$

$$= M_S \times K_{oc,Stot} \times K_{WS} \times U_M \times fract_{inf} \times \frac{A_S}{V_S}$$

$$= M_S \times K_{w,Stot} \times U_M \times fract_{inf} \times \frac{A_S}{V_S}$$

$$= M_S \times k_{LEACH}$$

Where:

- $k_{LEACH}(h^{-1}) = K_{w,Stot} \times U_M \times fract_{inf} \times \frac{1}{h_S}$ is the mass-based rate for soil leaching;
- M_S (kg) is the mass in soil compartment;
- $v_{oc,S}$ is the organic carbon volume fraction in soil compartment;
- $K_{oc,Stot}$ is the partition coefficient between organic carbon phase and soil compartment;
- $V_{oc,S}$ (m^3) is the volume of the organic carbon phase;
- k_S (h^{-1}) is the rate constant for soil degradation;
- $C_{oc,S}$ $(kg\ m^{-3})$ is the chemical concentration in the organic carbon phase;

- $Z_W\ (kg\ Pa^{-1}m^{-3}) = K_{WS} \times Z_S$ is the fugacity capacity of dissolved water phase;
- $K_{w,Stot} = K_{oc,Stot} \times K_{WS}$ is the partition coefficient between pore water phase and soil compartment;
- K_{WS} is the partition coefficient between dissolved water phase and organic carbon phase;
- $Z_S\ (kg\ Pa^{-1}m^{-3})$ is the fugacity capacity of organic carbon phase;
- $U_L\ (m\ h^{-1}) = U_M \times fract_{inf}$ is the leaching rate;
- $U_M\ (m\ h^{-1})$ is the rain rate;
- $fract_{inf}$ is the rain fraction infiltrating in soil;
- $D_{LEACH}\ (kg\ Pa^{-1}h^{-1})$ is the fugacity-based rate D for soil leaching;
- $f_S\ (Pa)$ is the soil fugacity
- $N_{LEACH,S}\ (kg\ h^{-1})$ is the soil leaching mass flux.

Runoff

$$N_{RUNOFF,SW} = f_S \times D_{RUNOFF} \quad \text{(Eq. 201)}$$

$$= f_S \times (U_W \times A_S \times Z_W + U_{SOLID} \times A_S \times Z_S)$$

$$= f_S \times (U_W \times A_S \times K_{WS} \times Z_S + U_{SOLID} \times A_S \times Z_S)$$

$$= f_S \times Z_S \times A_S \times (U_W \times K_{WS} + U_{SOLID})$$

$$= C_{oc,S} \times A_S \times (U_W \times K_{WS} + U_{SOLID})$$

$$= \frac{M_{oc,S}}{V_{oc,S}} \times A_S \times (U_W \times K_{WS} + U_{SOLID})$$

$$= M_{oc,S} \times A_S \times \frac{(U_W \times K_{WS} + U_{SOLID})}{V_{oc,S}}$$

$$= M_S \times v_{oc,S} \times K_{oc,Stot} \times A_S \times \frac{(U_W \times K_{WS} + U_{SOLID})}{V_{oc,S}}$$

$$= M_S \times K_{oc,Stot} \times A_S \times \frac{(U_W \times K_{WS} + U_{SOLID})}{V_S}$$

$$= M_S \times K_{oc,Stot} \times (U_W \times K_{WS} + U_{SOLID}) \times \frac{A_S}{V_S}$$

$$= M_S \times (U_W \times K_{WS} \times K_{oc,Stot} + U_{SOLID} \times K_{oc,Stot}) \times \frac{1}{h_S}$$

$$= M_S \times (U_W \times K_{w,Stot} + U_{SOLID} \times K_{oc,Stot}) \times \frac{1}{h_S}$$

$$= M_S \times (U_M \times fract_{runoff} \times K_{w,Stot} + U_{SOLID} \times K_{oc,Stot}) \times \frac{1}{h_S}$$

$$= M_S \times k_{RUNOFF}$$

Where:

- $k_{RUNOFF}(h^{-1}) = (U_M \times fract_{runoff} \times K_{w,Stot} + U_{SOLID} \times K_{oc,Stot}) \times \frac{1}{h_S}$ is the mass-based rate for soil runoff to water compartment;
- $M_S\ (kg)$ is the mass in soil compartment;
- $v_{oc,S}$ is the organic carbon volume fraction in soil compartment;
- $K_{oc,Stot}$ is the partition coefficient between organic carbon phase and soil compartment;
- $V_{oc,S}\ (m^3)$ is the volume of the organic carbon phase;
- $h_S\ (h^{-1})$ is the soil's height;
- $C_{oc,S}\ (kg\ m^{-3})$ is the chemical concentration in the organic carbon phase;
- $Z_W\ (kg\ Pa^{-1}m^{-3}) = K_{WS} \times Z_S$ is the fugacity capacity of dissolved water phase;
- $K_{w,Stot} = K_{oc,Stot} \times K_{WS}$ is the partition coefficient between pore water phase and soil compartment;
- K_{WS} is the partition coefficient between dissolved water phase and organic carbon phase;
- $Z_S\ (kg\ Pa^{-1}m^{-3})$ is the fugacity capacity of organic carbon phase;
- $U_{SOLID}\ (m\ h^{-1}) = U_M \times fract_{runoff}$ is the soil solid runoff rate;
- $U_W\ (m\ h^{-1}) = U_M \times fract_{runoff}$ is the water runoff rate;
- $U_M\ (m\ h^{-1})$ is the rain rate;
- $fract_{runoff}$ is the rain fraction that runoffs on soil;
- $D_{RUNOFF}\ (kg\ Pa^{-1}h^{-1})$ is the fugacity-based rate D for soil runoff to water;
- $f_S\ (Pa)$ is the soil fugacity
- $N_{RUNOFF,SW}\ (kg\ h^{-1})$ is the soil leaching mass flux.

Compared to eq. 116 of USEtox, $K_{oc,Stot}$ multiplies U_{SOLID} here.

Sedimentation

$$N_{SED,WSED} = f_W \times D_{SED} \qquad \text{(Eq. 202)}$$

$$= f_W \times U_{SED} \times A_W \times Z_{SUSP}$$

$$= f_W \times U_{SED} \times A_W \times K_{PW} \times Z_W$$

$$= C_{w,W} \times U_{SED} \times A_W \times K_{PW}$$

$$= \frac{M_{w,W}}{V_{w,W}} \times U_{SED} \times A_W \times K_{PW}$$

$$= M_W \times v_{w,W} \times K_{w,Wtot} \times K_{PW} \times U_{SED} \times \frac{A_W}{V_{w,W}}$$

$$= M_W \times v_{w,W} \times K_{w,Wtot} \times K_P \times dens_{susp} \times U_{DEP} \times v_{ss,W} \times \frac{A_W}{V_{w,W}} \times \frac{1}{1000}$$

And assuming that $V_{w,W} \approx V_W$

$$= M_W \times v_{w,W} \times K_{w,Wtot} \times K_P \times U_{DEP} \times v_{ss,W} \times dens_{susp} \times \frac{A_W}{V_W} \times \frac{1}{1000}$$

$$= M_W \times v_{w,W} \times K_{w,Wtot} \times K_P \times U_{DEP} \times C_{susp} \times \frac{A_W}{V_W} \times \frac{1}{1000}$$

$$= M_W \times fr\_m_{w,Wtot} \times K_P \times U_{DEP} \times C_{susp} \times \frac{A_W}{V_W} \times \frac{1}{1000}$$

$$= M_W \times k_{SED}$$

Where:

- $k_{SED}(h^{-1}) = fr\_m_{w,Wtot} \times K_P \times U_{DEP} \times C_{susp} \times \frac{1}{h_W} \times \frac{1}{1000}$ is the mass-based rate for sedimentation;
- $M_W\ (kg)$ is the mass in water compartment;
- $v_{w,W}$ is the dissolved water volume fraction in water compartment;
- $K_{w,Wtot}$ is the partition coefficient between dissolved water phase and water compartment;
- $V_{w,W}\ (m^3)$ is the volume of the dissolved water phase;
- $U_{SED}\ (m\,h^{-1}) = U_{DEP} \times \frac{C_{susp}}{dens_{susp}} = U_{DEP} \times v_{ss,W}$ is the suspended solids sedimentation rate;
- $U_{DEP}\ (m\,h^{-1})$ is the deposition velocity in freshwater;
- $C_{susp}\ (\frac{g_{ss}}{cm_W^3})$ is the concentration of suspended solids in water;
- $v_{ss,W}\ (\frac{cm_{ss}^3}{cm_W^3})$ is volume fraction of suspended solids in water;
- $1000\ (\frac{L_W}{m_W^3})$ is a conversion factor;
- $K_{PW} = K_P \times dens_{susp} \times \frac{1}{1000}$ is the partition coefficient between suspended solids and dissolved water phase;
- $dens_{susp}(\frac{g}{cm^3})$ is the density of suspended solids;
- $K_P\ (\frac{L_W}{kg_{ss}})$ is the partition coefficient between suspended solids and dissolved water phase;
- $V_W\ (m^3)$ is the volume of water compartment;
- $A_W(m^2)$ is the surface area of water compartment;
- $h_w\ (m)$ is the water compartment height;
- $C_{w,W}\ (kg\ m^{-3})$ is the chemical concentration in the dissolved water phase;
- $Z_W\ (kg\ Pa^{-1}m^{-3})$ is the fugacity capacity of dissolved water phase;
- $D_{SED}\ (kg\ Pa^{-1}h^{-1})$ is the fugacity-based rate D for sedimentation;
- $f_W\ (Pa)$ is the water fugacity;
- $N_{SED,WSED}(kg\ h^{-1})$ is the sedimentation mass flux of suspended solids to sediments.

Resuspension

$$N_{RESUSP,SEDW} = f_{SED} \times D_{RESUSP} \quad \text{(Eq. 203)}$$

$$= f_{SED} \times U_R \times \frac{A_{SED}}{V_{SED}} \times Z_{SED}$$

$$= C_{oc,SED} \times U_R \times \frac{A_{SED}}{V_{SED}}$$

$$= \frac{M_{oc,SED}}{V_{oc,SED}} \times U_R \times \frac{A_{SED}}{V_{SED}}$$

$$= M_{SED} \times v_{oc,SED} \times K_{oc,SEDtot} \times U_R \times \frac{A_{SED}}{V_{oc,SED}}$$

$$= M_{SED} \times K_{oc,SEDtot} \times U_R \times \frac{A_{SED}}{V_{SED}}$$

$$= M_{SED} \times k_{RESUSP}$$

Where:

- $k_{RESUSP}(h^{-1}) = K_{oc,SEDtot} \times U_R \times \frac{A_{SED}}{V_{SED}}$ is the mass-based rate for resuspension;
- M_{SED} (kg) is the mass in sediment compartment;
- $K_{oc,SEDtot}$ is the partition coefficient between organic carbon phase and sediment compartment;
- $V_{oc,SED}$ (m^3) is the volume of the organic carbon phase;
- U_R $(m\ h^{-1})$ is the resuspension velocity in freshwater;
- V_{SED} (m^3) is the volume of sediment compartment;
- $A_{SED}(m^2)$ is the surface area of sediment compartment;
- $C_{oc,SED}$ $(kg\ m^{-3})$ is the chemical concentration in the organic carbon phase;
- Z_{SED} $(kg\ Pa^{-1}m^{-3})$ is the fugacity capacity of organic carbon phase;
- D_{RESUSP} $(kg\ Pa^{-1}h^{-1})$ is the fugacity-based rate D for resuspension;
- f_{SED} (Pa) is the sediment fugacity;
- $N_{RESUSP,SEDW}(kg\ h^{-1})$ is the resuspension mass flux of suspended solids to water.

Water – sediment diffusion

$$N_{DIFF,WSED} = f_W \times D_T \quad \text{(Eq. 204)}$$

$$= f_W \times k_T \times A_{WSED} \times Z_W$$

$$= C_{w,W} \times k_T \times A_{WSED}$$

$$= \frac{M_{w,W}}{V_{w,W}} \times k_T \times A_{WSED}$$

$$= M_W \times v_{w,W} \times K_{w,Wtot} \times k_T \times \frac{A_{WSED}}{V_{w,W}}$$

And assuming that $V_{w,W} \approx V_W$

$$= M_W \times v_{w,W} \times K_{w,Wtot} \times k_T \times \frac{A_{WSED}}{V_W}$$

$$= M_W \times fr\_m_{w,Wtot} \times k_T \times \frac{A_{WSED}}{V_W}$$

$$= M_W \times fr\_m_{w,Wtot} \times k_T \times \frac{1}{h_W}$$

$$= M_W \times k_{T,WSED}$$

Where:

- $k_{T,WSED}(h^{-1}) = fr\_m_{w,Wtot} \times k_T \times \frac{1}{h_W}$ is the mass-based rate for water-sediments diffusion;
- $M_W\ (kg)$ is the mass in water compartment;
- $v_{w,W}$ is the dissolved water volume fraction in water compartment;
- $K_{w,Wtot}$ is the partition coefficient between dissolved water phase and water compartment;
- $V_{w,W}\ (m^3)$ is the volume of the dissolved water phase;
- $k_T\ (m\ h^{-1}) = k_{OSED} = \left(\frac{k_{T,w,W} \times k_{T,w,SED}}{k_{T,w,W} + k_{T,w,SED}}\right)^{-1}$ is the overall mass transfer coefficient for water-sediments diffusion. No partition coefficient is needed in the formula since the same phase is moving (dissolved water and pore water of sediments);
- $V_W\ (m^3)$ is the volume of water compartment;
- $A_W(m^2)$ is the surface area of water compartment;
- $h_w\ (m)$ is the water compartment height;
- $C_{w,W}\ (kg\ m^{-3})$ is the chemical concentration in the dissolved water phase;
- $Z_W\ (kg\ Pa^{-1}m^{-3})$ is the fugacity capacity of dissolved water phase;
- $D_T\ (kg\ Pa^{-1}h^{-1})$ is the fugacity-based rate D for water-sediments diffusion;
- $f_W\ (Pa)$ is the water fugacity;
- $N_{DIFF,WSED}(kg\ h^{-1})$ is the water-sediments diffusion mass flux.

<u>Sediment – water diffusion</u>

$$N_{DIFF,SEDW} = f_{SED} \times D_T \qquad \text{(Eq. 205)}$$

$$= f_{SED} \times k_T \times A_{WSED} \times Z_W$$

$$= C_{w,SED} \times k_T \times A_{WSED}$$

$$= \frac{M_{w,SED}}{V_{w,SED}} \times k_T \times A_{WSED}$$

$$= M_{SED} \times v_{w,SED} \times K_{w,SEDtot} \times k_T \times \frac{A_{WSED}}{V_{w,SED}}$$

$$= M_{SED} \times K_{w,SEDtot} \times k_T \times \frac{A_{WSED}}{V_{SED}}$$

$$= M_{SED} \times K_{w,SEDtot} \times k_T \times \frac{1}{h_{SED}}$$

$$= M_{SED} \times k_{T,SEDW}$$

Where:

- $k_{T,SEDW}\ (h^{-1}) = K_{w,SEDtot} \times k_T \times \frac{1}{h_{SED}}$ is the mass-based rate for sediments-water diffusion;
- $M_{SED}\ (kg)$ is the mass in sediment compartment;
- $v_{w,SED}$ is the dissolved water volume fraction in sediments compartment;
- $K_{w,SEDtot}$ is the partition coefficient between dissolved water phase and sediments compartment;
- $V_{w,SED}\ (m^3)$ is the volume of the dissolved water phase in sediments;
- $k_T\ (m\ h^{-1}) = k_{OSED} = \left(\frac{k_{T,w,W} \times k_{T,w,SED}}{k_{T,w,W} + k_{T,w,SED}}\right)^{-1}$ is the overall mass transfer coefficient for water-sediments diffusion. No partition coefficient is needed in the formula since the same phase is moving (dissolved water and pore water of sediments);
- $V_{SED}\ (m^3)$ is the volume of sediment compartment;
- $A_W(m^2)$ is the surface area of water and sediments compartment;
- $h_{SED}\ (m)$ is the sediments compartment height;
- $C_{w,SED}\ (kg\ m^{-3})$ is the chemical concentration in the dissolved water phase of sediments;
- $Z_W\ (kg\ Pa^{-1}m^{-3})$ is the fugacity capacity of dissolved water phase;
- $D_T\ (kg\ Pa^{-1}h^{-1})$ is the fugacity-based rate D for water-sediments diffusion;
- $f_{SED}\ (Pa)$ is the sediments fugacity;
- $N_{DIFF,SEDW}(kg\ h^{-1})$ is the sediments-water diffusion mass flux.

Further equation differences with USEtox formulas:

- Mass fraction of original species for water and soil are not considered at the moment;
- Differences in diffusion coefficient from soil Deff.s1L (eq. 105 of USEtox, effective advective transfer is not considered);
- Kaw does not vary with the scale;
- The alternate form in soil Ksolid,w is not considered (eq. 84 of USEtox) for water phase-soil total compartment partition coeff FRw.s1L (eq. 83 of USEtox) and also in sediment (eq. 86 of USEtox) for water phase-sediment total compartment partition coeff FRw.sd1L (eq. 85 of USEtox); also for Ksusp,w in SED.w1L.sd1L and for water

mass fraction FRw.w1L (eq.20 of USEtox). Dimensionless partition coefficient and volume fractions are considered at the moment in their substitution;

- Additional phenomena considered by USEtox: calculation of suspended matter concentration in freshwater (eq. 33).

Default parameters differences:

- RAINrate.L = 1.68E-08 m s^{-1} (value from Mackay: 6E-04 m h^{-1}); RAINrate.C = 2.22E-08 m s^{-1};
- IRRIGATION.L = 3E+04 m^3 (hypothesis: 62% of freshwater volume, as done in USEtox for the continental scale); IRRIGATION.C = 4.21E+11 m^3;
- vfish.w (local fish volume fraction) = 7E-06 (value from Mackay: 7 m^3 for a freshwater volume of 10^6 m^3); BIOmass.w1C = 1 kg fish per L water (if fish density is 1.3 kg L^{-1}, 0.77 L fish per L water);
- EROSION.L = 6.39E-12 m s^{-1} (value from Mackay: Solids runoff rate from soil = 0.2 mm y^{-1}); EROSION.C = 0.03 mm y^{-1};
- Organic carbon fraction in suspended particles = 0.04 (value from Mackay) vs CORGsusp1.C = 0.1;
- Organic carbon fraction in sediments = 0.04 (value from Mackay) vs CORGsd1.C = 0.05.

A.5 Constant rates k and fate results of the mass-based local-continental model

Table 63 Conversion procedures from fugacity to mass-based local rates. The calculation is performed in the Excel spreadsheet Mass-based local-continental model.xlsx

DIRECT CONVERSION FROM D VALUES

Local	k diffusion (h^{-1})	Formula
k_{DIFFAW}	9.12E-07	$D_{VAW}/(V_A \times Z_{Abulk})$
k_{DIFFWA}	1.00E-03	$D_{VAW}/(V_W \times Z_{Wbulk})$
k_{DIFFAS}	1.44E-03	$D_{VAS}/(V_A \times Z_{Abulk})$
k_{DIFFSA}	2.08E-02	$D_{VAS}/(V_S \times Z_{Sbulk})$

Local	k degradation (h^{-1})	Formula
$K_{DEG,A}$	4.08E-02	$D_{DEG,A}/(V_A \times Z_{Abulk})$
$K_{DEG,W}$	4.08E-03	$D_{DEG,W}/(V_W \times Z_{Wbulk})$
$K_{DEG,S}$	1.15E-04	$D_{DEG,S}/(V_S \times Z_{Sbulk})$

Local	k advection (h^{-1})	Formula
$k_{ADV,A}$	1.08E+01	$D_{ADV,A}/(V_A \times Z_{Abulk})$
$k_{ADV,W}$	3.60E+00	$D_{ADV,W}/(V_W \times Z_{Wbulk})$
k_{QAW}	2.63E-13	$D_{QAW}/(V_A \times Z_{Abulk})$
k_{MAW}	1.09E-08	$D_{MAW}/(V_A \times Z_{Abulk})$
k_{CAW}	3.16E-13	$D_{CAW}/(V_A \times Z_{Abulk})$
k_{QAS}	2.61E-11	$D_{QAS}/(V_A \times Z_{Abulk})$
k_{MAS}	1.08E-06	$D_{MAS}/(V_A \times Z_{Abulk})$
k_{CAS}	3.13E-11	$D_{CAS}/(V_A \times Z_{Abulk})$
$k_{RUNOFF,S}$	9.98E-09	$D_{RUNOFF,S}/(V_S \times Z_{Sbulk})$
$k_{RUNOFF,W}$	1.02E-05	$D_{RUNOFF,W}/(V_S \times Z_{Sbulk})$
k_{IRRIG}	1.17E-05	$D_{IRRIG}/(V_W \times Z_{Wbulk})$

ANALYTIC CONVERSION FROM D VALUES

Local	k diffusion (h^{-1})	Formula
k_{DIFFAW}	9.12E-07	$kow \times A_{AW}/V_A/K_{AW} \times K_{g,Atot}$
k_{DIFFWA}	1.00E-03	$kow \times A_{AW}/V_W \times K_{wdiss,Wtot}$
k_{DIFFAS}	1.44E-03	$K_{g,Atot} \times (1/(1/(kv \times A_{AS}) + 1/((B_{EA} + B_{EW} \times K_{WA} + B_{EOC} \times K_{SA})/Y^* A_{AS})))/V_A$
k_{DIFFSA}	2.08E-02	$K_{oc,Stot} \times (1/(1/(kv \times A_{AS} \times K_{AS}) + 1/((B_{EA} \times K_{AS} + B_{EW} \times K_{WA} + B_{EOC})/Y \times A_{AS})))/V_S$

Local	k degradation (h^{-1})	Formula
$K_{DEG,A}$	4.08E-02	$k_A \times v_{g,A} \times K_{g,Atot}$
$K_{DEG,W}$	4.08E-03	$k_W \times v_{w,W} \times K_{wdiss,Wtot}$
$K_{DEG,S}$	1.15E-04	$k_S \times v_{oc,S} \times K_{oc,Stot}$

Local	k advection (h^{-1})	Formula
$k_{ADV,A}$	1.08E+01	$G_A/V_A \times K_{g,Atot}$
$k_{ADV,W}$	3.60E+00	$(G_W+G_{PW} \times K_{PW})/V_W \times K_{wdiss,Wtot}$
k_{QAW}	2.63E-13	$U_Q \times v_Q \times A_{AW}/V_A \times K_{QA} \times K_{g,Atot}$
k_{MAW}	1.09E-08	$U_M \times A_{AW}/V_A \times K_{WA} \times K_{g,Atot}$
k_{CAW}	3.16E-13	$U_M \times A_{AW} \times Q \times v_Q/V_A \times K_{QA} \times K_{g,Atot}$
k_{QAS}	2.61E-11	$U_Q \times v_Q \times A_{AS}/V_A \times K_{QA} \times K_{g,Atot}$
k_{MAS}	1.08E-06	$U_M \times A_{AS}/V_A \times K_{WA} \times K_{g,Atot}$
k_{CAS}	3.13E-11	$U_M \times A_{AS} \times Q \times v_Q/V_A \times K_{QA} \times K_{g,Atot}$
$k_{RUNOFF,S}$	9.98E-09	$A_S \times U_{solid}/V_S \times K_{oc,Stot}$
$k_{RUNOFF,W}$	1.02E-05	$A_S \times U_W/V_S \times K_{WS} \times K_{oc,Stot}$
k_{IRRIG}	1.17E-05	$U_{IRRIG} \times A_{AS}/V_W \times K_{wdiss,Wtot}$

CONVERSION FROM D VALUES ACCORDING TO MCKONE AND BENNETT (2003)

Local	k diffusion (h^{-1})	Formula
k_{DIFFAW}	9.12E-05	$Y_W/(Z_{Abulk} \times d_A)$; $Y_W = D_{VAW}/A_{AW}$
k_{DIFFWA}	1.00E-03	$Y_W/(Z_{Wbulk} \times d_W)$; $Y_W = D_{VAW}/A_{AW}$
k_{DIFFAS}	1.45E-03	$Y_S/(Z_{Abulk} \times d_A)$; $Y_S = D_{VAS}/A_{AS}$
k_{DIFFSA}	2.09E-02	$Y_S/(Z_{Sbulk} \times d_S)$; $Y_S = D_{VAS}/A_{AS}$

Local	k advection (h^{-1})	Formula
k_{QAW}	2.63E-11	$Y_W/(Z_{Abulk} \times d_A)$; $Y_W = D_{QAW}/A_{AW}$
k_{MAW}	1.09E-06	$Y_W/(Z_{Abulk} \times d_A)$; $Y_W = D_{MAW}/A_{AW}$
k_{CAW}	3.16E-11	$Y_W/(Z_{Abulk} \times d_A)$; $Y_W = D_{CAW}/A_{AW}$
k_{QAS}	2.63E-11	$Y_S/(Z_{Abulk} \times d_A)$; $Y_S = D_{QAS}/A_{AS}$
k_{MAS}	1.09E-06	$Y_S/(Z_{Abulk} \times d_A)$; $Y_S = D_{MAS}/A_{AS}$
k_{CAS}	3.16E-11	$Y_S/(Z_{Abulk} \times d_A)$; $Y_S = D_{CAS}/A_{AS}$

Table 64 Conversion procedures from fugacity to mass-based continental rates

DIRECT CONVERSION FROM D VALUES

Continental	k diffusion (h^{-1})	Formula
k_{DIFFAW}	8.93E-07	$D_{VAW}/(V_A \times Z_{Abulk})$
k_{DIFFWA}	1.55E-03	$D_{VAW}/(V_W \times Z_{Wbulk})$
k_{DIFFAS}	3.43E-04	$D_{VAS}/(V_A \times Z_{Abulk})$
k_{DIFFSA}	2.09E-02	$D_{VAS}/(V_S \times Z_{Sbulk})$

Continental	k degradation (h^{-1})	Formula
$k_{DEG,\ A}$	4.08E-02	$D_{DEG,A}/(V_A \times Z_{Abulk})$
$k_{DEG,\ W}$	4.08E-03	$D_{DEG,W}/(V_W \times Z_{Wbulk})$
$k_{DEG,\ S}$	1.14E-04	$D_{DEG,S}/(V_S \times Z_{Sbulk})$

Continental	k advection (h^{-1})	Formula
$k_{ADV,A}$	8.39E-03	$D_{ADV,A}/(V_A \times Z_{Abulk})$
$k_{ADV,W}$	3.00E-05	$D_{ADV,W}/(V_W \times Z_{Wbulk})$
k_{QAW}	8.31E-14	$D_{QAW}/(V_A \times Z_{Abulk})$
k_{MAW}	3.45E-09	$D_{MAW}/(V_A \times Z_{Abulk})$
k_{CAW}	9.97E-14	$D_{CAW}/(V_A \times Z_{Abulk})$
k_{QAS}	6.23E-12	$D_{QAS}/(V_A \times Z_{Abulk})$
k_{MAS}	2.59E-07	$D_{MAS}/(V_A \times Z_{Abulk})$
k_{CAS}	7.48E-12	$D_{CAS}/(V_A \times Z_{Abulk})$
$k_{RUNOFF,S}$	1.00E-08	$D_{RUNOFF,S}/(V_S \times Z_{Sbulk})$
$k_{RUNOFF,W}$	1.02E-05	$D_{RUNOFF,W}/(V_S \times Z_{Sbulk})$
k_{IRRIG}	4.43E-06	$D_{IRRIG}/(V_W \times Z_{Wbulk})$

ANALYTIC CONVERSION FROM D VALUES

Continental	k diffusion (h^{-1})	Formula
k_{DIFFAW}	8.93E-07	$kow \times A_{AW}/V_A/K_{AW} \times K_{g,Atot}$
k_{DIFFWA}	1.55E-03	$kow \times A_{AW}/V_W \times K_{wdiss,Wtot}$
k_{DIFFAS}	3.43E-04	$K_{g,Atot} \times (1/(1/(kv \times A_{AS}) + 1/((B_{EA} + B_{EW} \times K_{WA} + B_{EOC} \times K_{SA})/Y^*A_{AS})))/V_A$
k_{DIFFSA}	2.09E-02	$K_{oc,Stot} \times (1/(1/(kv \times A_{AS} \times K_{AS}) + 1/((B_{EA} \times K_{AS} + B_{EW} \times K_{WA} + B_{EOC})/Y \times A_{AS})))/V_S$

Continental	k degradation (h^{-1})	Formula
$k_{DEG,\ A}$	4.08E-02	$k_A \times v_{g,A} \times K_{g,Atot}$
$k_{DEG,\ W}$	4.08E-03	$k_W \times v_{w,W} \times K_{wdiss,Wtot}$
$k_{DEG,\ S}$	1.15E-04	$k_S \times v_{oc,S} \times K_{oc,Stot}$

Continental	k advection (h^{-1})	Formula
$k_{ADV,A}$	8.39E-03	$G_A/V_A \times K_{g,Atot}$
$k_{ADV,W}$	3.00E-05	$(G_W+G_{PW} \times K_{PW})/V_W \times K_{wdiss,Wtot}$
k_{QAW}	8.31E-14	$U_Q \times v_Q \times A_{AW}/V_A \times K_{QA} \times K_{g,Atot}$
k_{MAW}	3.45E-09	$U_M \times A_{AW}/V_A \times K_{WA} \times K_{g,Atot}$
k_{CAW}	9.97E-14	$U_M \times A_{AW} \times Q \times v_Q/V_A \times K_{QA} \times K_{g,Atot}$
k_{QAS}	6.23E-12	$U_Q \times v_Q \times A_{AS}/V_A \times K_{QA} \times K_{g,Atot}$
k_{MAS}	2.59E-07	$U_M \times A_{AS}/V_A \times K_{WA} \times K_{g,Atot}$
k_{CAS}	7.48E-12	$U_M \times A_{AS} \times Q \times v_Q/V_A \times K_{QA} \times K_{g,Atot}$
$k_{RUNOFF,S}$	1.00E-08	$A_S \times U_{solid}/V_S \times K_{oc,Stot}$
$k_{RUNOFF,W}$	1.02E-05	$A_S \times U_W/V_S \times K_{WS} \times K_{oc,Stot}$
k_{IRRIG}	4.43E-06	$U_{IRRIG} \times A_{AS}/V_W \times K_{wdiss,Wtot}$
$k_{ADV,ACONTLOC}$	2.84E-07	$G_{ALOC}/V_{ACONT} \times K_{g,Atot}$
$k_{ADV,WCONTLOC}$	1.50E-07	$(G_{WLOC}+G_{PWLOC} \times K_{PW})/V_{WCONT} \times K_{wdiss,Wtot}$
$k_{RUNOFFCONT,LOC}$	1.13E-12	$(A_{SLOC} \times (U_{SOLID} + U_W \times K_{WS}))/V_{SCONT} \times K_{oc,Stot}$

CONVERSION FROM D VALUES ACCORDING TO MCKONE AND BENNETT (2003)

Continental	k diffusion (h^{-1})	Formula
k_{DIFFAW}	6.79E-05	$Y_W/(Z_{Abulk} \times d_A)$; $Y_W = D_{VAW}/A_{AW}$
k_{DIFFWA}	1.55E-03	$Y_W/(Z_{Wbulk} \times d_W)$; $Y_W = D_{VAW}/A_{AW}$
k_{DIFFAS}	3.48E-04	$Y_S/(Z_{Abulk} \times d_A)$; $Ys = D_{VAS}/A_{AS}$
k_{DIFFSA}	2.09E-02	$Y_S/(Z_{Sbulk} \times d_S)$; $Ys = D_{VAS}/A_{AS}$
k_{QAW}	6.32E-12	$Y_W/(Z_{Abulk} \times d_A)$; $Y_W = D_{QAW}/A_{AW}$
k_{MAW}	2.62E-07	$Y_W/(Z_{Abulk} \times d_A)$; $Y_W = D_{MAW}/A_{AW}$
k_{CAW}	7.58E-12	$Y_W/(Z_{Abulk} \times d_A)$; $Y_W = D_{CAW}/A_{AW}$
k_{QAS}	6.32E-12	$Y_S/(Z_{Abulk} \times d_A)$; $Ys = D_{QAS}/A_{AS}$
k_{MAS}	2.62E-07	$Y_S/(Z_{Abulk} \times d_A)$; $Ys = D_{MAS}/A_{AS}$
k_{CAS}	7.58E-12	$Y_S/(Z_{Abulk} \times d_A)$; $Ys = D_{CAS}/A_{AS}$

Table 65 Masses results for a benzene emission in each compartment in the mass-based local-continental model applying the analytic conversion procedure. Value in red highlights a difference between the mass obtained with the local-continental model (i.e. 4.15E-08 mol), the reason is under investigation and will be deepened in a future development.

Receiving compartment *i*	**M_i (mol) $E_{A,LOC}$ = 1 mol h^{-1}**	**M_i (mol) E_{WLOC} = 1 mol h^{-1}**	**M_i (mol) $E_{S,LOC}$ = 1 mol h^{-1}**
Loc. Air_{bulk}	9.22E-02	2.61E-05	9.17E-02
Loc. $Water_{bulk}$	4.17E-08	2.77E-01	1.35E-04
Loc. $Soil_{bulk}$	6.33E-03	1.57E-04	4.78E+01
Cont. Air_{bulk}	2.03E+01	5.59E+00	2.01E+01
Cont. $Water_{bulk}$	3.83E-03	1.76E+02	8.97E-02
Cont. $Soil_{bulk}$	3.31E-01	1.28E-01	3.29E-01